

Understanding Norovirus-Host Interactions:

Implications for Developing Novel Antiviral Strategies

Peifa Yu

The studies presented in this thesis were performed at the Laboratory of Gastroenterology and Hepatology, Erasmus MC-University Medical Center Rotterdam, the Netherlands.

The research was funded by:

- China Scholarship Council

Financial support for the printing of the thesis was provided by:
Erasmus University Rotterdam

© Copyright by Peifa Yu. All rights reserved.

No part of the thesis may be reproduced or transmitted, in any form, by any means, without express written permission of the author.

Cover and Layout design: the author of this thesis

Printing: Ridderprint | www.ridderprint.nl

ISBN: 978-94-6416-711-5

**Understanding Norovirus-Host Interactions:
Implications for Developing Novel Antiviral Strategies**
**Begrip van de interactie tussen norovirus en gastheer en de
consequenties daarvan voor nieuwe behandeling**

Thesis

to obtain the degree of Doctor from the
Erasmus University Rotterdam
by command of the
rector magnificus

Prof. dr. F.A. van der Duijn Schouten

and in accordance with the decision of the Doctorate Board

The public defense shall be held on

Tuesday 14th September 2021 at 10:30

by

Peifa Yu

born in Jinan, Shandong Province, China

Erasmus University Rotterdam



Doctoral Committee

Promoter:

Prof. dr. M.P. Peppelenbosch

Inner Committee:

Prof. dr. C.J. van der Woude

Prof. dr. F.J.M. van Kuppeveld

Dr. M.E. Wildenberg

Copromoter:

Dr. Q. Pan

Contents

Chapter 1	General introduction and outline of the thesis	1
Chapter 2	2'-Fluoro-2'-deoxycytidine inhibits murine norovirus replication and synergizes MPA, ribavirin and T705 <i>Archives of Virology, 2020, 165(11): 2605-2613</i>	15
Chapter 3	Lipopolysaccharide restricts murine norovirus infection in macrophages mainly through NF- κ B and JAK-STAT signaling pathway <i>Virology, 2020, 546: 109-121</i>	31
Chapter 4	Guanylate-binding protein 2 orchestrates innate immune responses against murine norovirus and is antagonized by the viral protein NS7 <i>Journal of Biological Chemistry, 2020, 295: 8036-8047</i>	59
Chapter 5	MDA5 against enteric viruses through induction of interferon-like response partially via the JAK-STAT cascade <i>Antiviral Research, 2020, 176: 104743</i>	83
Chapter 6	Murine norovirus replicase augments RIG-I-like receptors-mediated antiviral interferon response <i>Antiviral Research, 2020, 182: 104877</i>	109
Chapter 7	cGAS-STING effectively restricts murine norovirus infection but antagonizes the antiviral action of N-terminus of RIG-I in mouse macrophages <i>Gut Microbes, 2021 (in press)</i>	135
Chapter 8	Summary and Discussion	167
Chapter 9	Dutch Summary	173
Appendix	Acknowledgements Publications PhD Portfolio Curriculum Vitae	179

Chapter 1

General Introduction and Outline of The Thesis

Norovirus belongs to the *Caliciviridae* family and is a non-enveloped, positive single-stranded RNA virus. Following the introduction of rotavirus vaccines and the consequent reduction in the disease burden associated with rotavirus infection, now norovirus has become the main cause of outbreaks of viral gastroenteritis epidemics worldwide (1). Different from rotavirus, which is mainly a problem for young children, norovirus is prone to infect humans of all ages and is associated with 699 million gastroenteritis cases per year. The impact of norovirus on human societies is further aggravated by that it provokes approximately 200,000 deaths in children under 5 years of age in developing countries (2,3). Hence, norovirus poses a substantial burden on our species.

Epidemics of human norovirus (HuNV) infection often start with virus-contaminated food, but subsequent transmission of HuNV infection is predominantly by the fecal-oral route and through person-to-person contact. Symptoms associated with HuNV infection are diarrhea, vomiting, abdominal cramps and fever (4). Although norovirus gastroenteritis is usually self-limiting, severe cases may occur in infants, elderly or immunocompromised patients, the latter in particular recipients of orthotopic organ transplantation requiring immunosuppressive medication. In such patients chronic infection may develop accompanied by persistent gastrointestinal symptoms (5,6). Management of such patients is highly troublesome and often restricted to supportive therapy and it is fair to say that there is an urgent need for better therapeutic options.

Despite the substantial disease burden associated with norovirus, compared to other pathogens such as influenza virus and coronavirus, norovirus has been given less attention. One of the reasons of the paucity of information on the molecular details of HuNV infection is the absence of robust experimental models sustaining viral infection. Thus there is an urgent need for more research into the molecular pathology of norovirus infection in general and the establishment of better experimental models in particular. In this thesis I hope to address these issues, but before I shall sketch my strategy in this regard, I first need to introduce various biological aspects of both the virus and the associated infectious process.

Norovirus genomic composition

Noroviruses can infect a wide range of mammalian hosts, maybe even all mammalian species, and evident examples of mammals subject to norovirus infection include cattle, swine, mice and of course humans. With the continuous identification of new strains, proper taxonomy remains a challenge. Noroviruses have recently been classified into at least 10 genogroups (GI-GX) and two tentative genogroups, based on sequence variation in the capsid protein (VP1) and the RNA-dependent RNA polymerase (7). The viruses in the GI, GII, GIV, GVIII and GIX classes can infect humans, with GII being reported as to be dominant with respect to most of

human infections. The virus in GV is the murine norovirus (MNV). The variety in different strains necessitates careful evaluation before general statements on norovirus biology are made.

The genome of norovirus is approximately 7.5 kilobases (kb) in length and encodes three or four open reading frames (ORFs) (8,9). The 5'-end of the genome is covalently linked to a viral protein (VPg) and the 3'-end of the genome is polyadenylated (Fig. 1). The ORF1 encodes a polyprotein that is post-translationally cleaved into six non-structural proteins (NS1/2 to NS7) by the viral protease (NS6) (10). ORF2 encodes the major structural protein referred to as VP1 and in which shell (S) and protruding (P) domains are recognized. Within the P domain, there is a highly variable region, named P2, that contains sites that act as antigens in anti-norovirus immunity and interacts with histo-blood group antigens (HBGAs) (11,12). ORF3 encodes a minor structural protein (VP2) that is associated with capsid assembly and genome encapsidation, as well as cell entry of the virions into cytoplasm of host cells (13). Specific for MNV, an additional ORF (designated as ORF4) in the ORF2 coding region produces a protein named as virulence factor (VF1), and that acts as an antagonist of the innate antiviral immune response (9). The non-structural proteins are associated with the viral replication complex (RC) induced membrane clusters, and interaction with host factors to regulate cellular homeostasis and promote viral replication (14,15). Further information on the importance of specific sequence elements from the norovirus genome with host cell biology would help the design of rational approaches to combat disease associated with the virus.

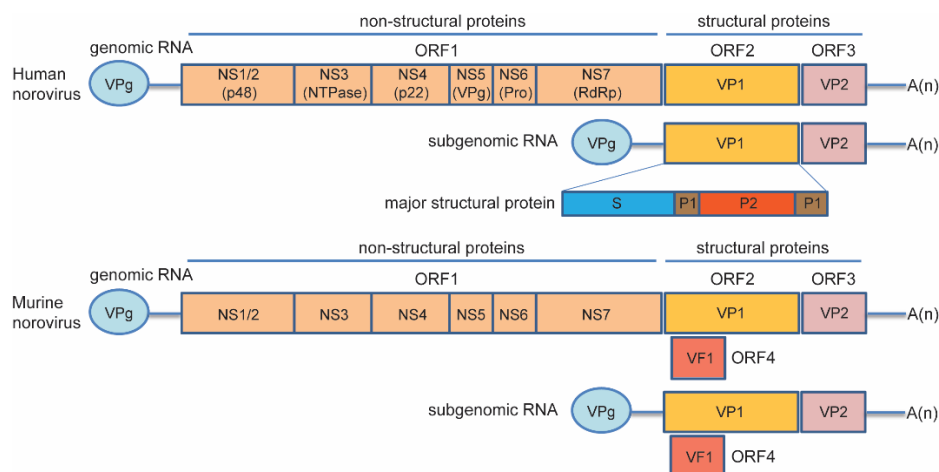


Figure 1. Genomic composition of the HuNV and MNV. (A) The 5'-end of HuNV genome is covalently linked to a viral protein (VPg) and the 3'-end of the genome is polyadenylated, consisting of three ORFs. ORF1 encodes a polyprotein that is cleaved by the viral protease NS6 into six non-structural proteins (NS1/2 to NS7). ORF2 and ORF3 are translated from a subgenomic RNA, encoding the structural protein VP1 and VP2, respectively. (B) MNV shares a similar genome organization with HuNV. Specifically, MNV has an additional ORF (designated as ORF4) overlapping with ORF2, named as virulence factor (VF1). Figure was adapted from (10).

Norovirus experimental models

The lack of in vitro culture systems that allow for robust infection and replication of HuNV has impeded of both understanding norovirus viral biology as well as of its interaction with human immunity. Consequently the development of antivirals and vaccines has been minimal. Nevertheless advances are made and the work towards establishment of cell culture models that support HuNV replication is gradually progressing. The HuNV GII.4 strain has been reported to have the capacity to infect human B cell lines, as deduced from a significant increase in viral genomic copy numbers following inoculation, whereas this experimental system also allowed the detection of the finding that HBGAs probably serve as a cofactor for binding and attachment of HuNV to B cells (16). Generally speaking, the establishment of human intestinal enteroids (HIEs) that contain multiple intestinal epithelial cell types, advances our understanding of the human intestinal epithelium and such structures constitute good culture systems for studying viral pathogenesis and viral-host interactions and their potential for norovirus research was quickly recognized. Already in 2016, HIEs derived from intestinal crypts were reported to support HuNV replication (17), and this observation was exploited in subsequent studies using this culture model to successfully uncover novel aspects of HuNV pathogenesis (18-20). Although HuNV replication following inoculation of experimental animals has been reported in some animal species including chimpanzees, gnotobiotic pigs, calves, and BALB/c Rag- γ c-deficient mice, these animal models are not suited for extensive experimentation and often only show viral replication of a short duration, and it is fair to say that the impact of such animal laboratory studies has been limited (21-24). Recently, studies have reported that HuNV GI and GII replicate and produce high titers in zebrafish (*Danio rerio*) larvae, which would constitute a simple and robust replication model and will facilitate studies of HuNV biology and development of antiviral strategies, even if translation to the human situation will not always be evident due to the substantial differences in biology and especially immunity between fish and mice (25). A replicon model in the Huh7 cell line that stably expresses a HuNV RNA replicon was developed by Chang and colleagues (26), and is currently widely used for studying antivirals against on HuNV replication, including ribavirin, mycophenolic acid (MPA) and calcineurin inhibitors (27,28). Further development of such models should prove instrumental for enlarging our insight in norovirus biology and uncover novel leads for improved treatment of disease.

Vaccines and treatment against norovirus infection

Currently, several candidate norovirus vaccines are in development, utilizing virus-like particles (VLPs), P particles, and recombinant adenoviruses as vectors for immune system antigen education. There are, however, no licensed norovirus vaccines yet, although a bivalent

GI.1/GII.4 VLP-based intramuscular vaccine (Phase IIb) and a GI.1 oral vaccine (Phase I) are currently undergoing evaluation in clinical trials, whereas others show promise in preclinical investigations (29). For now, however, there is evident lack of available vaccines or for that matter specific antiviral treatment. The development of specific antiviral drugs against norovirus infection may help bridge the time interval until effective vaccination becomes available.

Some potential inhibitors against norovirus have been identified and their possible efficacy for treating disease was demonstrated in relevant experimental models. For instance, ribavirin has been widely studied in general and been shown to exhibit a broad antiviral activity against multiple viruses, including norovirus (30). Clinical studies have reported that ribavirin treatment resulted in complete viral clearance in a subset of norovirus-infected patients, but treatment failure was observed as well (31). Thus the usefulness of this medication as monotherapy remains in doubt. Favipiravir, also known as T-705, has been approved for the treatment of influenza in Japan, and was repositioned to treat patients with Ebola virus infection (32,33). The medication has also been shown to be effective against norovirus, but its implementation in clinical practice for treating chronic norovirus infection is complicated by the observation that the drug is mutagenic in both mice and in patients (34). More general, despite the broad nature of clinical applications of various antiviral drug candidates, side effects and off-target effects continue to be problematic issues. It is clear that further research is necessary.

Host innate immune response following norovirus infection

Interferon (IFN)-mediated innate immune response provides a forward line of cell-autonomous defense against viral infections. Early viral recognition is possible through the presence of specific non-self motifs in viral particles that can bind pattern recognition receptors (PRRs). Important representatives of such receptors are the RIG-I-like receptors (RLRs) and Toll-like receptors (TLRs). RLRs mainly sense the viral replicative intermediates that accumulate in the cytosol following RNA virus infection (35). Three RLR members, including retinoic acid-inducible gene (RIG-I), melanoma differentiation associated gene 5 (MDA5) and laboratory of genetics and physiology gene 2 (LGP2), are widely expressed in mammalian cells and may all three contribute to defense against norovirus infection. All these three RLRs contain a distinctive C-terminal domain (CTD) that is linked to a helicase domain via a so-called 'pincer' sequence whereas RIG-I and MDA5 also possess two caspase activation and recruitment domains (CARDs) in their N-terminal domains (36). MDA5 has been described to act as a sensor that can recognize MNV infection (37). Silencing of RIG-I had no significant effect on viral replication in the HuNV replicon Huh-7 cell model (38), but RIG-I overexpression restricts norovirus replicon replication in this model, as well as MNV in human cells ectopically

expressing viral receptor (39,40). Upon binding with viral RNA, the CARD domains of MDA5 and RIG-I interact with the mitochondrial antiviral-signaling protein (MAVS, also known as IPS-1, VISA, or Cardif) to activate signaling cascades that leading to nuclear translocation of interferon-regulatory factors (IRFs, including IRF3 and IRF7) and nuclear factor κ B (NF- κ B), which in turn trigger the production of IFNs and proinflammatory cytokines (Fig. 2). Both HuNV and MNV are subject to cell-autonomous immune responses restricting viral replication, and hence are sensitive to IFNs (20,41).

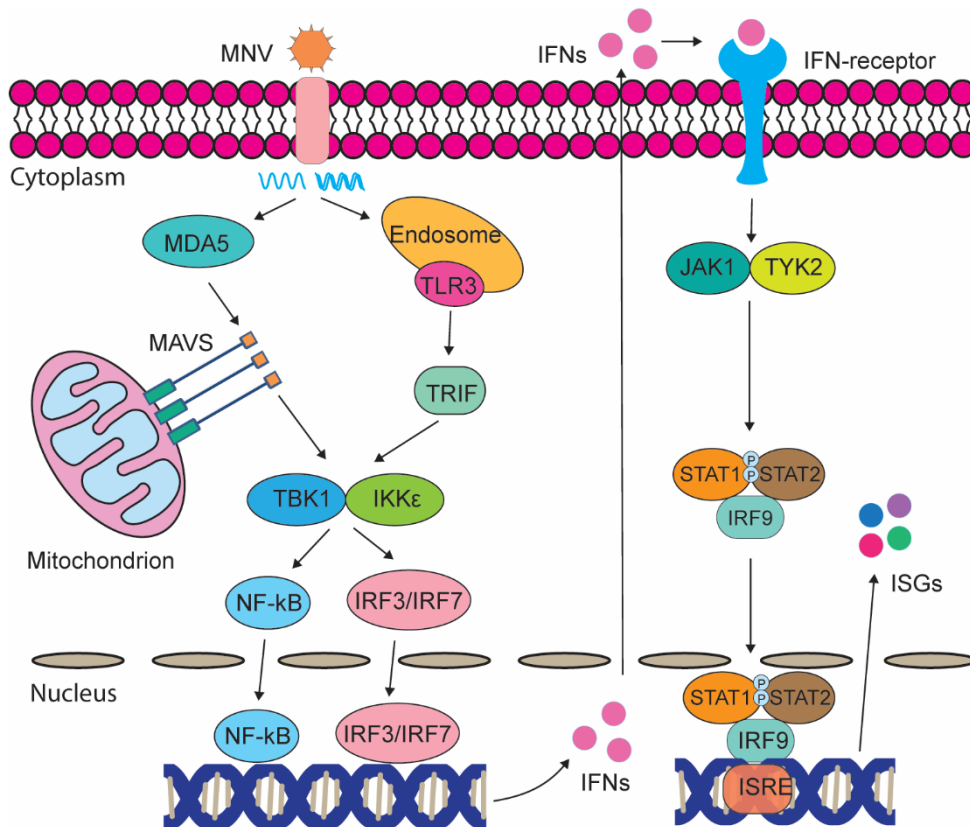


Figure 2. Recognition of MNV infection and MNV-induced IFN response. Upon infection, MNV is recognized by MDA5. The signals transduce through interaction with MAVS, and activates the downstream transcriptional factors, including NF- κ B and IRF3, leading to production of IFNs. TLR3 may also participate in MNV recognition. Then, the released IFNs bind to their receptors and further activate JAK/STAT signaling pathway, inducing transcription of hundreds of ISGs.

Activation of this signaling module, however, also provokes production and secretion of IFNs and leading to further cell-autonomous immunity while also preparing neighboring cells for viral attack through a paracrine mechanism. IFNs bind to plasma membrane transversing receptors and the binding of the receptors to their cognate ligands provokes intracellular activation of the Janus kinase/signal transducer and activator of transcription (JAK/STAT) signaling pathway, culminating in the induction of transcription of hundreds of IFN-stimulated genes (ISGs), and some of them are considered as ultimate antiviral effectors (42). For instance,

the STAT1-dependent innate immune response has been reported to be sufficient to prevent lethal MNV infection (43). IFN-stimulated gene 15 (ISG15) inhibits an early stage in the viral life cycle located upstream of viral genome transcription, at the viral entry/uncoating step (44). IFN-inducible GTPases, including the guanylate-binding proteins (GBPs), have recently been reported to exert broad antiviral activity, and are important for IFN- γ mediated inhibition of MNV replication by blocking the viral replication complexes formation (45,46). Thus a cell autonomous network potentially capable of norovirus infection is present in mammalian target cells for norovirus infection.

Indeed, TLRs can participate in such responses as well, recognizing the non-replicative incoming viral nucleic acids and subsequently triggering the production of IFNs and other cytokines, through different signal transduction cascades (35,36). Studies have demonstrated that virus like particles (VLPs) from GII.4 HuNV can induce activation of TLR2 and TLR5 (47). The use of TLR agonists as therapeutics is a rapidly growing area of research, and some TLR agonists (such as R-848, GS-9620 and R-837 for TLR7) have been reported to present anti-norovirus activity (48). Consistently, TLR3 deficient mice have a slight increase in viral titers upon MNV infection, indicating a minor tissue-specific role of TLR3 *in vivo* (37). Hence, stimulation of TLR-mediated anti-viral immunity should be considered a potential avenue for combating norovirus infection deserving further investigation.

The understanding of cell-autonomous immunity has recently gained a new impetus through the recognition of the importance of the inflammasome in this process. The inflammasome is located in the cytosol and is viewed as a multimeric signaling complex essential for coordinating host cell immune responses in response to invading pathogens and associated damage to the host. Accordingly, it is seen as critical for the initiation of both innate and adaptive immunity following infection with RNA viruses (49,50). Upon detecting activating signals, PRRs such as NLRP3 bind and engage the apoptosis-associated speck-like protein containing a CARD (ASC) to recruit and activate pro-caspase-1. The activated caspase-1 further cleaves pro-interleukin (IL)-1 β and pro-IL-18 into the mature forms of IL-1 β and IL-18, leading to the release from cells and executing a form of inflammatory cell death known as pyroptosis (49). Studies have reported that MNV persists much longer in NLRP6-deficient mice when compared with wild-type mice (51). MNV infection activates NLRP3 inflammasome and induces secretion of mature IL-1 β in primary bone marrow-derived macrophages (BMDMs) that primed with TLR2 agonist, and in STAT1-deficient BMDMs without TLR2 priming, while blocking the NLRP3 inflammasome activation presents a beneficial effect with regard to MNV-induced immunopathology in STAT1-deficient mice (52). The crosstalk between IFN immune response and inflammasome activation in response to norovirus infection remains to be studied.

Aim of this thesis

Norovirus is the most common etiology of diarrheal illness globally, causing both sporadic and epidemic infection. The quantity and quality of host immune responses in response to norovirus infection are essential for determining viral infection course and the clinical outcomes. Thus, there is clear need for gaining better understanding of virus-host interactions and to develop novel antiviral treatment against norovirus, which are the main aims of this thesis.

Outline of this thesis

Currently, no vaccination or specific antiviral treatment is available against norovirus, and consequently the virus inflicts globally untold misery and represents a clear global health burden. On a quest to identify novel avenues for controlling norovirus infection, in **Chapter 2**, I show that a nucleoside analogue, 2'-Fluoro-2'-deoxycytidine potently inhibits MNV replication in macrophages, and exerts moderate inhibition on HuNV replication in HG23 cells. Subsequently, I decided to identify the mechanisms the body uses for combating norovirus infection. Pursuing this research direction in **Chapter 3**, I show that MNV infection induces IL-1 β transcription but not release of mature IL-1 β . Pharmacological inflammasome inhibitors slightly reverse the inflammasome activator lipopolysaccharide (LPS)-mediated inhibition of viral replication. This antiviral effect mediated by LPS partially requires ISG induction mainly through NF- κ B and JAK-STAT signaling pathway in mouse macrophages.

Some ISGs are considered as ultimate antiviral effectors, and this class of ISGs includes guanylate-binding proteins (GBPs). Their role in constraining norovirus infection remained however enigmatic. Encouraged by the results obtained in my studies described in Chapter 3, in **Chapter 4**, I characterize the anti-MNV effects of GBP2. I observe the ISG is important for IFN- γ -dependent anti-MNV activity in murine macrophages, and potently inhibits MNV replication in HEK293T epithelial cells that are ectopically expressing MNV receptor (CD300lf) and thus susceptible to infection. Moreover, the viral replicase (NS7) antagonizes GBP2-mediated antiviral effects, suggesting relevant evolutionary pressure of this ISG on norovirus biology. As an ISG, MDA5 is an important cytoplasmic receptor sensing viral infection to trigger interferon production, but its functionality in combating norovirus infection remains obscure, prompting investigation in this respect. In **Chapter 5**, I show that human MDA5 restricts replication of several enteric viruses including HuNV. MDA5 overexpression induces some antiviral ISG induction through IFN-like response, without triggering functional IFN production, whereas blocking the JAK-STAT cascade only partially attenuates ISG induction and antiviral function of MDA5. Encouraged by these findings and prompted by the description of regulation of viral replicases of RLRs-mediated IFN responses in **Chapter 6**, I investigate the

regulation of MNV NS7 on human RIG-I and MDA5 mediated antiviral immune response. I show that viral NS7 enhances RIG-I and MDA5-triggered antiviral IFN response, which conceivably involves interactions with the caspase activation and recruitment domains (CARDs) of RIG-I and MDA5. Accordingly, RIG-I and MDA5 exert anti-MNV activity in human HEK293T cells expressing CD300lf, and this effect is further enhanced by NS7 overexpression, yielding further detailed insight into how the epithelium combats norovirus infection.

A last issue that I needed to address was clarifying the potential involvement of cGAS-STING regulation in response to RNA virus infection. Thus in **Chapter 7**, I investigate the role of cGAS-STING in the responses to MNV infection. I show knocking out mouse cGAS or STING leads to defects in induction of antiviral ISGs upon MNV infection and enhances viral replication in mouse macrophages, whereas cGAS and STING overexpression moderately increases ISG transcription but potently inhibits MNV replication in human HEK293T cells that ectopically expressing CD300lf. I further characterize that STING but not cGAS interacts with mouse RIG-I, and attenuates its N-terminus of RIG-I mediated antiviral effects.

Thus overall, I feel my studies significantly enhance our insight into the intricacies of host responses to norovirus infection, and I hope my studies will allow better development of antiviral strategies against norovirus infection.

References

1. Kollaritsch, H., Kundi, M., Giaquinto, C., et al. (2015) Rotavirus vaccines: a story of success. *Clin Microbiol Infect* 21, 735-743
2. Bartsch, S. M., Lopman, B. A., Ozawa, S., et al. (2016) Global economic burden of norovirus gastroenteritis. *PLoS One* 11, e0151219
3. Patel, M. M., Widdowson, M.A., Glass, R. I., et al. (2008) Systematic literature review of role of noroviruses in sporadic gastroenteritis. *Emerg Infect Dis* 14, 1224
4. Glass, R. I., Parashar, U. D., and Estes, M. K. (2009) Norovirus gastroenteritis. *New Engl J Med* 361, 1776-1785
5. Haessler, S., and Granowitz, E. V. (2013) Norovirus gastroenteritis in immunocompromised patients. *New Engl J Med* 368, 971-971
6. Chan, J., Mohammad, K. N., Zhang, L.Y., et al. (2021) Targeted Profiling of Immunological Genes during Norovirus Replication in Human Intestinal Enteroids. *Viruses* 13, 155
7. Chhabra, P., de Graaf, M., Parra, G. I., et al. (2019) Updated classification of norovirus genogroups and genotypes. *J Gen Virol* 100, 1393
8. Karst, S. M., Wobus, C. E., Goodfellow, I. G., et al. (2014) Advances in norovirus biology. *Cell Host Microbe* 15, 668-680
9. McFadden, N., Bailey, D., Carrara, G., et al. (2011) Norovirus regulation of the innate immune response and apoptosis occurs via the product of the alternative open reading frame 4. *PLoS Pathog* 7, e1002413
10. Thorne, L. G., and Goodfellow, I. G. (2014) Norovirus gene expression and replication. *J Gen Virol* 95, 278-291
11. Hutson, A. M., Atmar, R. L., Marcus, D. M., et al. (2003) Norwalk virus-like particle hemagglutination by binding to H histo-blood group antigens. *J Virol* 77, 405-415
12. Tan, M., Huang, P., Meller, J., et al. (2003) Mutations within the P2 domain of norovirus capsid affect binding to human histo-blood group antigens: evidence for a binding pocket. *J Virol* 77, 12562-12571
13. Vongpunsawad, S., Prasad, B. V., and Estes, M. K. (2013) Norwalk virus minor capsid protein VP2 associates within the VP1 shell domain. *J Virol* 87, 4818-4825
14. Hyde, J. L., Sosnovtsev, S. V., Green, K. Y., et al. (2009) Mouse norovirus replication is associated with virus-induced vesicle clusters originating from membranes derived from the secretory pathway. *J Virol* 83, 9709-9719
15. Hyde, J. L., Gillespie, L. K., and Mackenzie, J. M. (2012) Mouse norovirus 1 utilizes the cytoskeleton network to establish localization of the replication complex proximal to the microtubule organizing center. *J Virol* 86, 4110-4122
16. Jones, M. K., Watanabe, M., Zhu, S., et al. (2014) Enteric bacteria promote human and mouse norovirus infection of B cells. *Science* 346, 755-759
17. Ettayebi, K., Crawford, S. E., Murakami, K., et al. (2016) Replication of human noroviruses in stem cell-derived human enteroids. *Science* 353, 1387-1393
18. Lin, L., Han, J., Yan, T., et al. (2019) Replication and transcriptionomic analysis of human noroviruses in human intestinal enteroids. *Amer J Transl Res* 11, 3365
19. Lin, S.-C., Qu, L., Ettayebi, K., et al. (2020) Human norovirus exhibits strain-specific sensitivity to host interferon pathways in human intestinal enteroids. *Proc Nat Acad Sci USA* 117, 23782-23793
20. Hosmillo, M., Chaudhry, Y., Nayak, K., et al. (2020) Norovirus replication in human intestinal epithelial cells is restricted by the interferon-induced JAK/STAT signaling pathway and RNA polymerase II-mediated transcriptional responses. *mBio* 11
21. Bok, K., Parra, G. I., Mitra, T., et al. (2011) Chimpanzees as an animal model for human norovirus infection and vaccine development. *Proc Nat Acad Sci USA* 108, 325-330
22. Cheetham, S., Souza, M., Meulia, T., et al. (2006) Pathogenesis of a genogroup II human norovirus in gnotobiotic pigs. *J Virol* 80, 10372-10381

23. Souza, M., Azevedo, M. d. S. P. d., Jung, K., et al. (2008) Pathogenesis and immune responses in gnotobiotic calves after infection with the genogroup II. 4-HS66 strain of human norovirus. *J Virol* 82, 1777-1786
24. Taube, S., Kolawole, A. O., Höhne, M., et al. (2013) A mouse model for human norovirus. *MBio* 4
25. Van Dycke, J., Ny, A., Conceição-Neto, N., et al. (2019) A robust human norovirus replication model in zebrafish larvae. *PLoS Pathog* 15, e1008009
26. Chang, K.-O., Sosnovtsev, S. V., Belliot, G., et al. (2006) Stable expression of a Norwalk virus RNA replicon in a human hepatoma cell line. *Virology* 353, 463-473
27. Chang, K.-O., and George, D. W. (2007) Interferons and ribavirin effectively inhibit Norwalk virus replication in replicon-bearing cells. *J Virol* 81, 12111-12118
28. Dang, W., Yin, Y., Wang, Y., et al. (2017) Inhibition of calcineurin or IMP dehydrogenase exerts moderate to potent antiviral activity against norovirus replication. *Antimicrob Agents Chemother* 61
29. Mattison, C. P., Cardemil, C. V., and Hall, A. J. (2018) Progress on norovirus vaccine research: public health considerations and future directions. *Expert Rev Vaccines* 17, 773-784
30. Dang, W., Xu, L., Ma, B., et al. (2018) Nitazoxanide Inhibits Human Norovirus Replication and Synergizes with Ribavirin by Activation of Cellular Antiviral Response. *Antimicrob Agents Chemother* 62
31. Woodward, J. M., Gkrania-Klotsas, E., Cordero-Ng, A. Y., et al. (2015) The role of chronic norovirus infection in the enteropathy associated with common variable immunodeficiency. *Amer J Gastroenterol* 110, 320-327
32. Pharmacopoeia, J. (2011) Pharmaceutical and Food Safety Bureau. *Ministry of Health, Labour and Welfare, Tokyo*, 1723-1724
33. Sissoko, D., Laouenan, C., Folkesson, E., et al. (2016) Experimental Treatment with Favipiravir for Ebola Virus Disease (the JIKI Trial): A Historically Controlled, Single-Arm Proof-of-Concept Trial in Guinea. *PLoS Med* 13, e1001967
34. Ruis, C., Brown, L. K., Roy, S., et al. (2018) Mutagenesis in Norovirus in Response to Favipiravir Treatment. *New Engl J Med* 379, 2173-2176
35. Chow, K. T., Gale Jr, M., and Loo, Y.M. (2018) RIG-I and other RNA sensors in antiviral immunity. *Ann Rev Immunol* 36, 667-694
36. Streicher, F., and Jouvenet, N. (2019) Stimulation of innate immunity by host and viral RNAs. *Trends Immunol* 40, 1134-1148
37. McCartney, S. A., Thackray, L. B., Gitlin, L., et al. (2008) MDA-5 recognition of a murine norovirus. *PLoS Pathog* 4, e1000108
38. Guix, S., Asanaka, M., Katayama, K., et al. (2007) Norwalk virus RNA is infectious in mammalian cells. *J Virol* 81, 12238-12248
39. Dang, W., Xu, L., Yin, Y., et al. (2018) IRF-1, RIG-I and MDA5 display potent antiviral activities against norovirus coordinately induced by different types of interferons. *Antiviral Res* 155, 48-59
40. Yu, P., Li, Y., Li, Y., et al. (2020) Murine norovirus replicase augments RIG-I-like receptors-mediated antiviral interferon response. *Antiviral Res* 182, 104877
41. Emmott, E., Sorgeloos, F., Caddy, S. L., et al. (2017) Norovirus-mediated modification of the translational landscape via virus and host-induced cleavage of translation initiation factors. *Mol Cell Proteom* 16, S215-S229
42. Schoggins, J. W., Wilson, S. J., Panis, M., et al. (2011) A diverse range of gene products are effectors of the type I interferon antiviral response. *Nature* 472, 481-485
43. Karst, S. M., Wobus, C. E., Lay, M., et al. (2003) STAT1-dependent innate immunity to a Norwalk-like virus. *Science* 299, 1575-1578
44. Rodriguez, M. R., Monte, K., Thackray, L. B., et al. (2014) ISG15 functions as an interferon-mediated antiviral effector early in the murine norovirus life cycle. *J Virol* 88, 9277-9286
45. Biering, S. B., Choi, J., Halstrom, R. A., et al. (2017) Viral replication complexes are targeted by LC3-guided interferon-inducible GTPases. *Cell Host Microbe* 22, 74-85. e77

46. Yu, P., Li, Y., Li, Y., et al. (2020) Guanylate-binding protein 2 orchestrates innate immune responses against murine norovirus and is antagonized by the viral protein NS7. *J Biol Chem* 295, 8036-8047
47. Ponterio, E., Mariotti, S., Tabolacci, C., et al. (2019) Virus like particles of GII. 4 norovirus bind Toll Like Receptors 2 and 5. *Immunol Lett* 215, 40-44
48. Tuipulotu, D. E., Netzler, N. E., Lun, J. H., et al. (2018) TLR7 agonists display potent antiviral effects against norovirus infection via innate stimulation. *Antimicrob Agents Chemother* 62
49. Mathur, A., Hayward, J. A., and Man, S. M. (2018) Molecular mechanisms of inflammasome signaling. *J Leukocyte Biol* 103, 233-257
50. Lupfer, C., Malik, A., and Kanneganti, T.D. (2015) Inflammasome control of viral infection. *Curr Opin Virol* 12, 38-46
51. Wang, P., Zhu, S., Yang, L., et al. (2015) Nlrp6 regulates intestinal antiviral innate immunity. *Science* 350, 826-830
52. Dubois, H., Sorgeloos, F., Sarvestani, S. T., et al. (2019) Nlrp3 inflammasome activation and Gasdermin D-driven pyroptosis are immunopathogenic upon gastrointestinal norovirus infection. *PLoS Pathog* 15, e1007709

Chapter 2

2'-Fluoro-2'-deoxycytidine inhibits murine norovirus replication and synergizes MPA, ribavirin and T705

Peifa Yu, Yining Wang, Yunlong Li, Yang Li, Zhijiang Miao, Maikel P. Peppelenbosch, Qiuwei Pan

Archives of Virology, 2020, 165(11): 2605-2613.

Abstract

Noroviruses are the main causative agents for acute viral gastroenteritis worldwide. However, no vaccination or specific antiviral treatment is available, imposing a heavy global health burden. The nucleoside analogue 2'-Fluoro-2'-deoxycytidine (2'-FdC) has been reported to exert broad antiviral activities. Here, we report that 2'-FdC significantly inhibits murine norovirus replication in macrophages. This effect was partially reversed by exogenous supplementation of cytidine triphosphate. The combination of 2'-FdC with mycophenolic acid, ribavirin or favipiravir (T705), exerts synergistic antiviral effects. Our results indicate that 2'-FdC serves as a potential candidate for antiviral drug development against norovirus infection.

Keywords: 2'-Fluoro-2'-deoxycytidine, norovirus, replication, ISG, antiviral drug

Introduction

Human norovirus (HuNV) is a non-enveloped, positive single-stranded RNA virus [1]. Recently, noroviruses have been classified into at least 10 genogroups (GI-GX) on the basis of the VP1 amino acid sequence diversity [2]. Of these, viruses in the GI, GII, GIV, GVIII and GIX genogroups can infect humans and are a major cause of acute epidemic viral gastroenteritis worldwide [2]. It is estimated that noroviruses are responsible for 699 million gastroenteritis cases per year [3], and 200,000 deaths in children under 5 years of age in developing countries [4]. Although norovirus gastroenteritis is usually self-limiting, it has been recognized as an emerging burden in immunocompromised populations, particularly transplant recipients [5, 6]. However, research into HuNV infection has been hampered by the lack of availability of robust experimental models sustaining viral infection. Murine norovirus (MNV), capable of replicating in both cell culture and small-animal models, shares similar traits with HuNV in structural and genetic features, and has thus been widely used as a surrogate model [7, 8]. To date, no vaccination or specific antiviral treatment is available and clinical management is restricted to supportive care and oral rehydration. Thus, the development of specific antiviral drugs for norovirus infection is urgently needed.

Currently, potential inhibitors of noroviruses have been identified and some of these have been demonstrated efficacy in experimental models. Ribavirin has been widely studied and exhibits broad antiviral activity against multiple viruses including hepatitis C virus (HCV) [9], hemorrhagic fever virus [10], hepatitis E virus [11, 12], and norovirus [13]. Clinical studies have reported that ribavirin treatment resulted in complete viral clearance in a subset of norovirus infected patients, but treatment failure have occurred in two cases [14]. We previously have demonstrated that mycophenolic acid (MPA), a potent inhibitor of IMP dehydrogenase (IMPDH), can inhibit norovirus replication in cell culture [15]. Favipiravir, also known as T-705, has been approved for the treatment of influenza in Japan, and was repositioned to treat patients with Ebola virus infection [16, 17]. It has been shown to be effective against norovirus but the treatment can induce mutagenesis in mice and in patients, challenged the application of favipiravir for treating chronic norovirus infection [18].

Recently, 2'-fluoro-2'-deoxycytidine (2'-FdC), also known as 2'-deoxy-2'-fluorocytidine, has been reported to exert broad antiviral activity against HCV, Lassa virus, Crimean-Congo hemorrhagic fever virus and bunyaviruses [19-22]. Given the success of 2'-FdC against the abovementioned viruses, we aimed to investigate the potential antiviral activity of this compound against MNV replication

Materials and Methods

Reagents

2'-fluoro-2'-deoxycytidine was purchased from Biosynth Carbosynth and dissolved in Dimethyl sulfoxide (DMSO, Sigma, Zwijndrecht, the Netherlands). MPA (Sigma), ribavirin (BioConnect BV), T705 (BioVision), cytidine triphosphate (CTP; Sigma), guanosine triphosphate (GTP; Sigma), human IFN- α (Thermo Scientific, the Netherlands) and JAK inhibitor 1 (Santa Cruz Biotechnology, USA) were used. Rabbit polyclonal antisera to MNV NS1/2 [23] was kindly provided by Prof. Vernon K. Ward (School of Biomedical Sciences, University of Otago, New Zealand). β -actin antibody (#sc-47778) was purchased from Santa Cruz Biotechnology. IRDye® 800CW-conjugated goat anti-rabbit and goat anti-mouse IgGs (Li-Cor Bioscience, Lincoln, USA) were used as secondary antibodies, as appropriate.

Cells and viruses

RAW264.7 and J774A.1 were cultured in Dulbecco's modified Eagle's medium (DMEM; Lonza Verviers, Belgium) supplemented with 10% (vol/vol) heat-inactivated fetal calf serum (FCS; Hyclone, Logan, UT, USA), 100 μ g/mL of streptomycin, and 100 IU/mL of penicillin. Murine norovirus strains MNV-1 (MNV-1.CW1), the acutely cleared strain MNV^{CW3} and the persistent strain MNV^{CR6}, were produced by consecutively inoculating the virus (kindly provided by Prof. Herbert Virgin, Department of Pathology and Immunology, Washington University School of Medicine) into RAW264.7 cells [24]. Human Huh7 hepatocellular carcinoma cells harboring a genotype 1 HuNV replicon (HG23) were kindly provided by Dr. Kyeong-Ok Chang (Kansas State University) [25]. A neomycin resistant gene was engineered into ORF2, conferring HG23 resistance to neomycin. Gentamicin (G418; Gibco) was added to HG23 culture medium at 0.5 mg/mL for selection before experimentation.

TCID50

MNV was quantified by TCID50 assay. Briefly, 10-fold dilutions of MNV were inoculated into RAW264.7 cells grown in 96-well tissue culture plate at 1,000 cells/well. The plate was incubated at 37°C for another 5 days, followed by observing the cytopathic effect (CPE) of each well under a light scope. The TCID50 was calculated by using the Reed-Muench method.

Antiviral assay with MNV

The antiviral assay with MNV was initiated by inoculating the virus into RAW264.7 or J774A.1 cells at a multiplicity of infection (MOI) of 1. After 1 h of infection, cells were washed with phosphate-buffered saline (PBS) for two times to remove free viruses and were subsequently

treated with indicated compounds. For combination assay, RAW264.7 cells were infected with the virus for 1 h, then refreshed with the medium containing 2'-FdC, MPA, ribavirin or T705 alone or in combination, with indicated concentrations. After 20 h of treatment, total RNA, protein and the supernatant samples were collected and further analyzed by qRT-PCR, western-blotting and TCID₅₀ assay, respectively.

qRT-PCR

Total RNA was isolated with a Macherey NucleoSpin RNA II Kit (Bioke, Leiden, The Netherlands) and quantified with a Nanodrop ND-1000 (Wilmington, DE, USA). cDNA was synthesized from 500 ng of RNA using a cDNA synthesis kit (TaKaRa Bio, Inc., Shiga, Japan). The cDNA of all targeted genes were quantified by SYBR-Green-based (Applied Biosystems) real-time PCR on the StepOnePlus™ System (Thermo Fisher Scientific LifeSciences) according to the manufacturer's instructions. Human glyceraldehyde-3-phosphate dehydrogenase (GAPDH) and murine GAPDH genes were used as reference genes to normalize gene expression. The relative expression of targeted gene was calculated as $2^{-\Delta\Delta CT}$, where $\Delta\Delta CT = \Delta CT_{\text{sample}} - \Delta CT_{\text{control}}$ ($\Delta CT = CT[\text{targeted gene}] - CT[\text{GAPDH}]$). All primer sequences are listed in supplementary table 1.

Western blotting

Cultured cells were lysed in Laemmli sample buffer containing 0.1 M DTT and heated 5 mins at 95 °C, then loaded onto a 10% sodium dodecyl sulfate polyacrylamide gel electrophoresis (SDS-PAGE) gel. Then proteins were electrophoretically transferred onto a polyvinylidene difluoride (PVDF) membrane (pore size, 0.45 μm; Invitrogen) for 2 h with an electric current of 250 mA. Subsequently, the membrane was blocked with a mixture of 2.5 mL blocking buffer (Odyssey) and 2.5 mL PBS containing 0.05% Tween 20 for 1 h, followed by overnight incubation with primary antibodies (1:1000) at 4 °C. The membrane was washed three times and then incubated with IRDye-conjugated secondary antibody (1:5000) for 1 h. After washing three times, protein bands were detected with the Odyssey 3.0 Infrared Imaging System (Li-Cor Biosciences).

Confocal fluorescence microscopy

RAW264.7 or J774A.1 cells infected with MNV-1 (MOI 1) for 1 h, then refreshed with culture medium containing different concentrations of 2'-FdC in μ-slide 8-well chamber (Cat. no. 80826; ibidi GmbH) for 20 h. The cells were fixed with 4% paraformaldehyde in PBS, permeabilized with 0.2% Triton X-100, blocked with 5% skim milk for 1 h, reacted with the rabbit polyclonal antisera to MNV NS1/2, and stained with 4',6-diamidino-2-phenylindole (DAPI). Secondary antibody anti-rabbit IgG (H+L), F(ab')₂ Fragment (Alexa Fluor® 488

conjugate) was used. Imaging was performed on a Leica SP5 confocal microscopy using a 63x oil objective.

IC50 and CC50 calculation

The 50% inhibitory concentration (IC50) value and 50% cytotoxic concentration (CC50) were calculated based on the model $Y = \text{Bottom} + \frac{\text{Top} - \text{Bottom}}{1 + 10^{((\text{LogIC50} - X) * \text{HillSlope})}}$ using GraphPad Prism 5 software (GraphPad Prism 5; GraphPad Software Inc., La Jolla, CA, USA).

MTT assay

Cells were seeded into 96-well tissue culture plates and cell viability was assessed by adding 10 mM 3-(4,5-dimethyl-2-thiazolyl)-2,5-diphenyl-2H-tetrazolium bromide (MTT) (Sigma, Zwijndrecht, the Netherlands). After 3 h, the medium was replaced with 100 μ L of DMSO and was incubated at 37°C for 50 mins. The absorbance at 490 nm was recorded on the microplate absorbance reader (Bio-Rad, CA, USA).

Statistical analysis

Data are presented as the mean \pm SEM. Comparisons between groups were performed with Mann-Whitney test using GraphPad Prism 5.0 (GraphPad Software Inc., La Jolla, CA, USA). Differences were considered significant at a P value less than 0.05.

Results and discussion

To test the potential anti-norovirus activity of 2'-FdC, we used the surrogate model murine norovirus. We found that 2'-FdC significantly decreased the viral RNA and NS1/2 protein expression of MNV-1 in RAW264.7 cells, a murine macrophage cell line that is susceptible for MNV propagation (Fig. 1A and 1B). The inhibitory effects was further confirmed as shown the decreased viral NS1/2 expression by confocal fluorescence microscopy (Fig. 1C). Moreover, the viral titer was decreased by 2'-FdC (100 μ M) treatment (Fig. 1D). To further examine the antiviral effects, another murine macrophage cell line J774A.1 cells was used, and similar inhibitory effect of 2'-FdC against MNV-1 replication was found as shown the attenuated viral RNA and NS1/2 protein expression (supplementary Fig. 1).

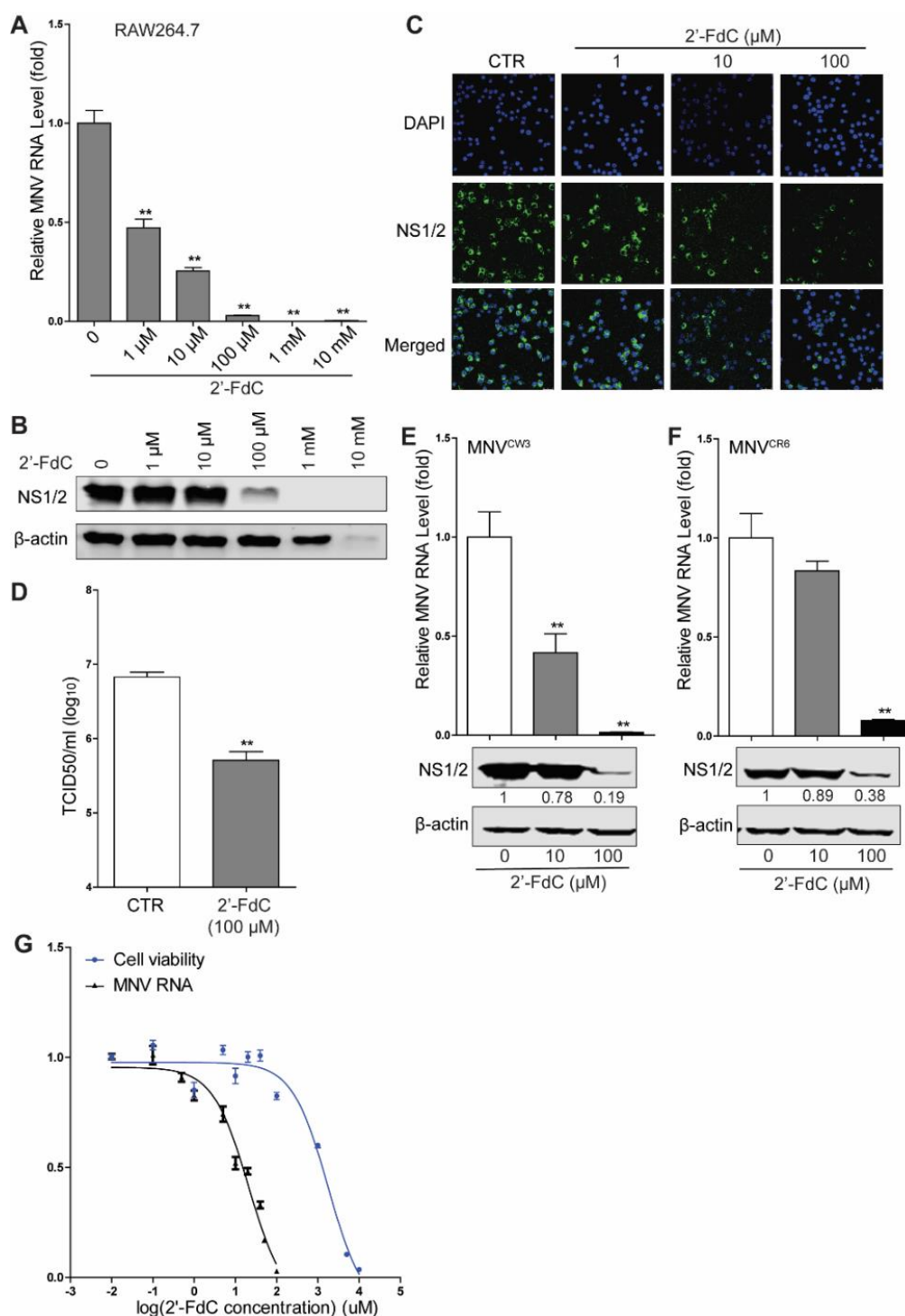


Figure 1. 2'-Fdc exerts anti-MNV activity in RAW264.7 cells. RAW264.7 cells were infected with MNV-1 (MOI 1) for 1 h, then refreshed with culture medium containing different concentrations of 2'-Fdc for 20 h. (A) The viral RNA level and (B) NS1/2 protein expression were analyzed by qRT-PCR (n = 6) and western blotting, respectively. (C) RAW264.7 cells were infected with MNV-1 (MOI 1) for 1 h, then refreshed with culture medium containing different concentrations of 2'-Fdc for 20 h. The viral NS1/2 protein expression was analyzed by confocal assay. (D) RAW264.7 cells were infected with MNV-1 (MOI 1) for 1 h, then untreated or treated with 2'-Fdc (100 μ M) for 20 h. The viral titers were determined by TCID50 assay (n = 6). RAW264.7 cells were infected with (E) MNV^{CW3} or (F) MNV^{CR6} at a MOI of 1

for 1 h, then untreated or treated with 2'-FdC (10 μ M and 100 μ M, respectively) for 20 h. The viral RNA level and NS1/2 protein expression were analyzed by qRT-PCR (n = 6) and western blotting, respectively. (G) RAW264.7 cells were uninfected or infected with MNV-1 (MOI 1) for 1 h, then untreated or treated with different concentrations of 2'-FdC for 20 h. The 50% cytotoxic concentration (CC50) (n = 16) and 50% inhibition concentration (IC50) (n = 4-6) against viral replication were calculated using GraphPad Prism 5 software. Data were normalized to the untreated control (set as 1). **P < 0.01. β -actin was used as a loading control. For immunoblot results (E and F), band intensity of NS1/2 protein in each lane was quantified by Odyssey software, and the quantification results were normalized to β -actin expression (control, set as 1).

With 2'-FdC emerging as a potential anti-MNV candidate, we further evaluated this antiviral effect on another two MNV strains with distinct biological behaviors, the acutely cleared strain MNV^{CW3} and the persistent strain MNV^{CR6}. Notably, 2'-FdC inhibited viral RNA replication and protein expression of both viral strains (Fig. 1E and 1F), respectively. In addition, the IC50 value of 2'-FdC against MNV-1 replication in RAW264.7 cells was 20.92 μ M (Fig. 1G), and CC50 of 2'-FdC to RAW264.7 cells was 1.768 mM (Fig. 1G). Moreover, we tested the antiviral effects of 2'-FdC on HuNV by using the HG23 cells harboring HuNV replicon, and found moderate inhibition on viral replication (Supplementary Fig. 2).

Nucleoside analogues have been reported to harnessing antiviral interferon response [13, 26]. Since interferon-stimulated genes (ISGs) are considered as the ultimate effectors against viral infection. However, we found that 2'-FdC did not significantly trigger ISG expression (supplementary Fig. 3A). By using a JAK inhibitor, we found that the inhibition of viral RNA level by 2'-FdC was not affected (supplementary Fig. 3B), suggesting that the antiviral effect of 2'-FdC does not require ISG induction. Theoretically, nucleoside analogues exert potential antiviral activity because they bind to the viral RNA polymerase active site to impede viral replication. Since 2'-FdC is an analogue of cytidine and fluorine is isosteric with a hydroxyl group, chemical conversion of 2'-FdC to the corresponding 2'-FdC-triphosphate (FdCTP) presented antiviral ability against HCV possibly targeting the viral NS5B enzyme [20]. Thus, we performed a competition assay by using CTP and GTP. Consistently, the results showed that CTP partially reversed the inhibitory effects of 2'-FdC on MNV replication from the viral RNA and protein levels (Fig. 2A and 2B), as well as the viral titers (Fig. 2D). In contrast, no significant effect of GTP on 2'-FdC mediated inhibition of viral replication was observed (Fig. 2C and 2D). Interestingly, we found that both CTP and GTP decreased the viral RNA level and NS1/2 protein expression (Fig. 2A-2D). It has been shown that MNV infection can induce viperin transcription in RAW264.7 cells [27], and viperin can convert CTP into 3'-deoxy-3',4'-dideoxy-CTP (ddhCTP), which can act as a chain terminator for the RNA-dependent RNA-polymerases and inhibit replication of ZIKA virus [28]. Moreover, exogenous CTP/GTP might compete with the endogenous usage of CTP/GTP for MNV replication [29]. These mechanism-of-actions might

partially explain the effects on MNV. These results suggested a potential mechanism of action of 2'-FdC against MNV, and it needs to be further investigated whether 2'-FdC exerts anti-MNV activity by targeting the viral replicase.

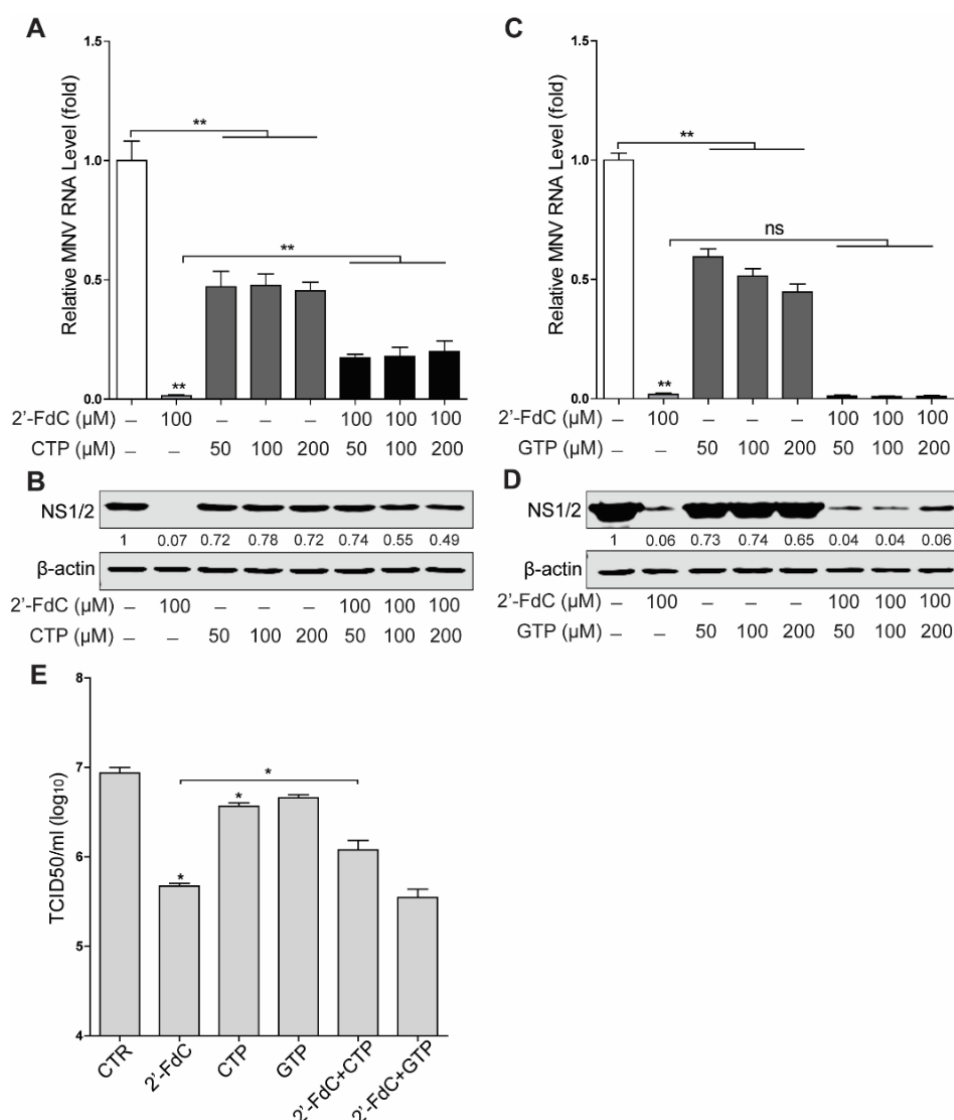


Figure 2. CTP but not GTP reverses 2'-FdC mediated inhibition of MNV replication. RAW264.7 cells were infected with MNV-1 (MOI 1) for 1 h, then untreated or treated with 2'-FdC, CTP or combinations with indicated concentrations for 20 h. (A) The viral RNA and (B) NS1/2 protein expression were analyzed by qRT-PCR (n = 6) and western blotting, respectively. RAW264.7 cells were infected with MNV-1 (MOI 1) for 1 h, then untreated or treated with 2'-FdC, GTP or combinations with indicated concentrations for 20 h. (C) The viral RNA and (D) NS1/2 protein expression were analyzed by qRT-PCR (n = 6) and western blotting, respectively. (E) RAW264.7 cells were infected with MNV-1 (MOI 1) for 1 h, then untreated or treated with 2'-FdC (100 μM), CTP (100 μM), GTP (100 μM) or combinations for 20 h. The viral titers were determined by TCID50 assay (n = 4). Data were normalized to the untreated control (set as 1). *P < 0.05; **P < 0.01. ns; not significant. β-actin was used as a loading control. For immunoblot results (B and D), band intensity of NS1/2 protein in each lane was quantified by Odyssey software, and the quantification results were normalized to β-actin expression (control, set as 1).

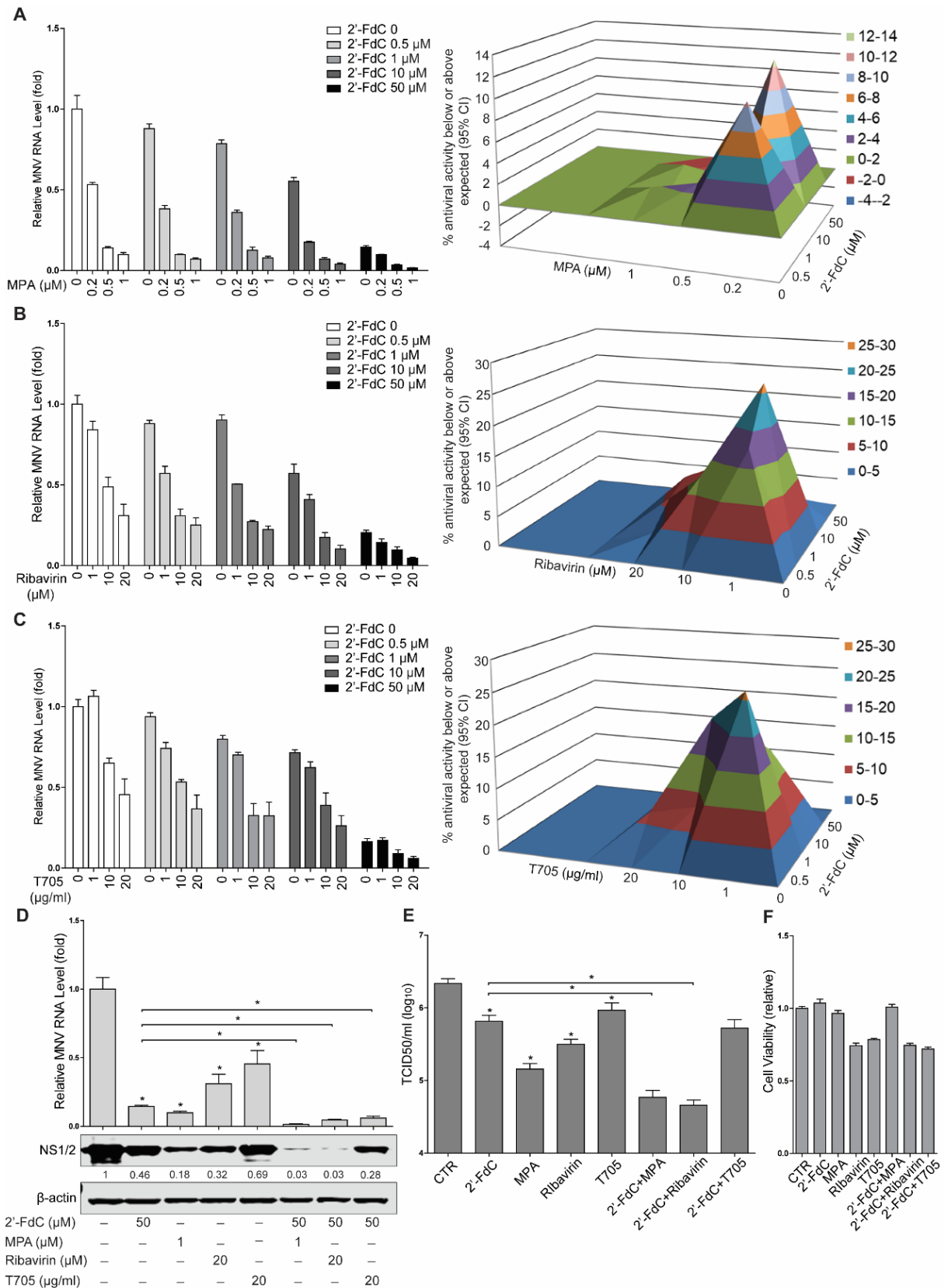


Figure 3. Synergistic anti-MNV effects of 2'-FdC with MPA, ribavirin or T-705. (A) RAW264.7 cells were infected MNV-1 (MOI 1) for 1 h, then untreated or treated with 2'-FdC and MPA with indicated concentrations for 20 h, alone or in combination. The combinatory effect of 2'-FdC and MPA on viral replication was analyzed by using qRT-PCR assay (n = 4) and the mathematical model MacSynergy. (B)

RAW264.7 cells were infected MNV-1 (MOI 1) for 1 h, then untreated or treated with 2'-FdC and ribavirin with indicated concentrations for 20 h, alone or in combination. The combinatory effect of 2'-FdC and ribavirin on viral replication was analyzed by using qRT-PCR assay (n = 2-4) and the mathematical model MacSynergy. (C) RAW264.7 cells were infected MNV-1 (MOI 1) for 1 h, then untreated or treated with 2'-FdC and T705 with indicated concentrations for 20 h, alone or in combination. The combinatory effect of 2'-FdC and T705 on viral replication was analyzed by using qRT-PCR assay (n = 4) and the mathematical model MacSynergy. The three-dimensional surface plot represents the differences (within 95% confidence interval) between actual experimental effects and theoretical additive effects of the combination at various concentrations of the two compounds. RAW264.7 cells were infected MNV-1 (MOI 1) for 1 h, then untreated or treated with 2'-FdC and MPA, ribavirin, or T705 with indicated concentrations for 20 h, alone or in combination. (D) The viral RNA level and NS1/2 protein expression, and (E) viral titers were analyzed by qRT-PCR (n = 4; data were derived from A, B and C), western blotting, and TCID50 (n = 4) assays, respectively. (F) RAW264.7 cells were untreated or treated with 2'-FdC (50 μ M), MPA (1 μ M), ribavirin (20 μ M), T705 (20 μ g/ml) or in combinations for 20 h. The cytotoxicity was determined by MTT assay (n = 16). *P < 0.05. β -actin was used as a loading control. For immunoblot results (D), band intensity of NS1/2 protein in each lane was quantified by Odyssey software, and the quantification results were normalized to β -actin expression (control, set as 1).

Since MPA, ribavirin and T705 have been reported to have anti-norovirus activity, a combined treatment of 2'-FdC with these compounds might be envisaged. To achieve better antiviral efficacy, we evaluated the combinatory antiviral effects of 2'-FdC with MPA by using the mathematical model MacSynergy [30]. Surprisingly, the results showed a moderate synergistic antiviral effect (36.57 μ M²%), which is greater than either 2'-FdC or MPA alone (Fig. 3A). Similar synergistic antiviral effects were observed when combining with ribavirin (99.18 μ M²%) or T705 (112.47 μ M²%) (Fig. 3B and 3C). To further confirm the synergistic antiviral effects, we evaluated viral protein expression and viral titers by using the high concentrations of the antivirals without major cytotoxicities (Fig. 3F). As shown in Fig. 3D and 3E, the viral NS1/2 protein expression and viral titers were further decreased by combination of the antivirals, supporting the synergistic antiviral effects of 2'-FdC with MPA, ribavirin or T705 against MNV replication.

Despite the wide clinical applications, potential side effects or unintended off-target effects should be considered for clinical usage of nucleoside analogues. Induction of mutagenesis by T705 treatment in patients has raised question for treating chronic norovirus infection [18]. Previous studies have reported that 2'-FdC exhibits delayed toxicity after prolonged exposure in 6- or 7-day assays, and no adverse clinical effects were observed in rats and woodchucks after 90 days of treatment [20]. Several derivatives of 2'-FdC have exerted promise as anti-HCV drugs with progress to clinical trials [31, 32]. However, due to the potential mitochondrial toxicity, long-term adverse effects of 2'-deoxynucleoside analogues treatment remain to be

concerned [33]. Thus, although 2'-FdC is an interesting antiviral compound, the potential adverse effects as well as combination with other compounds, should be carefully evaluated in future studies.

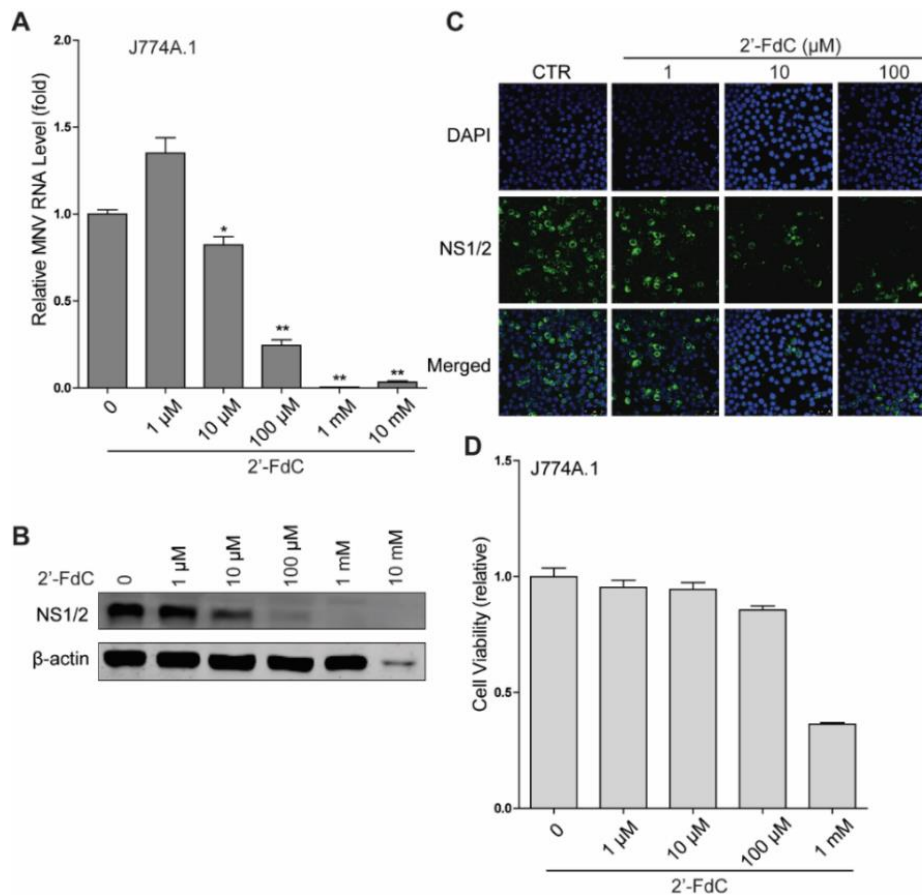
In conclusion, 2'-FdC exerts potent anti-MNV effects in macrophages. Importantly, 2'-FdC acts synergistically with the well-known antivirals including MPA, ribavirin and T705. Further studies are still required for evaluation of antiviral effects against HuNV infection in robust models by 2'-FdC or its derivatives. Nevertheless, our results have suggested that 2'-FdC can serve as a potential backbone for anti-norovirus drug design.

References

1. Karst, S. M., Wobus, C. E., Goodfellow, I. G., et al. (2014) Advances in norovirus biology. *Cell Host Microbe* 15, 668-680
2. Chhabra, P., de Graaf, M., Parra, G. I., et al. (2019) Updated classification of norovirus genogroups and genotypes. *J Gen Virol* 100, 1393-1406
3. Bartsch, S. M., Lopman, B. A., Ozawa, S., et al. (2016) Global Economic Burden of Norovirus Gastroenteritis. *PLoS One* 11, e0151219
4. Patel, M. M., Widdowson, M. A., Glass, R. I., et al. (2008) Systematic literature review of role of noroviruses in sporadic gastroenteritis. *Emerg Infect Dis* 14, 1224-1231
5. Ye, X., Van, J. N., Munoz, F. M., et al. (2015) Noroviruses as a Cause of Diarrhea in Immunocompromised Pediatric Hematopoietic Stem Cell and Solid Organ Transplant Recipients. *Am J Transplant* 15, 1874-1881
6. Bok, K., and Green, K. Y. (2012) Norovirus gastroenteritis in immunocompromised patients. *N Engl J Med* 367, 2126-2132
7. Wobus, C. E., Karst, S. M., Thackray, L. B., et al. (2004) Replication of Norovirus in cell culture reveals a tropism for dendritic cells and macrophages. *PLoS Biol* 2, e432
8. Wobus, C. E., Thackray, L. B., and Virgin, H. W. (2006) Murine norovirus: a model system to study norovirus biology and pathogenesis. *J Virol* 80, 5104-5112
9. Doss, W., Shiha, G., Hassany, M., et al. (2015) Sofosbuvir plus ribavirin for treating Egyptian patients with hepatitis C genotype 4. *J Hepatol* 63, 581-585
10. Andrei, G., and De Clercq, E. (1993) Molecular approaches for the treatment of hemorrhagic fever virus infections. *Antiviral Res* 22, 45-75
11. Dao Thi, V. L., Debing, Y., Wu, X., et al. (2016) Sofosbuvir Inhibits Hepatitis E Virus Replication In Vitro and Results in an Additive Effect When Combined With Ribavirin. *Gastroenterology* 150, 82-85 e84
12. Qu, C., Xu, L., Yin, Y., et al. (2017) Nucleoside analogue 2'-C-methylcytidine inhibits hepatitis E virus replication but antagonizes ribavirin. *Arch Virol* 162, 2989-2996
13. Dang, W., Xu, L., Ma, B., et al. (2018) Nitazoxanide Inhibits Human Norovirus Replication and Synergizes with Ribavirin by Activation of Cellular Antiviral Response. *Antimicrob Agents Chemother* 62
14. Woodward, J. M., Gkrania-Klotsas, E., Cordero-Ng, A. Y., et al. (2015) The role of chronic norovirus infection in the enteropathy associated with common variable immunodeficiency. *Am J Gastroenterol* 110, 320-327

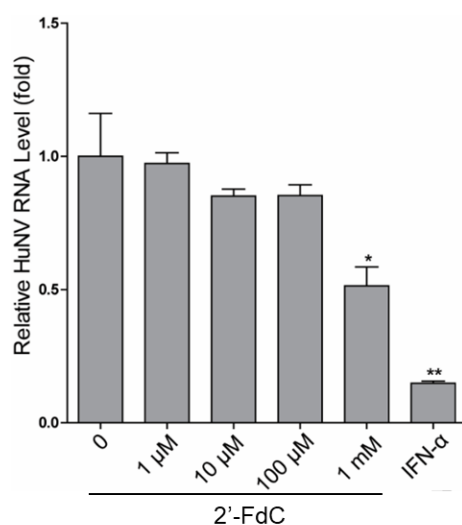
15. Dang, W., Yin, Y., Wang, Y., et al. (2017) Inhibition of Calcineurin or IMP Dehydrogenase Exerts Moderate to Potent Antiviral Activity against Norovirus Replication. *Antimicrob Agents Chemother* 61
16. Sissoko, D., Laouenan, C., Folkesson, E., et al. (2016) Experimental Treatment with Favipiravir for Ebola Virus Disease (the JIKI Trial): A Historically Controlled, Single-Arm Proof-of-Concept Trial in Guinea. *PLoS Med* 13, e1001967-e1001967
17. Pharmacopoeia, J. (2011) Pharmaceutical and Food Safety Bureau. *Ministry of Health, Labour and Welfare, Tokyo, 1723-1724*
18. Ruis, C., Brown, L.A. K., Roy, S., et al. (2018) Mutagenesis in norovirus in response to favipiravir treatment. *New Engl J Med* 379, 2173-2176
19. Stuyver, L. J., McBrayer, T. R., Whitaker, T., et al. (2004) Inhibition of the subgenomic hepatitis C virus replicon in huh-7 cells by 2'-deoxy-2'-fluorocytidine. *Antimicrob Agents Chemother* 48, 651-654
20. Smeets, D. F., Jung, K.-H., Westover, J., et al. (2018) 2'-Fluoro-2'-deoxycytidine is a broad-spectrum inhibitor of bunyaviruses in vitro and in phleboviral disease mouse models. *Antiviral Res* 160, 48-54
21. Welch, S. R., Guerrero, L. W., Chakrabarti, A. K., et al. (2016) Lassa and Ebola virus inhibitors identified using minigenome and recombinant virus reporter systems. *Antiviral Res* 136, 9-18
22. Welch, S. R., Scholte, F. E., Flint, M., et al. (2017) Identification of 2'-deoxy-2'-fluorocytidine as a potent inhibitor of Crimean-Congo hemorrhagic fever virus replication using a recombinant fluorescent reporter virus. *Antiviral Res* 147, 91-99
23. Davies, C., Brown, C. M., Westphal, D., et al. (2015) Murine norovirus replication induces G0/G1 cell cycle arrest in asynchronously growing cells. *J Virol* 89, 6057-6066
24. Wobus, C., Karst, S., Thackray, L., et al. (2004) Replication of Norovirus in cell culture reveals a tropism for dendritic cells and macrophages. *PLoS Biol* 2, 2076-2084
25. Chang, K.-O., Sosnovtsev, S. V., Belliot, G., et al. (2006) Stable expression of a Norwalk virus RNA replicon in a human hepatoma cell line. *Virology* 353, 463-473
26. Luthra, P., Naidoo, J., Pietzsch, C. A., et al. (2018) Inhibiting pyrimidine biosynthesis impairs Ebola virus replication through depletion of nucleoside pools and activation of innate immune responses. *Antiviral Res* 158, 288-302
27. Emmott, E., Sorgeloos, F., Caddy, S. L., et al. (2017) Norovirus-Mediated Modification of the Translational Landscape via Virus and Host-Induced Cleavage of Translation Initiation Factors. *Mol Cell Proteomics* 16, S215-S229
28. Gizzi, A. S., Grove, T. L., Arnold, J. J., et al. (2018) A naturally occurring antiviral ribonucleotide encoded by the human genome. *Nature* 558, 610-614
29. Jin, Z., Tucker, K., Lin, X., et al. (2015) Biochemical evaluation of the inhibition properties of favipiravir and 2'-C-methyl-cytidine triphosphates against human and mouse norovirus RNA polymerases. *Antimicrob agents Chemother* 59, 7504-7516
30. Prichard, M. N., and Shipman Jr, C. (1990) A three-dimensional model to analyze drug-drug interactions. *Antiviral Res* 14, 181-205
31. Pierra, C., Amador, A., Benzaria, S., et al. (2006) Synthesis and pharmacokinetics of valopicitabine (NM283), an efficient prodrug of the potent anti-HCV agent 2'-C-methylcytidine. *J Med Chem* 49, 6614-6620
32. Wedemeyer, H., Jensen, D., Herring Jr, R., et al. (2013) PROPEL: A randomized trial of mericitabine plus peginterferon alpha - 2a/ribavirin therapy in treatment - naïve HCV genotype 1/4 patients. *Hepatology* 58, 524-537
33. Arnold, J., Sharma, S., Feng, J., et al. (2012) Sensitivity of mitochondrial transcription and resistance of RNA polymerase II dependent nuclear transcription to antiviral ribonucleosides. *PLoS Pathog* 8, e1003030

Supplementary information

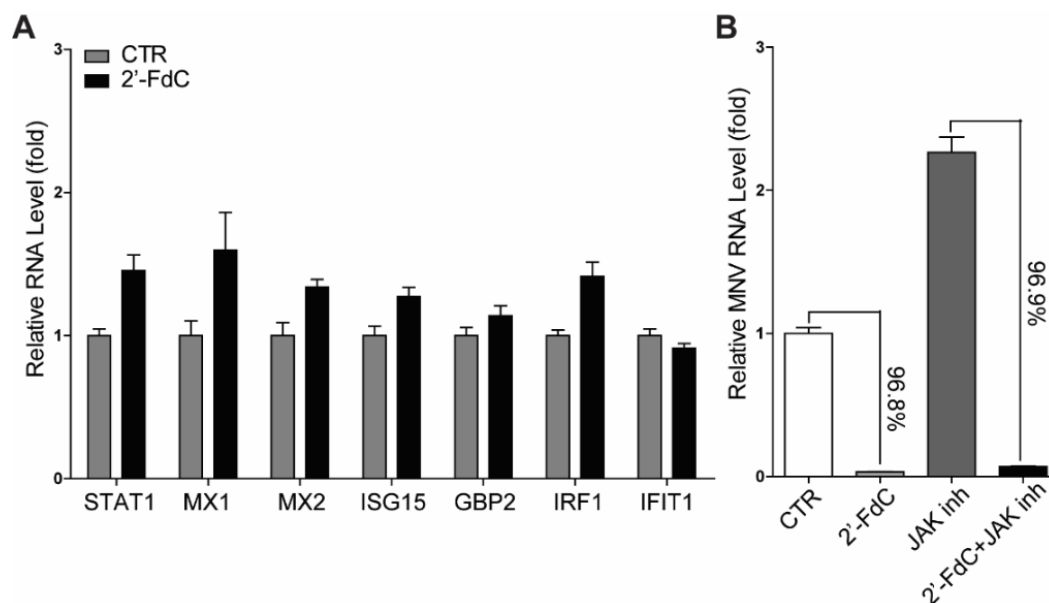


Supplementary Fig. 1
2'-FdC exerts anti-MNV activity in J774A.1 cells. J774A.1 cells were infected with MNV-1 (MOI 1) for 1 h, then refreshed with culture medium containing different concentrations of 2'-FdC for 20 h. (A) The viral RNA level and (B) NS1/2 protein expression were analyzed by qRT-PCR (n = 5-6) and western blotting, respectively. (C) J774A.1 cells were infected with MNV-1

(MOI 1) for 1 h, then refreshed with culture medium containing different concentrations of 2'-FdC for 20 h. The viral NS1/2 protein expression was analyzed by confocal assay. (D) J774A.1 were untreated or treated with 2'-FdC with different concentrations for 20 h. The cytotoxicity was determined by MTT assay (n = 28-32). Data were normalized to the untreated control (set as 1). *P < 0.5; **P < 0.01. β -actin was used as a loading control.



Supplementary Fig. 2 The anti-HuNV ability of 2'-FdC in HG23 cells. HG23 cells were untreated or treated with indicated concentrations of 2'-FdC or IFN- α (1000 IU/ml). After 2 days of treatment the antiviral activities were measured by qRT-PCR (n = 4-5). Data were normalized to the untreated control (set as 1). *P < 0.05; **P < 0.01.



Supplementary Fig. 3 The anti-MNV activity of 2'-FdC does not require ISG induction. (A) RAW264.7 cells were untreated or treated with 2'-FdC (100 μ M) for 20 h. The mRNA level of several ISGs were analyzed by qRT-PCR assay (n = 6). (B) RAW264.7 cells were infected with MNV-1 (MOI 1) for 1 h, then refreshed with culture medium containing 2'-FdC (100 μ M), JAK inhibitor 1 (5 μ g/ml) or combinations for 20 h. The viral RNA level was analyzed by qRT-PCR assay (n = 6). Data were normalized to the untreated control (set as 1).

Supplementary Table 1. Primers used for qRT-PCR.

Gene	F-sequence (5' to 3')	R-sequence (5' to 3')
MNV-1	CACGCCACCGATCTGTTCTG	GCGCTGCGCCATCACTC
mGAPDH	TTCCAGTATGACTCCACTCACGG	TGAAGACACCAGTAGACTCCACGAC
mSTAT1	GCCTCTCATTGTCACCGAAGAAC	TGGCTGACGTTGGAGATCACCA
mISG15	TGACGCAGACTGTAGACACG	TGGGGCTTTAGGCCATACTC
mMX1	GGGGAGGAAATAGAGAAAATGAT	GTTTACAAAGGGCTTGCTTGCT
mMX2	CCAGTTCCTCTCAGTCCCAAGATT	TACTGGATGATCAAGGGAACGTGG
mGBP2	ACCAGCTGCACTATGTGACG	TCAGAAGTGACGGGTTTTCC
mIRF1	CAGAGGAAAGAGAGAAAGTCC	CACACGGTGACAGTGCTGG
mIFIT1	CCATAGCGGAGGTGAATATC	GGCAGGACAATGTGCAAGAA
hGAPDH	TGTCCCCACCCCAATGTATC	CTCCGATGCCTGCTTCACTACCTT
HuNV ^a	CGYTGGATGCGNTTYCATGA	CTTAGACGCATCATCATTYAC

^aY = C + T; R = A + G; W = A+T; N = any

Chapter 3

Lipopolysaccharide restricts murine norovirus infection in macrophages mainly through NF- κ B and JAK-STAT signaling pathway

Peifa Yu, Yang Li, Yining Wang, Maikel P. Peppelenbosch, Qiuwei Pan

Virology, 2020, 546: 109-121.

Abstract

The inflammasome machinery has recently been recognized as an emerging pillar of innate immunity. However, little is known regarding the interaction between the classical interferon (IFN) response and inflammasome activation in response to norovirus infection. We found that murine norovirus (MNV-1) infection induces the transcription of IL-1 β , a hallmark of inflammasome activation, which is further increased by inhibition of IFN response, but fails to trigger the release of mature IL-1 β . Interestingly, pharmacological inflammasome inhibitors do not affect viral replication, but slightly reverse the inflammasome activator lipopolysaccharide (LPS)-mediated inhibition of MNV replication. LPS efficiently stimulates the transcription of IFN- β through NF- κ B, which requires the transcription factors IRF3 and IRF7. This activates downstream antiviral IFN-stimulated genes (ISGs) via the JAK-STAT pathway. Moreover, inhibition of NF- κ B and JAK-STAT signaling partially reverse LPS-mediated anti-MNV activity, suggesting additional antiviral mechanisms activated by NF- κ B. This study reveals additional insight in host defense against MNV infection.

Keywords: norovirus, inflammasome, interferon, lipopolysaccharide, macrophages

Introduction

Norovirus is a major cause of epidemic nonbacterial gastroenteritis worldwide. Currently, no vaccination or specific antiviral treatment is available except for supportive care and supplementation of fluids, exerting a great global economic burden and significant impact on public health (1). The lack of a robust human norovirus (HuNV) cell culture system is a key bottleneck for norovirus research. Recent studies have achieved some success in culturing HuNV in intestinal enteroid or B cells with modest viral replication level (2,3), and in zebrafish larvae (4) and human induced pluripotent stem cell-derived intestinal epithelial cells (5), but these systems have not been widely used. A HuNV subgenomic replicon model in Huh7 cell line is widely used, for instance for antiviral drug evaluation (6). Murine norovirus (MNV), permissive for replication in both cell culture and small-animal models, shares similar structural, biochemical and genetic features with HuNV, and thus has become a useful model for studying norovirus biology and associated pathology (7,8).

Innate immune response provides the first line of defense against viral infection through the recognition of pathogen associated molecular patterns (PAMPs) by its pattern recognition receptors (PRRs) including the recognized Toll-like receptors (TLRs), NOD-like receptors (NLRs), RIG-I like receptor (RLRs) and the cyclic GMP-AMP synthase (cGAS) (9). During viral replication, the accumulated nucleic acids within cells can be sensed by certain PRRs, and then rapidly activate the following intracellular transcription factors such as nuclear factor- κ B (NF- κ B) and IFN-regulatory factors (IRF3 and IRF7), leading to secretion of cytokines and chemokines including IFNs (10). The released IFNs bind to their receptors on the cell surface, and in turn activate Janus kinase (JAK)-signal transducer and activator of transcription (STAT) signaling pathway and further induce transcription of hundreds of IFN-stimulated genes (ISGs). A subset of ISGs are ultimate antiviral effectors limiting viral replication and spread (11). More recently, the inflammasome signaling has also been reported to exert a central role in the regulation of gastrointestinal health and disease (12). Inflammasomes are multiprotein complexes that induce downstream immune responses to specific pathogens and host cell damage (13). Once activated, inflammasomes can induce the activation of caspases and release of mature interleukin-1 β (IL-1 β) and IL-18, and execute a form of inflammatory cell death known as pyroptosis (12,13).

Lipopolysaccharide (LPS) is an important structural component of the outer membrane of gram-negative bacteria, acting as a potent inflammasome activator. Upon LPS recognition, TLR4 signaling can be activated by undergoing oligomerization and recruiting its downstream adaptors through interactions with the TIR (Toll-interleukin-1 receptor) domains, which further induces the proinflammatory cytokine expression and IFNs secretion through myeloid differentiation primary response gene 88 (MyD88)-dependent or MyD88-independent

pathways (14). Moreover, LPS has been reported to associate with non-canonical inflammasome activation by binding with caspase 11 and then cleaving gasdermin D to induce pyroptotic cell death (15).

Inflammasome activation is essential in controlling viral infection, such as rotavirus and influenza virus (16,17). Previous studies have reported that MNV-1 was rapidly cleared in wild-type mice (18), but persisted much longer in NLRP6-deficient mice (19), suggesting the potential involvement of inflammasome activation in norovirus infection. A recent study has revealed that MNV infection induced secretion of mature IL-1 β by activating NLRP3 inflammasome in primary bone marrow-derived macrophages (BMDMs) that primed with TLR2 agonist, and in STAT1 deficient BMDMs that without TLR2 priming (20). In this study, we investigated whether the IFN and inflammasome machineries interact and collectively respond to norovirus infection, and LPS-mediated anti-norovirus response.

Materials and methods

Reagents

Human IFN- α (Thermo Scientific, the Netherlands) and mouse IFN- γ (ab9922, Abcam) were dissolved in PBS. Lipopolysaccharide (LPS; L6529, Sigma) and adenosine 5-triphosphate disodium salt hydrate (ATP; A3377, Sigma) were dissolved in PBS. Stocks of JAK inhibitor 1 (Santa Cruz Biotech, CA), Bayer 11-7085 (Santa Cruz Biotech, CA), MCC950 (inh-mcc, Invivogen) and Ac-YVAD-cmK (inh-yvad, Invivogen) were dissolved in DMSO. Antibodies against phospho-STAT1 (Ser727) (#9177), STAT1 (#9172), MDA5 (D74E4, #5321) and IRF1 (D5E4, #8478), were purchased from Cell Signaling Technology. GBP2 antibody (11854-1-AP) was purchased from Proteintech. Rabbit polyclonal antisera to MNV NS1-2 (21) was kindly provided by Prof. Vernon K. Ward (School of Biomedical Sciences, University of Otago, New Zealand). β -actin antibody (#sc-47778) was purchased from Santa Cruz Biotechnology. IRDye[®] 800CW-conjugated goat anti-rabbit and goat anti-mouse IgGs (Li-Cor Bioscience, Lincoln, USA) were used as secondary antibodies, as appropriate.

Cell culture and viruses

RAW264.7 and J774A.1 cells were cultured in Dulbecco's modified Eagle's medium (DMEM; Lonza Verviers, Belgium) supplemented with 10% (vol/vol) heat-inactivated fetal calf serum (FCS; Hyclone, Logan, UT, USA), 100 μ g/mL of streptomycin, and 100 IU/mL of penicillin. Human Huh7 hepatocellular carcinoma cells harboring a genotype 1 HuNV replicon (HG23)

were kindly provided by Dr. Kyeong-Ok Chang (Kansas State University) (6). A neomycin resistant gene was engineered into ORF2, conferring HG23 resistance to neomycin. Gentamicin (G418; Gibco) was added to HG23 culture medium at 1.5 mg/mL for selection before experimentation. Mouse embryonic fibroblast cells (MEFs) (WT, NF- κ B^{-/-} and IRF3/7^{-/-}) were kindly provided by Dr. Sanna M. Mäkelä (National Institute for Health and Welfare Viral Infections Unit, Helsinki, Finland) with the permission of Dr. Michael J. Gale and Dr. A. Hoffmann (22). Wild-type (WT) MEFs and MEFs from STAT1^{-/-} mice were generously provided by Prof. Andrea Kröger (Helmholtz Centre for Infection Research) (23).

MNV-1 (murine norovirus strain MNV-1.CW1) was produced by inoculating the virus (kindly provided by Prof. Herbert Virgin, Department of Pathology and Immunology, Washington University School of Medicine) into RAW264.7 cells (7). The MNV-1 cultures were purified, aliquoted, and stored at -80 °C for all subsequent experiments. The MNV-1 stock was quantified three independent times by the 50% tissue culture infective dose (TCID₅₀).

TCID₅₀

MNV-1 was quantified by TCID₅₀ assay (24). Briefly, 10-fold dilutions of MNV-1 were inoculated into RAW264.7 cells grown in 96-well tissue culture plate at 1,000 cells/well. The plate was incubated at 37 °C for another 5 days, followed by observing the cytopathic effect (CPE) of each well under a light scope. The TCID₅₀ was calculated by using the Reed-Muench method.

MNV-1 infection in macrophages

To determine whether MNV-1 infection could activate the inflammasome, RAW264.7 (1X10⁵ cells/well) and J774A.1 (1X10⁵ cells/well) cells were plated at 12-well plate and were rested for 24 h at 37 °C. Cells were then either left uninfected or infected with MNV-1 at indicated multiplicity of infection (MOI) for 1 h at 37 °C. The MNV-1 inoculum was removed and the cells were washed three times with phosphate-buffered saline (PBS), and fresh medium was added back onto cells. LPS and ATP treated cells were set as positive control. Total RNA and cell supernatant samples were prepared at indicated time and stored at -80 °C before use.

For MNV-1 antiviral assay, RAW264.7 and J774A.1 cells were either left untreated or treated with LPS, IFN- γ or combination with indicated compounds for 6 h before inoculation with MNV-1 at 1 MOI. After 1 h inoculation, the cells were washed with PBS for three times to remove the residual viruses, and control medium or medium supplemented with LPS or mouse IFN- γ was added back onto cells. After 24 h of infection, total RNA, protein and supernatant samples were collected from the cells for further analysis.

HuNV antiviral assay

Twenty-four hours before experimentation, HG23 cells were cultured in the medium without gentamicin. HG23 cells were seeded into 48-well tissue culture plates (2.5×10^4 cells per well), treated with different concentrations of LPS or human IFN- α . After 48 h of treatment, total RNA was extracted from cells, and HuNV replication was determined by qRT-PCR analysis.

Enzyme-linked immunosorbent assay (ELISA)

Supernatant was analyzed for cytokine IL-1 β secretion by an ELISA kit (KMC0012; Invitrogen) according to manufacturer's instructions. The absorbance was measured at 450 nm in an automatic microplate reader. Results were calculated based on a standard curve.

Quantitative real-time polymerase chain reaction

Total RNA was isolated with a Macherey NucleoSpin RNA II Kit (Bioke, Leiden, The Netherlands) and quantified with a Nanodrop ND-1000 (Wilmington, DE, USA). During RNA isolation, DNase was added to remove genomic DNA according to the manufacturer's instructions. cDNA was synthesized from 500 ng of RNA using a cDNA synthesis kit (TaKaRa Bio, Inc., Shiga, Japan). The cDNA of all targeted genes transcript were quantified by SYBR-Green-based (Applied Biosystems) real-time PCR on the StepOnePlus™ System (Thermo Fisher Scientific Life Sciences) according to the manufacturer's instructions. Human glyceraldehyde-3-phosphate dehydrogenase (GAPDH) and murine GAPDH genes were used as reference genes to normalize gene expression. The relative expression of targeted gene was calculated as $2^{-\Delta\Delta C_T}$, where $\Delta\Delta C_T = \Delta C_T \text{sample} - \Delta C_T \text{control}$ ($\Delta C_T = C_T[\text{targeted gene}] - C_T[\text{GAPDH}]$). All primer sequences are listed in Supplementary Table 1 and Table 2.

Western blotting

Cultured cells were lysed in Laemmli sample buffer containing 0.1 M DTT and heated 5 mins at 95 °C, then loaded onto a 10% sodium dodecyl sulfate polyacrylamide gel electrophoresis (SDS-PAGE) gel, then proteins were electrophoretically transferred onto a polyvinylidene difluoride (PVDF) membrane (pore size, 0.45 μm ; Invitrogen) for 2 h with an electric current of 250 mA. Subsequently, the membrane was blocked with a mixture of 2.5 mL blocking buffer (Odyssey) and 2.5 mL PBS containing 0.05% Tween 20 for 1 h, followed by overnight incubation with primary antibodies (1:1000) at 4 °C. The membrane was washed 3 times and then incubated with IRDye-conjugated secondary antibody (1:5000) for 1 h. After washing 3 times, protein bands were detected with the Odyssey 3.0 Infrared Imaging System (Li-Cor Biosciences).

MTT assay

Cells were seeded into 96-well tissue culture plates and cell viability was assessed by adding 10 mM 3-(4,5-dimethyl-2-thiazolyl)-2,5-diphenyl-2H-tetrazolium bromide (MTT) (Sigma, Zwijndrecht, the Netherlands). After 3 h, the medium was replaced with 100 μ L of DMSO and was incubated at 37°C for another 50 mins. The absorbance at 490 nm was recorded on the microplate absorbance reader (Bio-Rad, CA, USA).

Statistical analysis

Data are presented as the mean \pm SEM. Comparisons between groups were performed with Mann-Whitney test using GraphPad Prism 5.0 (GraphPad Software Inc., La Jolla, CA, USA). Differences were considered significant at a *P* value less than 0.05.

Results

MNV-1 infection did not induce the release of mature IL-1 β , but increased its mRNA expression, which was further augmented by inhibition of IFN pathway in macrophages

To investigate whether MNV-1 can activate inflammasome, J774A.1 cells were used because of its permissiveness for MNV-1 infection and competence in inflammasome activation (7,25). We first determined the expression of IL-1 β and IL-18 as markers of inflammasome activation in J774A.1 cells treated with LPS (the component in the outer membrane of gram-negative bacteria) and ATP, the potent activators for inflammasome activation. We found that under stimulation by LPS and ATP, the mRNA and protein levels of IL-1 β were significantly increased (Fig. 1A-1C), and IL-18 mRNA level was moderately elevated (Fig. 1A). Although the IL-1 β mRNA level was modestly elevated in MNV-1 infected J774A.1 cells (Fig. 1B), no significant differences in IL-1 β protein level were observed in the supernatant of these cells (Fig. 1C). We confirmed active viral infection by detecting the viral NS1/2 protein in J774A.1 cells (Fig. 1D). In another macrophage cell line RAW264.7 cells, the IL-1 β and IL-18 mRNA levels were hardly changed upon MNV-1 infection (Supplementary Fig. 1). However, treatment with LPS and ATP also failed to induce the expression of these genes (Supplementary Fig. 1A and 1B), indicating possible defects of the inflammasome machinery in RAW264.7 cells, which is consistent with a previous study (26).

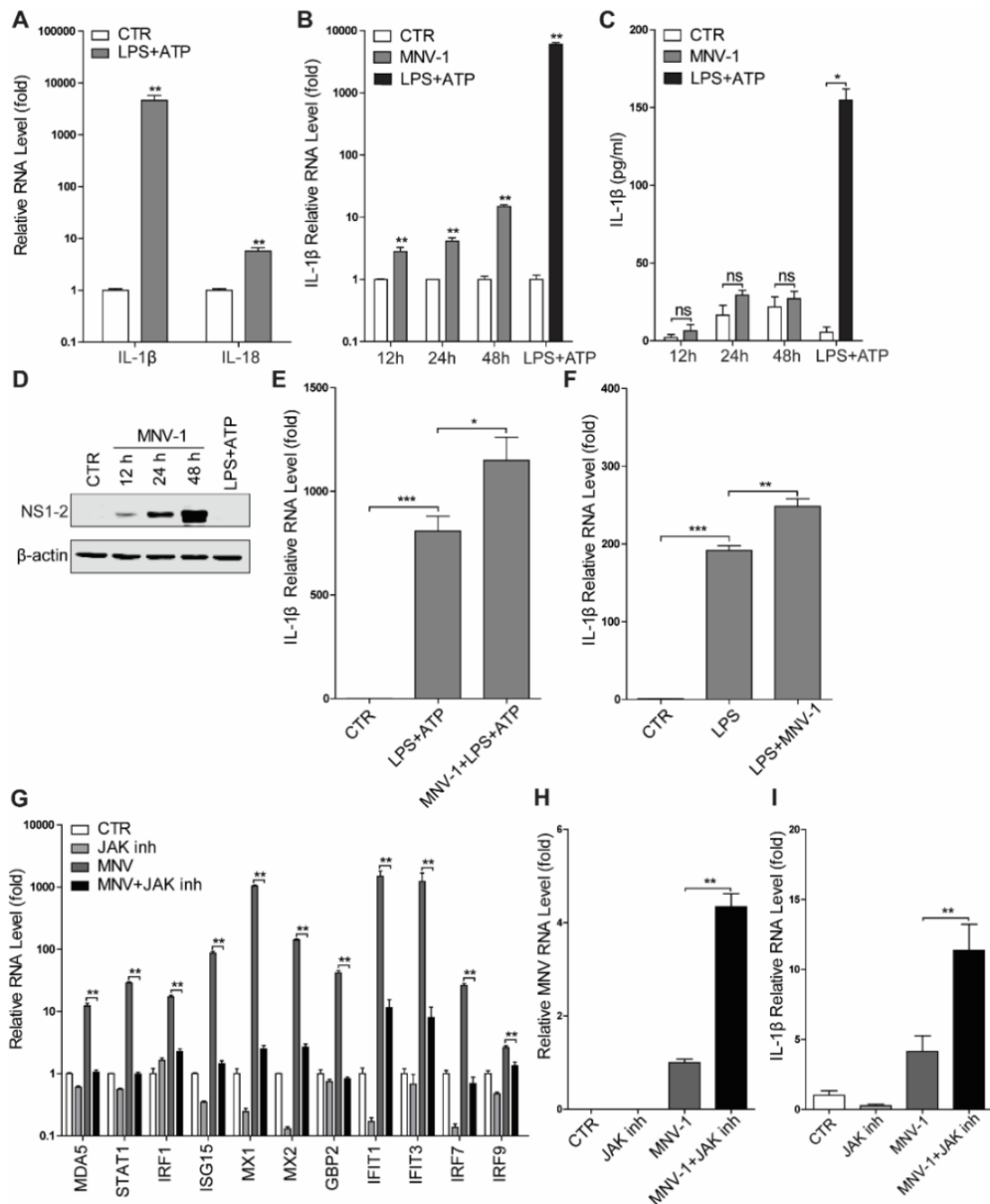


Figure 1. MNV-1 infection did not induce the release of mature IL-1 β , but increased its mRNA level in macrophages. J774A.1 cells were untreated or treated with LPS (400 ng/ μ l) for 4 h and then ATP (5 mM) for 40 mins, or left uninfected or infected with MNV-1 (MOI 1) for 24 h, and total RNA and cell culture supernatants were collected. mRNA levels of IL-1 β (A and B) (n = 6) and IL-18 (A) (n = 6), and protein level of IL-1 β (C) (n = 4) were analyzed by qRT-PCR and ELISA, respectively. Western blotting (D) was used to analyze the viral infection in J774A.1 cells at indicated times. (E) J774A.1 cells were uninfected or infected with MNV-1 (MOI 1) for 20 h, then treated with LPS (400 ng/ μ l) for 4 h and ATP (5 mM) for 40 mins. mRNA level of IL-1 β and cytotoxicity were analyzed by qRT-PCR (n = 8). (F) J774A.1 cells were untreated or treated with LPS (400 ng/ μ l) for 4 h then uninfected or infected with MNV-1 (MOI 1) for 24 h. mRNA level of IL-1 β and cytotoxicity were analyzed by qRT-PCR (n = 8). J774A.1 cells were untreated or treated with JAK inhibitor 1 (10 μ M) for 6 h then uninfected or infected with MNV-

1 (MOI 1) for 24 h. mRNA levels of indicated genes (G) (n = 6), MNV-1 RNA (H) (n = 6) and IL-1 β mRNA (I) (n = 6) were analyzed by qRT-PCR, respectively. Data were normalized to the untreated control (CTR, set as 1). *P < 0.05; **P < 0.01; ***P < 0.001; ns, not significant. β -actin was used as a loading control.

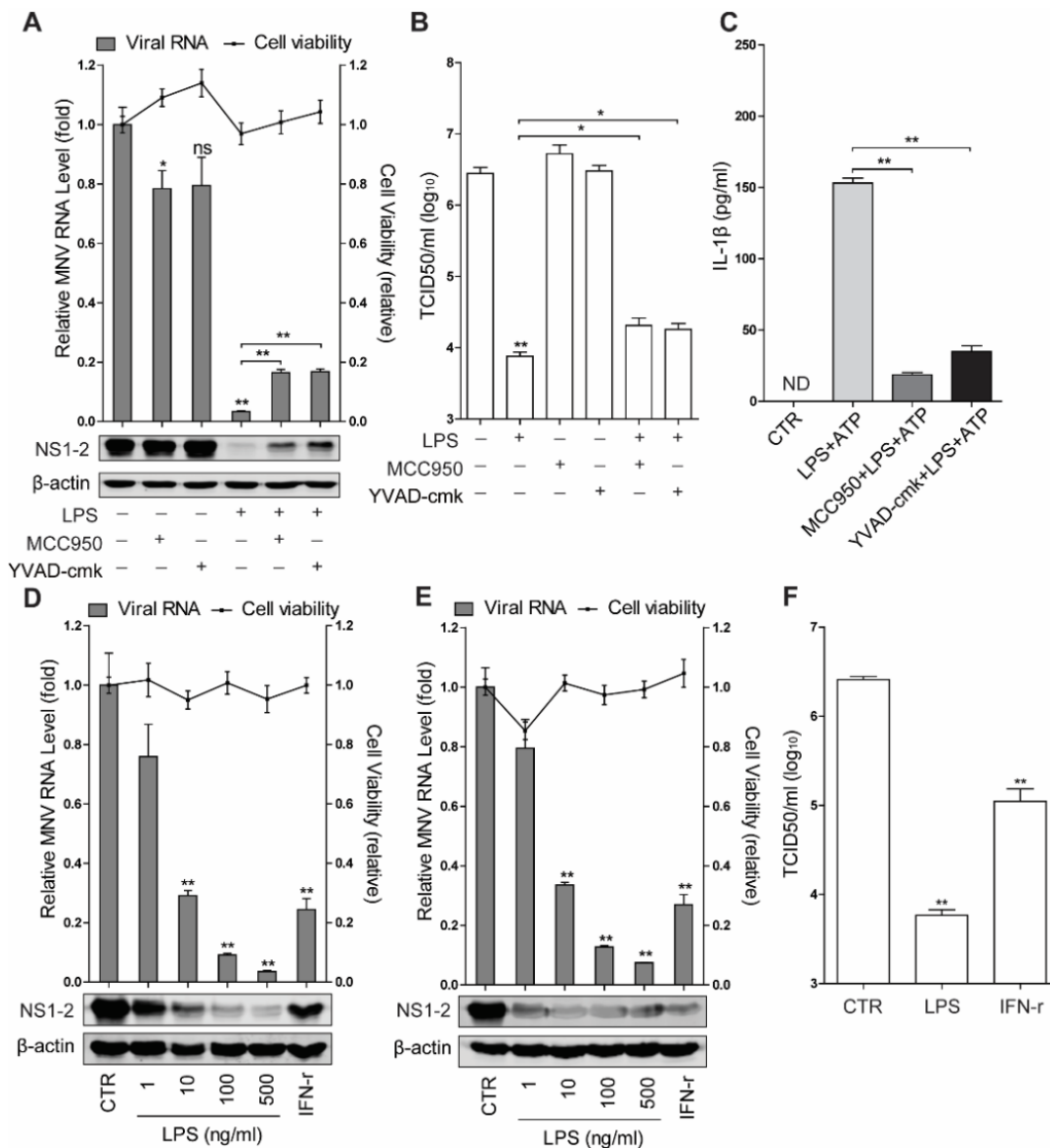


Figure 2. LPS potently inhibits MNV-1 replication largely independent of inflammasome. J774A.1 cells were treated with LPS (400 ng/ μ l), MCC950 (5 μ M), YVAD-cmk (5 μ M), or combination for 6 h, then infected with MNV-1 (MOI 1) for 24 h. (A) The viral RNA, NS1/2 protein and cytotoxicity were analyzed by qRT-PCR (n = 6), western blotting, and MTT (n = 16) assays, respectively. (B) The viral titers were also analyzed by TCID50 assay (n = 4-6). (C) J774A.1 cells were untreated or treated with LPS (400 ng/ μ l), MCC950 (5 μ M), YVAD-cmk (5 μ M), or combination for 4 h and then ATP (5 mM) for 40 mins. The cell culture supernatants were collected and used for analysis of IL-1 β by ELISA assay (n = 6). (D) RAW264.7 cells were untreated or treated with different concentrations of LPS as indicated, or IFN- γ (100 U/ml) for 6 h, then infected with MNV-1 (MOI 1) for 24 h. The viral RNA, NS1/2 protein and cytotoxicity were analyzed by qRT-PCR (n = 6), western blotting and MTT (n = 8) assay, respectively. (E) RAW264.7 cells were infected with MNV-1 (MOI 1) for 1 h, then added fresh medium or medium

supplemented with LPS at indicated concentrations or IFN- γ (100 U/ml) for 24 h. The viral RNA, NS1/2 protein and cytotoxicity were analyzed by qRT-PCR (n = 3 independent experiments with 2-3 replicates each), western blotting and MTT (n = 8) assays, respectively. (F) RAW264.7 cells were untreated or treated with different concentrations of LPS as indicated, or IFN- γ (100 U/ml) for 6 h, then infected with MNV-1 (MOI 1) for 24 h. The viral titers were analyzed by TCID₅₀ assay (n = 6). Data were normalized to the untreated control (CTR, set as 1). *P < 0.05; **P < 0.01; ns, not significant. ND, not determined. β -actin was used as a loading control.

We next investigated whether MNV-1 infection has a role in LPS-induced IL-1 β transcription. As expected, the IL-1 β mRNA level was further increased in MNV-1 infected J774A.1 cells by LPS and ATP stimulation (Fig. 1E), and this effect was also observed in LPS-pretreated cells (Fig. 1F). A recent study reported that MNV infection stimulated IL-1 β RNA transcription and protein release in STAT1 deficient BMDMs (20). Thus, we blocked the JAK-STAT pathway by using JAK-STAT inhibitor (JAK inhibitor 1), and found that inhibition of JAK-STAT pathway attenuated MNV-1 induced ISG transcription (Fig. 1G), but increased MNV-1 RNA level (Fig. 1H) and viral infection-induced IL-1 β mRNA transcription (Fig. 1I), which is in accordance with the recent study (20).

LPS potently inhibits MNV-1 replication largely independent of inflammasome

Norovirus cohabits with bacteria in the intestine. Co-infection of MNV and bacteria in macrophages has been reported to reduce the viral load (27,28). Thus, we further investigated the direct effects of bacteria-derived LPS on MNV-1 replication, and found that treatment with LPS potently inhibits viral replication in J774A.1 cells (Fig. 2A and 2B). However, this inhibitory effect on MNV-1 is only partially reversed by pharmacological inflammasome inhibitors MCC950 and YVAD-cmk, which did not affect viral replication (Fig. 2A and 2B) but decreased the release of mature IL-1 β triggered by LPS and ATP stimulation in J774A.1 cells (Fig. 2C).

We next evaluated the anti-MNV effect of LPS in RAW264.7 cells, which are incompetent of inflammasome activation (26). IFN- γ was used as a control. Pre-treatment with LPS potently inhibited viral RNA and NS1-2 protein levels in a dose-dependently manner (Fig. 2D). Similar effects were observed when cells were first infected with MNV-1 then subjected to treatment with LPS (Fig. 2E). Moreover, the viral titers were also decreased by LPS and IFN- γ pre-treatment (Fig. 2F).

These results urged us to investigate the antiviral effect of LPS on HuNV replication by using the Huh7-based HuNV replicon cells (HG23). After two days of treatment, LPS failed to but human IFN- α effectively restricted HuNV replication without triggering major cytotoxicities (Fig. 3A). It is widely recognized that IFNs exert antiviral effects via induction of the transcription of ISGs through JAK-STAT signaling pathway. We further revealed that

expression of type I IFNs (IFN- α and IFN- β) were not significantly induced by both LPS and IFN- α (Fig. 3B and 3C). However, IFN- α but not LPS triggered the expression and phosphorylation of STAT1 (Fig. 3D), and induction of ISGs including ISG15, IFIT1 and MX1 in HG23 cells (Fig. 3E). This is consistent with previous findings that hepatic epithelia cells do not respond to LPS stimulation (29). This previous study also showed that LPS suppresses IFN response in hepatocytes by upregulating ubiquitin-like protease 18 (USP18) expression, a negative regulator of type I IFN signaling (29). However, LPS stimulation did not affect USP18 gene transcription in our study (Fig. 3F). These results have demonstrated that LPS potently inhibits MNV replication in macrophages, but has no significant effect on HuNV replication in HG23 cells. This is probably related to the intrinsic property that epithelial HG23 cells are nonresponsive to LPS stimulation.

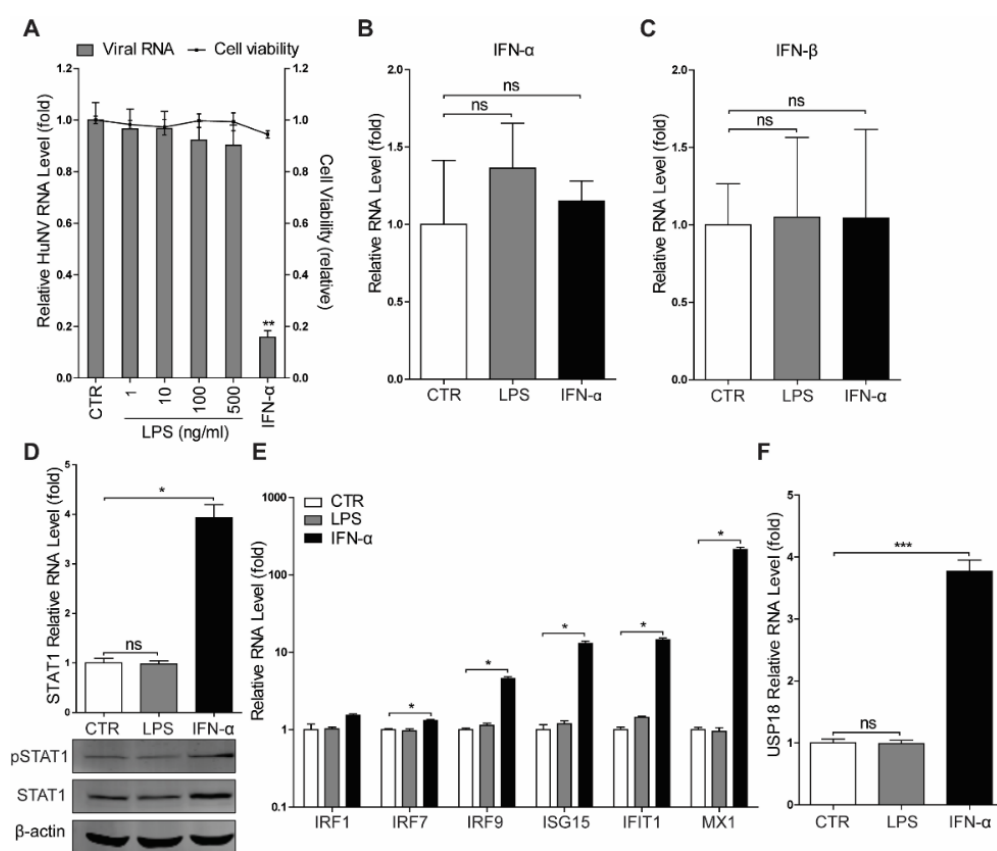


Figure 3. HuNV replication is not affected by LPS in the replicon model. (A) HG23 cells were untreated or treated with different concentrations of LPS as indicated, or IFN- α (200 IU/ml). After 2 days of treatment the antiviral activities and cytotoxicity were measured by qRT-PCR ($n = 6$) and MTT assay ($n = 16$), respectively. qRT-PCR analysis ($n = 4$) of mRNA levels of IFN- α (B), IFN- β (C), STAT1 (D upper panel), ISGs (E), USP18 (F) and western blotting analysis of STAT1 expression and phosphorylation (D lower panel) in HG23 cells untreated or treated with LPS (100 ng/ml) or IFN- α (200 IU/ml). Data were normalized to the untreated control (CTR, set as 1). * $P < 0.05$; ** $P < 0.01$; *** $P < 0.001$; ns, not significant. β -actin was used as a loading control.

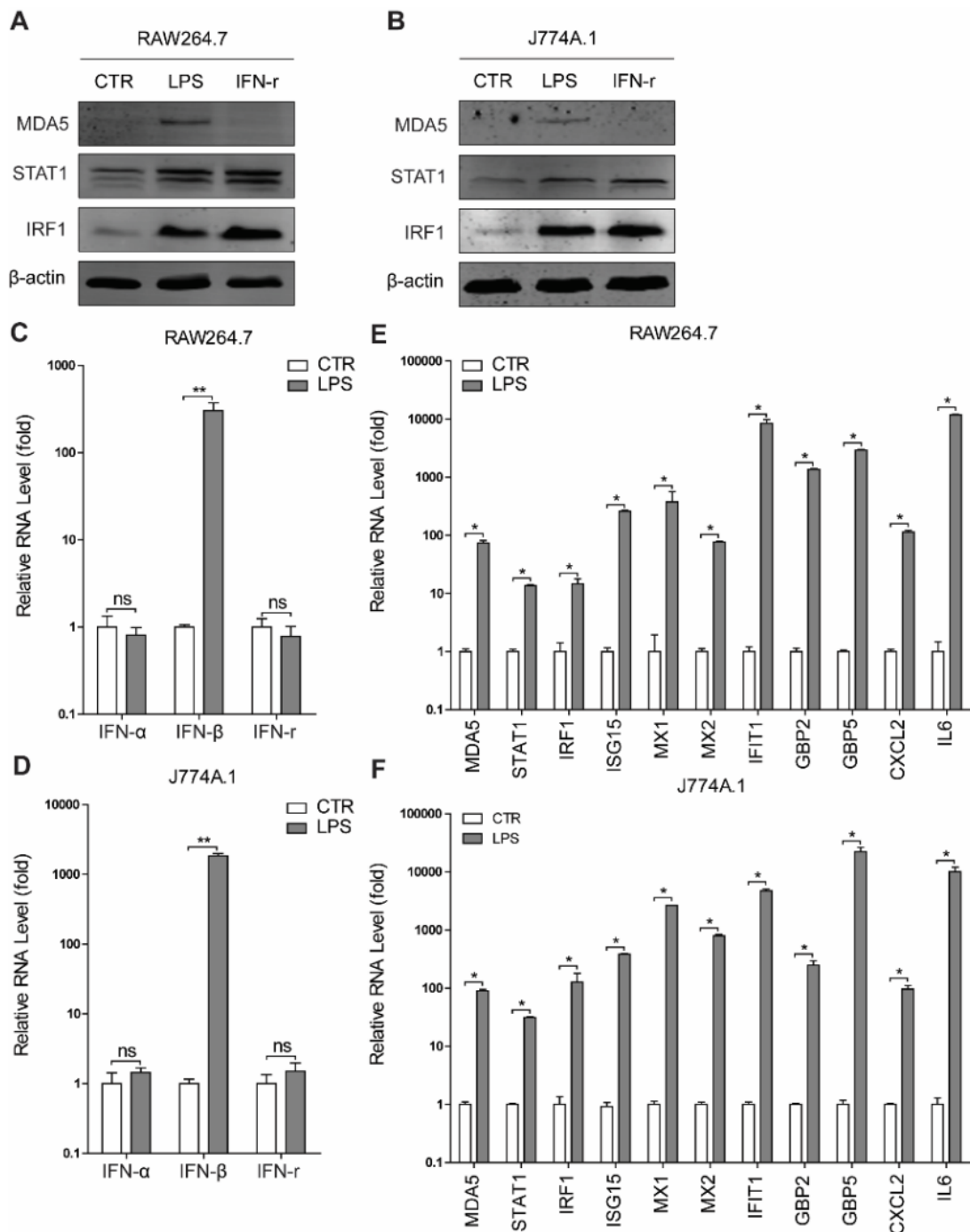
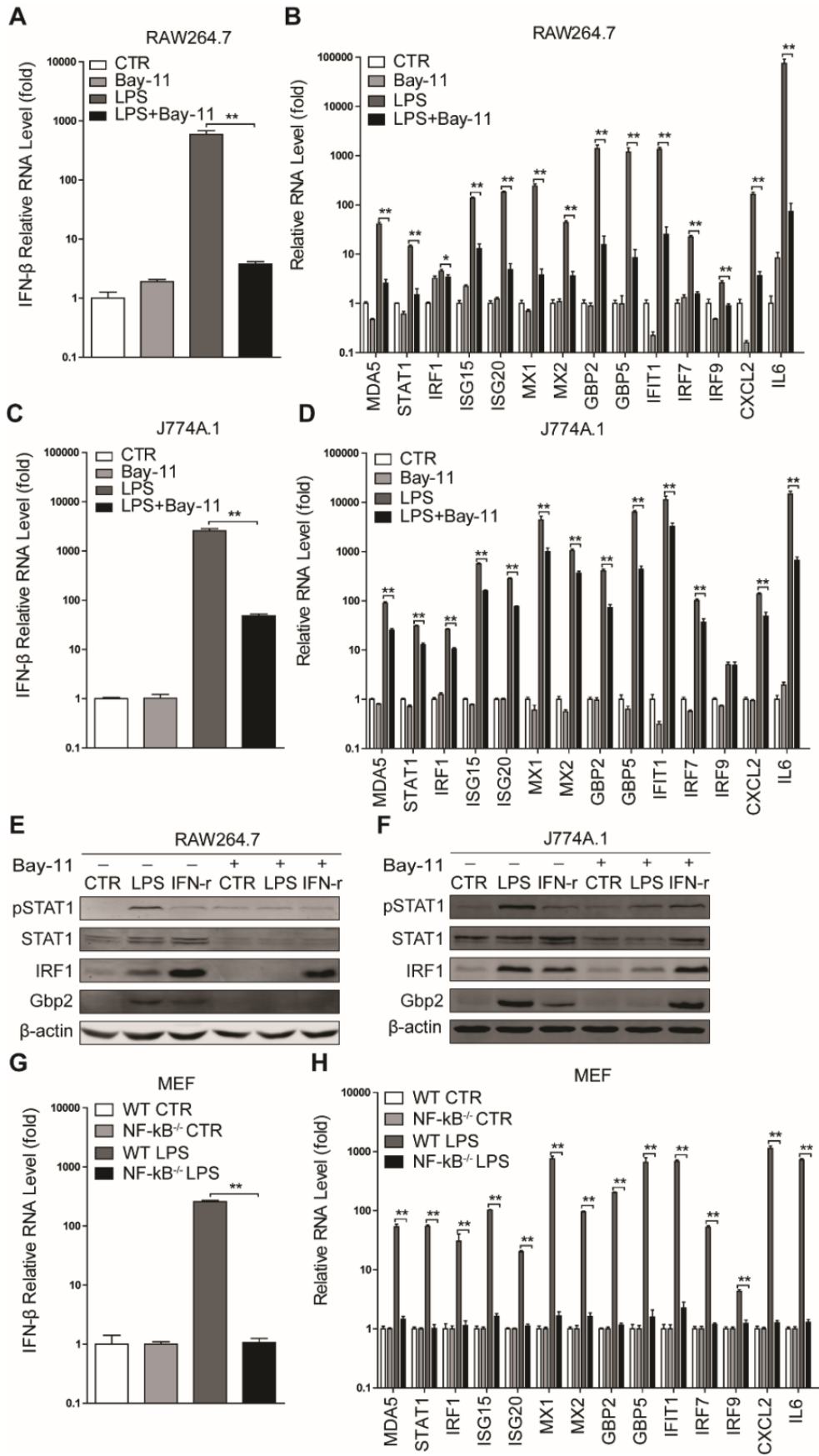


Figure 4. LPS stimulates the transcription of a wide range of ISGs. Western blotting analysis of ISG protein levels in RAW264.7 cells (A) and J774A.1 cells (B) untreated or treated with LPS (100 ng/ml) or IFN- γ (100 U/ml) for 6 h. qRT-PCR analysis of mRNA level of IFNs (C and D) (n = 6) and ISGs (E and F) (n = 4) in RAW264.7 cells and J774A.1 cells that untreated or treated with LPS (100 ng/ml) for 6 h, respectively. Data were normalized to the untreated control (CTR, set as 1). *P < 0.05; **P < 0.01; ns, not significant. β -actin was used as a loading control.



< Figure 5. NF-κB signaling is important for LPS-induced IFN-β and ISG transcription. Cells were untreated or treated with LPS (100 ng/ml), Bay 11-7085 (5 μM) or combination for 6 h. qRT-PCR analysis of IFN-β (A) and ISG (B) mRNA levels in RAW264.7 cells (n = 6). qRT-PCR analysis of IFN-β (C) and ISG (D) mRNA levels in J774A.1 cells (n = 6). Western blotting analysis of STAT1 expression and phosphorylation, and expression of IRF1 and GBP2 in RAW264.7 cells (E) and J774A.1 cells (F) untreated or treated with LPS (100 ng/ml), IFN-γ (100 U/ml), Bay 11-7085 (5 μM) or combination for 6 h. qRT-PCR analysis of mRNA levels of IFN-β (G) (n = 6) and ISGs (H) (n = 6) in WT and NF-κB^{-/-} MEFs untreated or treated with LPS (100 ng/ml) for 6 h. Data in (A, B, C, D and G) were normalized to the untreated control (CTR, set as 1). Data in (H) were normalized to untreated WT and NF-κB^{-/-} MEFs, respectively (both set as 1). *P < 0.05; **P < 0.01. β-actin was used as a loading control.

LPS stimulates the transcription of IFN-β and a wide range of ISGs

Given the dispensability of inflammasome in anti-MNV activity of LPS, we explored other possible mechanisms. It is generally recognized that LPS stimulation of macrophages induces production of many cytokines and inflammatory mediators including IRF-1, IL-6 and IFNs (30,31). We found that LPS stimulated the expression of the viral RNA sensor MDA5 in RAW264.7 and J774A.1 cells (Fig. 4A and 4B), and the increased transcription of IFN-β in both cell lines (Fig. 4C and 4D), respectively. ISGs are the ultimate antiviral effectors induced by IFNs through the JAK-STAT pathway. We found the activation of JAK-STAT pathway by detecting the increased expression of STAT1 at both the protein (Fig. 4A and 4B) and transcriptional levels (Fig. 4E and 4F), respectively. Moreover, the transcription of a wide range of ISGs was also stimulated by LPS (Fig. 4E and 4F), and IFN-γ treatment also induced the transcription of many ISGs in both cell lines (Supplementary Fig. 2). The induction of several important genes were further confirmed by immunoblotting (Fig. 4A and 4B).

NF-κB signaling is important for LPS-induced IFN-β and ISG transcription

It has been reported that recognition of LPS by TLR4 activates downstream transcription factors NF-κB, leading to the transcription of IFNs and ISGs (32). Thus, we further investigated whether NF-κB signaling is involved in LPS-induced IFN-β and ISG transcription in macrophages. Treatment with Bay 11-7085, a pharmacological inhibitor of NF-κB activation, largely inhibits LPS-triggered transcription of IFN-β (Fig. 5A and 5C) and most of the ISGs (Fig. 5B and 5D) in both macrophage cell lines. Moreover, this inhibitor also attenuated LPS-induced expression and phosphorylation of STAT1, as well as ISG expression such as IRF1 and GBP2 (Fig. 5E and 5F). Similarly, some ISGs induced by IFN-γ were also affected by Bay 11-7085 treatment in both cell lines (Supplementary Fig. 3).

To further determine the essential role of NF-κB pathway in LPS-induced ISG expression, wild-type (WT) and NF-κB deficient (NF-κB^{-/-}) MEFs were used. In NF-κB^{-/-} but not the WT cells, LPS

failed to induce the transcription of IFN- β (Fig. 5G). A similar ISG induction pattern was also observed in NF- κ B^{-/-} cells. All of the genes detected such as IRF1, ISG15, MX1 and GBP2 were significantly induced by LPS in WT cells but not in NF- κ B^{-/-} cells (Fig. 5H). Moreover, transcription of some ISGs induced by IFN- γ were largely decreased in NF- κ B^{-/-} cells (Supplementary Fig. 4A). Taken together, these findings revealed that NF- κ B pathway is important for LPS-induced IFN- β and ISG transcription.

IRF3 and IRF7 are important for LPS-induced IFN- β and ISG transcription

LPS as the ligand activates TLR4, which in turn phosphorylates downstream IRF3 and IRF7, leading to their nuclear translocation and induction of type I IFN genes and co-stimulatory molecules (32). Moreover, IRF3 and IRF7 have been reported to play an important role in controlling MNV-1 replication (33). Thus, by using WT and IRF3/7 deficient (IRF3/7^{-/-}) MEFs, we found that IFN- β was not induced by LPS in IRF3/7^{-/-} cells (Fig. 6A). Moreover, the detected genes induced by LPS in WT cells were reduced in IRF3/7^{-/-} cells (Fig. 6B). Compared to the WT cells, transcription of ISG15, ISG20, MX1 and IFIT1 appeared to be unchanged, while transcription of other ISGs such as IRF1, MX2, GBP2 and GBP5 induced by IFN- γ was decreased in IRF3/7^{-/-} cells (Supplementary Fig. 4B). These results suggested that IRF3 and IRF7 are also important for LPS-induced IFN- β and ISG transcription.

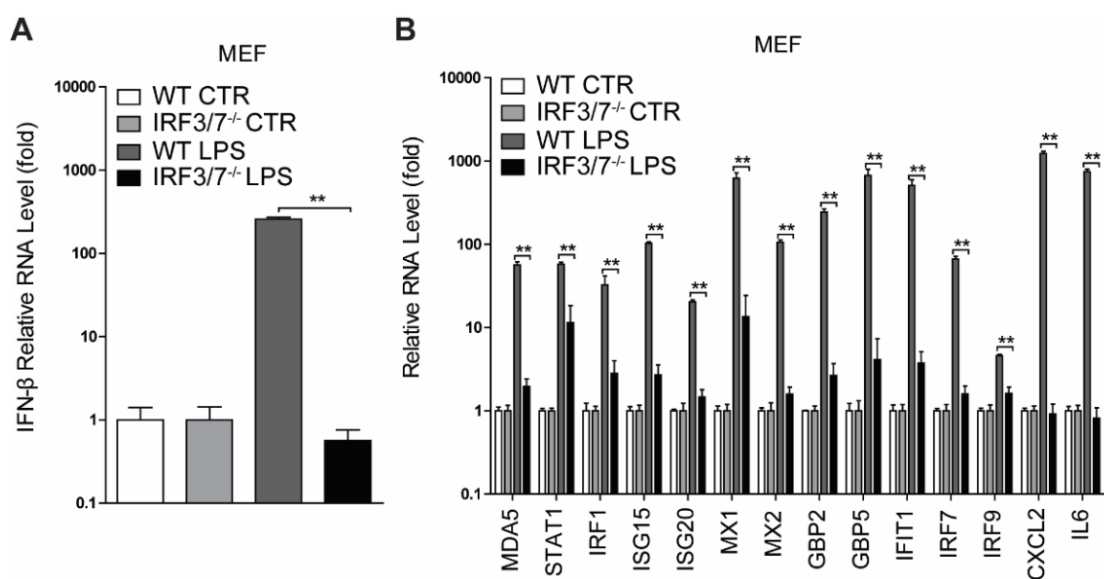


Figure 6. IRF3 and IRF7 are important for LPS-induced IFN- β and ISG transcription. qRT-PCR analysis of mRNA levels of IFN- β (A) (n = 6) and ISGs (B) (n = 6) in WT and IRF3/7^{-/-} MEFs untreated or treated with LPS (100 ng/ml) for 6 h. Data in (A) were normalized to the untreated control (CTR, set as 1). Data in (B) were normalized to untreated WT and IRF3/7^{-/-} MEFs, respectively (both set as 1). **P < 0.01.

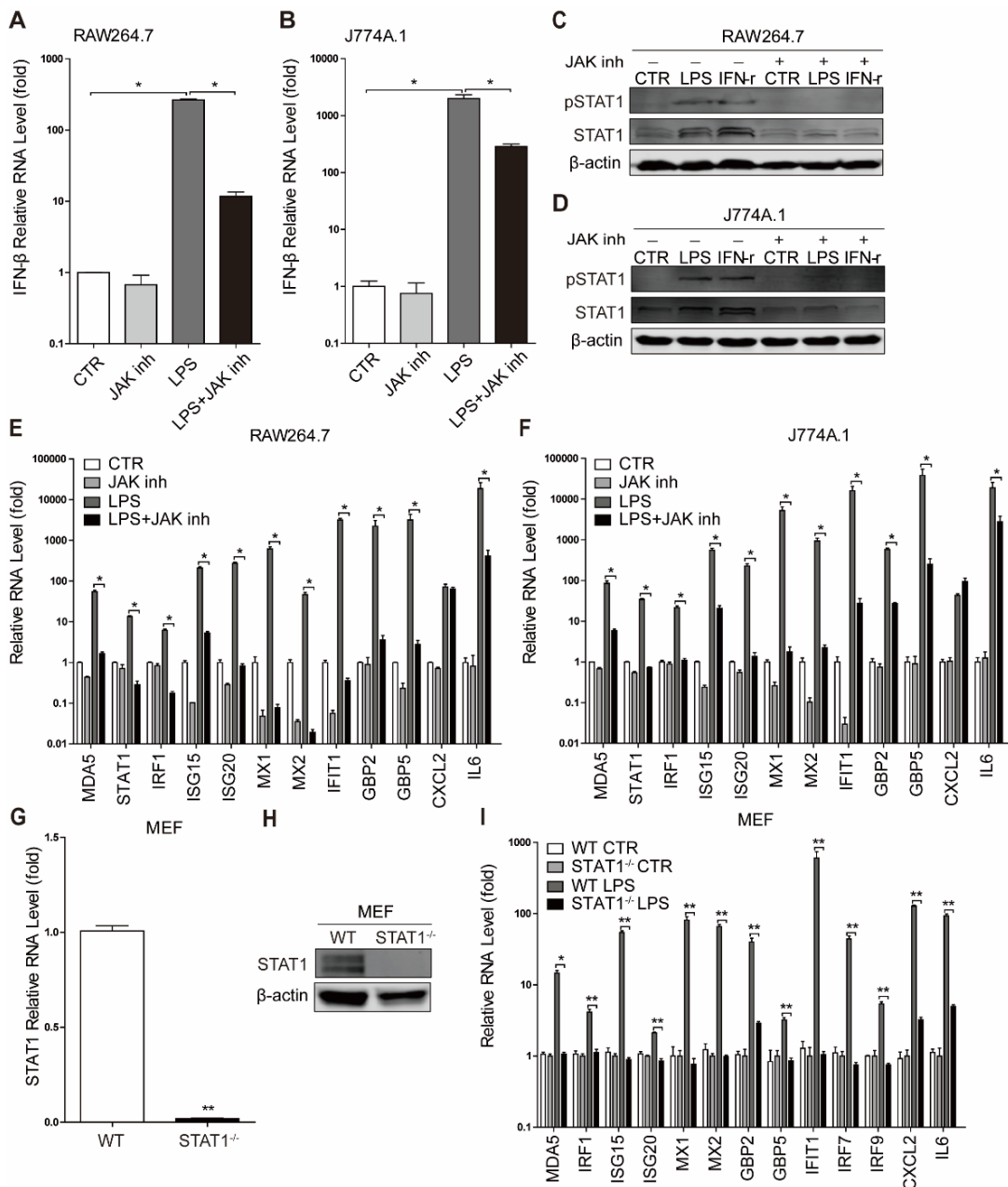


Figure 7. LPS induces ISG transcription largely through activation of JAK-STAT pathway. qRT-PCR analysis of IFN- β mRNA levels in RAW264.7 cells (A) and J774A.1 cells (B) untreated or treated with LPS (100 ng/ml) or JAK inhibitor 1 (10 μ M) for 6 h (n = 4). Western blotting analysis of STAT1 expression and phosphorylation in RAW264.7 cells (C) and J774A.1 cells (D) untreated or treated with LPS (100 ng/ml), IFN- γ (100 U/ml), JAK inhibitor 1 (10 μ M) or combination for 6 h. qRT-PCR analysis of ISG mRNA levels in RAW264.7 cells (E) and J774A.1 cells (F) untreated or treated with LPS (100 ng/ml), IFN- γ (100 U/ml), JAK inhibitor 1 (10 μ M) or combination for 6 h (n = 4). WT and STAT1^{-/-} MEFs were analyzed to determine the relative abundance of STAT1 mRNA level (G) by qRT-PCR (n = 6) and protein level (H) by western blotting. (I) qRT-PCR analysis of ISG mRNA levels in WT and STAT1^{-/-} MEFs untreated or treated with LPS (100 ng/ml) for 6 h (n = 6). Data in (A, B, E, F and G) were normalized to untreated control (CTR, set as 1). Data in (I) were normalized to untreated WT and STAT1^{-/-} MEFs, respectively (both set as 1). *P < 0.05; **P < 0.01. β -actin was used as a loading control.

LPS induces ISG transcription largely through activation of JAK-STAT pathway

The JAK-STAT signaling pathway has been shown to be essential for LPS-mediated gene expression in macrophages (34,35). Consistent with these results, we also observed that LPS induced the expression and phosphorylation of STAT1 in both RAW264.7 and J774A.1 cells, respectively (Fig. 7C and 7D). To determine whether ISG induction by LPS is through the activation of STAT1, we used JAK-STAT inhibitor to pharmacologically block the JAK-STAT pathway. We found that JAK inhibitor 1 partially blocked LPS induced transcription of IFN- β in both RAW264.7 and J774A.1 cells (Fig. 7A and 7B), while both the expression and phosphorylation of STAT1 triggered by LPS and IFN- γ were largely attenuated by this inhibitor (Fig. 7C and 7D). Next, we tested the mRNA level of some ISGs in LPS-stimulated macrophages treated with JAK inhibitor 1, and found that most of the LPS inducible genes were affected by JAK inhibitor 1 (Fig. 7E and 7F), without triggering major cytotoxicities (Supplementary Fig. 5D). In addition, the mRNA levels of these genes induced by IFN- γ were largely diminished by this inhibitor (Supplementary Fig. 5A and 5B).

To further confirm the ISG induction ability of LPS is partially dependent on the JAK-STAT pathway, we performed experiments with MEFs from WT and STAT1^{-/-} mice to examine the effect of STAT1 on ISG expression (Fig. 7G and 7H). We found that the abundance of detected ISGs triggered by LPS were also largely decreased in STAT1^{-/-} cells compared to those in WT cells (Fig. 7I). As a control, the transcription of IFN- γ induced ISGs was significantly blocked in STAT1^{-/-} cells (Supplementary Fig. 5C). Together, these results demonstrated that LPS activates ISG transcription largely through the activation of the JAK-STAT pathway.

In respect to the anti-MNV effects of LPS, we found that Bay 11-7085, the NF- κ B signaling inhibitor, partially reversed LPS and IFN- γ -mediated antiviral response against MNV-1 infection in RAW264.7 cells (Fig. 8A and 8E). Similar results were also observed in J774A.1 cells (Fig. 8B). Interestingly, the inhibitor alone enhanced viral replication (Fig. 8A, 8B and 8E), suggesting a basal defense mechanism of NF- κ B signaling against MNV-1 infection. Moreover, we also determined the role of JAK-STAT pathway in LPS-mediated antiviral activity and found that the anti-MNV activity of LPS was only moderately reversed, whereas the anti-MNV effect of IFN- γ was largely abolished by JAK inhibitor 1 (Fig. 8C-8E). Together, these results have demonstrated that NF- κ B cascade contributes to LPS-mediated control of MNV-1 replication partially through the JAK-STAT pathway.

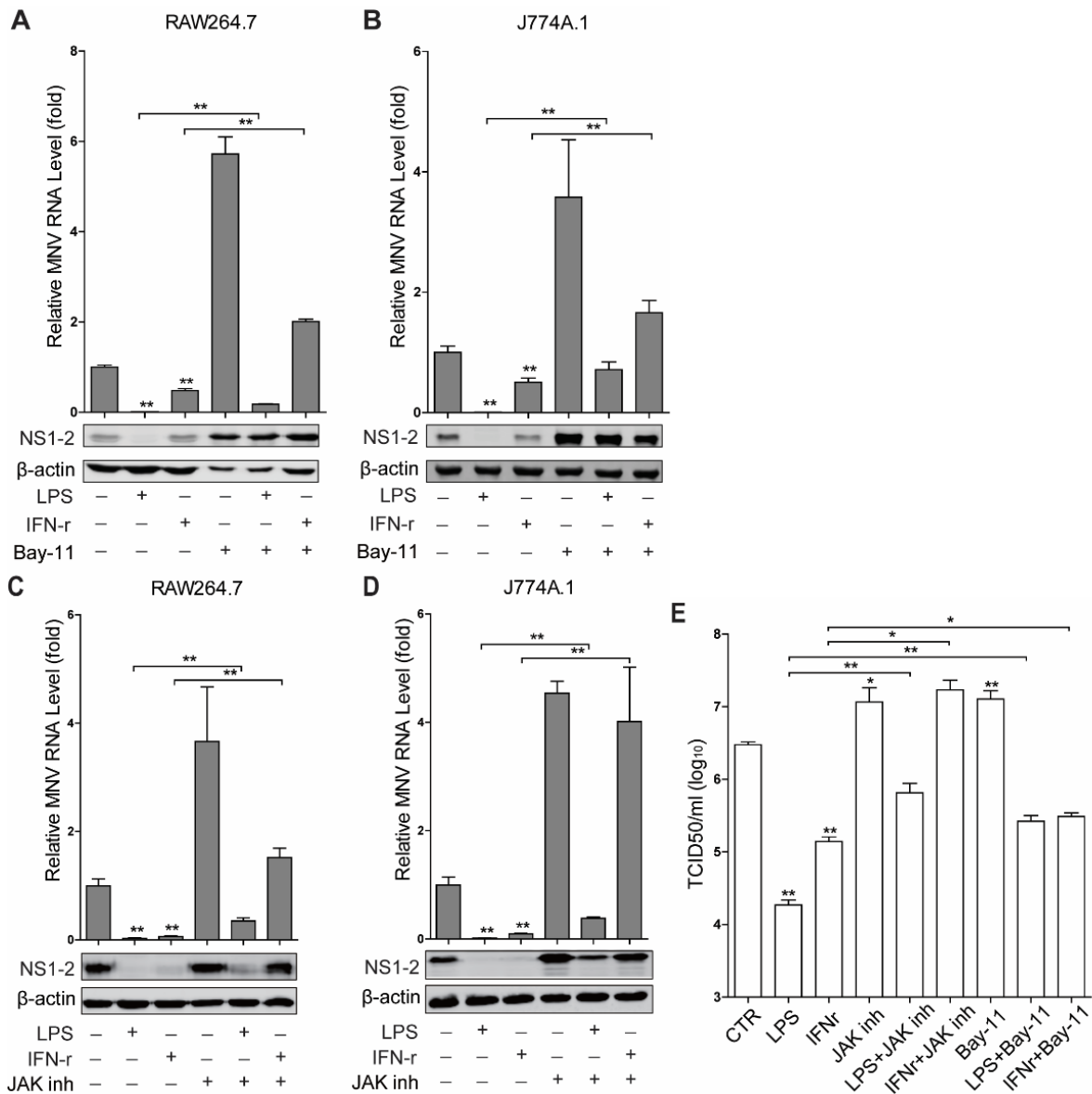


Figure 8. The NF-κB cascade contributes to LPS-mediated inhibition of MNV-1 replication partially through the JAK-STAT pathway. qRT-PCR (n = 6) and western blotting analysis of MNV-1 viral RNA and protein levels in RAW264.7 cells (A) and J774A.1 cells (B) untreated or treated with LPS (100 ng/ml), IFN-γ (100 U/ml), Bay 11-7085 (5 μM) or combination for 6 h, then infected with MNV-1 (MOI 1) for 24 h. qRT-PCR (n = 6) and western blotting analysis of MNV-1 viral RNA and protein levels in RAW264.7 cells (C) and J774A.1 cells (D) untreated or treated with LPS (100 ng/ml), IFN-γ (100 U/ml), JAK inhibitor 1 (10 μM) or combination for 6 h, then infected with MNV-1 (MOI 1) for 24 h. (E) The viral titers were also analyzed by TCID50 assay (n = 4-9). Data were normalized to the untreated control (CTR, set as 1). *P < 0.05; **P < 0.01. β-actin was used as a loading control.

Discussion

Innate immune response provides the first line of defense against viral infection. Studies have revealed that compared to wild-type mice, mice lacking either type I and type II IFN receptors or STAT1 have higher titers and succumb to lethal MNV infection (18,33), indicating the importance of IFNs in controlling norovirus infection. Besides IFNs, inflammasome signaling also has a central role in innate immune response against viral infections (16). Previous evidence indicated the potential role of inflammasome in norovirus replication (19). However, in this study, MNV-1 infection failed to adequately activate inflammasome activation in macrophages, although moderate activation of IL-1 β transcription was observed in J774A.1 cells. Similar results have been reported that MNV failed to secrete IL-1 β in WT BMDMs, but presented caspase-1 processing ability (20). In inflammasome-incompetent RAW264.7 cells, which lack the expression of ASC, one of the components for inflammasome complex formation (26), MNV-1 infection appeared not to affect IL-1 β transcription. A recent study reported that MNV infection induced mature IL-1 β secretion in STAT1 deficient BMDMs (20). Compared to MNV-1 infection alone, we also observed the increased IL-1 β transcription level induced by MNV-1 with JAK-STAT pathway inhibition. Studies have reported the crosstalk between IFN response and inflammasome activation (36). Here we revealed that inhibition of JAK-STAT pathway reduced MNV-1 infection triggered IFN response, but increased MNV-induced IL-1 β transcription. Moreover, decreased IFN response by inhibition of JAK-STAT pathway resulted in increased viral replication, which might further contribute to the upregulation of IL-1 β transcription. Thus, whether there is a potential crosstalk between IFN response and inflammasome activation in response to MNV infection needs to be further studied.

Norovirus and bacteria are cohabitants of the intestine. Gram-negative bacteria produce a large amount of LPS, which are naturally potent activators of inflammasome. It has been reported that hepatitis B virus (HBV) infection inhibits LPS-induced inflammasome activation, although HBV alone does not activate inflammasome (37). Moreover, studies have revealed that MNV infection can induced mature IL-1 β release in primed BMDMs with TLR2 agonist (Pam3CSK4) and TLR4 agonist (LPS) (20), and here we found that MNV-1 augmented LPS-induced IL-1 β transcription. Interestingly, we observed that LPS inhibited MNV-1 replication, but this inhibitory effect was only slightly reversed by inflammasome inhibitors, suggesting additional mechanisms contributing to the anti-MNV activity of LPS. These inhibitors might have a negative role on LPS-triggered expression of inflammatory factors, which could aid to LPS-mediated antiviral response against MNV infection to some extent. However, we do not exclude that there could be more active interactions of norovirus with inflammasome in other cell types, which deserve to be further investigated. Moreover, blocking NLRP3 inflammasome

activation has been reported to reduce MNV-induced immunopathology in STAT1-deficient mice (20). In addition, we found that inflammasome inhibitors alone appear not to affect the viral replication, and similar results were also demonstrated that MNV replication rates were not affected in WT or NLRP3^{-/-} BMDMs (20).

As a type of PRRs, TLRs are responsible for the recognition of infectious agents leading to activation of innate immune response (38). It has been reported that TLR7 activation by its agonists displays potent antiviral effects against norovirus infection by stimulating innate immune response genes (39). As a ligand of TLR4, LPS can activate transcription factors NF- κ B and IRFs, leading to the activation of IFN signaling (32). IFNs are central to the innate control of MNV infection (40-42). Here we found that LPS potently induces IFN- β transcription, and pharmacological inhibition of NF- κ B signaling significantly blunts LPS-triggered IFN- β transcription, which is further confirmed in NF- κ B deficient cells. Moreover, transcription factors IRF3 and IRF7 can regulate IFN-mediated inhibition of MNV-1 replication (33), and we found in this study that IFN- β transcription induced by LPS is largely attenuated in IRF3 and IRF7 deficient cells.

ISGs are regarded as the ultimate antiviral effectors, and several ISGs such as IRF1, ISG15 and GBP2 have been reported to mediate the anti-norovirus effect of IFN (43-46). In this study, we found that LPS also potently triggers ISG expression via the transcription factors including NF- κ B, IRF3 and IRF7. Moreover, blocking NF- κ B signaling attenuates LPS and IFN- γ mediated control of MNV-1 replication. JAK-STAT pathway is essential for IFN-induced ISG expression (34,47) and host innate immunity against MNV infection (18). We revealed that induction of ISGs triggered by LPS or IFN- γ are dramatically decreased by inhibition of the JAK-STAT pathway, which also largely abolishes IFN- γ mediated inhibition for MNV-1 replication. However, blocking this pathway partially reverses LPS-mediated anti-MNV ability. This indicates that LPS-triggered ISGs are partially responsible for its antiviral response against MNV-1 infection in macrophages, and other unknown antiviral mechanisms mediated by LPS may be involved. Furthermore, the non-canonical mechanisms regulating ISG transcription have been reported (48). Induction of ISGs via NF- κ B cascade might do not require JAK-STAT signaling, and this may account for the partial restoration of MNV replication by the inhibitors.

Accumulating evidences have demonstrated the interaction between gut microbiota and intestinal viruses including norovirus (49-51). Several mechanisms have been reported on how intestinal viruses interact with bacteria. On one hand, gut microbiota has been revealed to facilitate MNV replication through an antagonistic mechanism to IFN- λ in the intestine (50), and prompt HuNV infection in intestinal B cells (51). Bacterial component of the enteric microbiome plays an essential role in the establishment of viral persistent infection. For instance, histo-blood group antigen (HBGA)-like substances improve virion stability and

protect HuNV from acute heat stress (52), and infection of B cells (51). It has been also reported that LPS binding promotes viral infectivity by enhancing virion stability and cell attachment (53,54), but fails to enhance HuNV infection of B cells *in vitro* (51), and inhibits MNV-1 replication in macrophages in this study. On the other hand, previous studies have presented the antagonistic mechanisms that *Enterobacter cloacae*, a member of enteric commensal bacteria specifically binds HuNV, and inhibits virus infectivity in gnotobiotic pigs by enhancing the gut immunity (55). In addition, the microbiota-host interaction can also modulate the production of immune system molecules, resulting in anti-MNV effects. Thus, the interactions between intestinal bacteria and viruses collectively modulate the infection outcomes.

In summary, our study demonstrates that MNV-1 moderately triggers IL-1 β transcription, and is augmented by inhibition of IFN pathway in macrophages. Importantly, LPS potently inhibits MNV-1 replication, might through inflammasome to some extent but mainly via the NF- κ B cascade. Activation of NF- κ B by LPS drives the expression of IFN- β through IRF3 and IRF7. This activates the downstream antiviral ISGs via the JAK-STAT pathway. Moreover, inhibition of NF- κ B and JAK-STAT signaling partially reversed the anti-MNV activity of LPS, suggesting additional antiviral mechanisms activated by NF- κ B, which need to be further studied. Our study has revealed new insight in virus-cell interactions, and may provide rationale for new therapeutic development against norovirus infection.

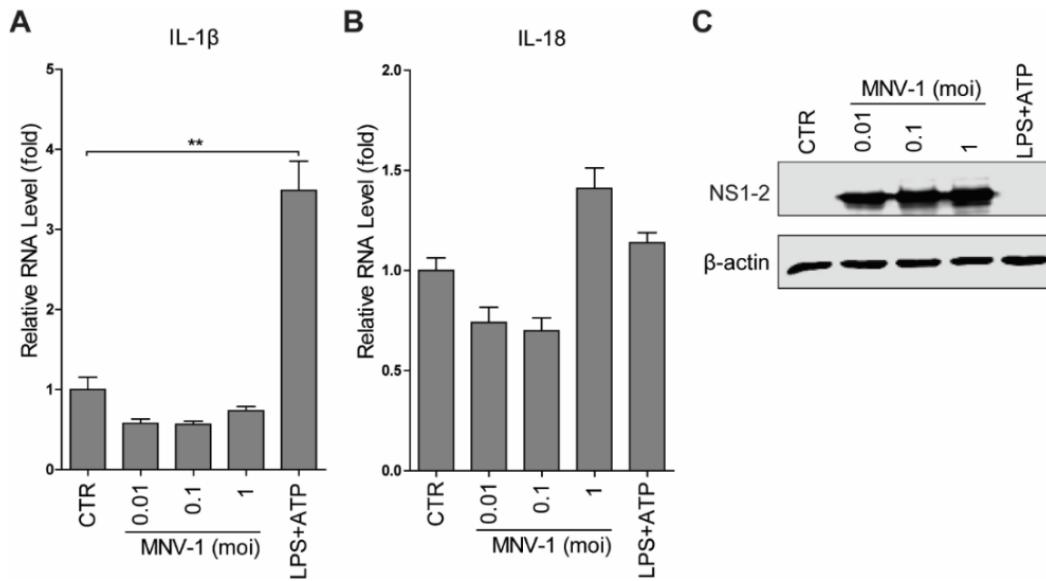
References

1. Karst, S. M., Wobus, C. E., Goodfellow, I. G., et al. (2014) Advances in norovirus biology. *Cell Host Microbe* 15, 668-680
2. Ettayebi, K., Crawford, S. E., Murakami, K., et al. (2016) Replication of human noroviruses in stem cell-derived human enteroids. *Science*, aaf5211
3. Jones, M. K., Grau, K. R., Costantini, V., et al. (2015) Human norovirus culture in B cells. *Nature Protoc* 10, 1939
4. Van Dycke, J., Ny, A., Conceicao-Neto, N., et al. (2019) A robust human norovirus replication model in zebrafish larvae. *PLoS Pathog* 15, e1008009
5. Sato, S., Hisaie, K., Kurokawa, S., et al. (2019) Human Norovirus Propagation in Human Induced Pluripotent Stem Cell-Derived Intestinal Epithelial Cells. *Cell Mol Gastroenterol Hepatol* 7, 686-688 e685
6. Chang, K.-O., Sosnovtsev, S. V., Belliot, G., et al. (2006) Stable expression of a Norwalk virus RNA replicon in a human hepatoma cell line. *Virology* 353, 463-473
7. Wobus, C. E., Karst, S. M., Thackray, L. B., et al. (2004) Replication of Norovirus in cell culture reveals a tropism for dendritic cells and macrophages. *PLoS Biol* 2, e432
8. Wobus, C. E., Thackray, L. B., and Virgin, H. W. (2006) Murine norovirus: a model system to study norovirus biology and pathogenesis. *J Virol* 80, 5104-5112
9. Wu, J., and Chen, Z. J. (2014) Innate immune sensing and signaling of cytosolic nucleic acids. *Annu Rev Immunol* 32, 461-488

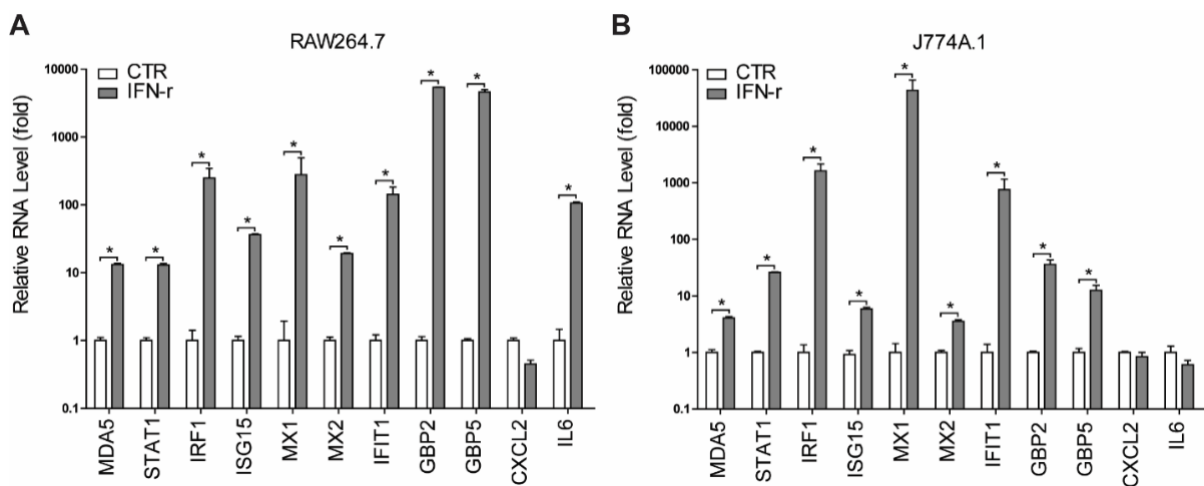
10. Schneider, W. M., Chevillotte, M. D., and Rice, C. M. (2014) Interferon-stimulated genes: a complex web of host defenses. *Annu Rev Immunol* 32, 513-545
11. Schoggins, J. W., Wilson, S. J., Panis, M., et al. (2011) A diverse range of gene products are effectors of the type I interferon antiviral response. *Nature* 472, 481
12. Man, S. M. (2018) Inflammasomes in the gastrointestinal tract: infection, cancer and gut microbiota homeostasis. *Nat Rev Gastroenterol Hepatol*, 1
13. Chen, I. Y., and Ichinohe, T. (2015) Response of host inflammasomes to viral infection. *Trends Microbiol* 23, 55-63
14. Lu, Y. C., Yeh, W. C., and Ohashi, P. S. (2008) LPS/TLR4 signal transduction pathway. *Cytokine* 42, 145-151
15. Broz, P., and Dixit, V. M. (2016) Inflammasomes: mechanism of assembly, regulation and signalling. *Nat Rev Immunol* 16, 407-420
16. Zhu, S., Ding, S., Wang, P., et al. (2017) Nlrp9b inflammasome restricts rotavirus infection in intestinal epithelial cells. *Nature* 546, 667
17. Ichinohe, T., Lee, H. K., Ogura, Y., et al. (2009) Inflammasome recognition of influenza virus is essential for adaptive immune responses. *J Exp Med* 206, 79-87
18. Karst, S. M., Wobus, C. E., Lay, M., et al. (2003) STAT1-dependent innate immunity to a Norwalk-like virus. *Science* 299, 1575-1578
19. Wang, P., Zhu, S., Yang, L., et al. (2015) Nlrp6 regulates intestinal antiviral innate immunity. *Science* 350, 826-830
20. Dubois, H., Sorgeloos, F., Sarvestani, S. T., et al. (2019) Nlrp3 inflammasome activation and Gasdermin D-driven pyroptosis are immunopathogenic upon gastrointestinal norovirus infection. *PLoS Pathog* 15, e1007709
21. Baker, E. S. (2012) *Characterisation of the NS1-2 and NS4 proteins of murine norovirus*, University of Otago
22. Mäkelä, S. M., Österlund, P., Westenius, V., et al. (2015) RIG-I signaling is essential for influenza B virus-induced rapid interferon gene expression. *J Virol*, 01576-01515
23. Nandakumar, R., Finsterbusch, K., Lipps, C., et al. (2013) Hepatitis C virus replication in mouse cells is restricted by IFN-dependent and-independent mechanisms. *Gastroenterology* 145, 1414-1423. e1411
24. Hwang, S., Alhatlani, B., Arias, A., et al. (2014) Murine norovirus: propagation, quantification, and genetic manipulation. *Curr Protoc Microbiol* 33, 15K. 12.11-15K. 12.61
25. Hirano, S., Zhou, Q., Furuyama, A., et al. (2017) Differential Regulation of IL-1 β and IL-6 Release in Murine Macrophages. *Inflammation* 40, 1933-1943
26. He, W.-t., Wan, H., Hu, L., et al. (2015) Gasdermin D is an executor of pyroptosis and required for interleukin-1 β secretion. *Cell Res* 25, 1285
27. Agnihothram, S. S., Basco, M. D. S., Mullis, L., et al. (2015) Infection of murine macrophages by *Salmonella enterica* serovar Heidelberg blocks murine norovirus infectivity and virus-induced apoptosis. *PLoS One* 10, e0144911
28. Li, D., Breiman, A., Le Pendu, J., et al. (2016) Anti-viral Effect of *Bifidobacterium adolescentis* against Noroviruses. *Front Microbiol* 7, 864
29. MacParland, S. A., Ma, X.-Z., Chen, L., et al. (2016) LPS and TNF- α inhibit interferon-signaling in hepatocytes by increasing USP18 expression. *J Virol* 02557-02515
30. Guha, M., and Mackman, N. (2001) LPS induction of gene expression in human monocytes. *Cell Signal* 13, 85-94
31. Beutler, B., and Rietschel, E. T. (2003) Innate immune sensing and its roots: the story of endotoxin. *Nat Rev Immunol* 3, 169
32. Moynagh, P. N. (2005) TLR signalling and activation of IRFs: revisiting old friends from the NF- κ B pathway. *Trends Immunol* 26, 469-476
33. Thackray, L. B., Duan, E., Lazear, H. M., et al. (2012) Critical role for IRF-3 and IRF-7 in type I interferon-mediated control of murine norovirus replication. *J Virol* 01824-01812

34. Ohmori, Y., and Hamilton, T. A. (2001) Requirement for STAT1 in LPS - induced gene expression in macrophages. *J Leukocyte Biol* 69, 598-604
35. Kovarik, P., Stoiber, D., Novy, M., et al. (1998) Stat1 combines signals derived from IFN - γ and LPS receptors during macrophage activation. *EMBO J* 17, 3660-3668
36. Kopitar-Jerala, N. (2017) The role of interferons in inflammation and inflammasome activation. *Front Immunol* 8, 873
37. Yu, X., Lan, P., Hou, X., et al. (2017) HBV inhibits LPS-induced NLRP3 inflammasome activation and IL-1 β production via suppressing the NF- κ B pathway and ROS production. *J Hepatol* 66, 693-702
38. Hertzog, P. J., O'Neill, L. A., and Hamilton, J. A. (2003) The interferon in TLR signaling: more than just antiviral. *Trends Immunol* 24, 534-539
39. Tuipulotu, D. E., Netzler, N. E., Lun, J. H., et al. (2018) TLR7 agonists display potent antiviral effects against norovirus infection via innate stimulation. *Antimicrob Agents Chemother*, 02417-02417
40. Changotra, H., Jia, Y., Moore, T. N., et al. (2009) Type I and type II interferons inhibit the translation of murine norovirus proteins. *J Virol* 83, 5683-5692
41. Hwang, S., Maloney, N. S., Bruinsma, M. W., et al. (2012) Nondegradative role of Atg5-Atg12/Atg16L1 autophagy protein complex in antiviral activity of interferon gamma. *Cell Host Microbe* 11, 397-409
42. Nice, T. J., Baldrige, M. T., McCune, B. T., et al. (2015) Interferon- λ cures persistent murine norovirus infection in the absence of adaptive immunity. *Science* 347, 269-273
43. Maloney, N. S., Thackray, L. B., Goel, G., et al. (2012) Essential cell autonomous role for interferon regulatory factor 1 in interferon- γ -mediated inhibition of norovirus replication in macrophages. *J Virol*, 01564-01512
44. Rodriguez, M. R., Monte, K., Thackray, L. B., et al. (2014) ISG15 functions as an interferon-mediated antiviral effector early in the murine norovirus life cycle. *J Virol*, 01422-01414
45. Biering, S. B., Choi, J., Halstrom, R. A., et al. (2017) Viral replication complexes are targeted by LC3-guided interferon-inducible GTPases. *Cell Host Microbe* 22, 74-85. e77
46. Orchard, R. C., Sullender, M. E., Dunlap, B. F., et al. (2019) Identification of antinorovirus genes in human cells using genome-wide CRISPR activation screening. *J Virol* 93, e01324-01318
47. Shuai, K., and Liu, B. (2003) Regulation of JAK-STAT signalling in the immune system. *Nat Rev Immunol* 3, 900
48. Wang, W., Xu, L., Su, J., et al. (2017) Transcriptional Regulation of Antiviral Interferon-Stimulated Genes. *Trends Microbiol* 25, 573-584
49. Miura, T., Sano, D., Suenaga, A., et al. (2013) Histo-blood group antigen-like substances of human enteric bacteria as specific adsorbents for human noroviruses. *J Virol* 87, 9441-9451
50. Baldrige, M. T., Nice, T. J., McCune, B. T., et al. (2015) Commensal microbes and interferon- λ determine persistence of enteric murine norovirus infection. *Science* 347, 266-269
51. Jones, M. K., Watanabe, M., Zhu, S., et al. (2014) Enteric bacteria promote human and mouse norovirus infection of B cells. *Science* 346, 755-759
52. Li, D., Breiman, A., Le Pendu, J., et al. (2015) Binding to histo-blood group antigen-expressing bacteria protects human norovirus from acute heat stress. *Front Microbiol* 6, 659
53. Kuss, S. K., Best, G. T., Etheredge, C. A., et al. (2011) Intestinal microbiota promote enteric virus replication and systemic pathogenesis. *Science* 334, 249-252
54. Robinson, C. M., Jesudhasan, P. R., and Pfeiffer, J. K. (2014) Bacterial lipopolysaccharide binding enhances virion stability and promotes environmental fitness of an enteric virus. *Cell Host Microb* 15, 36-46
55. Lei, S., Samuel, H., Twitchell, E., et al. (2016) Enterobacter cloacae inhibits human norovirus infectivity in gnotobiotic pigs. *Sci Rep* 6, 25017

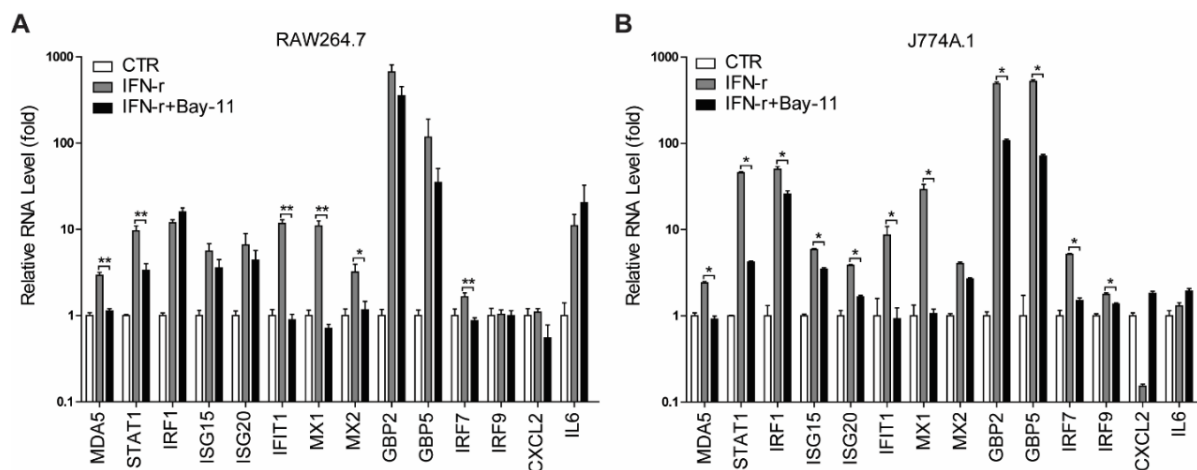
Supplementary information



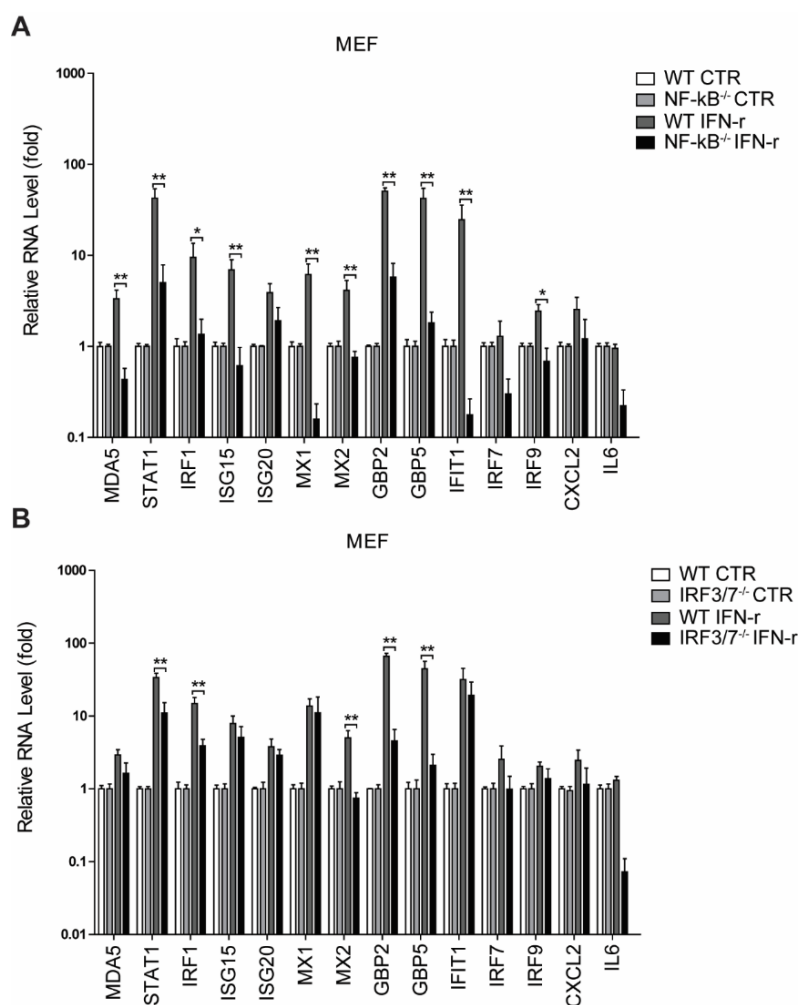
Supplementary Fig. 1 IL-1 β and IL-18 mRNA level were not upregulated by MNV-1 infection in RAW264.7 cells. RAW264.7 cells were untreated or treated with LPS (400 ng/ μ l) for 4 h and then ATP (5 mM) for 40 mins, or left uninfected or infected with MNV-1 at indicated MOIs for 24 h. mRNA levels of IL-1 β (A) and IL-18 (B), and viral infection were analyzed by qRT-PCR (n = 6) and western blotting, respectively. Data were normalized to the untreated control (CTR, set as 1). **P < 0.01. β -actin was used as a loading control.



Supplementary Fig. 2 IFN- γ activates ISG transcription in macrophages. qRT-PCR analysis of ISG mRNA levels in RAW264.7 cells (A) (n = 4), and J774A.1 cells (B) (n = 4) untreated or treated with IFN- γ (100 ng/ μ l) for 6 h. Data were normalized to the untreated control (CTR, set as 1). *P < 0.05.

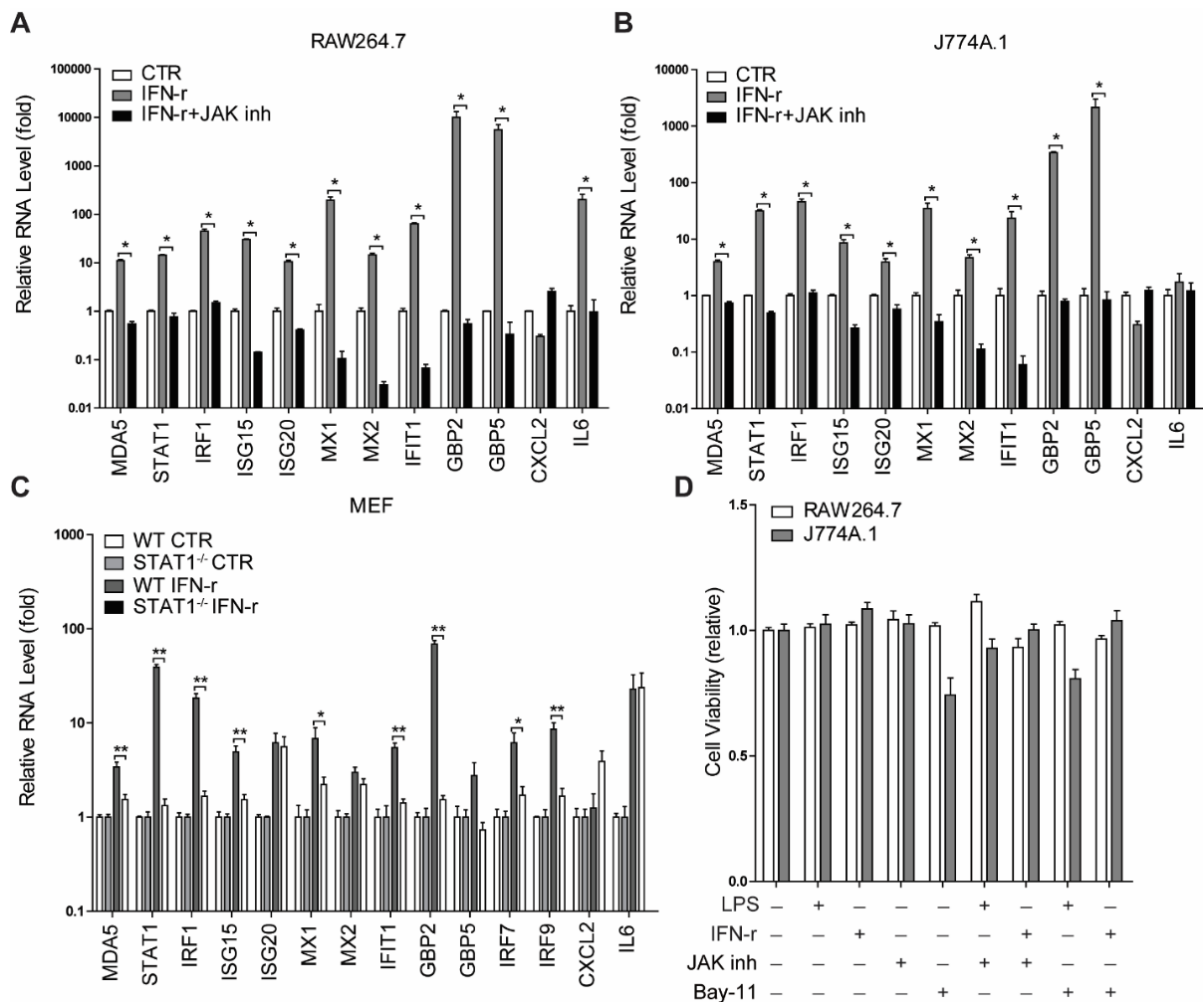


Supplementary Fig. 3 Bay 11-7085 partially diminishes IFN- γ -induced ISG transcription in macrophages. qRT-PCR analysis of ISG mRNA levels in RAW264.7 cells (A) ($n = 6$) and J774A.1 cells (B) ($n = 4$) untreated or treated with IFN- γ (100 ng/ μ l), Bay 11-7085 (5 μ M) or combination for 6 h. Data were normalized to the untreated control (CTR, set as 1). * $P < 0.05$; ** $P < 0.01$.



Supplementary Fig. 4 The ISG induction ability of IFN- γ is attenuated in NF- κ B $^{-/-}$ and IRF3/7 $^{-/-}$ cells. (A) qRT-PCR analysis of ISG mRNA levels in WT and NF- κ B $^{-/-}$ MEFs untreated or treated with IFN- γ (100

ng/ml) for 6 h (n = 6). (B) qRT-PCR analysis of ISG mRNA levels in WT and IRF3/7^{-/-} MEFs untreated or treated with IFN- γ (100 ng/ml) for 6 h (n = 6). Data were normalized to untreated WT and NF- κ B^{-/-} or IRF3/7^{-/-} MEFs, respectively (both set as 1). *P < 0.05; **P < 0.01.



Supplementary Fig. 5 The ISG induction ability of IFN- γ is dependent on JAK-STAT pathway. qRT-PCR analysis of ISG mRNA levels in RAW264.7 cells (A) (n = 4) and J774A.1 cells (B) (n = 4) that untreated or treated with IFN- γ (100 ng/ μ l), JAK inhibitor 1 (10 μ M) or combination for 6 h. (C) qRT-PCR analysis of ISG mRNA levels in WT and STAT1^{-/-} MEFs untreated or treated with IFN- γ (100 ng/ml) for 6 h (n = 6). (D) Cell viability was determined by MTT assay in RAW264.7 and J774A.1 cells untreated or treated with LPS (100 ng/ml), IFN- γ (100 U/ml), JAK inhibitor 1 (10 μ M), Bay 11-7085 (5 μ M) or combination for 6 h (n = 16). Data in (A, B and D) were normalized to the untreated control (CTR, set as 1). Data in (C) were normalized to untreated WT and STAT1^{-/-} MEFs, respectively (both set as 1). *P < 0.05; **P < 0.01.

Supplementary Table 1. qRT-PCR primer sequences (mouse)

Gene	F-Sequences (5' to 3')	R-Sequences (5' to 3')
mGAPDH	TTCCAGTATGACTCCACTCACGG	TGAAGACACCAGTAGACTCCACGAC
mIL-1 β	GCCACCTTTTGACAGTGATGAG	ATGTGCTGCTGCGAGATTTG
mIL-18	CAGGCCTGACATCTTCTGCAA	TCTGACATGGCAGCCATTGT
mIFN- α	GGATGTGACCTTCCTCAGACTC	ACCTTCTCCTGCGGGAATCCAA
mIFN- β	AAGAGTTACTGCTTTCATC	CACTGTCTGCTGGTGGAGTTCATC
mIFN- γ	GATATCTGGAAGGAAGTGGCAAAG	AGAGATAATCTGGCTCGGCTCTGCAGGAT
mMDA5	GTGATGACGAGGCCAGCAGTTG	ATTCATCCGTTTCGTCCAGTTTCA
mSTAT1	GCCTCTCATTGTCACCGAAGAAC	TGGCTGACGTTGGAGATCACCA
mIRF1	CAGAGGAAAGAGAGAAAGTCC	CACACGGTGACAGTGCTGG
mISG15	TGACGCAGACTGTAGACACG	TGGGGCTTTAGGCCATACTC
mISG20	CAATGCCCTGAAGGAGGATA	TGTAGCAGGCGCTTACACAG
mMX1	GGGGAGGAAATAGAGAAAATGAT	GTTTACAAAGGGCTTGCTTGCT
mMX2	CCAGTTCCTCTCAGTCCCAAGATT	TACTGGATGATCAAGGGAACGTGG
mGbp2	ACCAGCTGCACTATGTGACG	TCAGAAGTGACGGGTTTTCC
mGbp5	GTGACAGAAGTACAGACTTGC	CATGCCATTGGCTTGCAAGTC
mIFIT1	CCATAGCGGAGGTGAATATC	GGCAGGACAATGTGCAAGAA
mIFIT2	TCAGCACCTGCTTCATCCAA	CACCTTCGGTATGGCAACTT
mOAS2	CATCCTTCTGCACCAGCTCA	TCAGTAGCTCCAGAACCCA
mIRF7	CCTCTGCTTTCTAGTGATGCCG	CGTAAACACGGTCTTGCTCCTG
mIRF9	CAACATAGGCGGTGGTGGCAAT	GTTGATGCTCCAGGAACACTGG
mCXCL2	CGCTGTCAATGCCTGAAGAC	ACACTCAAGCTCTGGATGTTCTTG
mIL6	AGTCCGGAGAGGAGACTTCA	TTGCCATTGCACAACCTTTT
MNV-1	CACGCCACCGATCTGTTCTG	GCGCTGCGCCATCACTC

Supplementary Table 2. qRT-PCR primer sequences (human)

Gene	F-Sequences (5' to 3')	R-Sequences (5' to 3')
GAPDH	TGTCCCCACCCCAATGTATC	CTCCGATGCCTGCTTCACTACCTT
IFN- α	GACTCCATCTTGGCTGTGA	TGATTTCTGCTCTGACAACCT
IFN- β	CTTGGATTCTACAAAGAAGCAG	TCCTCCTTCTGGAAGTCTGCA
STAT1	ATGGCAGTCTGGCGCTGAATT	CCAAACCAGGCTGGCACAATTG
IRF1	GAGGAGGTGAAAGACCAGAGCA	TAGCATCTCGGCTGGACTTCGA
ISG15	CTCTGAGCATCCTGGTGAAGAA	AAGGTCAGCCAGAACAGGTCGT
MX1	GGCTGTTTACCAGACTCCGACA	CACAAAGCCTGGCAGCTCTCTA
IFIT1	GCCTTGCTGAAGTGTGGAGGAA	ATCCAGGCGATAGGCAGAGATC
IRF7	CCACGCTATACCATCTACCTGG	GCTGCTATCCAGGGAAGACACA
IRF9	CCACCGAAGTTCAGGTAACAC	AGTCTGCTCCAGCAAGTATCGG
USP18	AGGAGAAGCGTCCCTTTCCA	TGGTCCTTAATCAGGTTCCAGAG
HuNV GI-specific primer ^a	CGYTGGATGCGNTTYCATGA	CTTAGACGCATCATCATTYAC

a: Y = C + T; R = A + G; W = A+T; N = any

Chapter 4

Guanylate-binding protein 2 orchestrates innate immune responses against murine norovirus and is antagonized by the viral protein NS7

Peifa Yu, Yang Li, Yunlong Li, Zhijiang Miao, Maikel P. Peppelenbosch, Qiuwei Pan

Journal of Biological Chemistry, 2020, 295: 8036-8047.

Abstract

Noroviruses are the main causative agents of acute viral gastroenteritis, but the host factors that restrict their replication remain poorly identified. Guanylate-binding proteins (GBPs) are IFN-inducible GTPases that exert broad antiviral activity and are important mediators of host defenses against viral infections. Here we show that both IFN- γ -stimulation and murine norovirus (MNV) infection induce GBP2 expression in murine macrophages. Results from loss- and gain-of-function assays indicated that GBP2 is important for IFN- γ -dependent anti-MNV activity in murine macrophages. Ectopic expression of MNV receptor (CD300lf) in human HEK293T epithelial cells conferred susceptibility to MNV infection. Importantly, GBP2 potently inhibited MNV in these human epithelial cells. Results from mechanistic dissection experiments revealed that the N-terminal G domain of GBP2 mediates these anti-MNV effects. R48A and K51A substitutions in GBP2, associated with loss of GBP2 GTPase activity, attenuated the anti-MNV effects of GBP2. Finally, we found that non-structural protein 7 (NS7) of MNV co-localizes with GBP2 and antagonizes the anti-MNV activity of GBP2. These findings reveal that GBP2 is an important mediator of host defenses against murine norovirus.

Keywords: murine norovirus (MNV), guanylate-binding protein 2 (GBP2), interferon-stimulated gene (ISG), non-structural protein 7 (NS7), antiviral restriction factor

Introduction

Human norovirus (HuNV) infection is the major cause of epidemic nonbacterial gastroenteritis worldwide (1,2). Currently, there is no vaccination or specific antiviral treatment available. Clinical management is limited to supportive care and oral rehydration, and HuNV imposes a heavy global health burden (3). Thus defining improved anti-HuNV therapy represents an urgent clinical need. Research into HuNV infection, however, has been hampered by the lack of robust experimental models. Murine norovirus (MNV), capable of replicating in both cell culture and small-animal models, shares similar traits with HuNV in structural and genetic features, and has thus been widely used as a surrogate model (4,5). The recent discovery of the MNV receptor (CD300lf) has now enabled MNV infection in human cells by ectopically expressing this receptor. This has resulted in improved understanding of the mechanisms underlying viral replication and the identification of cellular factors as potential antiviral targets (6,7).

Noroviruses are non-enveloped, positive single-stranded RNA virus belonging to the *Caliciviridae* family. The genome is about 7.5 kb in length that encodes three or four ORFs (3,8). The 5' proximal ORF1 encodes a polyprotein that is post-translationally cleaved into six non-structural proteins (NS1/2 to NS7). ORF2 and ORF3 encoding the major and minor structural proteins are referred as VP1 and VP2, respectively, which are translated from a subgenomic RNA. VP2 has been reported to possess important functions in viral replication and virion stability but may also corrupt host immune response (9). Specific for MNV, ORF4 overlaps with ORF2, and produces an additional protein called virulence factor (VF1). VF1 has been reported to antagonize innate immune response to MNV infection (8,9). MNV NS1/2 protein is associated with cell tropism and mediates resistance to interferon- λ (IFN- λ)-mediated clearance used for treating persistent viral infection (10). NS7 is the viral RNA-dependent RNA polymerase that can also modulate innate immune response (11,12). However, the exact interactions of these viral proteins with host innate antiviral immunity remain poorly understood.

IFN-mediated innate immune responses provide the first line of host defense against viral infections. Specific viral components sensed by pathogen recognition receptors including Toll-like receptors and RIG-I-like receptors lead to IFN production (13,14). The released IFNs bind to their cognate receptors to activate Janus kinase (JAK)/signal transducer and activator of transcription (STAT) signaling pathway, resulting in the transcription of hundreds of interferon-stimulated genes (ISGs). A subset of ISGs are considered as the ultimate antiviral effectors limiting viral replication and spread (15). Currently, only a few ISGs have been identified to inhibit MNV infection including interferon regulatory factor 1 (IRF1) and

interferon-stimulated gene 15 (ISG15) (16,17). Thus, it is largely unknown which factors are important for effective cell-autonomous defense against MNV infection.

Interesting candidate molecules to act in the defense against MNV infection are the guanylate-binding proteins (GBPs). They are members of the superfamily of IFN-inducible GTPases with many typical characteristics of ISGs. These proteins are composed of three distinct domains including the N-terminal globular GTPase domain containing all motifs responsible for nucleotide binding and hydrolysis (G domain), the following helical part presenting as the middle domain (M domain), and the C-terminal GTPase effector domain (E domain) (18,19). To date, seven human GBPs and 11 murine GBPs as well as two mouse pseudogenes encoding GBPs have been identified (20,21). Apart from host resistance against bacterial and protozoan pathogens (18,22,23), GBPs (e.g., GBP1, GBP2 and GBP5) have been reported to exert broad antiviral activity against human immunodeficiency virus (HIV), Zika virus, hepatitis C virus (HCV), classical swine fever virus (CSFV) and influenza virus (24-27). They are capable of regulating inflammasome activation (28,29), and this plays a role in controlling replication of rotavirus and influenza virus (30,31). A recent study has indicated that IFN- γ -mediated inhibition of MNV replication and help to block the viral replication complexes formation (32). In this study, we detailed investigated the regulation and function of GBP2 in MNV infection, revealing an important role in orchestrating host response to MNV infection.

Materials and methods

Reagents

Mouse IFN- γ (ab9922, Abcam) was dissolved in PBS. Stocks of JAK inhibitor 1 (SC-204021, Santa Cruz Biotechnology) was dissolved in Dimethyl sulfoxide (DMSO, Sigma) with a final concentration of 5 mg/ml. Puromycin (P8833, Sigma) was dissolved in PBS with a final concentration of 10 mg/mL. Q5[®] Site-Directed Mutagenesis Kit (NEB) was used. GBP2 antibody (11854-1-AP) was purchased from Proteintech. STAT1 (#9172) antibody was purchased from Cell Signaling Technology. Rabbit polyclonal antisera to MNV NS1/2 was kindly provided by Prof. Vernon K. Ward (School of Biomedical Sciences, University of Otago, New Zealand) (33). β -actin antibody (#sc-47778) was purchased from Santa Cruz Biotechnology. Secondary antibodies including IRDye[®] 800CW-conjugated goat anti-rabbit and goat anti-mouse IgGs (Li-Cor Bioscience, Lincoln, USA), and anti-rabbit IgG (H+L), F(ab')₂ Fragment (Alexa Fluor[®] 488 Conjugate) and anti-mouse IgG(H+L), F(ab')₂ Fragment (Alexa Fluor 594 conjugate) were used, as appropriate.

Cells and viruses

RAW264.7, J774A.1, Cos-1 and human embryonic kidney (HEK293T) cells were cultured in Dulbecco's modified Eagle's medium (DMEM; Lonza Verviers, Belgium) supplemented with 10% (vol/vol) heat-inactivated fetal calf serum (FCS; Hyclone, Logan, UT, USA), 100 µg/mL of streptomycin, and 100 IU/mL of penicillin. MNV-1 (murine norovirus strain MNV-1.CW1) (4) was produced by consecutively inoculating the virus (kindly provided by Prof. Herbert Virgin, Department of Pathology and Immunology, Washington University School of Medicine) into RAW264.7 cells. The MNV-1 cultures were purified, aliquoted, and stored at -80°C for all subsequent experiments. The MNV-1 stock was quantified three independent times by the 50% tissue culture infective dose (TCID₅₀).

TCID₅₀

MNV-1 was quantified by TCID₅₀ assay. Briefly, 10-fold dilutions of MNV-1 were inoculated into RAW264.7 cells grown in 96-well tissue culture plate at 1,000 cells/well. The plate was incubated at 37°C for another 5 days, followed by observing the cytopathic effect (CPE) of each well under a light scope. TCID₅₀ was calculated by using the Reed-Muench method.

Plasmid construction and cell transfection

The full-length mouse GBP2 gene was amplified from IFN-γ-stimulated RAW264.7 cells and cloned into pcDNA3.1/Flag-HA (Addgene), pcDNA3.1/Myc-His (provided by Dr. Shuaiyang Zhao, Chinese Academy of Agricultural Sciences), and the lentiviral vector pCDH-CMV-MCS-EF1-GFP-T2A-Puro (Sanbio BV) to generate pFlag-GBP2, pMyc-GBP2 and pCDH-GBP2, respectively. The truncated mutants of GBP2 were further amplified and cloned into the Flag-tagged and lentiviral vectors, respectively. The MNV NS7 gene was amplified from cDNA that was extracted from MNV-1 infected RAW264.7 cells, and cloned into Flag- and Myc-tagged empty vectors, respectively. The Flag-CD300lf vector was kindly provided by Prof. Herbert Virgin (Department of Pathology and Immunology, Washington University School of Medicine) (6). All primer sequences used for plasmid construction are listed in supplementary table 1.

HEK293T cells were transfected with various plasmids at indicated concentrations using FuGENE HD Transfection Reagent (catalog no. E2311; Promega) according to the manufacturer's instructions. Where necessary, the appropriate empty vector was used to maintain a constant amount of plasmid DNA per transfection. At 6 h post-transfection (hpt), fresh DMEM containing 10% FCS replaced the transfection mixture, and the cells were incubated at 37 °C.

Silencing or overexpressing mouse GBP2 by lentiviral vectors

Lentiviral pLKO.1 knockdown vectors (Sigma-Aldrich) targeting mouse GBP2 were obtained from the Erasmus Biomics Center. The lentiviral pseudoparticles were produced in HEK293T cells as previously described (34). After a pilot study, the shRNA vectors exerting optimal gene knockdown were selected. These shRNA sequences are listed in supplementary table 2. Stable gene knockdown cells were generated after lentiviral vector transduction and puromycin (5 µg/mL; Sigma) selection. For stable expression, GBP2 wild-type and truncated overexpression lentiviral vectors were used to generate the GBP2 stable expression RAW264.7 cell lines. Meanwhile, control shRNA and the lentiviral empty vectors were also used as control, respectively.

qRT-PCR

Total RNA was isolated with a Macherey NucleoSpin RNA II Kit (Bioke, Leiden, The Netherlands) and quantified with a Nanodrop ND-1000 (Wilmington, DE, USA). cDNA was synthesized from 500 ng of RNA using a cDNA synthesis kit (TaKaRa Bio, Inc., Shiga, Japan). The cDNA of all targeted genes transcript were quantified by SYBR-Green-based (Applied Biosystems) real-time PCR on the StepOnePlus™ System (Thermo Fisher Scientific Life Sciences) according to the manufacturer's instructions. Human glyceraldehyde-3-phosphate dehydrogenase (GAPDH) and murine GAPDH genes were used as reference genes to normalize gene expression. The relative expression of targeted gene was calculated as $2^{-\Delta\Delta C_T}$, where $\Delta\Delta C_T = \Delta C_{T\text{sample}} - \Delta C_{T\text{control}}$ ($\Delta C_T = C_T[\text{targeted gene}] - C_T[\text{GAPDH}]$). All primer sequences are listed in supplementary table 3.

Western blotting

Cultured cells were lysed in Laemmli sample buffer containing 0.1 M DTT and heated 5 mins at 95°C, then loaded onto a 10% sodium dodecyl sulfate polyacrylamide gel electrophoresis (SDS-PAGE) gel. Proteins were electrophoretically transferred onto a polyvinylidene difluoride (PVDF) membrane (pore size, 0.45 µm; Invitrogen) for 2 h with an electric current of 250 mA. Subsequently, the membrane was blocked with a mixture of 2.5 mL blocking buffer (Odyssey) and 2.5 mL PBS containing 0.05% Tween 20 for 1 h, followed by overnight incubation with primary antibodies (1:1000) at 4°C. The membrane was washed 3 times and then incubated with IRDye-conjugated secondary antibody (1:5000) for 1 h. After washing 3 times, protein bands were detected with the Odyssey 3.0 Infrared Imaging System (Li-Cor Biosciences).

Confocal fluorescence microscopy

HEK293T and Cos-1 cells (3×10^4 cells/well) were cotransfected with pFlag-GBP2 and pMyc-NS7 (1 µg/each) into µ-slide 8-well chamber (Cat. no. 80826; ibidi GmbH) at 37°C for 24 h. The cells were fixed with 4% paraformaldehyde in PBS, permeabilized with 0.2% Triton X-100,

blocked with 5% skim milk for 1 h, reacted with the appropriate antibody, and stained with 4',6-diamidino-2-phenylindole (DAPI). Antibodies used in this study were mouse anti-Flag Mab (F1804; Sigma-Aldrich), rabbit anti-Myc PAb (Cell Signaling), and anti-rabbit IgG (H+L), F(ab')₂ Fragment (Alexa Fluor® 488 Conjugate) or anti-mouse IgG(H+L), F(ab')₂ Fragment (Alexa Fluor 594 conjugate) secondary antibodies. Imaging was performed on a Leica SP5 confocal microscopy using a 63x oil objective.

Statistical analysis

Data are presented as the mean ± SD. Comparisons between groups were performed with Mann-Whitney test using GraphPad Prism 5.0 (GraphPad Software Inc., La Jolla, CA, USA). Differences were considered significant at a P value less than 0.05.

Results

IFN- γ stimulation upregulates GBP2 expression in mouse macrophages

IFN- γ signaling can potently inhibit MNV replication and induce expression of GBPs. In this study, we observed upregulation of GBP2 following IFN- γ treatment in RAW264.7 and J774A.1 cells (Fig. 1A and 1B), two murine macrophage cell lines susceptible to MNV infection. This effect appears to be mediated by canonical JAK/STAT-mediated IFN signaling as the pharmacological compound JAK inhibitor 1 blocked IFN- γ -induced GBP2 expression both on mRNA (Fig. 1C and 1D) and protein levels (Fig. 1E) in RAW264.7 and J774A.1 cells. Furthermore, IFN- γ failed to stimulate GBP2 expression in STAT1 deficient mouse embryonic fibroblasts (MEFs) (Fig. 1F and 1G). We thus concluded that upregulation of GBP2 is part of the canonical IFN- γ response.

GBP2 enhances IFN- γ -mediated inhibition of MNV-1 replication in mouse macrophages

We next examined whether MNV infection could induce GBP2 expression. Interestingly, inoculation of both in RAW264.7 cells (Fig. 2A and 2B) and J774A.1 cells (Fig. 2C) with MNV-1 upregulated GBP2. To investigate the functional implication, we silenced GBP2 expression in RAW264.7 cells by lentiviral shRNAs. The efficacy of this approach was confirmed both with or without IFN- γ treatment (Fig. 3A-3C). Although GBP2 silence *per se* has no major effect on MNV-1 replication, this strategy decreased anti-MNV activity of IFN- γ (Fig. 3D). This is in accordance with a study demonstrating that MNV replicates to a high level in GBP2 deficient

murine bone marrow derived macrophages (BMDMs) in the presence of IFN- γ (33). Thus GBP2 is necessary for the anti-MNV activity of IFN- γ . Furthermore, we succeeded with stable GBP2 overexpression employing a lentiviral vector (Fig. 4A and 4B). This did not affect MNV-1 RNA level (Fig. 4C), but augmented IFN- γ -mediated inhibition of MNV-1 RNA transcription and NS1/2 protein expression (Fig. 4D-4G), as well as the viral titers (Fig. 4H). Thus GBP2 is an important mediator of IFN- γ -triggered inhibition of MNV-1 replication in murine macrophages.

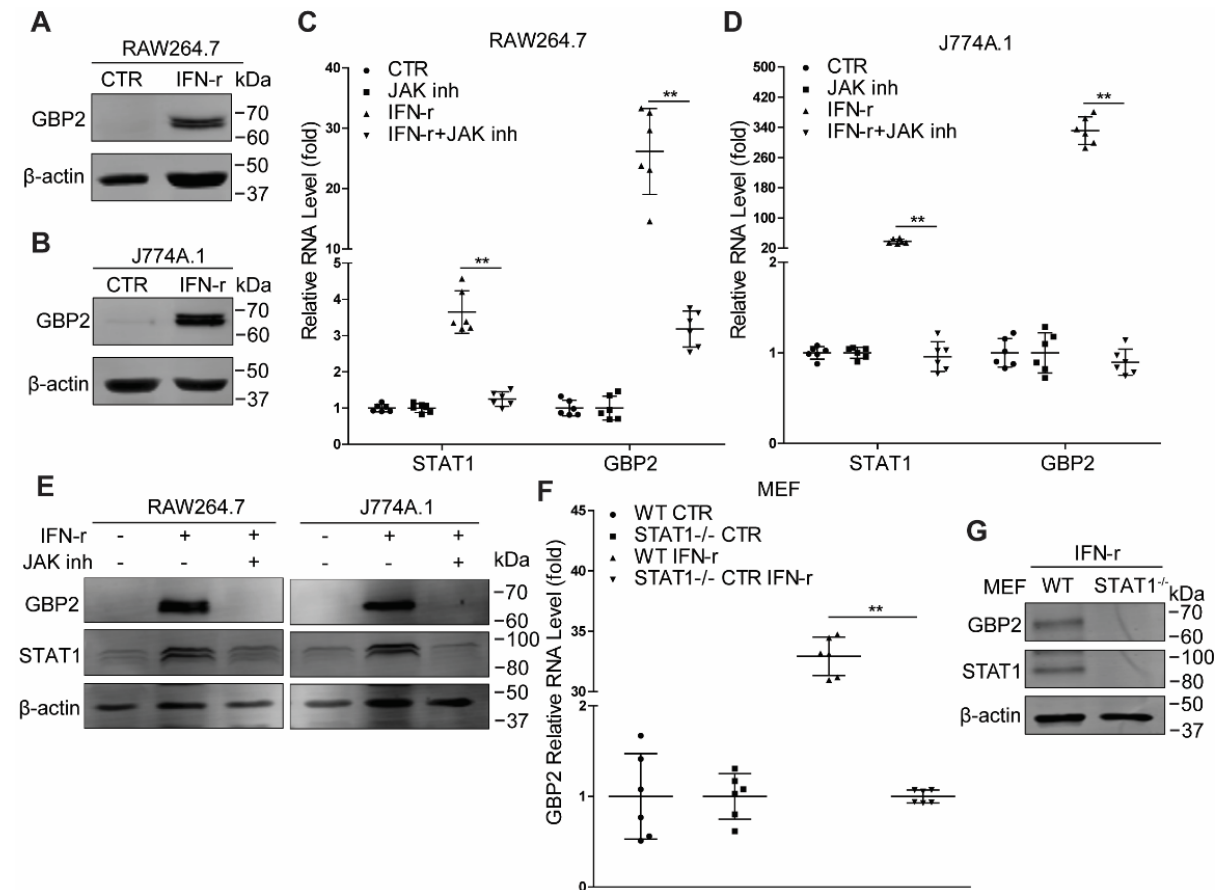


Figure 1. IFN- γ stimulation triggers GBP2 expression in mouse macrophages. Western blotting analysis of GBP2 expression in RAW264.7 (A) and J774A.1 (B) cells that were treated or untreated with IFN- γ (100 U/ml) for 24 h. RAW264.7 and J774A.1 cells were treated or untreated with IFN- γ (100 U/ml) or JAK inhibitor 1 (10 μ M) for 4 h or 6 h, respectively. mRNA (C; n = 6 and D; n = 6), and protein (E) levels of STAT1 and GBP2 were analyzed by qRT-PCR and western blotting, respectively. (F) WT and STAT1^{-/-} MEFs were untreated or treated with IFN- γ (100 U/ml) for 6 h. The mRNA level of GBP2 was analyzed by qRT-PCR (n = 6). (G) Expression of STAT1 and GBP2 in WT and STAT1^{-/-} MEFs treated with IFN- γ (100 U/ml) for 6 h were analyzed by western blotting. Data in (C and D) were normalized to the untreated and JAK inhibitor treated cells (both set as 1). Data in (F) were normalized to untreated WT and STAT1^{-/-} MEFs, respectively (both set as 1). **P < 0.01. β -actin was used as a loading control.

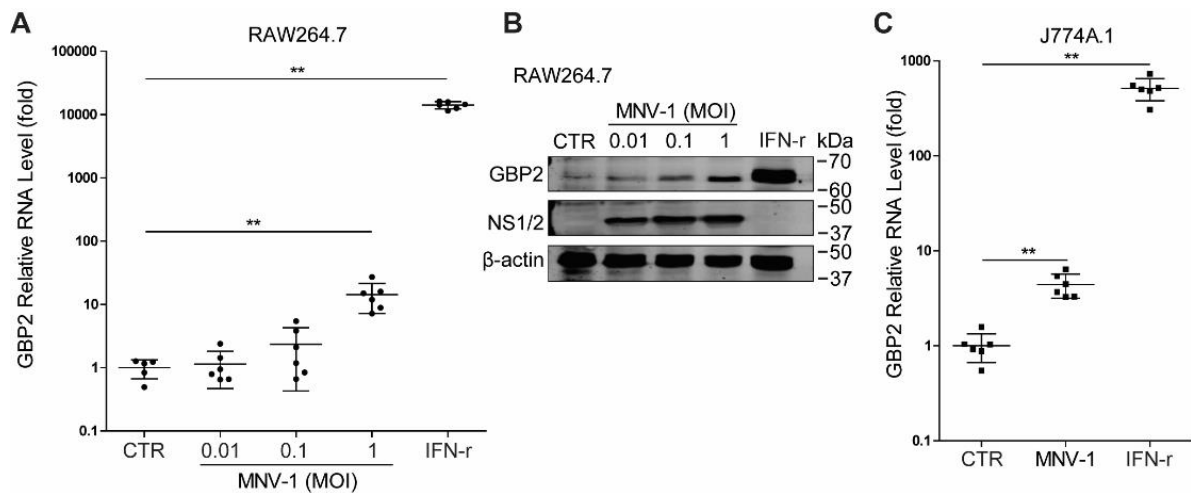


Figure 2. MNV-1 infection upregulates GBP2 expression. RAW264.7 cells were infected with MNV-1 at indicated MOIs or treated with IFN- γ (100 U/ml) for 24 h. (A) The GBP2 mRNA level was analyzed by qRT-PCR (n = 5-6). (B) Expression of GBP2 and MNV NS1/2 were analyzed by western blotting. (C) J774A.1 cells were infected with MNV-1 at a MOI of 1, or treated with IFN- γ (100 U/ml) for 24 h. mRNA level of GBP2 was analyzed by qRT-PCR (n = 6). Data were normalized to the untreated control (CTR, set as 1). **P < 0.01. β -actin was used as a loading control.

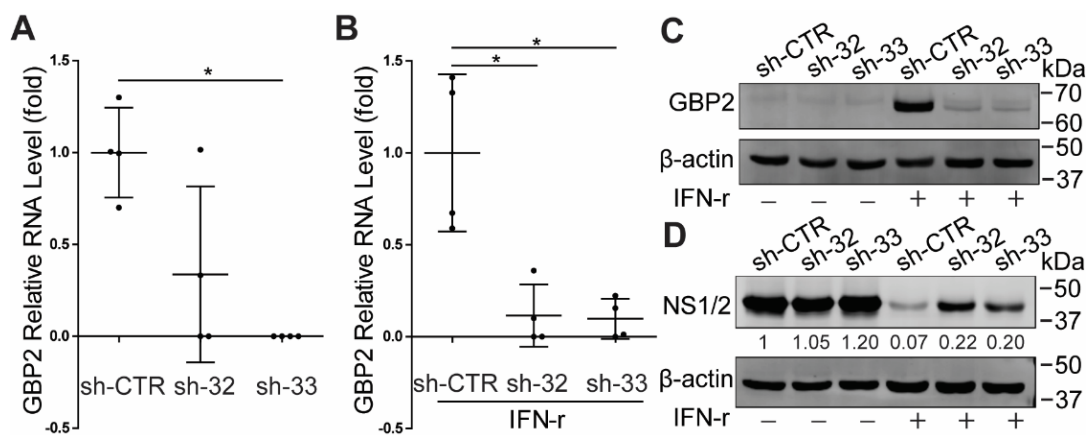


Figure 3. Knockdown of GBP2 attenuates IFN- γ -mediated inhibition of MNV-1 NS1/2 protein expression in mouse macrophages. (A) qRT-PCR analysis of GBP2 knockdown by lentiviral shRNA vectors in RAW264.7 cells (n = 4). (B) qRT-PCR analysis of GBP2 knockdown by lentiviral shRNA vectors in RAW264.7 cells that were stimulated with IFN- γ (100 U/ml) for 6 h (n = 4). (C) Western blotting analysis of GBP2 knockdown by lentiviral shRNA vectors in RAW264.7 cells without or with IFN- γ (100 U/ml) treatment. (D) GBP2-knockdown RAW264.7 cells were infected with MNV-1 at a MOI of 1 for 1 h, then untreated or treated with IFN- γ (100 U/ml) for 24 h. The viral NS1/2 protein level was analyzed by western blotting. Data in (A and B) were normalized to the control (CTR, set as 1). *P < 0.05. β -actin was used as a loading control.

GBP2 overexpression restricts MNV-1 replication in human epithelial cells

Discovery of the MNV receptor (CD300lf) has enabled MNV infection in human cells by ectopic expression of this receptor (6). We found that transfection with FLAG-tagged CD300lf allowed MNV-1 replication in human HEK293T cells (Fig. 5A). Studies have reported that the anti-MNV ability of IFN- γ is impaired in human HAP1 cells with complete loss of GBPs (33). To further examine whether GBP2 exerts anti-norovirus activity in human cells, HEK293T cells were co-transfected with FLAG-tagged CD300lf and different concentrations of GBP2 vectors for 24 h, and subsequently infected with MNV-1 for another 24 h. Mirroring the results in murine macrophages, GBP2 overexpression alone can inhibit MNV-1 shown at both viral RNA (Fig. 5B) and protein levels (Fig. 5C). Furthermore, transfection with Myc-tagged GBP2 into CD300lf expressing HEK293T cells confirmed the inhibitory effects on MNV-1 (Fig. 5D-5F). Thus a role for GBP2 in constraining MNV replication is not restricted to murine macrophages but also extends to human epithelial cells.

Of note, several ISGs with broad antiviral activity, including IRF1, RIG-I and MDA5, have been shown to activate the transcription of many other ISGs (15,35-37). To address whether GBP2 also exerts its action in a similar manner, we measured the transcriptional level of several selected ISGs in RAW264.7 cells in the absence or presence of stable GBP2 overexpression. Overexpression GBP2 did not affect the expression of these tested ISGs (Fig. S1A). This was further confirmed in HEK293T cells (Fig. S1B). These results suggest that the antiviral activity of GBP2 is independent of ISG induction.

The N-terminus of GBP2 is essential for the anti-MNV activity

Structural analysis of human GBP1 has revealed three distinct domains, including the N-terminal globular GTPase domain (G domain), the following two helical part presenting as the middle domain (M domain), and the C-terminal GTPase effector domain (E domain) (19). Based on the human GBP1 structure, we predicted and modelled the mouse GBP2 protein structure (Fig. S2) by using the online software SWISS-MODEL (RRID:SCR_018123) and mapped GBP2 into three corresponding domains (Fig. 6A). To investigate which domain is responsible for the antiviral actions, we constructed Flag-tagged truncated mutants of GBP2, and verified their expression in HEK293T cells (Fig. 6B). Their anti-MNV activities were examined in HEK293T cells transfected with Flag-tagged CD300lf. We found that the G and GM domains of GBP2 inhibited viral replication shown at both viral RNA and protein levels (Fig. 6C and 6D). In contrast, the M, ME and E domains did not exert anti-MNV activity (Fig. 6C and 6D). To further confirm, we established stable expression of GBP2 truncated mutants in RAW264.7 cells (Fig. 6E). These cells were infected with MNV-1 then treated with IFN- γ for 24 h. We found that the G and GM domains of GBP2 enhanced IFN- γ -mediated anti-MNV activity,

whereas the remaining domains appeared not to influence viral replication (Fig. 6F-6H). Taken together, the N-terminus of GBP2 is indispensable for restricting MNV-1 replication in human cells and augmenting IFN- γ -mediated anti-MNV ability in murine macrophages.

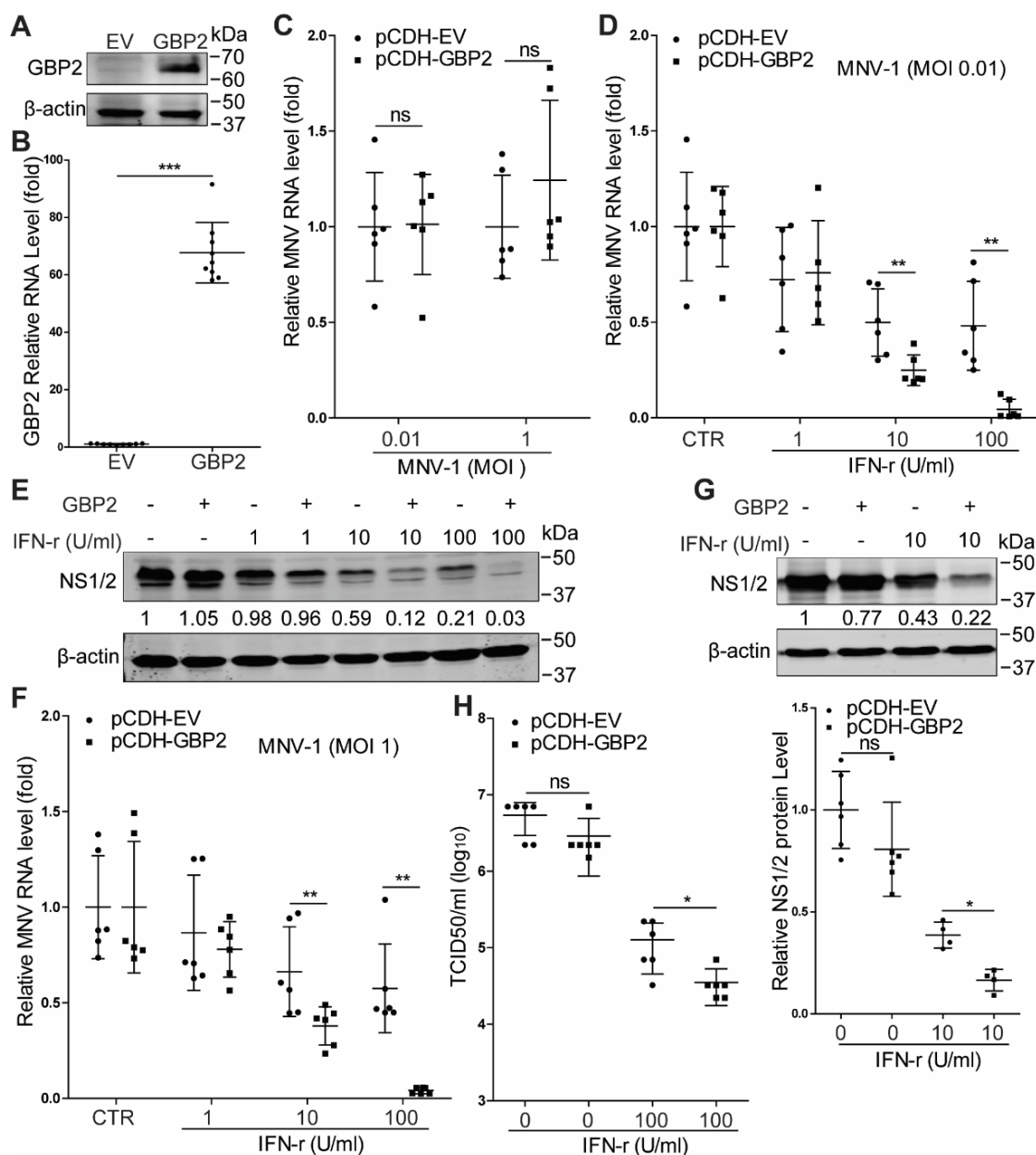


Figure 4. GBP2 overexpression enhances IFN- γ -mediated inhibition of MNV-1 replication in mouse macrophages. (A) HEK293T cells were transfected with pCDH-GBP2 (1 ug) or the empty vectors (1 ug) for 24 h. Western blotting analysis of GBP2 expression by using rabbit anti-GBP2 antibody (1: 1000). (B) qRT-PCR analysis of GBP2 overexpression by lentiviral vectors in RAW264.7 cells (n = 9). (C) qRT-PCR analysis of MNV RNA level (n = 6) in GBP2 stable expression cells that were infected with MNV-1 with indicated MOIs. qRT-PCR (D) analysis of MNV RNA level (n = 5-6) and western blotting (E) analysis of MNV NS1/2 expression in GBP2 stable expression cells that were infected with MNV-1 (MOI 0.01) for 1 h, then treated with indicated concentrations of IFN- γ for 24 h. qRT-PCR (F) analysis of MNV RNA level (n = 6) and western blotting (G) analysis (n = 4-6) of MNV NS1/2 expression in GBP2 stable

expression cells that were infected with MNV-1 (MOI 1) for 1 h, then treated with indicated concentrations of IFN- γ for 24 h. (H) TCID50 assay analysis of viral titers in the supernatants from GBP2 stable expression cells that were infected with MNV-1 (MOI 1) for 1 h, then untreated or treated with IFN- γ for 24 h (n = 6). Data in (B, C, G lower panel and H) were normalized to the untreated control (set as 1). Data in (D and F) were normalized to untreated EV and GBP2 stable expression cells, respectively (both set as 1). *P < 0.05; **P < 0.01; ***P < 0.001; ns, not significant. β -actin was used as a loading control.

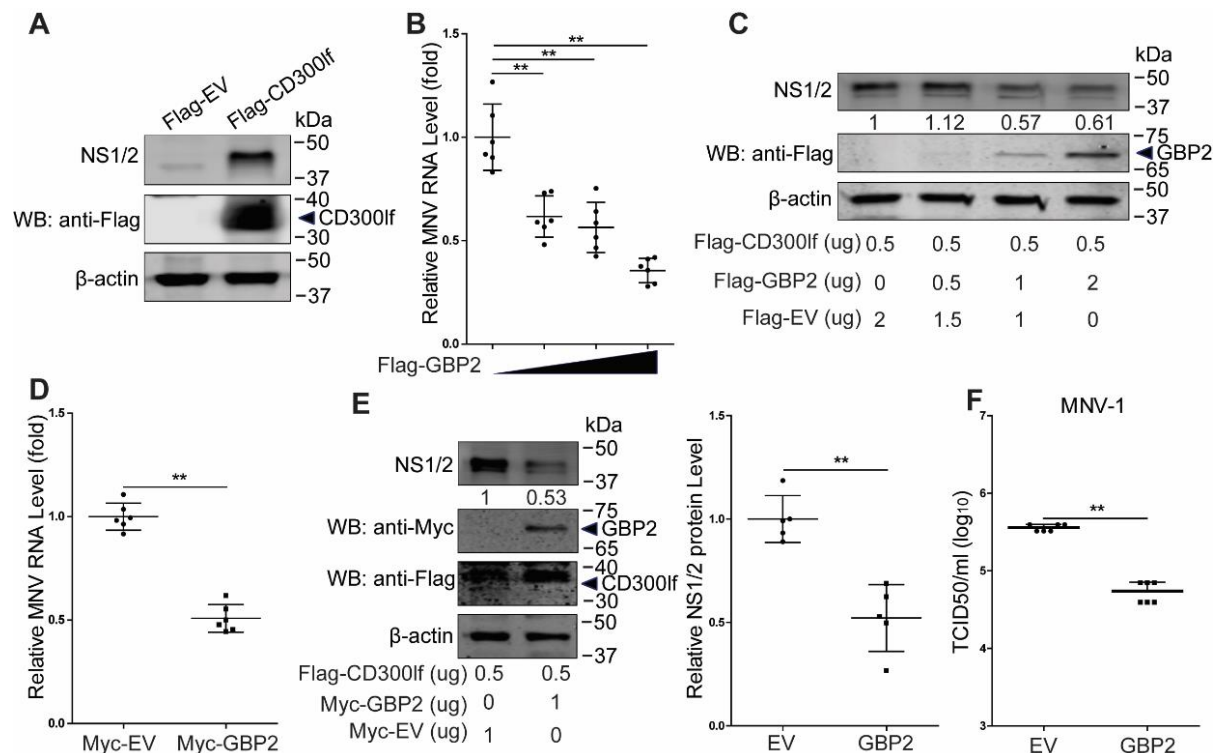


Figure 5. GBP2 restricts MNV-1 replication in human epithelial cells. (A) HEK2923T cells were transfected with the pFlag-CD300lf (0.5 ug) or the empty vectors (0.5 ug) for 24 h, then infected with MNV-1 at MOI of 1 for 24 h. Western blotting analysis of MNV-1 infection by detecting the viral NS1/2 protein. qRT-PCR analysis of MNV RNA (B) (n = 6), and western blotting analysis of MNV NS1/2 and GBP2 proteins (C) in HEK293T cells that were transfected with pFlag-CD300lf (0.5 ug) and pFlag-GBP2 or empty vectors with indicated concentrations, then infected with MNV-1 at MOI of 1 for 24 h. HEK293T cells were transfected with pFlag-CD300lf (0.5 ug) and pMyc-GBP2 (1 ug) or empty vectors (1 ug) for 24 h, then infected with MNV-1 at MOI of 1 for 24 h. The viral RNA and NS1/2 protein levels were analyzed by qRT-PCR (D) (n = 6) and western blotting (E) (n = 5), respectively. (F) HEK293T cells were transfected with pFlag-CD300lf (0.5 ug) and pMyc-GBP2 (1 ug) or empty vectors (1 ug), then infected with MNV-1 at MOI of 1 for 24 h. Viral titers in the supernatants were analyzed by TCID50 assay (n = 6). Data in (B, D, E right panel and F) were normalized to the EV control (set as 1). **P < 0.01. β -actin was used as a loading control.

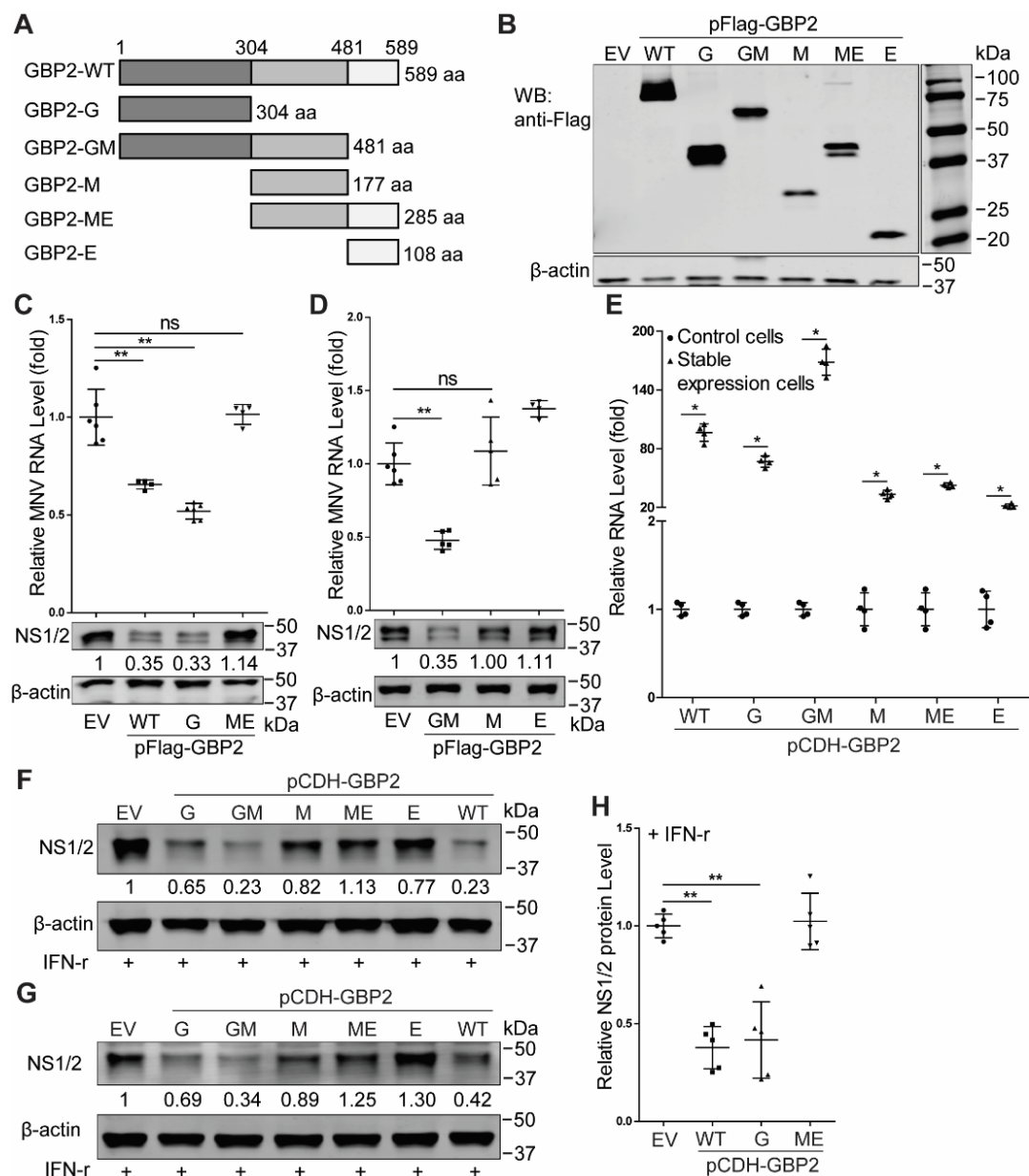


Figure 6. The N-terminus of GBP2 is essential for its anti-MNV activity. (A) Schematic representation of the protein domains of GBP2. (B) Expression of full-length or truncated forms of GBP2. The indicated expression plasmids were transfected into HEK293T cells for 24 h, and the cell lysates were analyzed by western blotting using antibodies against Flag tag and β -actin. (C and D) qRT-PCR ($n = 4-6$) and western blotting analysis of MNV RNA level and NS1/2 protein in HEK293T cells that transfected with pFlag-CD300lf (0.5 μ g) and indicated plasmids (1 μ g) for 24 h, then infected with MNV-1 (MOI 1) for another 24 h. (E) Identification of stable expression of GBP2 truncated mutants by lentiviral vectors in RAW264.7 cells by qRT-PCR assay ($n = 4$). Western blotting analysis of MNV NS1/2 protein level in RAW264.7 cells with stable expression of GBP2 truncated mutants by lentiviral vectors that were infected with MNV-1 at a MOI of 0.01 (F), or at a MOI of 1 (G) for 1 h, then treated with IFN- γ (10 U/ml) for 24 h. (H) Viral NS1/2 protein expression by western blotting was statistically analyzed ($n = 5$). Data in (C, D, E and H) were normalized to the EV control (set as 1). * $P < 0.05$; ** $P < 0.01$; ns, not significant. β -actin was used as a loading control.

The R48 and K51 residues are critical for GBP2 mediated anti-MNV activity

It has been reported that the GTPase activity of GBPs is important for the antiviral activity (27,38). The R48 and K51 residues are important for its GTPase activity of both hGBP1 (38,39), and mGBP2 (40). Thus, we constructed two GBP2 mutants including GBP2 (R48A) and GBP2 (K51A) (Fig. 7A), and confirmed their expression in HEK293T cells (Fig. 7B). To determine the antiviral effects of these two GBP2 mutants, we transfected the constructed mutants and viral receptor vectors into HEK293T cells, then infected with MNV-1 for 24 h. Compared with the wild-type GBP2, these two mutants failed to restrict MNV-1 at both viral RNA (Fig. 7C), and NS1/2 protein levels (Fig. 7D). Measuring viral titers in the supernatants of infected cells further confirmed these results (Fig. 7E). Thus, the R48 and K51 residues of GBP2 are essential for its anti-MNV activity.

MNV NS7 antagonizes the antiviral activity of GBP2

Studies have reported that the viral replicase has a negative regulation on porcine GBP1 mediated inhibition of CSFV (27) and human GBP1 mediated restriction of HCV (36). Thus, we next determined whether the MNV replicase NS7 has a role on GBP2 mediated antiviral activity. We co-transfected pFlag-GBP2 and pFlag-NS7 into HEK293T cells. We found that GBP2 expression was not affected by NS7 expression (Fig. 8A), and NS7 did not affect viral NS1/2 protein expression (Fig. 8B). Moreover, confocal microscopy indicated that besides localization in the nucleus, NS7 could co-localize with GBP2 in the cytoplasm of the cells (Fig. 8C and 8D). To further investigate NS7 on GBP2 mediated antiviral activity, we co-transfected pFlag-CD300lf, pFlag-GBP2 and pMyc-NS7 into HEK293T cells, then infected with MNV-1 for 24 h. We found that NS7 attenuated GBP2 mediated anti-MNV effects shown at both viral RNA and NS1/2 protein levels (Fig. 8E and 8F). These results indicated a potential antagonistic effects of NS7 on GBP2 mediated anti-MNV activity.

Discussion

GBPs as a group of IFN-induced proteins are essential for innate immune response against intracellular bacterial, viral and protozoan pathogens (18,22,25). With respect to viruses, it has been shown that human GBP1 can restrict replication of vesicular stomatitis virus and encephalomyocarditis virus (41), whereas several GBPs have been linked to host defense against HIV, CSFV and influenza virus (25,27,42). A recent study suggested potential interactions between this family of GTPases and norovirus replication (32). Here we further show that GBP2 effectively responds to and defends murine norovirus infection. Our findings

fit well with the increasing momentum and support for the notion that IFN- γ -inducible GTPases are crucial for cell-autonomous host defense against viral infection in general and norovirus in particular (7). We first demonstrated that GBP2 mediates IFN- γ -triggered anti-MNV activity in murine macrophages, whereas GBP2 alone is not sufficient to inhibit MNV. By exploiting ectopic expression of the viral receptors (6), we conferred susceptibility of human HEK293T cells to MNV infection. We further demonstrated that GBP2 alone is sufficient to potently inhibit MNV in human epithelial cells, without requiring the presence of IFN- γ . We speculate that the disparity in requiring IFN- γ may be attributed to the differences in species, cell types and the expression patterns of GBP2.

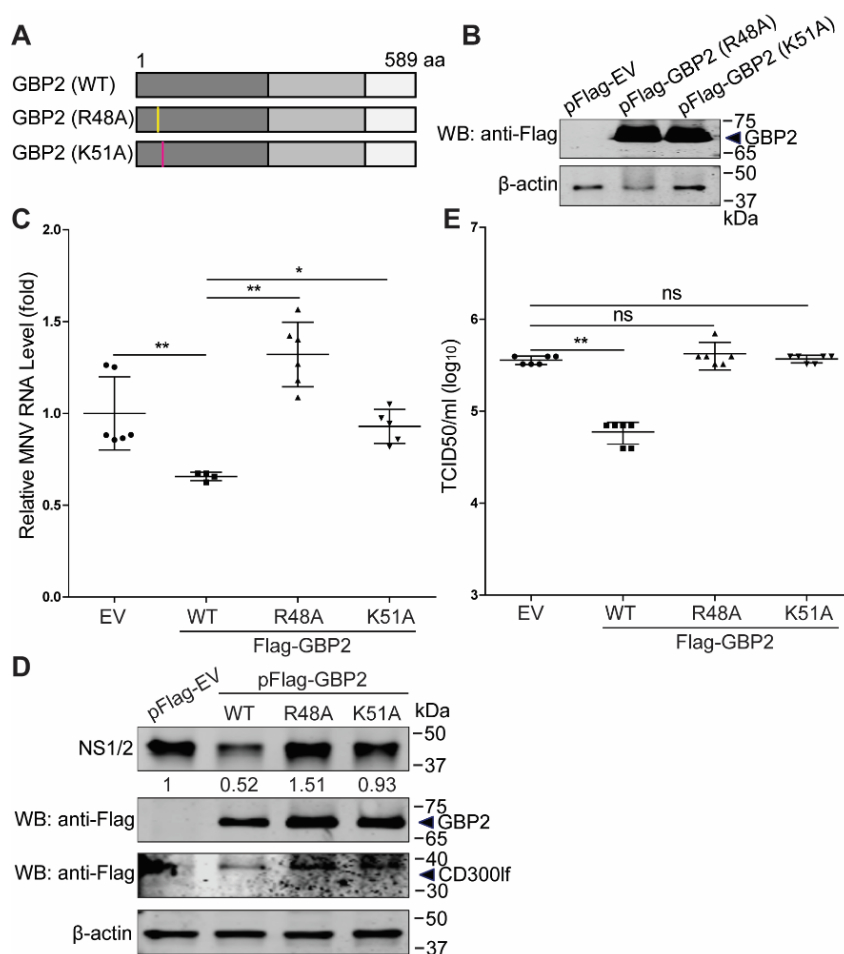


Figure 7. The R48 and K51 residues of GBP2 are critical for its anti-MNV activity. (A) Schematic representation of the GBP2 mutations. (B) Expression of GBP2 mutations. The indicated expression plasmids were transfected into HEK293T cells for 24 h, and the cell lysates were analyzed by western blotting using antibodies against Flag tag and β -actin. HEK293T cells were transfected with pFlag-CD300lf (0.5 μ g), and pFlag-GBP2 (WT), pFlag-GBP2 (R48A), pFlag-GBP2 (K51A) or empty vectors for 24 h, then infected with MNV-1 at a MOI of 1 for 24 h. The MNV RNA (C) ($n = 4-6$), and NS1/2 protein (D) levels were analyzed by qRT-PCR and western blotting, respectively. (E) The viral titers in the supernatants were examined by TCID50 assay ($n = 6$). Data in (C and E) were normalized to the EV control (set as 1). * $P < 0.05$; ** $P < 0.01$; ns, not significant. β -actin was used as a loading control.

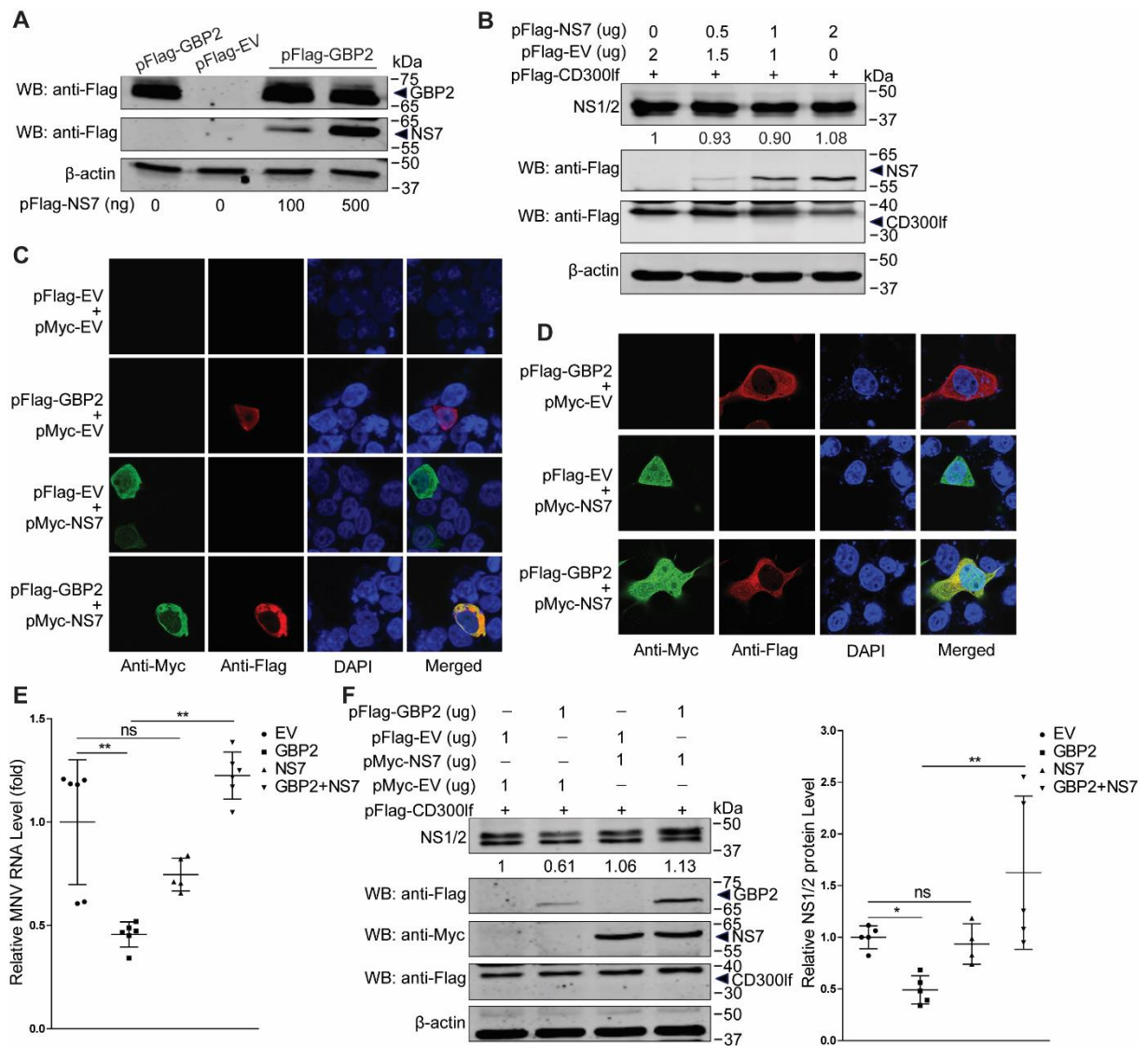


Figure 8. MNV NS7 antagonizes GBP2 mediated anti-MNV activity. (A) HEK293T cells were co-transfected with pFlag-GBP2 (1 ug) and pFlag-EV (1 ug) or pFlag-NS7 with indicated concentrations for 24 h. The cell lysates were collected for analysis by western blotting. (B) HEK293T cells were co-transfected with pFlag-CD300lf (0.5 ug) and pFlag-EV or pFlag-NS7 with indicated concentrations for 24 h, then infected with MNV-1 (MOI 1) for 24 h. The cell lysates were collected for analysis by western blotting using antibodies against the NS1/2, Flag tag and β -actin. Co-localization of GBP2 with MNV NS7 was examined. Expression plasmids pFlag-GBP2 (1 ug) and pMyc-NS7 (1 ug) or the vectors (1 ug) were co-transfected into HEK293T (C) and Cos-1 (D) cells and subjected to a confocal assay, respectively. HEK293T cells were cotransfected with pFlag-CD300lf (0.5 ug), pFlag-GBP2, pMyc-NS7 or the empty vectors with indicated concentrations for 24 h, then infected with MNV-1 (MOI 1) for 24 h. The total RNA and cell lysates were collected and analyzed by qRT-PCR (E) (n = 5-6), and western blotting (F) (n = 4-5). Data in (E and F right panel) were normalized to the EV control (set as 1). *P < 0.05; **P < 0.01; ns, not significant. β -actin was used as a loading control.

Although ISGs are known as antiviral effectors, their mode-of-actions are diverse including direct and indirect anti-viral actions. Some ISGs have been linked to immunity against norovirus infection. IRF1 has been reported to contribute to IFN- γ -mediated inhibition of MNV replication in macrophages (16). This may be an indirect effect as shown in the setting of hepatitis E virus (HEV) infection. IRF1 activates STAT1 to induce the expression of a wide range of ISGs that eventually inhibit HEV replication (35). ISG15 inhibits an early step of the MNV life cycle upstream of viral genome transcription (17). GBP1 has been reported to restrict DENV replication by modulating NF- κ B activity, leading to the production of antiviral and pro-inflammatory cytokines (43). As seen in this study, the inhibition of MNV replication by GBP2 appears to be independent of ISG induction. Interestingly, recent studies have shown an association between GBPs and inflammasome activation. The inflammasome machinery is essential for host defense against viral pathogens (28,29). MNV infection triggers NLRP3 inflammasome activation in primary BMDMs with STAT1 deficiency or in TLR2-primed BMDMs (44). MNV infection persists much longer in NLRP6-deficient compared with the wild-type mice (45). It is thus tempting to suggest that GBP2 functions through inflammasome activation and this scenario should be investigated in future experimentation.

Structurally, hGBP1 can be mapped into three domains with distinct functionality (19). The N-terminal domain of GBP1 is responsible for the antiviral activity against influenza A virus (IAV), HCV and CSFV infections (27,38,39). The C-terminal domain of mGBP2 dictates the recruitment to the *Toxoplasma gondii* parasitophorous vacuole and contributes to control of its replication (18). Based on the hGBP1 structure (PDB, 1f5n) (19), we modeled the different domains of mouse GBP2 including the G, M and E domains. By constructing the truncated mutants of GBP2, we found that the N-terminal G-domain is important for the anti-MNV activity in human epithelial cells, and for augmenting IFN- γ -mediated anti-MNV response in murine macrophages.

The R48 and K51 residues within the N-terminal domain are essential for the GTPase activity and antiviral function of GBP1 (27,38). Arg-48 in the P-loop is highly conserved across different GBPs, and functions as a GTPase-activating “arginine finger” involved in the multimerization process. The R48A mutant has much weaker GTPase activity (40). Lys-51 (K51A) mutation in mouse GBP2 leads to a nearly complete loss of function including hydrolysis, dimerization and nucleotide binding (40). In this study, we found that the R48A and K51A mutants attenuate the anti-MNV effects of GBP2, suggesting the potential requirement of GTPase activity. Viruses have developed sophisticated strategies to evade host defense (46). MNV NS1/2 interacts with host protein VAPA to enhance viral replication (47), NS3 interacts with microtubule-associated protein GEF-H1, which plays a role in immune detection of viral replication (48). MNV NS7 is the viral replicase, and catalyzes replication of the viral genome. NS7 presents a diffused pattern both in cell cytoplasm and nucleus (49,50). In this study, we

revealed that NS7 co-localizes with GBP2 in the cytoplasm by transient expression, and antagonizes GBP2 mediated anti-MNV activity. Viral replicases including NS5B of HCV and NS5A of CSFV, and NS1 of IAV have been reported to interact with GBP1 (38,39), and attenuate GBP1-mediated antiviral activity (27,38). Thus, the potential interaction of NS7 with GBP2, and possible inhibitory role on GTPase activity of GBP2 are interesting to be further studied.

In summary, MNV-1 infection activates the expression of GBP2, an IFN-inducible GTPase. GBP2 orchestrates innate immune defense against MNV independent of its N-terminus. However, MNV NS7 can co-localize with GBP2 in the cytoplasm, and antagonize GBP2 mediated anti-MNV activity. These findings shed new light on norovirus-host interactions, and shall be helpful for better understanding the pathogenesis and developing new antiviral strategies.

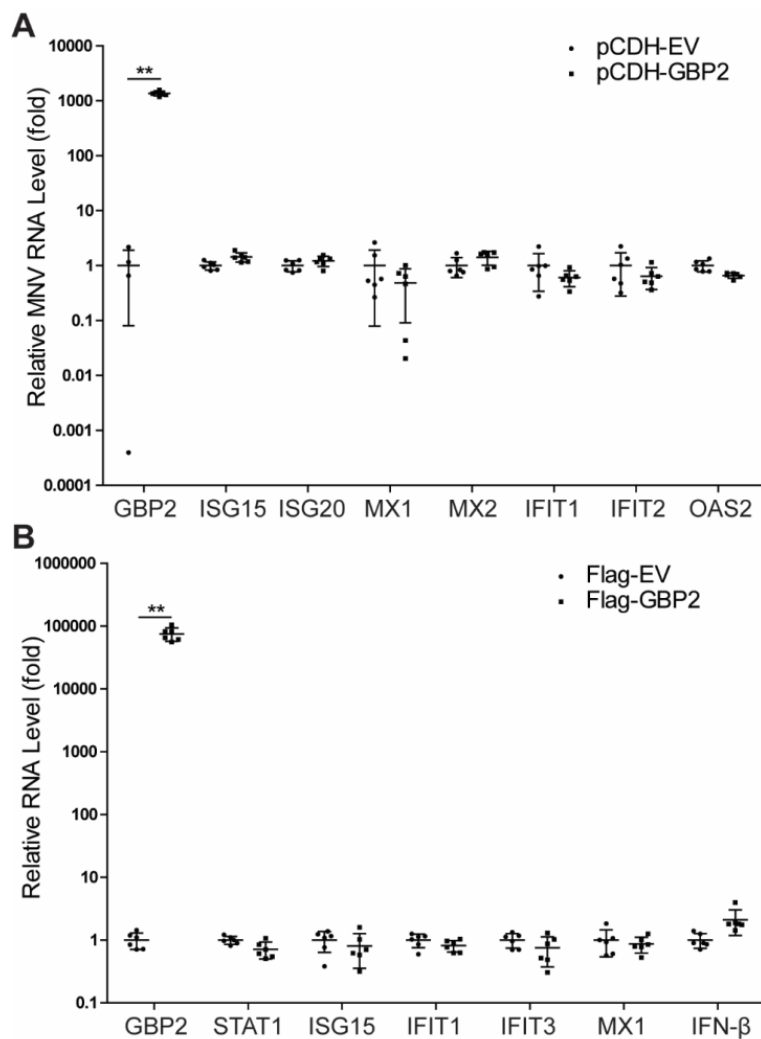
References

1. Glass, R. I., Parashar, U. D., and Estes, M. K. (2009) Norovirus gastroenteritis. *New Engl J Med* 361, 1776-1785
2. Bok, K., and Green, K. Y. (2012) Norovirus gastroenteritis in immunocompromised patients. *New Engl J Med* 367, 2126-2132
3. Karst, S. M., Wobus, C. E., Goodfellow, I. G., et al. (2014) Advances in norovirus biology. *Cell Host Microbe* 15, 668-680
4. Wobus, C. E., Karst, S. M., Thackray, L. B., et al. (2004) Replication of Norovirus in cell culture reveals a tropism for dendritic cells and macrophages. *PLoS Biol* 2, e432
5. Wobus, C. E., Thackray, L. B., and Virgin, H. W. (2006) Murine norovirus: a model system to study norovirus biology and pathogenesis. *J Virol* 80, 5104-5112
6. Orchard, R. C., Wilen, C. B., Doench, J. G., et al. (2016) Discovery of a proteinaceous cellular receptor for a norovirus. *Science* 353, 933-936
7. Orchard, R. C., Sullender, M. E., Dunlap, B. F., et al. (2019) Identification of antinorovirus genes in human cells using genome-wide CRISPR activation screening. *J Virol* 93, e01324-01318
8. McFadden, N., Bailey, D., Carrara, G., et al. (2011) Norovirus regulation of the innate immune response and apoptosis occurs via the product of the alternative open reading frame 4. *PLoS Pathog* 7, e1002413
9. Zhu, S., Regev, D., Watanabe, M., et al. (2013) Identification of immune and viral correlates of norovirus protective immunity through comparative study of intra-cluster norovirus strains. *PLoS Pathog* 9, e1003592
10. Lee, S., Liu, H., Wilen, C. B., et al. (2019) A Secreted Viral Nonstructural Protein Determines Intestinal Norovirus Pathogenesis. *Cell Host Microbe* 25, 845-857.e845
11. Högbom, M., Jäger, K., Robel, I., et al. (2009) The active form of the norovirus RNA-dependent RNA polymerase is a homodimer with cooperative activity. *J Gen Virol* 90, 281-291
12. Subba-Reddy, C. V., Goodfellow, I., and Kao, C. C. (2011) VPg-primed RNA synthesis of norovirus RNA-dependent RNA polymerases by using a novel cell-based assay. *J Virol* 85, 13027-13037
13. Wu, J., and Chen, Z. J. (2014) Innate immune sensing and signaling of cytosolic nucleic acids. *Ann Rev Immunol* 32, 461-488

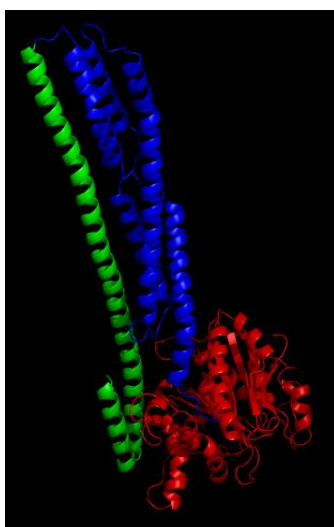
14. Wang, W., Xu, L., Su, J., et al. (2017) Transcriptional Regulation of Antiviral Interferon-Stimulated Genes. *Trends Microbiol* 25, 573-584
15. Schoggins, J. W., Wilson, S. J., Panis, M., et al. (2011) A diverse range of gene products are effectors of the type I interferon antiviral response. *Nature* 472, 481
16. Maloney, N. S., Thackray, L. B., Goel, G., et al. (2012) Essential cell autonomous role for interferon regulatory factor 1 in interferon- γ -mediated inhibition of norovirus replication in macrophages. *J Virol*, 01564-01512
17. Rodriguez, M. R., Monte, K., Thackray, L. B., et al. (2014) ISG15 functions as an interferon-mediated antiviral effector early in the murine norovirus life cycle. *J Virol*, 01422-01414
18. Degrandi, D., Kravets, E., Konermann, C., et al. (2013) Murine guanylate binding protein 2 (mGBP2) controls *Toxoplasma gondii* replication. *Proc Nat Acad Sci USA* 110, 294-299
19. Prakash, B., Praefcke, G. J. K., Renault, L., et al. (2000) Structure of human guanylate-binding protein 1 representing a unique class of GTP-binding proteins. *Nature* 403, 567
20. Kresse, A., Konermann, C., Degrandi, D., et al. (2008) Analyses of murine GBP homology clusters based on in silico, in vitro and in vivo studies. *BMC Genom* 9, 158
21. Man, S. M., Place, D. E., Kuriakose, T., et al. (2017) Interferon-inducible guanylate-binding proteins at the interface of cell-autonomous immunity and inflammasome activation. *J Leukocyte Biol* 101, 143-150
22. Wandel, M. P., Pathe, C., Werner, E. I., et al. (2017) GBPs inhibit motility of *Shigella flexneri* but are targeted for degradation by the bacterial ubiquitin ligase IpaH9. 8. *Cell Host Microbe* 22, 507-518. e505
23. Li, P., Jiang, W., Yu, Q., et al. (2017) Ubiquitination and degradation of GBPs by a *Shigella* effector to suppress host defence. *Nature* 551, 378
24. Braun, E., Hotter, D., Koepke, L., et al. (2019) Guanylate-Binding Proteins 2 and 5 Exert Broad Antiviral Activity by Inhibiting Furin-Mediated Processing of Viral Envelope Proteins. *Cell Rep* 27, 2092-2104. e2010
25. Krapp, C., Hotter, D., Gawanbacht, A., et al. (2016) Guanylate binding protein (GBP) 5 is an interferon-inducible inhibitor of HIV-1 infectivity. *Cell Host Microbe* 19, 504-514
26. Itsui, Y., Sakamoto, N., Kurosaki, M., et al. (2006) Expressional screening of interferon-stimulated genes for antiviral activity against hepatitis C virus replication. *J Viral Hepat* 13, 690-700
27. Li, L.-F., Yu, J., Li, Y., et al. (2016) Guanylate-Binding Protein 1, an Interferon-Induced GTPase, Exerts an Antiviral Activity against Classical Swine Fever Virus Depending on Its GTPase Activity. *J Virol* 90, 4412-4426
28. Shenoy, A. R., Wellington, D. A., Kumar, P., et al. (2012) GBP5 promotes NLRP3 inflammasome assembly and immunity in mammals. *Science*, 1217141
29. Meunier, E., Wallet, P., Dreier, R. F., et al. (2015) Guanylate-binding proteins promote activation of the AIM2 inflammasome during infection with *Francisella novicida*. *Nat Immunol* 16, 476
30. Ichinohe, T., Lee, H. K., Ogura, Y., et al. (2009) Inflammasome recognition of influenza virus is essential for adaptive immune responses. *J Exp Med* 206, 79-87
31. Zhu, S., Ding, S., Wang, P., et al. (2017) Nlrp9b inflammasome restricts rotavirus infection in intestinal epithelial cells. *Nature* 546, 667
32. Biering, S. B., Choi, J., Halstrom, R. A., et al. (2017) Viral replication complexes are targeted by LC3-guided interferon-inducible GTPases. *Cell Host Microbe* 22, 74-85. e77
33. Davies, C., Brown, C. M., Westphal, D., et al. (2015) Murine norovirus replication induces G0/G1 cell cycle arrest in asynchronously growing cells. *J Virol* 89, 6057-6066
34. Wang, Y., Zhou, X., Debing, Y., et al. (2014) Calcineurin inhibitors stimulate and mycophenolic acid inhibits replication of hepatitis E virus. *Gastroenterology* 146, 1775-1783
35. Xu, L., Zhou, X., Wang, W., et al. (2016) IFN regulatory factor 1 restricts hepatitis E virus replication by activating STAT1 to induce antiviral IFN-stimulated genes. *FASEB J* 30, 3352-3367
36. Dang, W., Xu, L., Yin, Y., et al. (2018) IRF-1, RIG-I and MDA5 display potent antiviral activities against norovirus coordinately induced by different types of interferons. *Antiviral Res* 155, 48-59

37. Xu, L., Wang, W., Li, Y., et al. (2017) RIG-I is a key antiviral interferon-stimulated gene against hepatitis E virus regardless of interferon production. *Hepatology* 65, 1823-1839
38. Itsui, Y., Sakamoto, N., Kakinuma, S., et al. (2009) Antiviral effects of the interferon-induced protein guanylate binding protein 1 and its interaction with the hepatitis C virus NS5B protein. *Hepatology* 50, 1727-1737
39. Zhu, Z., Shi, Z., Yan, W., et al. (2013) Nonstructural protein 1 of influenza A virus interacts with human guanylate-binding protein 1 to antagonize antiviral activity. *PLoS One* 8, e55920
40. Kravets, E., Degrandi, D., Weidtkamp-Peters, S., et al. (2012) The GTPase activity of murine guanylate-binding protein 2 (mGBP2) controls the intracellular localization and recruitment to the parasitophorous vacuole of *Toxoplasma gondii*. *J Biol Chem* 287, 27452-27466
41. Anderson, S. L., Carton, J. M., Lou, J., et al. (1999) Interferon-induced guanylate binding protein-1 (GBP-1) mediates an antiviral effect against vesicular stomatitis virus and encephalomyocarditis virus. *Virology*, 256: 8-14.
42. Feng, J., Cao, Z., Wang, L., et al. (2017) Inducible GBP5 mediates the antiviral response via interferon-related pathways during influenza A virus infection. *J Innate Immun* 9, 419-435
43. Pan, W., Zuo, X., Feng, T., et al. (2012) Guanylate-binding protein 1 participates in cellular antiviral response to dengue virus. *Virology* 9, 292
44. Dubois, H., Sorgeloos, F., Sarvestani, S. T., et al. (2019) Nlrp3 inflammasome activation and Gasdermin D-driven pyroptosis are immunopathogenic upon gastrointestinal norovirus infection. *PLoS Pathog* 15, e1007709
45. Wang, P., Zhu, S., Yang, L., et al. (2015) Nlrp6 regulates intestinal antiviral innate immunity. *Science* 350, 826-830
46. Li, Y., Qu, C., Yu, P., et al. (2019) The Interplay between Host Innate Immunity and Hepatitis E Virus. *Viruses* 11
47. McCune, B. T., Tang, W., Lu, J., et al. (2017) Noroviruses Co-opt the Function of Host Proteins VAPA and VAPB for Replication via a Phenylalanine-Phenylalanine-Acidic-Tract-Motif Mimic in Nonstructural Viral Protein NS1/2. *mBio* 8
48. Fritzlir, S., White, P. A., and Mackenzie, J. M. (2019) The Microtubule-Associated Innate Immune Sensor GEF-H1 Does Not Influence Mouse Norovirus Replication in Murine Macrophages. *Viruses* 11, 47
49. Fernandez-Vega, V., Sosnovtsev, S. V., Belliot, G., et al. (2004) Norwalk virus N-terminal nonstructural protein is associated with disassembly of the Golgi complex in transfected cells. *J Virol* 78, 4827-4837
50. Hyde, J. L., and Mackenzie, J. M. (2010) Subcellular localization of the MNV-1 ORF1 proteins and their potential roles in the formation of the MNV-1 replication complex. *Virology* 406, 138-148

Supplementary information



Supplementary Fig. 1 GBP2 does not trigger ISG expression. (A) qRT-PCR analysis of ISG mRNA levels in GBP2 stable expression RAW264.7 cells by lentiviral-based vectors (n = 4-6). (B) qRT-PCR analysis of ISG mRNA levels in HEK293T cells that transfected with pFlag-GBP2 or empty vectors (n = 6). Data were normalized to the EV control (set as 1). **P < 0.01.



Supplementary Fig. 2 A predicted model of the tertiary structure of mouse GBP2. Based on the human GBP1 structure (PDB, 1f5n), the structure of mouse GBP2 protein (NCBI Reference Sequence: NP_034390) was predicted by using the online software SWILL-MODEL, where the G domain (7 - 304 aa) is in red, the M domain (305 - 481 aa) in blue, and the E domain (482 - 581 aa) in green. aa, amino acid.

Supplementary Table 1. The primers used for plasmid construction

Primer	Sequence (5'to 3')	Usage
pFlag-GBP2-F	TGCTCTAGAGCCTCAGAGATCCACATGTCCGGAAC	Amplification of GBP2
pFlag-GBP2-R	CGGGGTACCGATCAGAGTATAGTGCACTTCCCAG	
pFlag-GBP2_G-F	TGCTCTAGAGCCTCAGAGATCCACATGTCCGGAAC	Amplification of GBP2
pFlag-GBP2_G-R	TTGCGGCCGCTCAATTGCTGATGGCACCAAC	(G domain)
pFlag-GBP2_GM-F	TGCTCTAGAGCCTCAGAGATCCACATGTCCGGAAC	Amplification of GBP2
pFlag-GBP2_GM-R	TTGCGGCCGCTCATGTGAGTGACTGATCCGTC	(GM domain)
pFlag-GBP2_M-F	TGCTCTAGAATGGGGTCTCTCCCCTGCATGGA	Amplification of GBP2
pFlag-GBP2_M-R	TTGCGGCCGCTCATGTGAGTGACTGATCCGTC	(M domain)
pFlag-GBP2_ME-F	TGCTCTAGAATGGGGTCTCTCCCCTGCATGGA	Amplification of GBP2
pFlag-GBP2_ME-R	CGGGGTACCTCAGAGTATAGTGCACTTCCCAGAC	(ME domain)
pFlag-GBP2_E-F	TGCTCTAGAGAGGCAGCAAAGGAGGTAGAAGA	Amplification of GBP2
pFlag-GBP2_E-R	CGGGGTACCTCAGAGTATAGTGCACTTCCCAGAC	(E domain)
pMyc-GBP2-F	TGCTCTAGAATGGCCTCAGAGATCCACATGTCCGG	Amplification of GBP2
pMyc-GBP2-R	CGGGGTACCGAGTATAGTGCACTTCCCAGACG	
pCDH-GBP2-F	TGCTCTAGAATGGCCTCAGAGATCCACATGTCCGG	Amplification of GBP2
pCDH-GBP2-R	TTGCGGCCGCTCAGAGTATAGTGCACTTCCCAGAC	
pCDH-GBP2_G-F	TGCTCTAGAATGGCCTCAGAGATCCACATGTCCGG	Amplification of GBP2
pCDH-GBP2_G-R	TTGCGGCCGCTCATGTGAGTGACTGATCCGTC	(G domain)
pCDH-GBP2_GM-F	TGCTCTAGAATGGCCTCAGAGATCCACATGTCCGG	Amplification of GBP2
pCDH-GBP2_GM-R	TTGCGGCCGCTCATGTGAGTGACTGATCCGTC	(GM domain)
pCDH-GBP2_M-F	TGCTCTAGAATGGGGTCTCTCCCCTGCATGGA	Amplification of GBP2
pCDH-GBP2_M-R	TTGCGGCCGCTCATGTGAGTGACTGATCCGTC	(M domain)
pCDH-GBP2_ME-F	TGCTCTAGAATGGGGTCTCTCCCCTGCATGGA	Amplification of GBP2
pCDH-GBP2_ME-R	TTGCGGCCGCTCAGAGTATAGTGCACTTCCCAGAC	(ME domain)
pCDH-GBP2_E-F	TGCTCTAGAATGGAGGCAGCAAAGGAGGTAGAAG	Amplification of GBP2
pCDH-GBP2_E-R	TTGCGGCCGCTCAGAGTATAGTGCACTTCCCAGAC	(E domain)
pFlag-NS7-F	TGCTCTAGAGGACCCCCATGCTTCCCCGCCCTCA	Amplification of MNV
pFlag-NS7-R	CGGAATTCTTACTCATCCTCATTACAAAGAC	NS7
pMyc-NS7-F	CTAGCTAGCATGGGACCCCCATGCTTCCCCGCCCTCA	Amplification of MNV
pMyc-NS7-R	CGGGATCCCTCATCCTCATTACAAAGACTGC	NS7

Supplementary Table 2. Lentiviral shRNA sequences

No.	Gene	Accession	Sequences	Target Sequence
sh-32	mouse	NM_01026	CCGGGCGACTGTGCATCAGGAAATTCTCGAG	GCGACTGTGCATCA
	GBP2	0.1	AATTCCTGATGCACAGTCGCTTTTTG	GGAAATT
sh-33	mouse	NM_01026	CCGGCATCAGGAAATTCTTTCCAAACTCGAGT	CATCAGGAAATTCT
	GBP2	0.1	TTGGAAAGAATTCCTGATGTTTTG	TTCCAAA

Supplementary Table 3. The primers used for qRT-PCR

Gene	F-Sequences (5' to 3')	R-Sequences (5' to 3')
mGAPDH	TTCCAGTATGACTCCACTCACGG	TGAAGACACCAGTAGACTCCACGAC
mSTAT1	GCCTCTCATTGTCACCGAAGAAC	TGGCTGACGTTGGAGATACCA
mIRF1	CAGAGGAAAGAGAGAAAGTCC	CACACGGTGACAGTGCTGG
mISG15	TGACGCAGACTGTAGACACG	TGGGGCTTTAGGCCATACTC
mISG20	CAATGCCCTGAAGGAGGATA	TGTAGCAGGCGCTTACACAG
mMX2	CCAGTTCCTCTCAGTCCCAAGATT	TACTGGATGATCAAGGGAACGTGG
mGbp2 ^a	ACCAGCTGCACTATGTGACG	TCAGAAGTGACGGGTTTTCC
mOAS2	CATCCTTCTGCACCAGCTCA	TCAGTAGCTCCCAGAACCCA
mIFIT1	CCATAGCGGAGGTGAATATC	GGCAGGACAATGTGCAAGAA
mGBP2-M ^b	AGTCTCTGGATCTGCACAGG	GAGCTGATGAGACATCCATG
mGBP2-E ^c	TCGAGCTGATGATGCAGCAG	TCTCATTCTCGAATCCTTCC
hGAPDH	TGTCCCACCCCAATGTATC	CTCCGATGCCTGCTTCACTACCTT
hSTAT1	ATGGCAGTCTGGCGGCTGAATT	CCAAACCAGGCTGGCACAATTG
hIRF1	GAGGAGGTGAAAGACCAGAGCA	TAGCATCTCGGCTGGACTTCGA
hISG15	CTCTGAGCATCCTGGTGAGGAA	AAGGTCAGCCAGAACAGGTCGT
hMX1	GGCTGTTTACCAGACTCCGACA	CACAAAGCCTGGCAGCTCTCTA
hIFIT1	GCCTTGCTGAAGTGTGGAGGAA	ATCCAGGCGATAGGCAGAGATC
MNV-1	CACGCCACCGATCTGTTCTG	GCGCTGCGCCATCACTC

a, the primers were used for detection of the WT, G and GM domain of mGBP2; b, the primers were used for detection of the M and ME domain of mGBP2; c, the primers were used for detection of the E domain of mGBP2.

Chapter 5

MDA5 against enteric viruses through induction of interferon-like response partially via the JAK-STAT cascade

Yang Li, **Peifa Yu**, Changbo Qu, Pengfei Li, Yunlong Li, Zhongren Ma, Wenshi Wang, Robert de Man, Maikel P. Peppelenbosch, Qiuwen Pan

Antiviral Research, 2020, 176: 104743

Abstract

Enteric viruses including hepatitis E virus (HEV), human norovirus (HuNV), and rotavirus are causing global health issues. The host interferon response constitutes the first-line defense against viral infections. Melanoma Differentiation-Associated protein 5 (MDA5) is an important cytoplasmic receptor sensing viral infection to trigger interferon production, and on the other hand it is also an interferon-stimulated gene (ISG). In this study, we investigated the effects and mode-of-action of MDA5 on the infection of enteric viruses. We found that MDA5 potently inhibited HEV, HuNV and rotavirus replication in multiple cell models. Overexpression of MDA5 induced transcription of important antiviral ISGs through interferon-like (IFN-like) response, without triggering of functional IFN production. Interestingly, MDA5 activates the expression and phosphorylation of STAT1, which is a central component of the JAK-STAT cascade and a hallmark of antiviral IFN response. However, genetic silencing of STAT1 or pharmacological inhibition of the JAK-STAT cascade only partially attenuated the induction of ISG transcription and the antiviral function of MDA5. Thus, we have demonstrated that MDA5 effectively inhibits HEV, HuNV and rotavirus replication through provoking a non-canonical IFN-like response, which is partially dependent on JAK-STAT cascade.

Keywords: MDA5, innate immunity, ISGs, interferon

Introduction

There are over 100 types of viruses excreted in feces, which collectively known as enteric viruses. Among these, hepatitis E virus (HEV) has been recognized as an emerging zoonotic virus, representing a major cause of acute hepatitis worldwide. Although it is often self-limiting, high mortality rate has been reported in pregnant women. Human norovirus (HuNV) and rotavirus are the leading causes of acute gastroenteritis. Interestingly, all three types of viruses can cause chronic infection in immunocompromised organ transplantation patients (1-4), highlighting the essential role of host immunity in determining the outcome of these infections.

Innate immune system is the first line of host defense against viral infection and plays a critical role in clearance of pathogen (5). Upon infection, pathogen-associated molecular patterns (PAMPs) are recognized by pattern recognition receptor (PRRs), such as toll-like receptors (TLRs) and retinoic acid inducible gene I (RIG-I)-like receptors (RLRs) (6,7). Subsequently, PRRs initiate downstream signaling pathway to produce a panel of cytokines, in particular, the antiviral interferons (IFNs). Mechanistically, type I and III IFN bind to their receptors on the cell surface to initiate signal cascades. This binding triggers the phosphorylation of STAT1 and STAT2, which subsequently bind to IRF9 to form a interferon-stimulated gene factor 3 (ISGF3) complex. ISGF3 translocates to the nucleus to drive expression of interferon-stimulated genes (ISGs) to establish antiviral states (8).

Melanoma Differentiation-Associated protein 5 (MDA5) is an important cytoplasmic receptor, a member of RLRs, which participates in recognition of different RNA viruses. Upon the detection of viral RNA ligand, MDA5 recruits mitochondrial antiviral signaling (MAVS, also known as IPS-1, VISA, or Cardif) (9) to activate IRF3/7 and NF- κ B, and eventually triggers interferon and inflammatory responses. On the other hand, MDA5 is also an important antiviral ISG. MDA5 has been reported to potently inhibit the replication of Sindbis virus (SINV), West Nile virus (WNV) and Venezuelan equine encephalitis virus (VEEV) (10). Thus, the antiviral mechanisms may directly through pathogen recognition pathway or directly act as an antiviral ISG. However, how MDA5 exactly exerts antiviral action against different types of viruses remains largely under investigated.

Materials and methods

Reagents

Human IFN- α (Sigma-Aldrich, H6166) was dissolved in PBS. Stocks of JAK inhibitor 1 (SC-204021, Santa Cruz Biotechnology, Santa Cruz, CA, USA) were dissolved in DMSO with a final concentration of 5 mg/ml. Dimethyl sulfoxide (DMSO, Sigma, Zwijndrecht, the Netherlands) was used as vehicle control. Phospho-STAT1 (Tyr701) (58D6, Rabbit mAb, 9167), STAT1 (Rabbit mAb, 9172), RIG-I (D14G6, Rabbit mAb, 3743), PKR (D7F7, Rabbit mAb, 12297), MDA5 (IFIH1) (D74E4, Rabbit mAb, 5321) antibodies were obtained from Cell Signaling Technology (Danvers, MA, USA). β -actin antibody (mouse monoclonal, sc-47778) was obtained from Santa Cruz Biotechnology (Santa Cruz, CA, USA). Anti-rabbit and anti-mouse IRDye-conjugated secondary antibodies (Li-Cor Biosciences, Lincoln, NE, USA) were also used.

Cell culture

Huh7 and PLC/PRF/5 (PLC) human hepatoma cells, Huh7-STAT1 knockout cells, HEK293T cells and Caco2 cells were cultured in DMEM (Lonza Biowhittaker, Verviers, Belgium) complemented with 10% (v/v) fetal calf serum (FCS) (Hyclone, Logan, UT, USA), 100 IU/ml penicillin and 100 mg/ml streptomycin. For the ISRE reporter model (Huh7-ISRE-Luc), Huh7 cells were transduced with a lentiviral transcriptional reporter system expressing the firefly luciferase gene driven by a promoter containing multiple ISRE promoter elements (SBI Systems Biosciences, Mountain View, CA, USA). Luciferase activity represents ISRE promoter activation (11).

Viruses and cell culture models

In this study, multiple cell lines were used for HEV replication, including a human hepatoma cell lines, Huh7 and PLC. For the full-length HEV model, a plasmid construct containing the full-length HEV genome (Kernow-C1 p6 clone; GenBank Accession Number JQ679013) was used to generate HEV genomic RNA with the Ambion mMessage mMachine in vitro RNA transcription Kit (Thermo Fisher Scientific Life Sciences). Huh7 and PLC cells were electroporated with full-length HEV genome RNA, to generate consecutive HEV-infected cell models, Huh7-p6 and PLC-p6. For the subgenomic HEV model, a construct containing subgenomic HEV in which the portion of HEV ORF2 was replaced with the in-frame Gaussia princeps luciferase reporter gene to yield p6-Luc (12). Huh7 cells were electroporated with HEV subgenomic RNA to generate an HEV subgenomic model, Huh7-p6-Luc, in which the accumulation of secreted luciferase serves as a reporter for HEV replication. HG23 (Huh7 cells

containing a stable subgenomic HuNV replicon) (13). Gentamicin (G418; Gibco) was added to HG23 culture medium at 1.5 mg/mL for selection before experimentation.

Gene knockdown and overexpression by lentiviral vectors

For gene knockdown, pLKO.1-based lentiviral vectors (Sigma-Aldrich) targeting MDA5 and non-targeted control vector (shCTR) were obtained from the Biomics Center in Erasmus Medical Center. Lentiviral pseudoparticles were generated in HEK293T cells. To generate a stable gene-knockdown cell line, PLC cells were transduced with lentiviral particles for 48 h. Subsequently, transduced cells were cultured with medium containing 2.5 mg/ml puromycin (Sigma-Aldrich). Because the vectors also express a puromycin resistance gene, cell lines showing optimal gene knockdown after selection, were chosen. pTRIP.CMV.IVsb.ISG.ires.TagRFP-based MDA5 overexpression vector was a kind gift from Prof. Charles M. Rice (Rockefeller University, New York, NY, USA) (10). Meanwhile, Photinus pyralis luciferase (Fluc) was used as the control (also kind gifts from Prof. Charles M. Rice). Target cell lines were seeded into 12-well plates at a density of 6×10^4 cells per well and transduced with lentiviral pseudoparticles at 37°C for 24, 48, or 72 h. The transduction time of each experiment is described in the legend of each figure, along with the control vector used.

Quantification of viral replication

MDA5 was transduced in Huh7-p6 and PLC-p6 cell models. HEV RNA level was quantified 48 h after transduction by qRT-PCR. MDA5 was transduced in HG23 cells and rotavirus infected Caco2 cells. HuNV and rotavirus RNA level were quantified 48 h after transduction by qRT-PCR, respectively. Intracellular gene expression was quantified by SYBR-Green-based (Applied Biosystems SYBR Green PCR Master Mix; Thermo Fisher Scientific Life Sciences) real-time PCR with the StepOnePlus System (Thermo Fisher Scientific Life Sciences). GAPDH was used as housekeeping genes, and all gene expression levels (relative) were normalized to GAPDH using the $2^{-\Delta\Delta Ct}$ method. For HEV-related Gaussia luciferase analysis (HEV-p6-Luc), the activity of secreted luciferase in the cell culture medium was measured by BioLux Gaussia Luciferase Flex Assay Kit (New England Biolabs, Ipswich, MA, USA), according to the manufacturer's instructions. Luciferase activity was quantified with a LumiStar Optima luminescence counter (BMG Lab Tech, Offenburg, Germany). For the firefly and Photinus pyralis luciferases, luciferin potassium salt (100 mM; Sigma-Aldrich) was added to the cells and incubated for 10 min at 37°C, and luciferase activity was measured.

IFN production bioassay

Cells were seeded into 6-well plates at a density of 1×10^5 cells per well and transduced with MDA5 or control lentiviral particles at 37°C. After 72 h, lentiviral particles were removed, and

cells were washed 3 times with PBS and cultured for another 72 h. The cultured supernatant was subsequently collected and filtered through a 0.45mm pore size membrane and added to Huh7-ISRE-Luc reporter cells which are sensitive to IFNs.

Immunoblot analysis

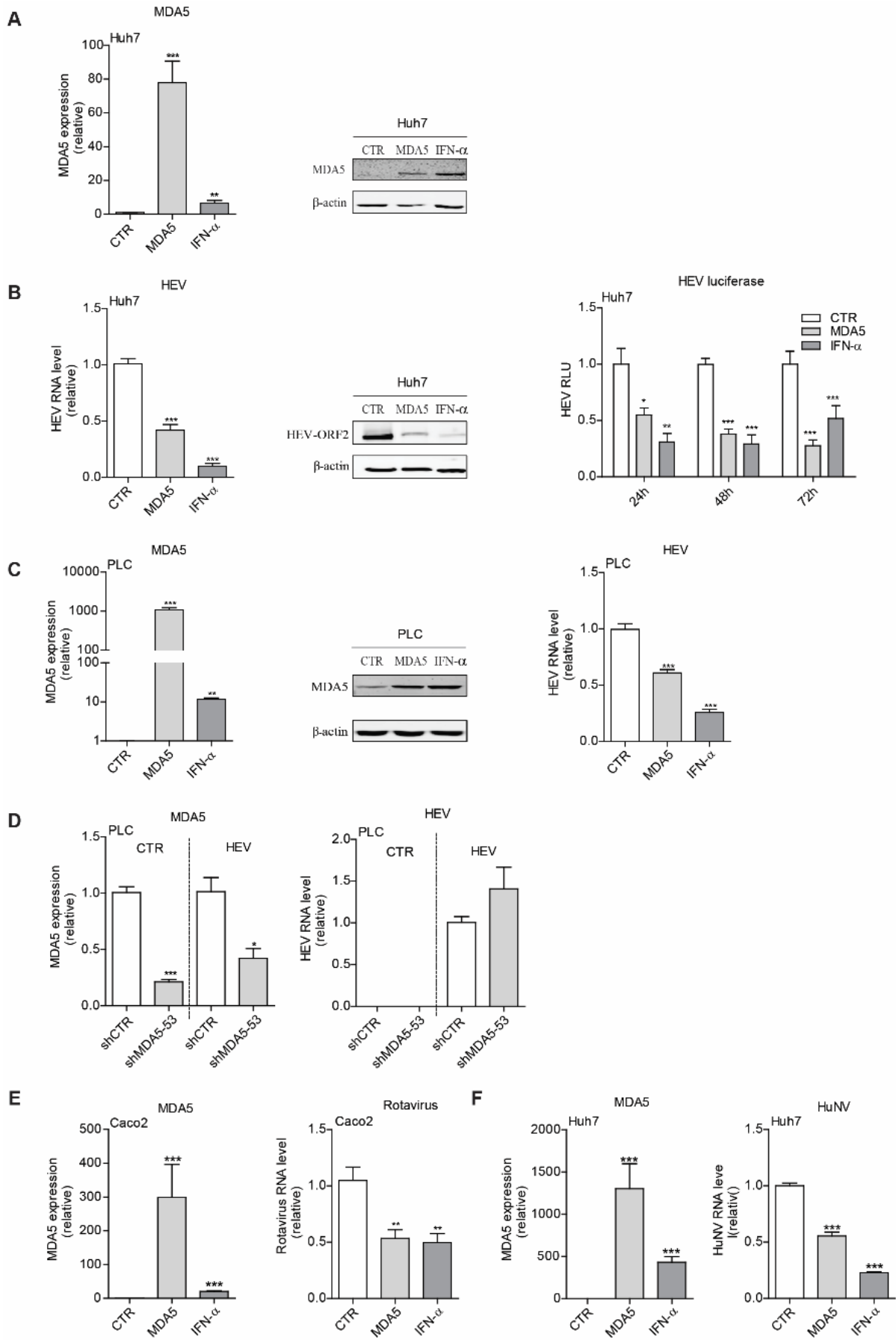
Lysate was heated at 95°C for 5 min. Proteins were subjected to a 10% sodium dodecyl sulfate polyacrylamide gel (SDS-PAGE), separated at 100 V for 100min, and electrophoretically transferred onto a PVDF membrane (pore size: 0.45 mm; Thermo Fisher Scientific Life Sciences) for 100 min with an electric current of 230 mA. Subsequently, the membrane was blocked with blocking buffer (Li-Cor Biosciences) in PBS containing 0.05% Tween-20. Membranes were incubated with primary antibodies overnight at 4°C. Rabbit anti-MDA5 (1:1000), p-STAT1 (1:1000), STAT1 (1:1000), RIG-I (1:1000), PKR (1:1000) antibodies or mouse anti- β -actin (1:1000) were diluted in blocking buffer. The membrane was washed 3 times, followed by incubation for 1 h with anti-rabbit or anti-mouse IRDye-conjugated secondary antibodies (1:5000; Li-Cor Biosciences) at room temperature. β -actin served as the loading standard. The membrane was scanned by Odyssey Infrared Imaging System (Li-Cor Biosciences). Results were visualized with Odyssey 3.0 software. Band intensity data of each immunoblot was also quantified by Odyssey Software.

MTT assay

Cells were seeded in 96-well plates, and 10mM 3-(4,5-dimethylthiazol-2-yl)-2,5-diphenyltetrazolium bromide (MTT) (Sigma-Aldrich) was added. The plate was incubated at 37°C with 5% CO₂ for 3 h, then the medium was removed, added 100 μ L of DMSO to each well, afterward the plate was incubated at 37°C for 1h. The absorbance was read on the microplate absorbance reader (Bio-Rad, Hercules, CA, USA) at a wavelength of 490 nm.

Statistical analysis

GraphPad Prism 5 software was used for data analysis using a Mann-Whitney test. All results were presented as mean \pm standard errors of the means (SEM). P values of less than 0.05 (single asterisks in figures) were considered statistically significant; whereas P values less than 0.01 (double asterisks) and 0.001 (triple asterisks) were considered highly significant.



< Figure 1. MDA5 inhibits the replication of different enteric viruses. (A) Quantitative RT-PCR analysis and immunoblot analysis of MDA5 expression in Huh7-p6 cells transduced with MDA5 or Fluc vector or treated with IFN- α (1000 IU/mL) for 48 hours. (B) Quantitative RT-PCR analysis and immunoblot analysis of HEV RNA level and HEV ORF2 protein level in Huh7-p6 cells transduced with MDA5 or Fluc vector or treated with IFN- α (1000 IU/mL) for 48 hours and analysis of HEV-related Gaussia luciferase activity in Huh7-p6-luciferase cells transduced with MDA5 or Fluc vector or treated with IFN- α (1000 IU/mL) for 24, 48, or 72 hours. (C) Quantitative RT-PCR analysis and immunoblot analysis of MDA5 expression and quantitative RT-PCR analysis of HEV RNA level in PLC-p6 cells transduced with MDA5 or Fluc vector or treated with IFN- α (1000 IU/mL) for 48 hours. (D) PLC cells transduced with lentiviral short hairpin RNA vector targeting MDA5 or scramble control. Stable MDA5 knockdown or scramble control PLC cells were infected with HEV for 48 hours. Quantitative RT-PCR analysis of MDA5 expression level and HEV RNA level (E) Quantitative RT-PCR analysis of MDA5 expression and rotavirus RNA level in Caco2 cells transduced with MDA5 or Fluc vector or treated with IFN- α (1000 IU/mL) for 48 hours. (F) Quantitative RT-PCR analysis of MDA5 expression and HuNV RNA level in HG23 cells transduced with MDA5 or Fluc vector or treated with IFN- α (1000 IU/mL) for 48 hours. Data were normalized to the Fluc control (CTR, set as 1) or to the scramble control (shCTR, set as 1). Data are means \pm SEM of three independent experiments with 2-4 biological repeats for each. *P < 0.05, **P < 0.01, ***P < 0.001. Abbreviation: CTR, control; RLU, relative luciferase unit; sh, short hairpin.

Results

MDA5 potently inhibits HEV, HuNV and rotavirus replication

To evaluate the effects of MDA5 on enteric viruses, we have employed multiple cell culture models of HEV, HuNV and rotavirus infections. For HEV, two Huh7-based HEV models (Huh7-p6 and Huh7-p6-Luc) were used. Lentiviral mediated MDA5 overexpression was confirmed in Huh7-p6 cells at mRNA and protein levels (Fig. 1A). In both models, MDA5 overexpression significantly inhibited HEV replication (Fig. 1B). Next, we confirmed the anti-HEV activity in PLC cell model (PLC-p6) (Fig. 1C). Conversely, gene silencing of MDA5 by RNAi appears to facilitate HEV replication, although not statistically significant (Fig. 1D).

Next, we found that MDA5 overexpression also significantly inhibits rotavirus and HuNV replication in Caco2 and Huh7 cells, respectively (Fig. 1E, 1F). These results have demonstrated that MDA5 has a broad antiviral activity against enteric viruses, and encouraged us to further explore the mechanism-of-action.

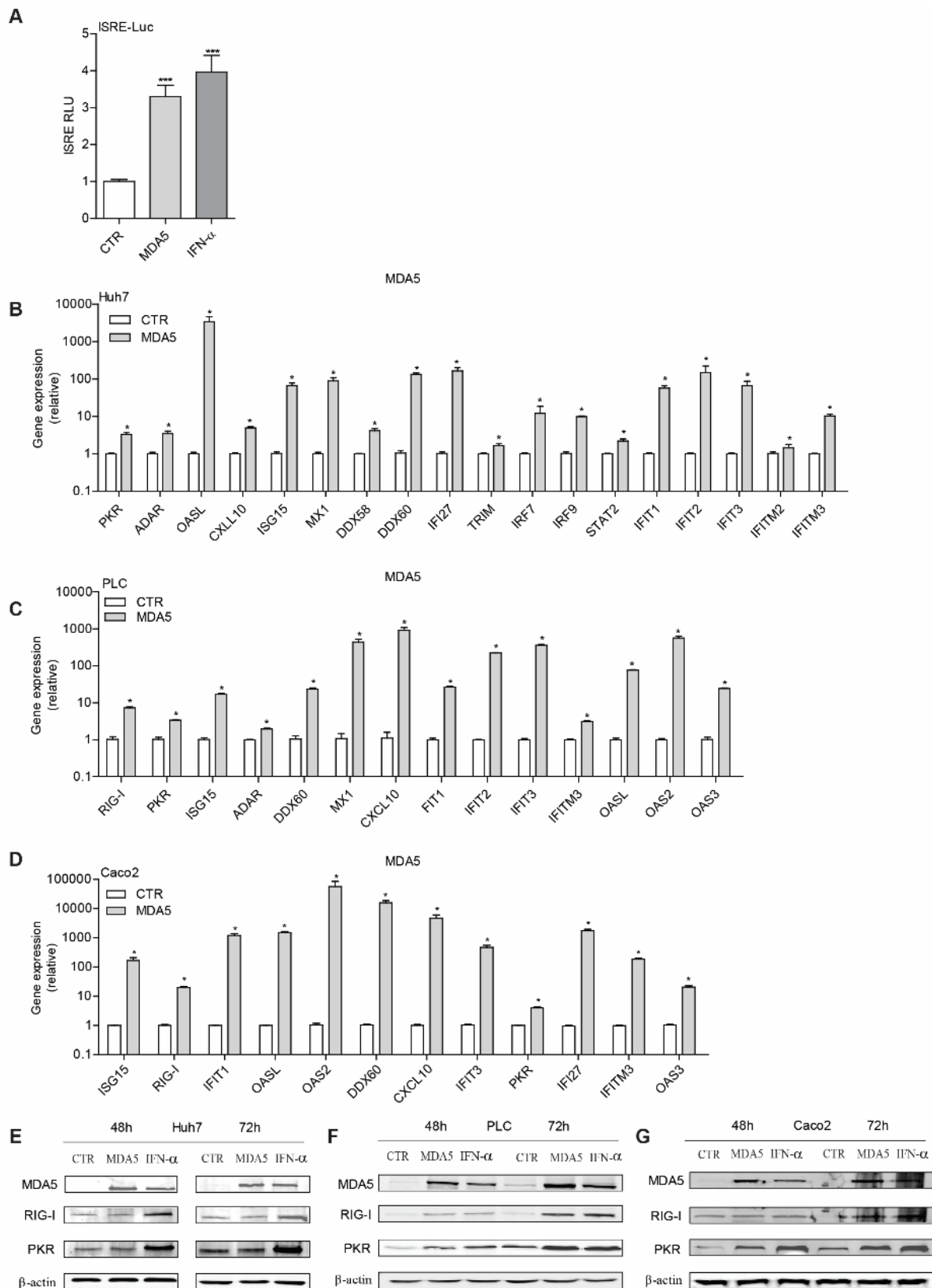


Figure 2. MDA5 triggers the transcription of a range of antiviral ISGs. (A) Analysis of ISRE-related *firefly* luciferase activity in Huh7-ISRE-Luc cells transduced with MDA5 or Fluc vector or treated with IFN- α (1000 IU/mL) for 48 hours. (B) Quantitative RT-PCR analysis of ISG mRNA level in Huh7-p6 cells, (C) PLC-p6 cells, and (D) Caco2 cells transduced with MDA5 or Fluc vector for 48 hours. (E) Immunoblot

analysis of ISG protein level in Huh7-p6 cells, (F) PLC-p6 cells, and (G) Caco2 cells transduced with MDA5 or Fluc vector for 48 or 72 hours. Data were normalized to the Fluc control (CTR, set as 1). Data are means \pm SEM of three independent experiments with 2-4 biological repeats for each. *P < 0.05; **P < 0.01; ***P < 0.001. Abbreviation: CTR, control.

MDA5 triggers the transcription of a range of antiviral ISGs through IFN-like response

In general, IFNs active ISGF3 complex, which binds to IFN-stimulated response element (ISRE) motifs in nucleus to drives ISGs transcription. Usually upon sensing of particular viruses, MDA5 triggers IFNs production, which subsequently induce ISG expression. Here, we employed a transcriptional report system that mimics IFN response with a reporter luciferase gene that was driven by multiple ISRE (ISRE-Luc). Surprisingly, similar to IFN- α treatment, MDA5 overexpression in naïve cells already potently increased ISRE-luciferase activity (Fig. 2A). Activation of ISRE usually leads to the transcription of ISGs that contain this motifs in their promoter regions. Consistently, MDA5 overexpression stimulated the transcription of a large panel of ISGs in Huh7, PLC and Caco2 cells (Fig. 2B, 2C, and 2D). The induction level of ISG transcription by MDA5 is similar to that by IFN- α treatment (Supporting Fig. 1A, 1B, and 1C), whereas the induction patterns are different. The expression of several important ISGs was further confirmed by immunoblotting at protein level (Fig. 2E, 2F, and 2G). These results suggested that MDA5 induces ISG expression through triggering IFN-like response.

Overexpression of MDA5 does not induce the production of functional IFNs

Since MDA5 induced antiviral ISG transcription through IFN-like response, we examined whether MDA5 overexpression triggers IFN production. At mRNA level, MDA5 overexpression did not induce IFN- α and IFN- β , but moderately induced IFN- λ expression in Huh7, PLC and Caco2 cells (Fig. 3A, 3B, and 3C). More importantly, we investigated whether there is production of functional IFNs by testing conditioned medium (supernatant) from MDA5 overexpressed Huh7, PLC or Caco2 cells (Fig. 3D). In the ISRE-based IFN reporter assay, treatment with these conditioned medium collected did not trigger ISRE activation (Fig. 3E, 3F, and 3G). These results demonstrated that MDA5 overexpression does not trigger the production of functional IFNs in these cell models.

Overexpression of MDA5 upregulates STAT1 expression and phosphorylation

Given the dispensability of IFN production in MDA5-triggered IFN-like response, we next investigated the effect on STAT1, a central component of the JAK-STAT cascade. At mRNA level, similar to IFN- α treatment, MDA5 overexpression significantly upregulated STAT1 expression in Huh7, PLC and Caco2 cells (Fig. 4A, 4B, and 4C). This was further confirmed at total protein

levels of STAT1 in these cell models (Fig. 4E, 4F, and 4G). Phosphorylation of STAT1 is hallmark of the activation of JAK-STAT cascade by IFNs. We found the activation of p-STAT1, at 701 site, by MDA5 overexpression, similar to IFN- α treatment (Fig. 4H, 4I, and 4J).

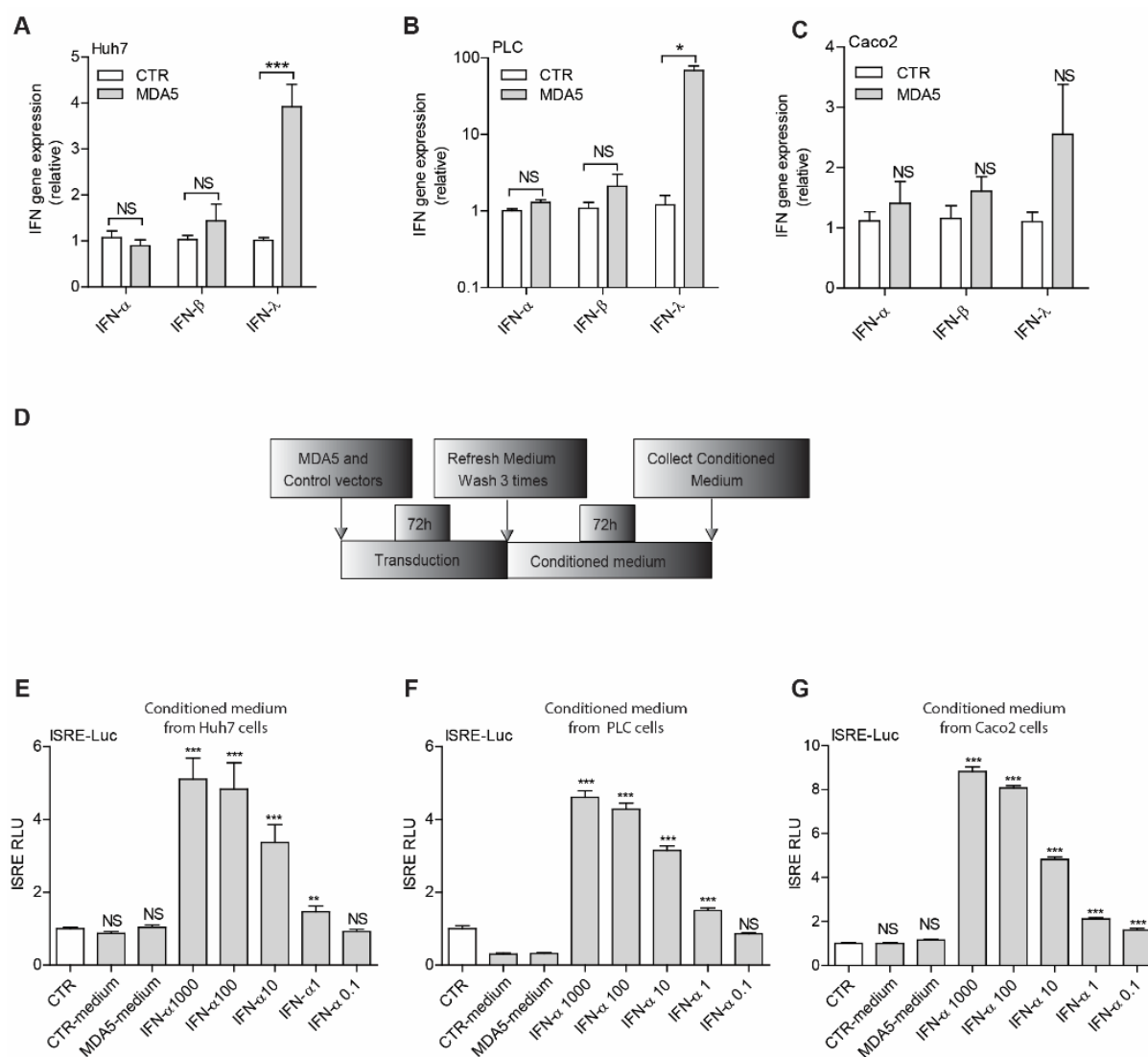


Figure 3. MDA5 overexpression did not induce the production of functional IFNs. (A) Quantitative RT-PCR analysis of IFN gene mRNA level in Huh7-p6 cells, (B) PLC-p6 cells and (C) Caco2 cells transduced with MDA5 or Fluc vector for 48h. (D) Production of conditioned medium (supernatant). Cells were transduced with MDA5 or Fluc (control) vector for 72 hours; then, the cells were washed five times, and medium was refreshed. Cells were cultured for another 72 hours, and supernatant was collected as conditioned medium. (E) Analysis of ISRE-related firefly luciferase activity in Huh7-ISRE-Luc cells treated with conditioned medium from Huh7-p6 cells, (F) PLC-p6 cells and (G) Caco2 cells or various concentrations of IFN- α for 48 hours. Data were normalized to the Fluc control (CTR, set as 1). Data are means \pm SEM of three independent experiments with 2-4 biological repeats for each. *P < 0.05; **P < 0.01; ***P < 0.001; Abbreviation: ns, not significant ; CTR, control; RLU, relative luciferase unit.

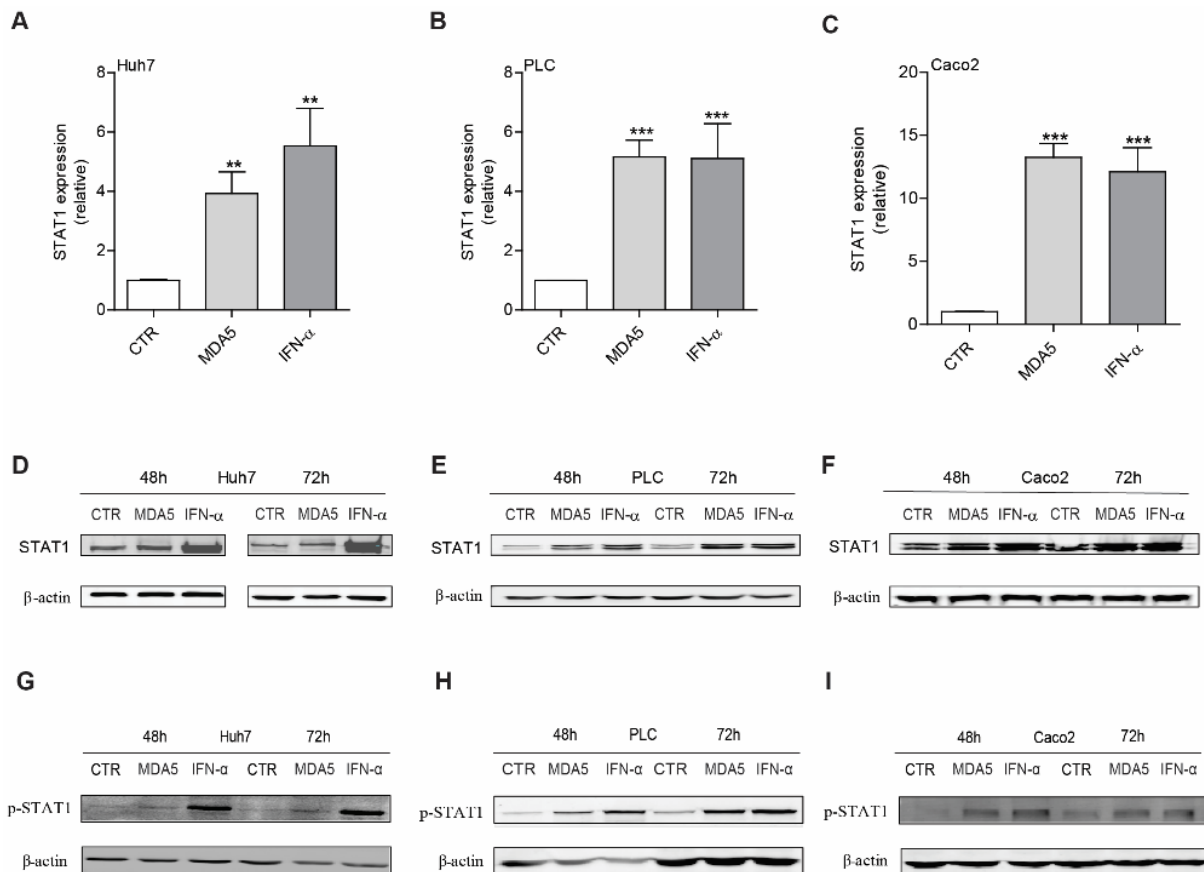
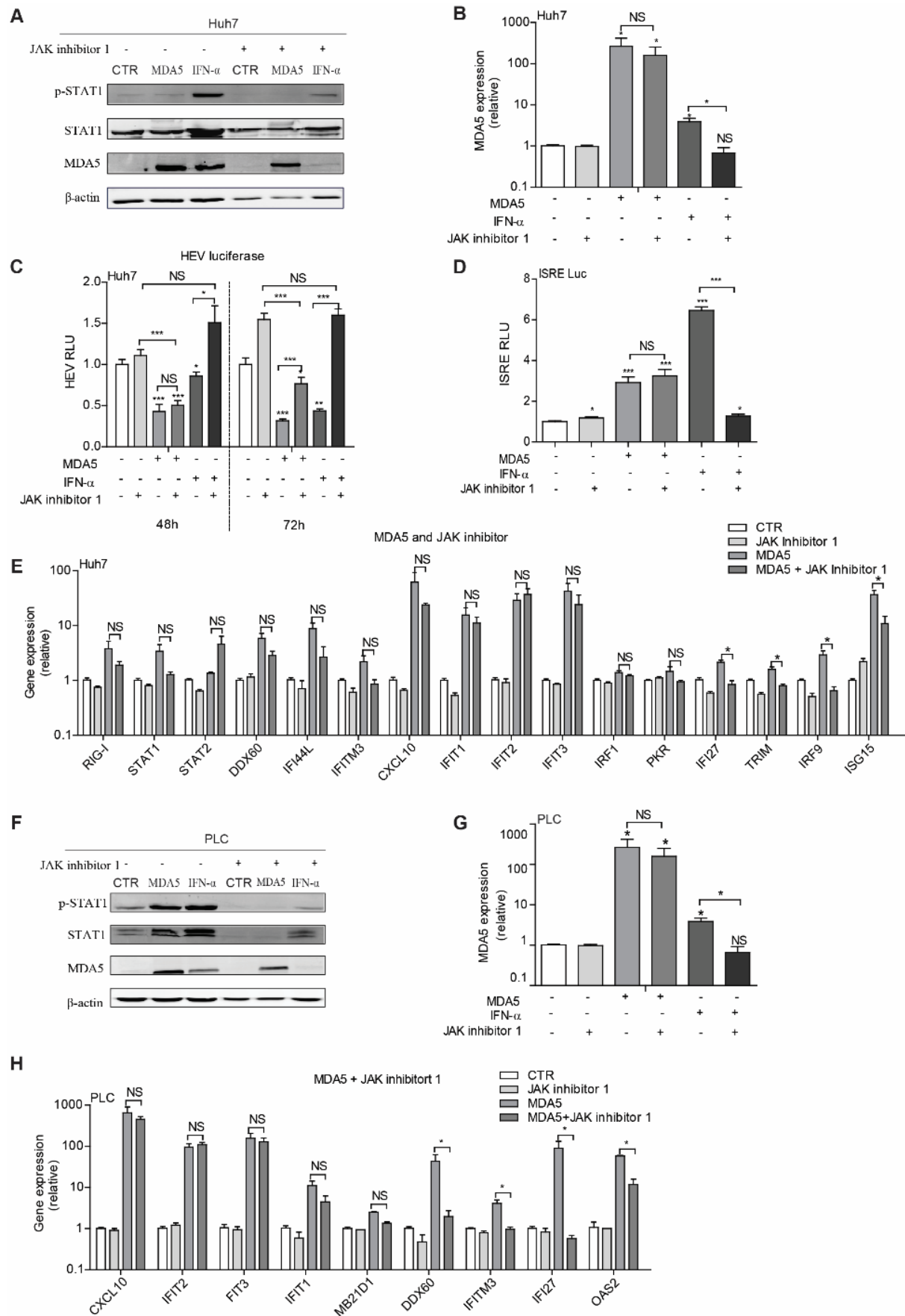


Figure 4. MDA5 overexpression activates STAT1 expression and phosphorylation. (A) Quantitative RT-PCR analysis of STAT1 mRNA level in Huh7-p6 cells, (B) PLC-p6 cells and (C) Caco2 cells transduced with MDA5 or Fluc vector for 48h. (D) Immunoblot analysis of STAT1 expression in Huh7-p6 cells, (E) PLC-p6 cells and (F) Caco2 cells transduced with MDA5 vector or treated with IFN- α (1000 IU/MI) for 48 or 72 hours. (G) Immunoblot analysis of p-STAT1 (Tyr701) expression in Huh7-p6 cells, (H) PLC-p6 cells and (I) Caco2 cells transduced with MDA5 vector or treated with IFN- α (1000 IU/MI) for 48 or 72 hours. Data were normalized to the Fluc control (CTR, set as 1). Data are means \pm SEM of three independent experiments with 2-4 biological repeats for each. *P < 0.05; **P < 0.01; ***P < 0.001; Abbreviation: CTR, control.

The effect of JAK-STAT pathway on MDA5-mediated antiviral ability and triggered ISG transcription

Because MDA5 activates STAT1 expression and phosphorylation, we further investigated the role of JAK-STAT pathway on MDA5-mediated ISG transcription and antiviral activity. We firstly used JAK inhibitor 1 to pharmacologically block the JAK-STAT pathway. As expected, MDA5 or IFN- α -induced p-STAT1 were effectively blocked by JAK inhibitor (Fig. 5A), whereas lentiviral-delivered MDA5 overexpression was not affected by the inhibitor in Huh7 cells (Fig. 5A, 5B). Surprisingly, the anti-HEV activity of MDA5 only partially attenuated, whereas the anti-HEV activity of IFN- α was totally blocked by JAK inhibitor 1 (Fig. 5C). Consistently, MDA5-



< Figure 5. JAK inhibitor 1 partially attenuates MDA5-induced ISG transcription and anti-HEV activity.

(A) Immunoblot analysis of p-STAT1 (Tyr701) expression and ISG protein levels in Huh7 cells transduced with MDA5 vector or treated with IFN- α (1000 IU/mL) or JAK inhibitor 1 (10 μ M) for 48 hours. (B) Quantitative RT-PCR analysis of MDA5 mRNA levels in Huh7 cells transduced with MDA5 vector or treated with IFN- α (1000 IU/mL) or JAK inhibitor 1 (10 μ M) for 48 hours. (C) Analysis of HEV-related Gaussia luciferase activity in Huh7-p6-luciferase cells transduced with MDA5 or Fluc vector or treated with IFN- α (1000 IU/mL) or JAK inhibitor 1 (10 μ M) for 48 hours. (D) Analysis of ISRE-related firefly luciferase activity in Huh7-ISRE-Luc cells transduced with MDA5 or Fluc vector or treated with IFN- α (1000 IU/mL) or JAK inhibitor 1 (10 μ M) for 48 hours. (E) Quantitative RT-PCR analysis of ISG mRNA levels in Huh7 cells transduced with MDA5 vector or Fluc control or JAK inhibitor 1 (10 μ M) for 48 hours. (F) Immunoblot analysis of p-STAT1 (Tyr701) expression and ISG protein levels in PLC cells transduced with MDA5 vector or treated with IFN- α (1000 IU/mL) or JAK inhibitor 1 (10 μ M) for 48 hours. (G) Quantitative RT-PCR analysis of MDA5 mRNA levels in PLC cells transduced with MDA5 vector or treated with IFN- α (1000 IU/mL) or JAK inhibitor 1 (10 μ M) for 48 hours. (H) Quantitative RT-PCR analysis of ISG mRNA levels in PLC cells transduced with MDA5 vector or Fluc control or JAK inhibitor 1 (10 μ M) for 48 hours. Data were normalized to the Fluc control (CTR, set as 1). Data are means \pm SEM of three independent experiments with 2-4 biological repeats for each. *P < 0.05; **P < 0.01; ***P < 0.001; Abbreviation: ns, not significant; CTR, control.

induced ISRE activation was hardly affected by this inhibitor, whereas ISRE activation induced by IFN- α was totally blocked (Fig. 5D). Subsequently, we measured the mRNA level of many antiviral ISGs in MDA5-overexpressed Huh7 cells treated with JAK inhibitor 1. Expectedly, only a small fraction of ISGs was affected by the inhibitor (Fig. 5E). In contrast, IFN- α -induced ISGs transcription was totally blocked by the inhibitor (Supporting Fig. 2A). Similar results were observed in PLC cells (Fig. 5F, 5G, 5H, and supporting Fig. 2B).

To further confirm, we overexpressed MDA5 in STAT1 knockout (STAT1^{-/-}) and wildtype Huh7 cells (Fig. 6A, 6B). Although MDA5 failed to induce p-STAT1 in STAT1^{-/-} cells (Fig. 6B), it induced a similar level of ISG transcript compared with in wildtype Huh7 cells (Fig. 6C). In contrast, IFN- α failed to induce ISGs in STAT1^{-/-} cells (Supporting Fig. 3A).

In HuNV and rotavirus models, we observed similar results that the induction of ISGs and antiviral activity of MDA5 only partially attenuated, but the effects of IFN- α was totally blocked by JAK inhibitor 1 (Fig. 7, and supporting Fig. 4A, 4B). Collectively, these results demonstrated that the induction of ISG transcription and the anti-enteric virus activity of MDA5 only partially depend on JAK-STAT cascade.

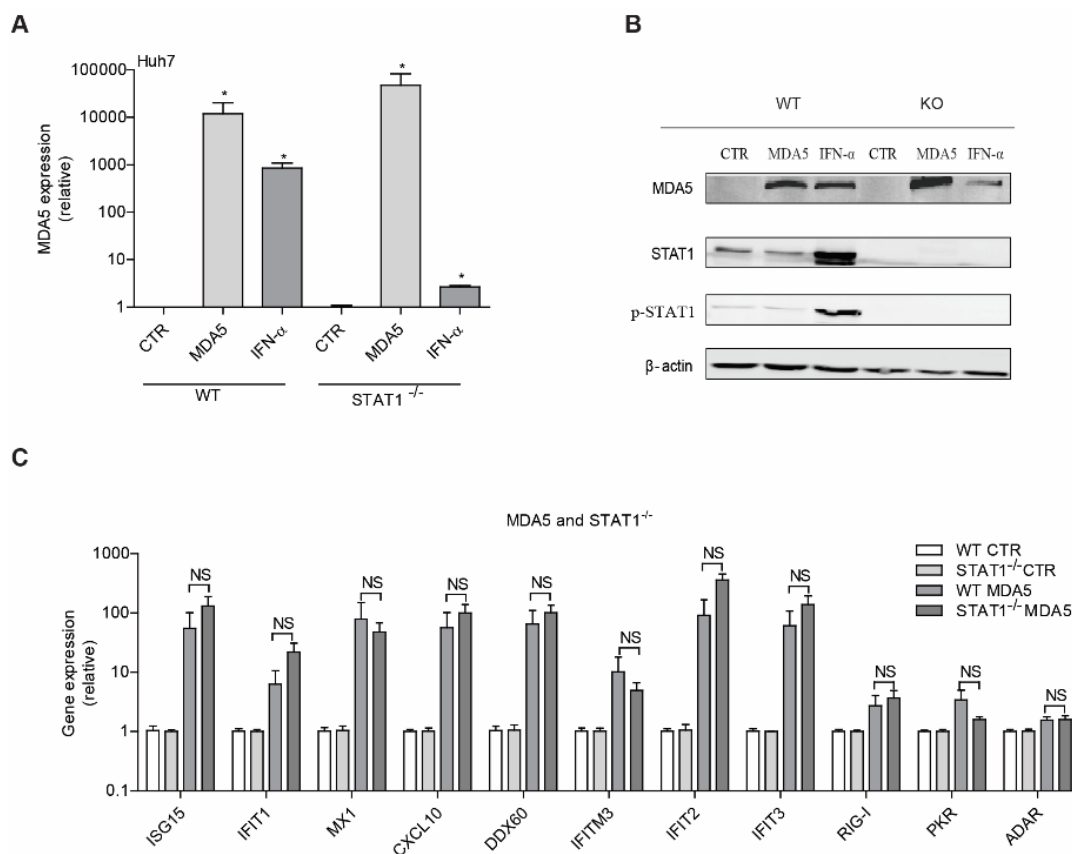


Figure 6 MDA5-induced ISG transcription was not affected in STAT1 knockout cells. (A) Quantitative RT-PCR analysis of MDA5 mRNA levels in WT and STAT1^{-/-} Huh7 cells transduced with MDA5 vector or Fluc control for 48 hours. (B) Immunoblot analysis of ISG protein level in WT and STAT1^{-/-} Huh7 cells transduced with MDA5 vector or Fluc control for 48 hours. (C) Quantitative RT-PCR analysis of ISG mRNA levels in WT and STAT1^{-/-} Huh7 cells transduced with MDA5 vector or Fluc for 48 hours. Data were normalized to the Fluc control (CTR, set as 1). Data are means \pm SEM of three independent experiments with 2-4 biological repeats for each. *P < 0.05; **P < 0.01; ***P < 0.001. Abbreviation: ns, not significant; CTR, control.

Discussion

Our study shows that MDA5 is a broad antiviral factor against enteric virus infection, including HEV, HuNV and rotavirus. Overexpression of MDA5 induces the phosphorylation of STAT1 and triggers the transcription of a panel of antiviral ISGs, without requirement of functional IFN production. Knockout or pharmacological inhibition of STAT1 only partially blocked the induction of ISG transcription and the antiviral activity of MDA5.

The innate immune system is the first line of defense against viral infection. One predominant characteristic is the rapid and spectrum of resistance to infection through recognition of viral

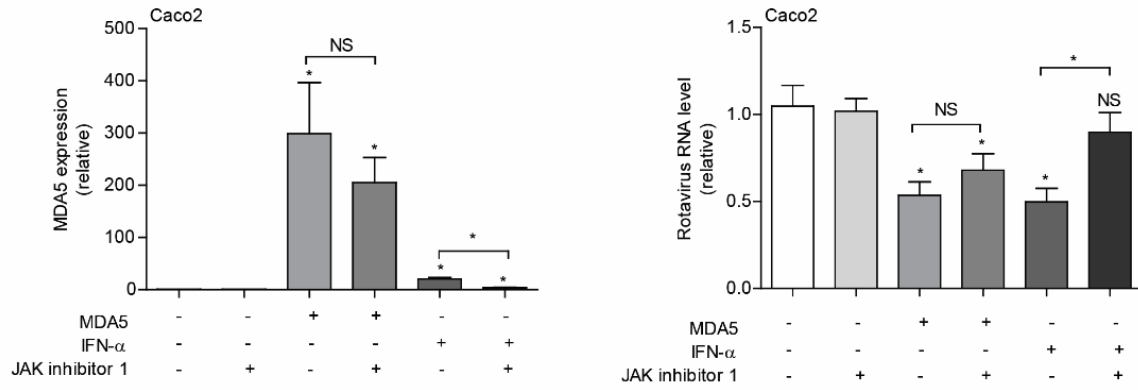
components by host PRRs, which initiate signal cascade transduction that triggers the production and secretion of IFNs. Subsequently, IFNs stimulate transcription of ISGs through JAK-STAT pathway to establish antiviral state. Among of them, only small subset of ISGs have antiviral effects (10). Previous results have shown that MDA5 plays important role in defending against a wide range of viral infections (14-17). Consistent with these reports, we found that MDA5 significantly inhibits enteric viruses replication in multiple cell models.

MDA5 is a main cytoplasmic sensor, which recognizes the viral RNA to trigger downstream antiviral signaling (16-19). Classically, virus infection induces MDA5 activation and mediates IFNs production through MAVS-IRF3 signal pathway. Several studies have demonstrated that MDA5 induce IFN- α or IFN- β production during virus infection (16,20). In turn, IFNs combat viral infection and exert immune regulatory roles through induction of ISGs. In this study, we found that MDA5 induced transcription and expression of many ISGs, and most of these have been reported to have antiviral activity (10,21-23). However, the expression pattern of ISGs induced by MDA5 is different from IFN- α treatment. For instance, in Huh7 cells, overexpression of MDA5 highly activates the expression of IFIT2, IFIT3 and CXCL10, whereas the expression of PKR and IFI27 is highly activated by IFN- α treatment. This indicates non-canonical mechanisms of MDA5 in promoting ISG transcription.

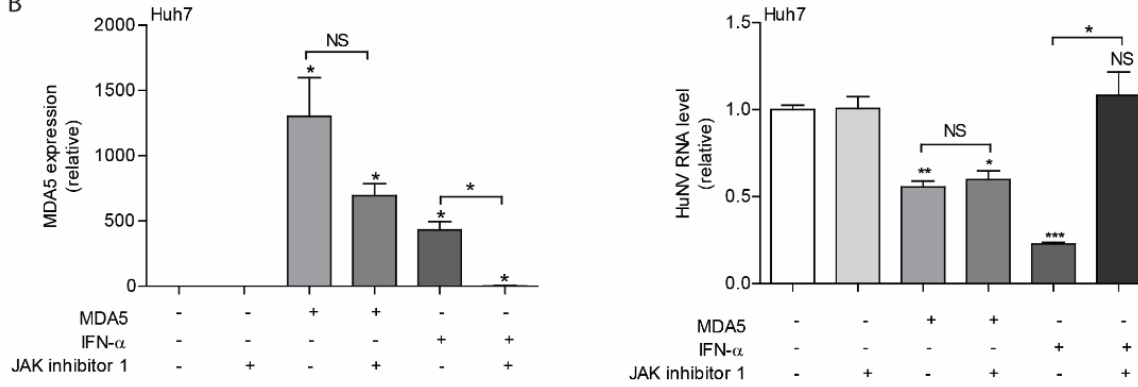
For rotavirus infection, it has been reported that MDA5 and RIG-I are important sensors to trigger IFN response through MAVS, whereas MDA5 silencing significantly decreased IFN production (24). However, we have previously demonstrated that in culture of intestinal epithelial cell line or organoids, infection of rotavirus increased IFN gene transcription, but not the production of IFN proteins (25). Consistently, in the different models of this study, MDA5 did not induce the production of IFNs, but provoked a non-canonical IFN-like response. Similar actions have been previously observed for RIG-I and IFN regulatory factor 1 (IRF1) in inhibiting HEV replication in epithelial cell lines (22,23). Mechanistically, this remains an intriguing question that how these broad antiviral factors can trigger ISG transcription without the requirement of IFN production?

It has been previously reported that RIG-I overexpression triggers STAT1 expression and activation (22,26). Similarly, we found that overexpression of MDA5 also activates STAT1 expression and phosphorylation at the 701 site. STAT1 phosphorylation is the hallmark of JAK-STAT activation cascade, the downstream cascade of IFN pathway. Interestingly, genetic silencing of STAT1 or pharmacological inhibition of JAK-STAT pathway only partially attenuated ISG induction and antiviral activity of MDA5, whereas completely blocked IFN- α -induced ISG transcription and antiviral activity. It has been reported that these non-classical antiviral mechanisms are also very important in antiviral defense. For instance, there are different forms of ISGF3 complexes, and some function independent of the JAK-STAT pathway.

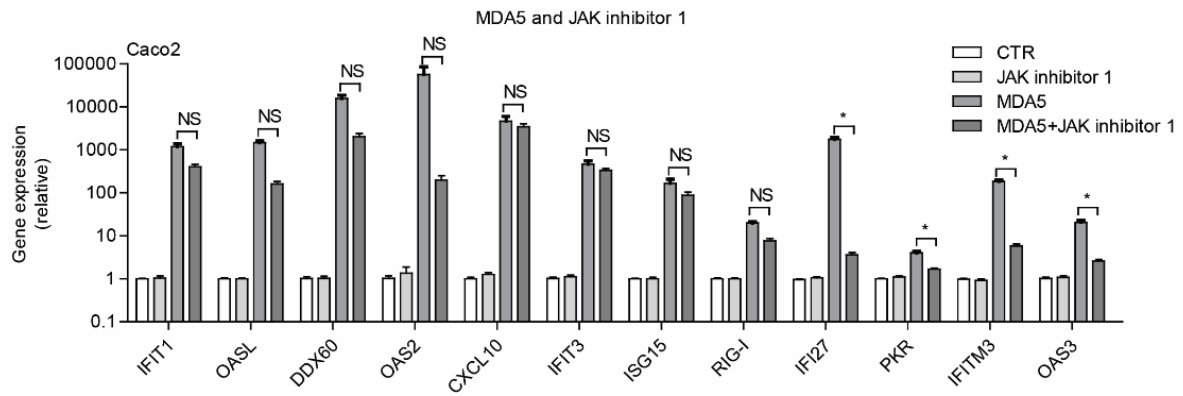
A



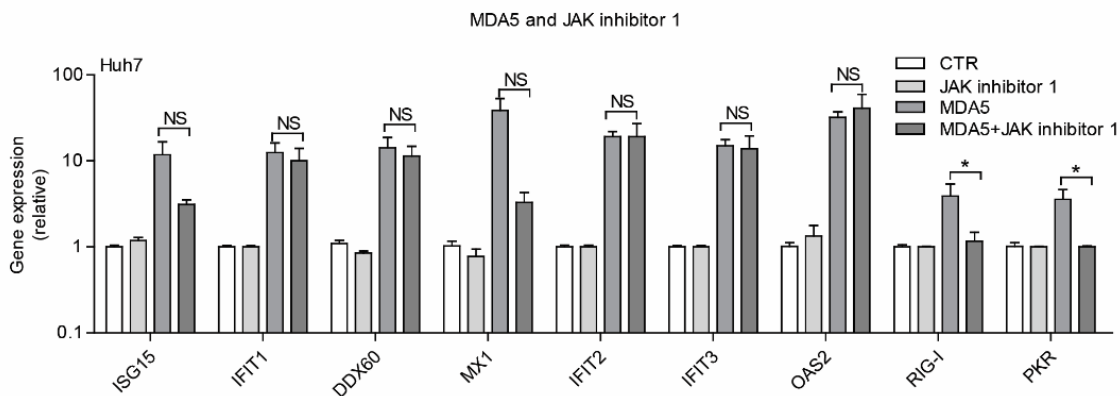
B



C



D



< Figure 7. MDA5 inhibits rotavirus and HuNV replication and induced ISG transcription partially via JAK-STAT pathway (A) Quantitative RT-PCR analysis of MDA5 mRNA levels or rotavirus RNA level in Caco2 cells transduced with MDA5 vector or treated with IFN- α (1000 IU/mL) or JAK inhibitor 1 (10 μ M) for 48 hours. (B) Quantitative RT-PCR analysis of MDA5 mRNA levels or HuNV RNA level in HG23 cells transduced with MDA5 vector or treated with IFN- α (1000 IU/mL) or JAK inhibitor 1 (10 μ M) for 48 hours. (C) Quantitative RT-PCR analysis of ISG mRNA levels in Caco2 cells or (D) HG23 cells transduced with MDA5 vector or treated with IFN- α (1000 IU/mL) or JAK inhibitor 1 (10 μ M) for 48 hours. Data are means \pm SEM of three independent experiments with 2-4 biological repeats for each. *P < 0.05; **P < 0.01; ***P < 0.001. Abbreviation: ns, not significant; CTR, control

Unphosphorylated ISGF3 (u-ISGF3) complex has been demonstrated to drive antiviral ISG expression and protect from viral infections at homeostatic status (27,28). The STAT2-IRF9 complex can also regulate antiviral activity and ISG expression without the presence of STAT1 (29). Thus, our findings on MDA5 have added new knowledge to the non-classical IFN responses.

In summary, MDA5 potently inhibits the infection of enteric viruses, including HEV, HuNV and rotavirus. It provokes an antiviral IFN-like response without requirement of IFN production, but is partially dependent on the JAK-STAT cascade. These findings have revealed non-canonical actions of MDA5 on viral infection, and the detailed mechanisms deserve further investigation.

References

1. Kamar, N., Selves, J., Mansuy, J. M., et al. (2008) Hepatitis E virus and chronic hepatitis in organ-transplant recipients. *N Engl J Med* 358, 811-817
2. Zhou, X., de Man, R. A., de Knegt, R. J., et al. (2013) Epidemiology and management of chronic hepatitis E infection in solid organ transplantation: a comprehensive literature review. *Rev Med Virol* 23, 295-304
3. Bok, K., and Green, K. Y. (2012) Norovirus gastroenteritis in immunocompromised patients. *N Engl J Med* 367, 2126-2132
4. Yin, Y., Metselaar, H. J., Sprengers, D., et al. (2015) Rotavirus in organ transplantation: drug-virus-host interactions. *Am J Transplant* 15, 585-593
5. Medzhitov, R., and Janeway, C., Jr. (2000) Innate immunity. *N Engl J Med* 343, 338-344
6. O'Neill, L. A., and Bowie, A. G. (2010) Sensing and signaling in antiviral innate immunity. *Curr Biol* 20, R328-333
7. Jensen, S., and Thomsen, A. R. (2012) Sensing of RNA viruses: a review of innate immune receptors involved in recognizing RNA virus invasion. *J Virol* 86, 2900-2910
8. Schneider, W. M., Chevillotte, M. D., and Rice, C. M. (2014) Interferon-stimulated genes: a complex web of host defenses. *Annu Rev Immunol* 32, 513-545
9. Seth, R. B., Sun, L., Ea, C. K., et al. (2005) Identification and characterization of MAVS, a mitochondrial antiviral signaling protein that activates NF-kappaB and IRF 3. *Cell* 122, 669-682

10. Schoggins, J. W., Wilson, S. J., Panis, M., et al. (2011) A diverse range of gene products are effectors of the type I interferon antiviral response. *Nature* 472, 481-485
11. Pan, Q., de Ruyter, P. E., Metselaar, H. J., et al. (2012) Mycophenolic acid augments interferon-stimulated gene expression and inhibits hepatitis C Virus infection in vitro and in vivo. *Hepatology* 55, 1673-1683
12. Shukla, P., Nguyen, H. T., Faulk, K., et al. (2012) Adaptation of a genotype 3 hepatitis E virus to efficient growth in cell culture depends on an inserted human gene segment acquired by recombination. *J Virol* 86, 5697-5707
13. Chang, K. O., Sosnovtsev, S. V., Belliot, G., et al. (2006) Stable expression of a Norwalk virus RNA replicon in a human hepatoma cell line. *Virology* 353, 463-473
14. Dang, W., Xu, L., Yin, Y., et al. (2018) IRF-1, RIG-I and MDA5 display potent antiviral activities against norovirus coordinately induced by different types of interferons. *Antiviral Res* 155, 48-59
15. Lu, H. L., and Liao, F. (2013) Melanoma differentiation-associated gene 5 senses hepatitis B virus and activates innate immune signaling to suppress virus replication. *J Immunol* 191, 3264-3276
16. Zhang, Z., Filzmayer, C., Ni, Y., et al. (2018) Hepatitis D virus replication is sensed by MDA5 and induces IFN-beta/lambda responses in hepatocytes. *J Hepatol* 69, 25-35
17. Cao, X., Ding, Q., Lu, J., et al. (2015) MDA5 plays a critical role in interferon response during hepatitis C virus infection. *J Hepatol* 62, 771-778
18. Kuo, R. L., Kao, L. T., Lin, S. J., et al. (2013) MDA5 plays a crucial role in enterovirus 71 RNA-mediated IRF3 activation. *PLoS One* 8, e63431
19. Wei, L., Cui, J., Song, Y., et al. (2014) Duck MDA5 functions in innate immunity against H5N1 highly pathogenic avian influenza virus infections. *Vet Res* 45, 66
20. Pham, A. M., Santa Maria, F. G., Lahiri, T., et al. (2016) PKR Transduces MDA5-Dependent Signals for Type I IFN Induction. *PLoS Pathog* 12, e1005489
21. Schoggins, J. W., MacDuff, D. A., Imanaka, N., et al. (2014) Pan-viral specificity of IFN-induced genes reveals new roles for cGAS in innate immunity. *Nature* 505, 691-695
22. Xu, L., Wang, W., Li, Y., et al. (2017) RIG-I is a key antiviral interferon-stimulated gene against hepatitis E virus regardless of interferon production. *Hepatology* 65, 1823-1839
23. Xu, L., Zhou, X., Wang, W., et al. (2016) IFN regulatory factor 1 restricts hepatitis E virus replication by activating STAT1 to induce antiviral IFN-stimulated genes. *FASEB J* 30, 3352-3367
24. Broquet, A. H., Hirata, Y., McAllister, C. S., et al. (2011) RIG-I/MDA5/MAVS are required to signal a protective IFN response in rotavirus-infected intestinal epithelium. *J Immunol* 186, 1618-1626
25. Hakim, M. S., Chen, S., Ding, S., et al. (2018) Basal interferon signaling and therapeutic use of interferons in controlling rotavirus infection in human intestinal cells and organoids. *Sci Rep* 8, 8341
26. Jiang, L. J., Zhang, N. N., Ding, F., et al. (2011) RA-inducible gene-I induction augments STAT1 activation to inhibit leukemia cell proliferation. *Proc Natl Acad Sci U S A* 108, 1897-1902
27. Wang, W., Yin, Y., Xu, L., et al. (2017) Unphosphorylated ISGF3 drives constitutive expression of interferon-stimulated genes to protect against viral infections. *Sci Signal* 10
28. Sung, P. S., Cheon, H., Cho, C. H., et al. (2015) Roles of unphosphorylated ISGF3 in HCV infection and interferon responsiveness. *Proc Natl Acad Sci U S A* 112, 10443-10448
29. Blaszczyk, K., Olejnik, A., Nowicka, H., et al. (2015) STAT2/IRF9 directs a prolonged ISGF3-like transcriptional response and antiviral activity in the absence of STAT1. *Biochem J* 466, 511-524

Supplementary information

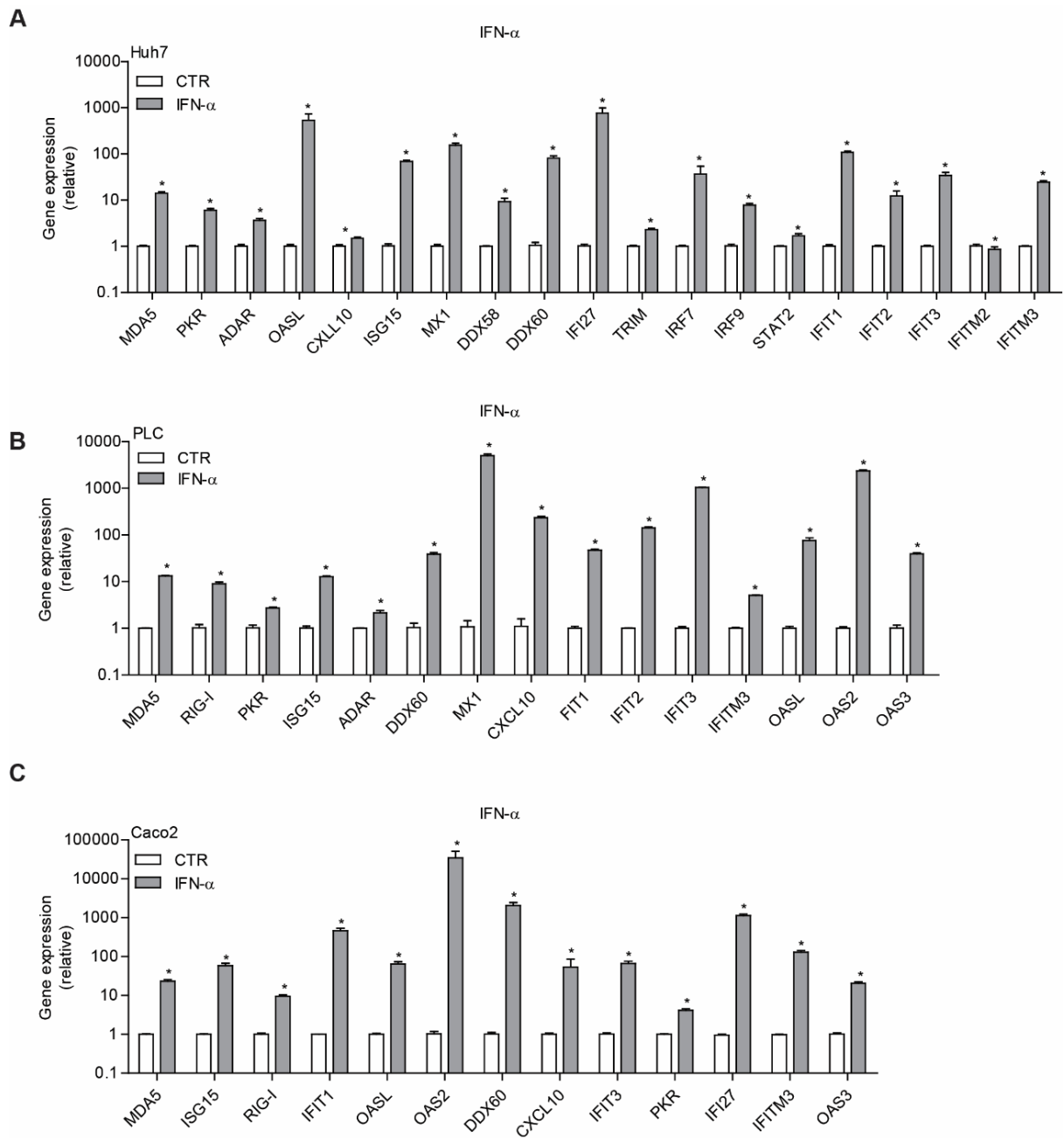


Fig. S1 IFN- α induce a range of antiviral ISG transcription. (A) Quantitative RT-PCR analysis of ISG mRNA level in Huh7, (B) PLC or (C) Caco2 cells treated or untreated with IFN- α (1000 IU/mL) for 48 hours. Data were normalized to the untreated control (CTR, set as 1). Data are means \pm SEM of three independent experiments. Abbreviation: CTR, control.

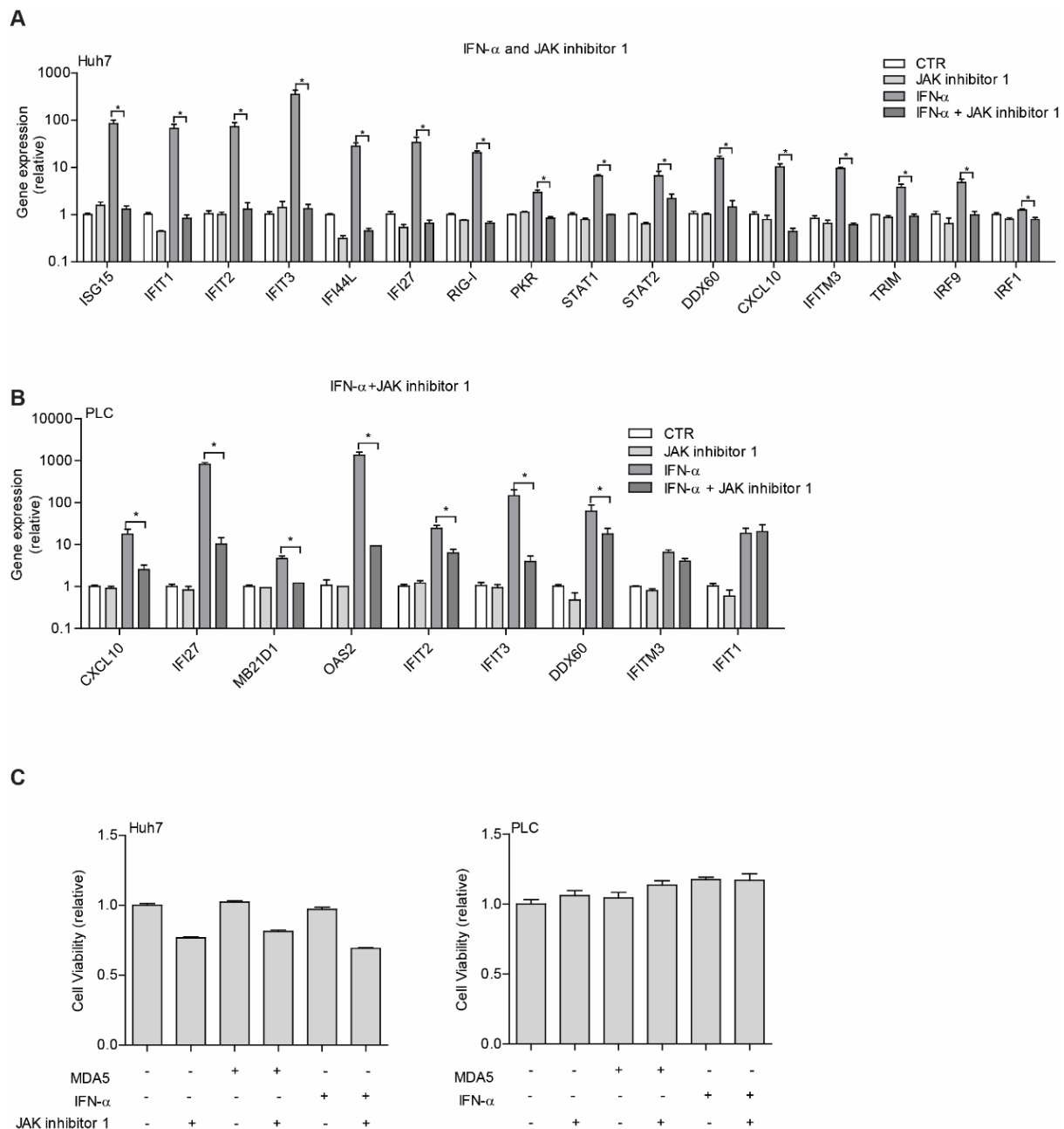


Fig. S2 JAK inhibitor 1 totally blocked IFN- α -induced ISG transcription. (A) Quantitative RT-PCR analysis of ISG mRNA levels in Huh7 or (B) PLC cells treated with IFN- α (1000 IU/mL) or JAK inhibitor 1 (10 μ M) for 48 hours. (C) MTT assay analysis of cell viability in Huh7 or PLC cells transduced with MDA5 vector or treated with IFN- α (1000 IU/mL) or JAK inhibitor 1 (10 μ M) for 48 hours. Data were normalized to the untreated control (CTR, set as 1). Data are means \pm SEM of three independent experiments. Abbreviation: CTR, control.

A

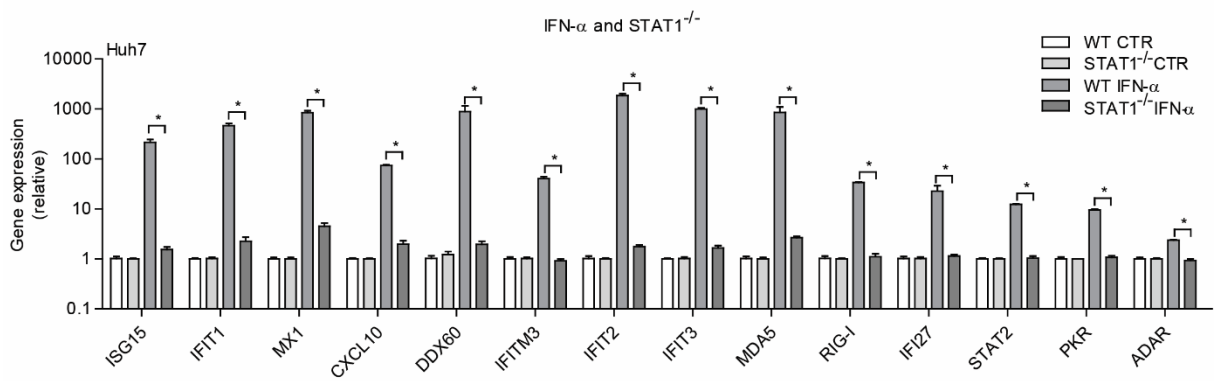


Fig. S3 IFN- α does not induce ISG transcription in STAT1 deficient cells. (A) Quantitative RT-PCR analysis of ISG mRNA levels in WT and STAT1^{-/-} Huh7 cells with IFN- α (1000 IU/mL) for 48 hours. Data were normalized to the untreated WT and STAT1^{-/-} cells, respectively (Both set as 1). Data are means \pm SEM of three independent experiments. Abbreviation: CTR, control.

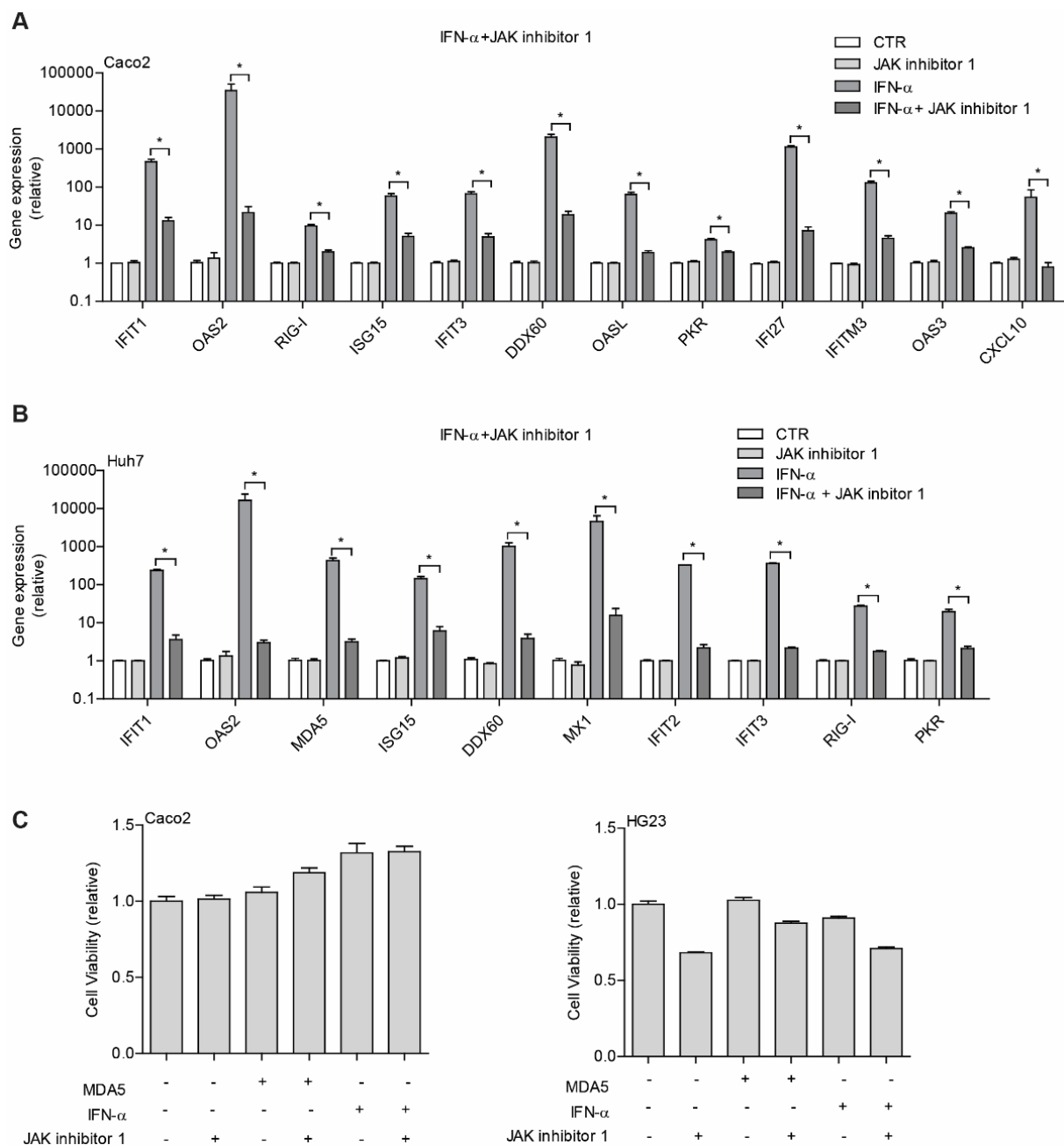


Fig. S4 JAK inhibitor 1 totally blocked IFN- α -induced ISG transcription. (A) Quantitative RT-PCR analysis of ISG mRNA levels in Caco2 cells or (B) Huh7 cells treated with IFN- α (1000 IU/mL) or JAK inhibitor 1 (10 μ M) for 48 hours. (C) MTT assay analysis of cell viability in Caco2 or HG23 cells transduced with MDA5 vector or treated with IFN- α (1000 IU/mL) or JAK inhibitor 1 (10 μ M) for 48 hours. Data were normalized to the untreated control (CTR, set as 1). Data are means \pm SEM of three independent experiments. Abbreviation: CTR, control.

Supplementary Table 1. Lentiviral shRNA sequence

No.	Gene	Accession	Sequences	Target Sequences
shMDA5	IFIH1	NM_022168.2	CCGGCCCATGACACAGAATGAAC AACTCGAGTTGTTTCATTCTGTGTC ATGGGTTTTTG	CCCATGACACAGAAT GAACAA

Supplementary Table 2. Primer sequences

Gene	F-Sequences (5' to 3')	R-Sequences (5' to 3')
HEV	ATCGGCCAGAAGTTGGTTTTTAC	CCGTGGCTATAACTGTGGTCT
HuNV	CGYTGGATGCGNTTYCATGA	CTTAGACGCATCATCATTYAC
RTV	TGGTTAACGCAGGATCGGA	AACCTTTCCGCGTCTGGTAG
GAPDH	GTCTCCTCTGACTTCAACAGCG	ACCACCCTGTTGCTGTAGCCAA
MDA5 (IFIH1)	GCTGAAGTAGGAGTCAAAGCCC	CCACTGTGGTAGCGATAAGCAG
RIG-I (DDX58)	CACCTCAGTTGCTGATGAAGGC	GTCAGAAGGAAGCACTTGCTACC
ADAR	TCCGTCTCCTGTCCAAAGAAGG	TTCTTGCTGGGAGCACTCACAC
PKR	GAAGTGGACCTCTACGCTTTGG	TGATGCCATCCCGTAGGTCTGT
CXCL10	GGTGAGAAGAGATGTCTGAATCC	GTCCATCCTTGAAGCACTGCA
ISG15	CTCTGAGCATCCTGGTGAGGAA	AAGGTCAGCCAGAACAGGTCGT
MX1	GGCTGTTTACCAGACTCCGACA	CACAAAGCCTGGCAGCTCTCTA
DDX60	GGTGTTTTACCAGGGAGTATCG	CCAGTTTTGGCGATGAGGAGCA
IFI27	CGTCCTCCATAGCAGCCAAGAT	ACCCAATGGAGCCCAGGATGAA
STAT1	ATGGCAGTCTGGCGGCTGAATT	CCAAACCAGGCTGGCACAATTG
STAT2	CAGGTCACAGAGTTGCTACAGC	CGGTGAACTTGCTGCCAGTCTT
IFIT1	GCCTTGCTGAAGTGTGGAGGAA	ATCCAGGCGATAGGCAGAGATC
IRF1	GAGGAGGTGAAAGACCAGAGCA	TAGCATCTCGGCTGGACTTCTGA
IRF7	CCACGCTATACCATCTACCTGG	GCTGCTATCCAGGGAAGACACA
IRF9	CCACCGAAGTTCCAGGTAACAC	AGTCTGCTCCAGCAAGTATCGG
IFIT2	GGAGCAGATTCTGAGGCTTTGC	GGATGAGGCTCCAGACTCCAA
IFIT3	CCTGGAATGCTTACGGCAAGCT	GAGCATCTGAGAGTCTGCCCAA
IFITM2	GGCTTCATAGCATTTCGCTACTC	AGATGTTCCAGGCACTTGGCGGT
IFITM3	CTGGGCTTCATAGCATTTCGCT	AGATGTTCCAGGCACTTGGCGGT
OAS2	GCTTCCGACAATCAACAGCCAAG	CTTGACGATTTTGTGCCGCTCG
OASL	GTGCCTGAAACAGGACTGTTGC	CCTCTGCTCCACTGTCAAGTGG
IFI44L	TGCACTGAGGCAGATGCTGCG	TCATTGCGGCACACCAGTACAG
IFN- α	TGGGCTGTGATCTGCCTCAAAC	CAGCCTTTTGGAACTGGTTGCC
IFN- β	CTTGATTCTACAAAGAAGCAGC	TCCTCCTTCTGGAAGTCTGCA
IFN- λ	GGAAGACAGGAGAGCTGCAACT	AACTGGGAAGGGCTGCCACATT

Chapter 6

Murine norovirus replicase augments RIG-I-like receptors-mediated antiviral interferon response

Peifa Yu, Yang Li, Yunlong Li, Zhijiang Miao, Yining Wang, Maikel P. Peppelenbosch, Qiuwei Pan

Antiviral Research, 2020, 182: 104877.

Abstract

Noroviruses are the main causative agents for acute viral gastroenteritis worldwide. RIG-I-like receptors (RLRs) triggered interferon (IFN) activation is essential for host defense against viral infections. In turn, viruses have developed sophisticated strategies to counteract host antiviral response. This study aims to investigate how murine norovirus (MNV) replicase interacts with RLRs-mediated antiviral IFN response. Counterintuitively, we found that the MNV replicase NS7 enhances the activation of poly (I:C)-induced IFN response and the transcription of downstream interferon-stimulated genes (ISGs). Interestingly, NS7 protein augments RIG-I and MDA5-triggered antiviral IFN response, which conceivably involves direct interactions with the caspase activation and recruitment domains (CARDs) of RIG-I and MDA5. Consistently, RIG-I and MDA5 exert anti-MNV activity in human HEK293T cells with ectopic expression of viral receptor CD300lf. This effect requires the activation of JAK/STAT pathway, and is further enhanced by NS7 overexpression. These findings revealed an unconventional role of MNV NS7 as augmenting RLRs-mediated IFN response to inhibit viral replication.

Keywords: norovirus, NS7, RIG-I, MDA5, ISGs

Introduction

Human noroviruses (HuNV) are positive sense single-stranded RNA viruses belonging to the *Caliciviridae* family (1). Although they are the major causes of epidemic nonbacterial gastroenteritis worldwide (2,3), progress on norovirus research has been hampered by the lack of robust cell culture systems. The closely related murine norovirus (MNV) shares similar structural and genetic features with HuNV and can efficiently propagate *in vitro* and *in vivo* (4,5). Importantly, the recent discovery of the MNV receptor (CD300lf) breaks the barriers for viral infection in human cells, and enables the study of MNV in human cell models (6,7).

The MNV genome is approximately 7.5 kilo bases (kb) in length that encodes four open reading frames (ORFs) (1,8). ORF1 encodes a polyprotein that is post-translationally cleaved into six non-structural proteins (NS1/2 to NS7), while ORF2 and ORF3 encode the major and minor structural proteins that referred to as VP1 and VP2, respectively (9). ORF4 overlaps with ORF2, and encodes the virulence factor (VF1), which can antagonize innate immune response to MNV infection (8,9). The non-structural proteins are associated with the viral replication complex induced membrane clusters, and interaction with host factors to regulate cellular homeostasis and promote viral replication (10,11). NS7 is the viral RNA-dependent RNA polymerase (RdRp) (12,13), responsible for viral replication.

Interferon (IFN)-mediated innate immune response provides a forward line of cell-autonomous defense against viral infections (14). Upon infection, viral components can be recognized by specific pathogen recognition receptors including the RIG-I-like receptors (RLRs) RIG-I and MDA5, which subsequently activate IFN response (15,16). MDA5 has been demonstrated as a predominant sensor of MNV (17), whereas inactivating RIG-I signaling has no effects on HuNV replication (18). RIG-I and MDA5 contain the N-terminal caspase-recruitment domains (CARDs), which can recruit and interact with the CARD-containing adaptor named mitochondrial antiviral signaling protein (also known as IPS-1, VISA or Cardif) (19,20). The interaction stimulates downstream signaling pathways including activation of transcriptional factors NF- κ B and IRF3, and further induces type I IFN production (20,21). The released IFNs bind to their receptors and in turn activate Janus kinase (JAK)/signal transducer and activator of transcription (STAT) signaling pathway, leading to transcription of hundreds of interferon-stimulated genes (ISGs), some of which are considered as the ultimate antiviral effectors restricting viral replication (22).

Many viruses have developed sophisticated strategies to counteract the host IFN signaling. For instance, MNV VF1 can inhibit RLRs-mediated IFN response (9), and VP2 has been reported to possess important functions in viral replication and modulation of the host immune response (9). Studies have reported the regulation of viral replicases on RIG-I and MDA5

mediated IFN response. Semliki Forest virus (SFV) RdRp can induce IFN- β through the RIG-I and MDA5 pathways by converting host cell RNA into 5'-ppp RNA (23). Furthermore, transgenic mice stably expressing RdRp encoded by Theiler's murine encephalomyelitis virus (TMEV) can dramatically upregulate antiviral ISGs and confer profound resistance to ECMV challenge, and is refractory to HIV-1 infection in THP-1 cells (24). Recently, transgenic mice with similar antiviral mechanisms against retrovirus infection have also been documented (25). Previous studies have revealed that RNAs synthesized by transiently expression of norovirus RdRp can stimulate RIG-I-dependent reporter luciferase production via the IFN- β promoter (26). However, a recent study showed that the replicases of enterovirus 71 (EV71) and coxsackievirus B3 inhibit MDA5-mediated IFN activation through interaction with MDA5 (27). Given the importance and complicity of interactions between viral replicases with the host innate immunity, this study aims to investigate the role of MNV NS7 on regulating RLRs-mediated IFN activation and antiviral response.

Materials and methods

6

Reagents

Poly (I:C) (HMW) (Bio-Connect BV) was dissolved in distilled water. Stocks of JAK inhibitor 1 (SC-204021, Santa Cruz Biotechnology, Santa Cruz, CA, USA) were dissolved in DMSO (DMSO, Sigma, Zwijndrecht, the Netherlands) with a final concentration of 5 mg/ml. Halt™ Protease Inhibitor Cocktail (100X) was purchased from Thermo Fisher Scientific. Rabbit polyclonal antisera to MNV NS1/2 was kindly provided by Prof. Vernon K. Ward (School of Biomedical Sciences, University of Otago, New Zealand) (28). Rabbit polyclonal antisera to MNV NS7 was kindly provided by Prof. Ian Goodfellow (Department of Pathology, University of Cambridge, UK) (29). Mouse anti-RIG-I (clone 1C3, Sigma) and mouse anti-MDA5 (Proteintech) antibodies were used. β -actin antibody (#sc-47778) was purchased from Santa Cruz Biotechnology. IRDye® 800CW-conjugated goat anti-rabbit and goat anti-mouse IgGs (Li-Cor Bioscience, Lincoln, USA) were used as secondary antibodies, as appropriate.

Cells and viruses

RAW264.7 and human embryonic kidney (HEK293T) cells were cultured in Dulbecco's modified Eagle's medium (DMEM; Lonza Verviers, Belgium) supplemented with 10% (vol/vol) heat-inactivated fetal calf serum (FCS; Hyclone, Logan, UT, USA), 100 μ g/mL of streptomycin, and 100 IU/mL of penicillin. MNV-1 (murine norovirus strain MNV-1.CW1) (4) was kindly provided by Prof. Herbert Virgin (Department of Pathology and Immunology, Washington

University School of Medicine), and produced by inoculating the virus into RAW264.7 cells. The MNV-1 cultures were purified, aliquoted, and stored at $-80\text{ }^{\circ}\text{C}$ for all subsequent experiments. The MNV-1 stock was quantified three independent times by the 50% tissue culture infective dose (TCID₅₀).

TCID₅₀

TCID₅₀ assay was performed to quantify the viral titers. Briefly, 10-fold dilutions of MNV-1 were inoculated into RAW264.7 cells grown in 96-well tissue culture plate at 1,000 cells/well. The plate was incubated at $37\text{ }^{\circ}\text{C}$ for another 5 days, followed by observing the cytopathic effect (CPE) of each well under a light scope. The TCID₅₀ was calculated by using the Reed-Muench method.

Plasmid construction and cell transfection

The full length human RIG-I was amplified from a plasmid containing human RIG-I (kindly provided by Prof. Xuetao Cao, Nankai University, China) (30), and cloned into pcDNA3.1/Flag-HA (Addgene). The CARD domain of RIG-I was amplified and cloned into pcDNA3.1/Flag-HA and pcDNA3.1/Myc-His (kindly provided by Dr. Shuaiyang Zhao, Chinese Academy of Agricultural Sciences, China) vectors, respectively. The remaining domain of RIG-I without CARDS (pFlag-RIG-I_ΔCARD) was amplified and cloned into pcDNA3.1/Flag-HA vector. The full length and CARD domain of human MDA5 were amplified from pTRIP.CMV.IVSb.ISG.ires.TagRFP-based hMDA5 overexpression vector (kindly provided by Prof. Charles M. Rice, Rockefeller University, New York, USA) (22), and cloned into pcDNA3.1/Flag-HA vector. The Myc-tagged plasmid containing the CARD domain of MDA5 and the related empty vectors were kindly provided by Dr. Rei-Lin Kuo (Chang Gung University, Taiwan, China) (27). The MNV NS7 gene was amplified from cDNA that prepared from MNV-1 infected RAW264.7 cells, and cloned into Flag- and Myc-tagged vectors, respectively. The related N- and C-terminus of NS7 were also amplified and cloned into Flag-tagged vectors, respectively. The pFlag-CD300lf plasmid was kindly provided by Prof. Herbert Virgin (Department of Pathology and Immunology, Washington University School of Medicine, USA) (6). The primers used for plasmid construction are listed in supplementary table 1.

HEK293T cells were transfected with various plasmids at indicated concentrations using FuGENE HD Transfection Reagent (E2311; Promega) according to the manufacturer's instructions. Where necessary, the appropriate empty vectors were used to maintain a constant amount of plasmid DNA per transfection.

qRT-PCR

Total RNA was isolated with a Macherey NucleoSpin RNA II Kit (Bioke, Leiden, The Netherlands) and quantified with a Nanodrop ND-1000 (Wilmington, DE, USA). cDNA was synthesized from 500 ng of RNA using a cDNA synthesis kit (TaKaRa Bio, Inc., Shiga, Japan). The cDNA of all targeted genes were quantified by SYBR-Green-based (Applied Biosystems) real-time PCR on the StepOnePlus™ System (Thermo Fisher Scientific LifeSciences) according to the manufacturer's instructions. Human glyceraldehyde-3-phosphate dehydrogenase (GAPDH) and murine GAPDH genes were used as reference genes to normalize gene expression. The relative expression of targeted gene was calculated as $2^{-\Delta\Delta C_T}$, where $\Delta\Delta C_T = \Delta C_{T\text{sample}} - \Delta C_{T\text{control}}$ ($\Delta C_T = C_T[\text{targeted gene}] - C_T[\text{GAPDH}]$). All primer sequences are listed in supplementary table 2.

Western blotting

Cultured cells were lysed in Laemmli sample buffer containing 0.1 M DTT and heated 5 mins at 95 °C, then loaded onto a 10% sodium dodecyl sulfate polyacrylamide gel electrophoresis (SDS-PAGE) gel. Then proteins were further electrophoretically transferred onto a polyvinylidene difluoride (PVDF) membrane (pore size, 0.45 μm; Invitrogen) for 2 h with an electric current of 250 mA. Subsequently, the membrane was blocked with a mixture of 2.5 mL blocking buffer (Odyssey) and 2.5 mL PBS containing 0.05% Tween 20 for 1 h, followed by overnight incubation with primary antibodies (1:1000) at 4 °C. The membrane was washed 3 times and then incubated with appropriate IRDye-conjugated secondary antibody for 1 h. After washing 3 times, protein bands were detected with the Odyssey 3.0 Infrared Imaging System (Li-Cor Biosciences).

Co-immunoprecipitation

HEK293T cells (1×10^5 cells/well) were co-transfected with pMyc-NS7 and pFlag-RIG-I WT, pFlag-RIG-I_CARD or pFlag-MDA5_CARD (1.5 μg/each) in 12-well tissue culture plate. At 48 h post-transfection, the cells were washed twice with cold PBS and lysed with cold NP-40 lysis buffer at 4 °C for 30 minutes. Halt™ Protease Inhibitor Cocktail (Thermo Fisher Scientific) was added in the lysis steps according to the manufacturer's instructions. The cells collected by scraping and lysates were cleared by centrifugation at 12,000 rpm for 10 minutes at 4 °C. 10% of the supernatants were taken as input control, and the remaining supernatants were incubated with a mouse anti-Flag MAb (F1804; Sigma-Aldrich) at 4 °C for 2 h, and then incubated with protein A/G plus-agarose (sc-2003; Santa Cruz) overnight at 4 °C. The agaroses were centrifuged and washed three times, and the bound proteins were analyzed by western blotting.

Confocal fluorescence microscopy

HEK293T cells (3×10^4 cells/well) were co-transfected with pFlag-RIG-I WT, pFlag-RIG-I_CARD, pFlag-MDA5 WT or pFlag-MDA5_CARD and pMyc-NS7 (1 μ g/each) into μ -slide 8-well chamber (Cat. no. 80826; ibidi GmbH) for 24 h. In addition, HEK293T cells were co-transfected with pFlag-CD300lf and pMyc-RIG-I_CARD or pMyc-MDA5_CARD for 24 h, then infected with MNV-1 for 20 h. The cells were fixed with 4% paraformaldehyde in PBS, permeabilized with 0.2% Triton X-100, blocked with 5% skim milk for 1 h, reacted with the appropriate antibody, and stained with 4',6-diamidino-2-phenylindole (DAPI). Antibodies used included mouse anti-Flag Mab (F1804; Sigma-Aldrich), rabbit anti-Myc Mab (71D10; Cell Signaling), mouse anti-Myc Mab (9B11; Cell Signaling), rabbit anti-NS7 antisera, and anti-rabbit IgG (H+L), F(ab')₂ Fragment (Alexa Fluor[®] 488 and 594 conjugate) or anti-mouse IgG(H+L), F(ab')₂ Fragment (Alexa Fluor 488 and 594 conjugate) secondary antibodies. Imaging was performed on a Leica SP5 confocal microscopy using a 63x oil objective.

Antiviral assay with MNV

HEK293T cells (8×10^4 cells/well) were co-transfected with pFlag-CD300lf and pFlag-RIG-I_WT, pFlag-RIG-I_CARD, pFlag-MDA5_WT, or pFlag-MDA5_CARD with indicated concentrations in 24-well tissue culture plate for 24 h, then infected with MNV-1 for 20 h. The total RNA, supernatants and protein samples were collected and used for determination of antiviral activity of RIG-I and MDA5. To determine whether MNV NS7 could regulate RLRs-mediated antiviral response, HEK293T cells were co-transfected with pFlag-CD300lf and pFlag-RIG-I_WT, pFlag-RIG-I_CARD, pFlag-MDA5_WT, pFlag-MDA5_CARD, or pFlag-NS7 for 24 h, followed with infection of MNV-1 for 20 h. The total RNA and protein samples were collected for further analysis.

Statistical analysis

Data are presented as the mean \pm SEM. Comparisons between groups were performed with Mann-Whitney test using GraphPad Prism 5.0 (GraphPad Software Inc., La Jolla, CA, USA). Differences were considered significant at a P value less than 0.05.

Results

MNV NS7 enhances RIG-I triggered IFN response

To examine the effects of MNV RdRp on IFN response, we first tested in the context of poly(I:C) triggered IFN response. We found that viral NS7 alone did not affect IFN- β transcription, but enhanced poly(I:C) triggered IFN- β transcription (supplementary Fig. 1A) and transcription of ISGs including IFIT1 and IFIT3 (supplementary Fig. 1B). Besides TLR3, RIG-I and MDA5 have been implicated in the recognition of poly(I:C) and the subsequent induction of IFN response (31,32). To investigate whether MNV NS7 could regulate RIG-I-mediated IFN signaling, HEK293T cells were co-transfected with pFlag-RIG-I_WT and pFlag-NS7 for 24 h (Fig. 1A). We found that NS7 overexpression alone did not trigger IFN response, but enhanced RIG-I induced IFN- β transcription (Fig. 1B), as well as the downstream ISG transcription (Fig. 1C). It has been reported that the CARDs of RIG-I are responsible for signal transduction and activation of IRF-3 and NF- κ B, as well as subsequent IFN response (16). Thus, we constructed the truncated RIG-I domains (Fig. 1D) and further investigated whether NS7 also augments RIG-I_CARD and RIG-I_ΔCARD triggered IFN activation. We found that RIG-I_CARD induced IFN- β and ISG transcription were enhanced by NS7 (Fig. 1E and 1F). The helicase domain of RIG-I (RIG-I_ΔCARD) has been reported to have negative regulatory effects by blocking newcastle disease virus-induced IRF3 activation (Yoneyama et al., 2004). Consistently, we found RIG-I_ΔCARD did not trigger IFN activation, which was also not further triggered by NS7 (Fig. 1E and 1F). These results demonstrated that MNV NS7 positively regulates RIG-I mediated IFN signaling.

Interaction and co-localization of MNV NS7 with RIG-I

It has been reported that the replicases of EV71 and CVB3 inhibit MDA5 triggered IFN signaling through interaction with the CARDs of MDA5 (27). This prompted us to investigate whether there is an interaction between NS7 and RIG-I. HEK293T cells were co-transfected with Flag-tagged RIG-I and Myc-tagged NS7 for 48 h. The lysates of transfected cells were subjected to immunoprecipitation by anti-Flag resin, and our results showed that RIG-I could precipitate with NS7 protein (Fig. 2A). As aforementioned, the CARDs of RIG-I is able to activate the IFN response, which is further increased by MNV NS7 expression (Fig. 1F). We further demonstrated the interaction between NS7 and RIG-I_CARD in HEK293T cells co-transfected with Flag-tagged RIG-I_CARD and Myc-tagged NS7 (Fig. 2B). Moreover, we examined the localization of NS7 with RIG-I proteins in cells. Confocal microscopy revealed that besides nucleus localization, MNV NS7 could co-localize with either RIG-I or the CARDs of RIG-I in the cytoplasm (Fig. 2C). These data demonstrated that MNV NS7 interacts with RIG-I and its N-

terminus (CARDs), and this interaction might explain the augment of RIG-I mediated IFN activation by NS7.

NS7 interacts with MDA5 and enhances MDA5 triggered ISG transcription

Next, we examined the effect of MNV NS7 on another RLR, MDA5. We co-transfected the pTRIP.CMV.IVsb.ISG.ires.TagRFP-MDA5 and pFlag-NS7 into HEK293T cells for 24 h, and

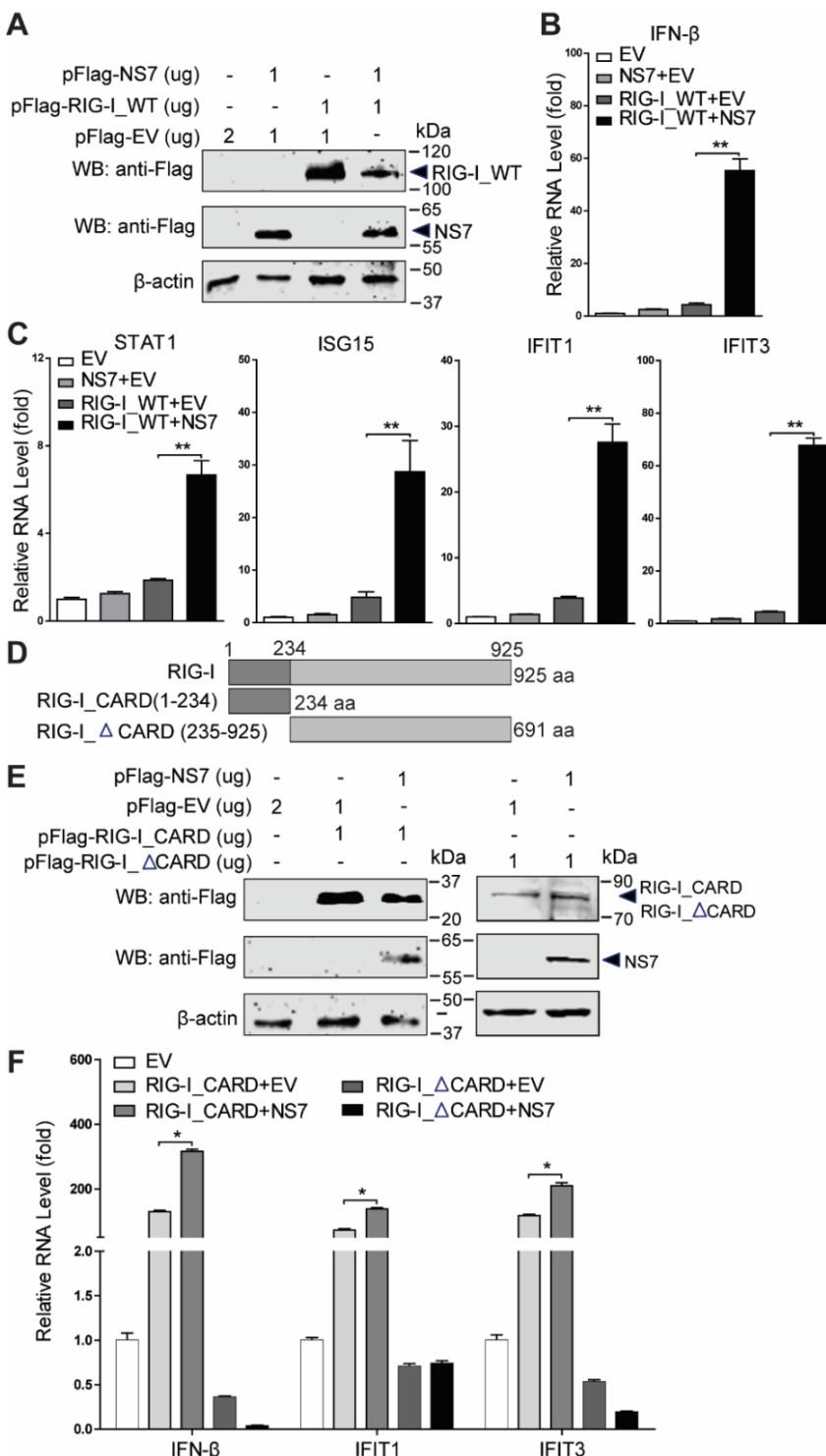


Figure 1. MNV NS7 enhances RIG-I triggered IFN response.

HEK293T cells were transfected with pFlag-RIG-I_WT, pFlag-NS7, or empty vectors with indicated concentrations for 24 h. (A) The protein expression of transfected vectors was analyzed by western blotting. (B) The IFN- β mRNA level was analyzed by qRT-PCR assay (n = 6). (C) The mRNA levels of STAT1, ISG15, IFIT1 and IFIT3 were analyzed by qRT-PCR assay (n = 6). (D) Schematic representation of truncated RIG-I domains. HEK293T cells were transfected with pFlag-RIG-I_CARD, pFlag-RIG-I_ΔCARD, or empty vectors with indicated concentrations for 24 h. (E) The protein expression of transfected vectors was analyzed by western blotting. (F) The mRNA levels of IFN- β , IFIT1 and IFIT3 were analyzed by qRT-PCR assay (n = 4-8). Data (B, C and F) were normalized to the EV control (set as 1). *P < 0.05; **P < 0.01. β -actin was used as a loading control.

found that NS7 overexpression enhanced MDA5 induced IFN- β transcription (Fig. 3A). Because the CARDS of MDA5 alone could initiate IFN activation and ISG transcription (27), we further determined whether NS7 could trigger MDA5_CARD mediated IFN response. We co-transfected the Myc-tagged MDA5_CARD and NS7 into HEK293T cells (Fig. 3B), and found

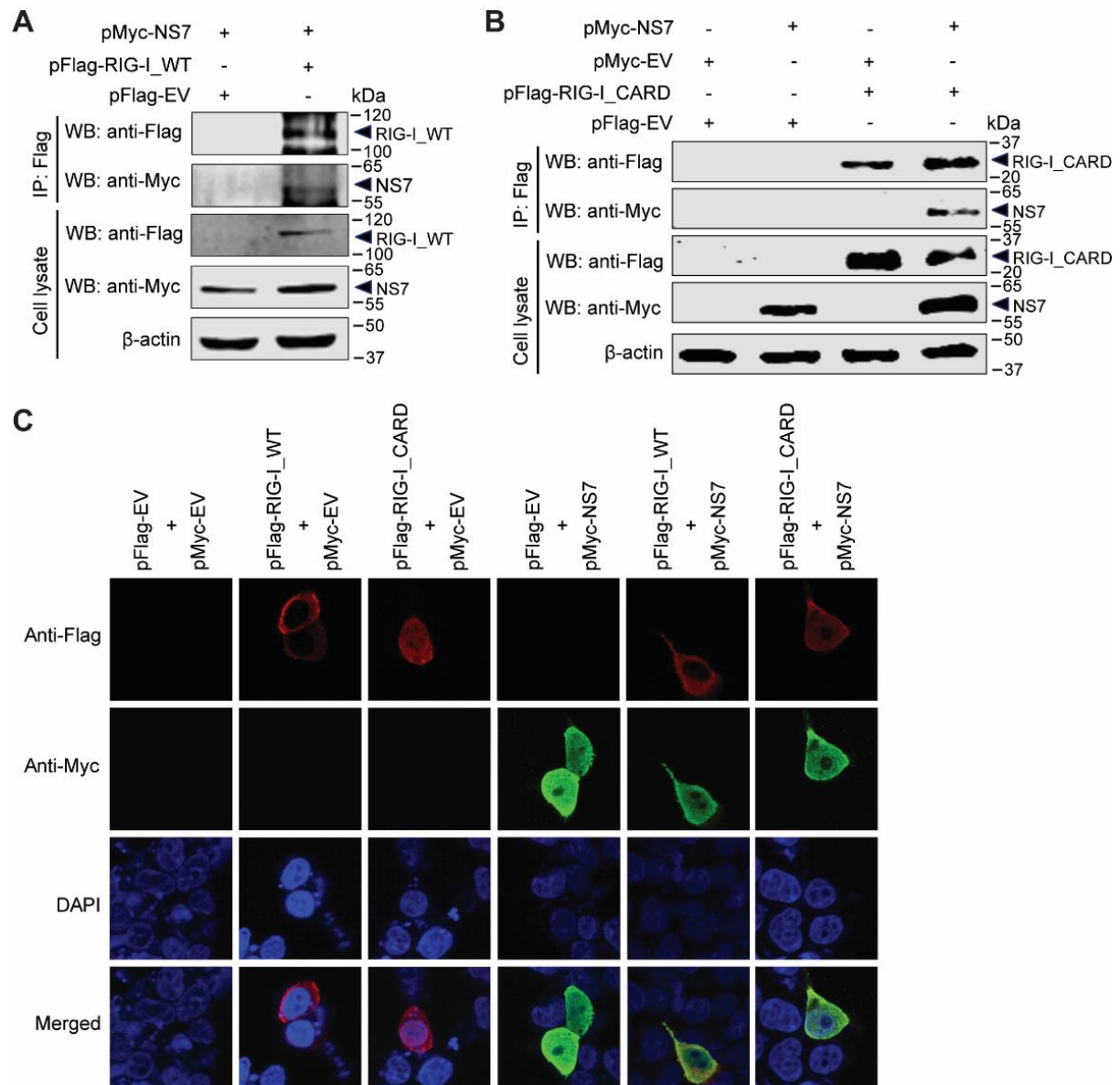
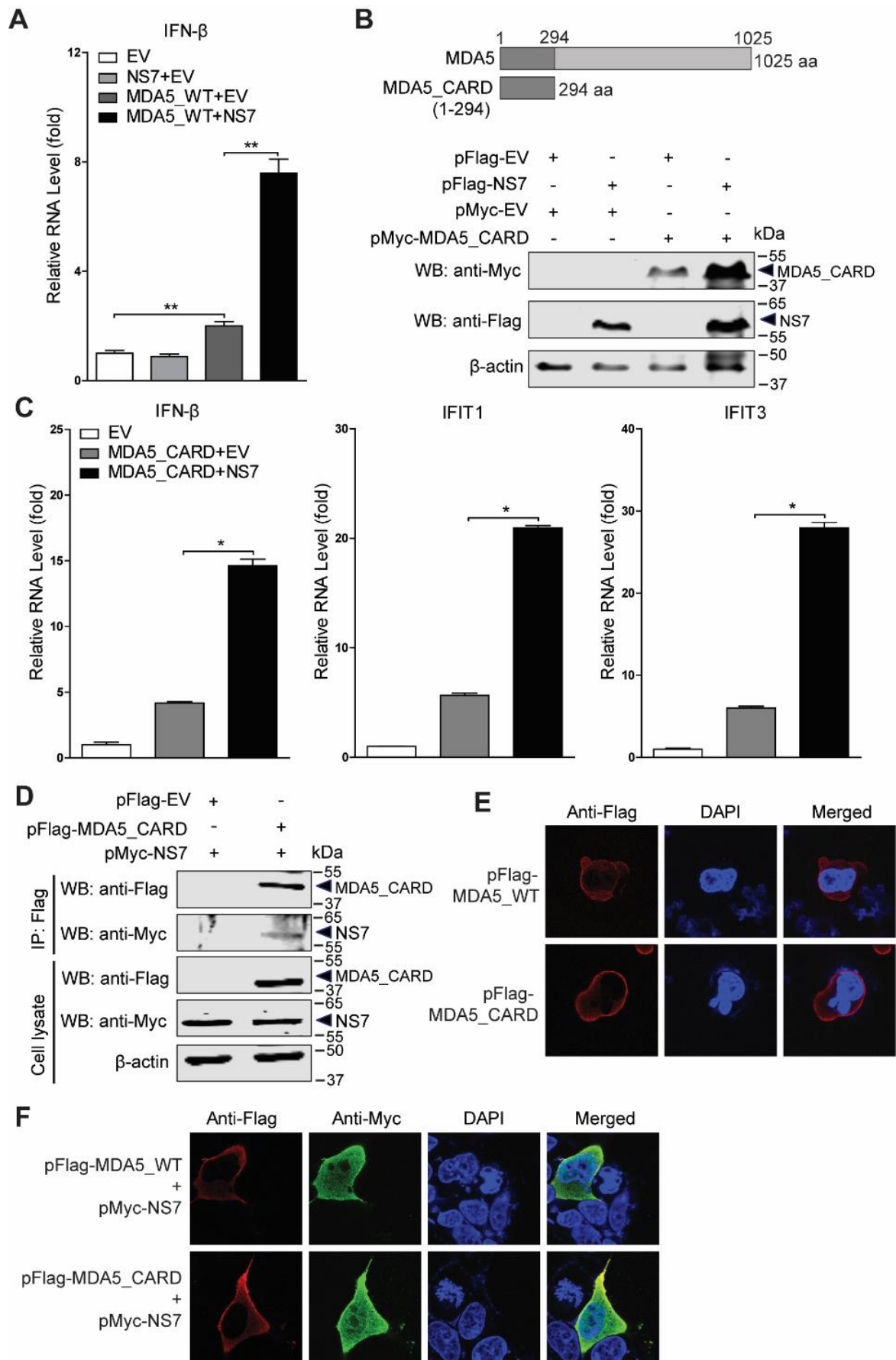


Figure 2. Interaction and co-localization of MNV NS7 with RIG-I. (A) HEK293T cells were transfected with pMyc-NS7 (1.5 μ g) and pFlag-RIG-I_WT (1.5 μ g), or empty vectors for 48 h. Co-IP was performed using anti-Flag MAb (1:1000). The precipitated proteins were analyzed by western blotting using antibodies against the Flag and Myc tags. (B) HEK293T cells were transfected with pMyc-NS7 (1.5 μ g) and pFlag-RIG-I_CARD (1.5 μ g), or empty vectors for 48 h. Co-IP was performed using anti-Flag MAb (1:1000). The precipitated proteins were analyzed by western blotting using antibodies against the Flag and Myc tags. (C) Co-localization of RIG-I and RIG-I_CARD with NS7. Expression plasmids pMyc-NS7 and pFlag-RIG-I_WT, pFlag-RIG-I_CARD, or empty vectors (1 μ g/each) were transfected into HEK293T cells for 24 h and then subjected to a confocal assay. β -actin was used as a loading control.



< Figure 3. NS7 interacts with MDA5 and enhances MDA5 triggered ISG transcription. (A) qRT-PCR analysis of IFN- β mRNA level in HEK293T cells that were transfected with pFlag-NS7, pLuc-MDA5, or empty vectors (1 μ g/each) for 24 h (n = 6). (B) Schematic representation of CARD domain of MDA5. HEK293T cells were transfected with pFlag-NS7, pMyc-MDA5_CARD, or empty vectors (1 μ g/each) for 24 h. Western blotting analysis of the expression of indicated transfected vectors. (C) The mRNA levels of IFN- β , IFIT1 and IFIT3 were analyzed by qRT-PCR assay (n = 4). (D) HEK293T cells were transfected with pMyc-NS7 (1.5 μ g) with pFlag-MDA5_CARD (1.5 μ g), or empty vectors for 48 h. Co-IP was performed using anti-Flag MAb (1:1000). The precipitated proteins were analyzed by western blotting using antibodies against the Flag and Myc tags. (E) Confocal analysis of expression and localization of MDA5 and MDA5_CARD in HEK293T cells that were transfected with pFlag-MDA5_WT and pFlag-MDA5_CARD (1 μ g/each) for 24 h. MDA5 and MDA5_CARD in HEK293T cells that were transfected with pFlag-MDA5_WT and pFlag-MDA5_CARD (1 μ g/each) for 24 h. (F) Co-localization of MDA5 or MDA5_CARD with NS7. Expression plasmids pMyc-NS7 and pFlag-MDA5_WT, or pFlag-MDA5_CARD (1 μ g/each) were transfected into HEK293T cells for 24 h and then subjected to a confocal assay. Data (A and C) were normalized to the EV control (set as 1). *P < 0.05; **P < 0.01. β -actin was used as a loading control.

that IFN- β transcription activated by MDA5_CARD was further increased by co-expression of MNV NS7 (Fig. 3C). Consistently, this effect was also observed on the induction of downstream antiviral ISGs including IFIT1 and IFIT3 (Fig. 3C). Similar to the interaction with the CARDs of RIG-I, we found that NS7 also interacts with the CARDs of MDA5 (Fig. 3D). Furthermore, we also investigated the localization of NS7 with MDA5 proteins in HEK293T cells by confocal microscopy. The results showed the expression and localization of Flag-tagged MDA5 and its CARDs in the cytoplasm (Fig. 3E), which also co-localized with MNV NS7 in the cytoplasm, while NS7 also diffused in the nucleus (Fig. 3F).

We next investigated whether the N- or C-terminus of NS7 are responsible for the effects on RIG-I and MDA5 mediated IFN activation. The N- or C-terminus of NS7 with Flag tag were constructed (supplementary Fig. 2A and 2B). HEK293T cells were co-transfected with Flag-tagged CARDs of RIG-I or MDA5, and N- or C-terminus of NS7. At 24 h post-transfection, we found that the upregulation of IFN- β , IFIT1 and IFIT3 transcription triggered by CARDs of RIG-I or MDA5 was slightly enhanced by N-terminus of NS7 (supplementary Fig. 2C and 2D). The C-terminus of NS7 appeared not to affect RIG-I_CARD but inhibited MDA5_CARD mediated IFN activation (supplementary Fig. 2C and 2D). These results collectively suggested that the intact of MNV NS7 is essential for effective augmentation of RIG-I and MDA5 mediated IFN activation.

Co-localization of NS7 with the CARDS of RIG-I and MDA5 in MNV infected human cells

Ectopic expression of the MNV receptor mouse CD300lf breaks the species barriers for MNV infection in human cells (6). Thus, we determined MNV replication by immunoblotting viral NS1/2 protein in human HEK293T cells that were transfected with Flag-tagged CD300lf and infected with the virus (Fig. 4A). In addition, we confirmed viral replication by targeting viral NS7 protein with rabbit anti-NS7 antisera using confocal microscopy (Fig. 4B). We next examined co-localization of MNV NS7 with the CARDS of RIG-I and MDA5 in infected cells. In order to avoid the influence by the Flag tag of MNV receptor, we co-transfected the pFlag-CD300lf with pMyc-RIG-I_CARD or pMyc-MDA5_CARD into HEK293T cells for 24 h (Fig. 4C), then infected with MNV-1 for 20 h. The results showed that besides nucleus localization, MNV NS7 can co-localize with the CARDS of RIG-I and MDA5 in the cytoplasm of infected cells (Fig. 4D), which is in accordance with previous studies demonstrating the diffuse of NS7 protein in

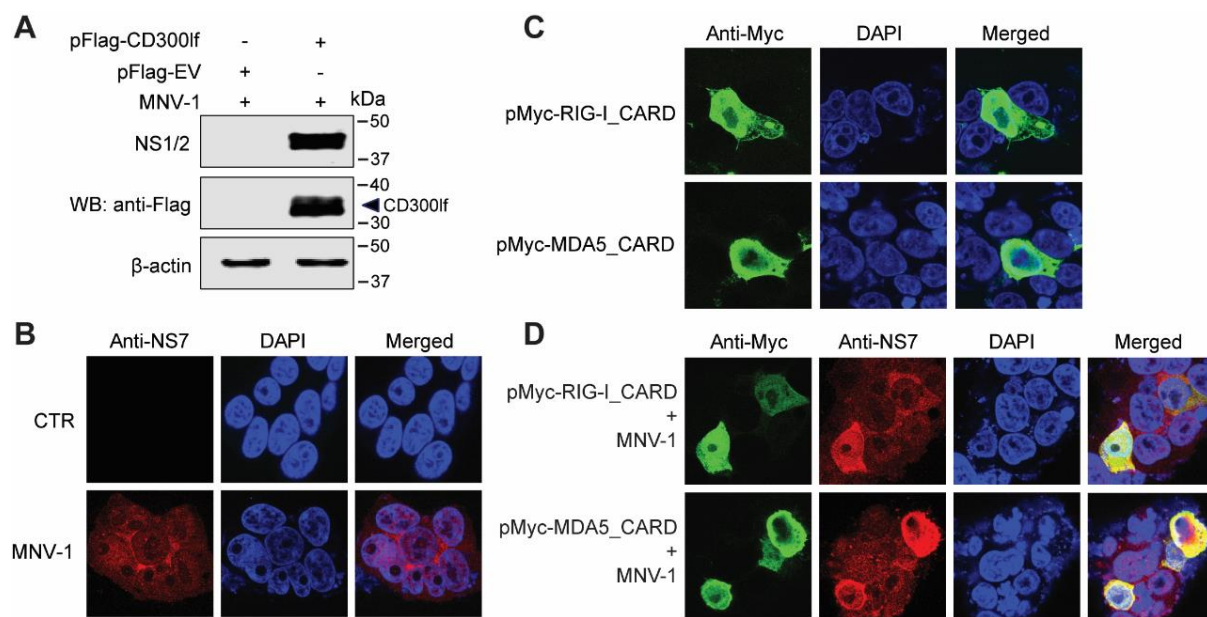


Figure 4. Co-localization of viral NS7 with the CARDS of RIG-I and MDA5 in MNV infected human cells.

(A) HEK293T cells were transfected with pFlag-CD300lf (1 μ g) or empty vectors (1 μ g) for 24 h, then infected with MNV-1 for 20 h. Expression of viral NS1/2 protein and the transfected vectors were analyzed by western blotting. (B) HEK293T cells were transfected with pFlag-CD300lf (1 μ g) for 24 h, then uninfected or infected with MNV-1 for 20 h. Expression of viral NS7 protein was analyzed by confocal assay. (C) HEK293T cells were transfected with pMyc-RIG-I_CARD (1 μ g) or pMyc-MDA5_CARD (1 μ g) for 24 h. The expression and localization of RIG-I_CARD and MDA5_CARD were analyzed by confocal assay. (D) HEK293T cells were transfected with pFlag-CD300lf (0.5 μ g) and pMyc-RIG-I_CARD (1 μ g) or pMyc-MDA5_CARD (1 μ g) for 24 h, then infected with MNV-1 for 20 h. Co-localization of RIG-I_CARD or MDA5_CARD with NS7 in MNV-1 infected cells was analyzed by confocal assay.

the cytoplasm and nuclear in infected cells (10). The activator of TLR3 signaling, poly (I:C) triggers IFN response involving RIG-I and MDA5 activation. Thus, we used poly (I:C) to activate the endogenous RIG-I and MDA5, and confirmed co-localization of RIG-I (supplementary Fig. 3A) and MDA5 (supplementary Fig. 3B) with viral NS7 in MNV-infected HEK293T cells. In addition, we found anti-MNV effects of poly (I:C) in HEK293T cells expressing MNV receptor (supplementary Fig. 3C).

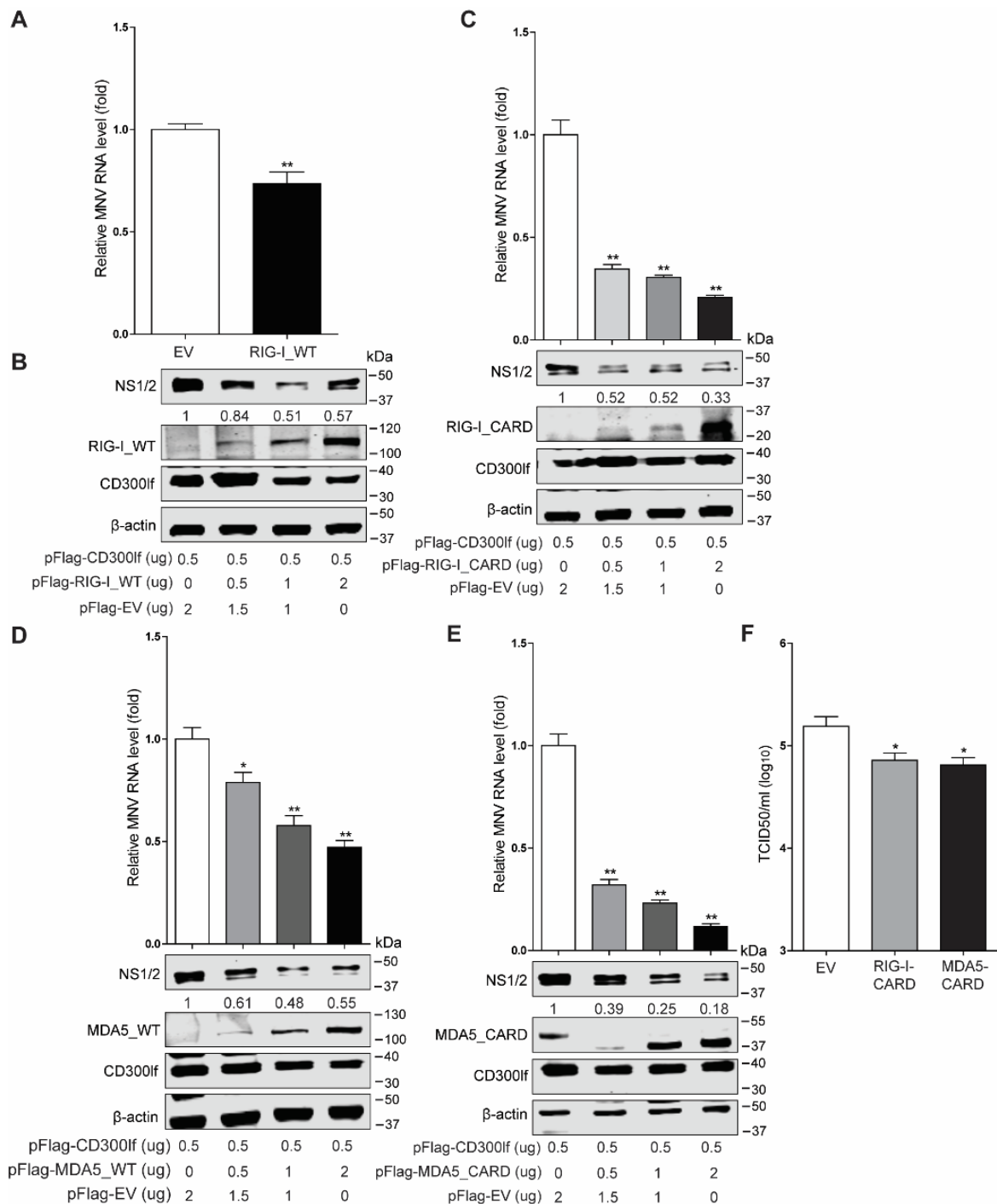


Figure 5. RIG-I or MDA5 overexpression restricts MNV replication. (A) HEK293T cells were transfected with pFlag-CD300lf (0.5 μg) and pFlag-RIG-I_WT (1 μg), or empty vectors (1 μg) for 24 h, then infected

with MNV-1 for 20 h. The viral RNA level was analyzed by qRT-PCR assay (n = 6). (B) HEK293T cells were transfected with pFlag-CD300lf and pFlag-RIG-I_WT, or empty vectors with indicated concentrations for 24 h, then infected with MNV-1 for 20 h. The expression of viral NS1/2 and transfected vectors was analyzed by western blotting. (C) HEK293T cells were transfected with pFlag-CD300lf and pFlag-RIG-I_CARD, or empty vectors with indicated concentrations for 24 h, then infected with MNV-1 for 20 h. The viral RNA level, and the expression of viral NS1/2 and transfected vectors were analyzed by qRT-PCR (n = 6) and western blotting, respectively. (D) HEK293T cells were transfected with pFlag-CD300lf and pFlag-MDA5_WT, or empty vectors with indicated concentrations for 24 h, then infected with MNV-1 for 20 h. The viral RNA level, and the expression of viral NS1/2 and transfected vectors were analyzed by qRT-PCR (n = 6) and western blotting, respectively. (E) HEK293T cells were transfected with pFlag-CD300lf and pFlag-MDA5_CARD, or empty vectors with indicated concentrations for 24 h, then infected with MNV-1 for 20 h. The viral RNA level, and the expression of viral NS1/2 and transfected vectors were analyzed by qRT-PCR (n = 6) and western blotting, respectively. (F) HEK293T cells were transfected with pFlag-CD300lf (0.5 µg) and pFlag-RIG-I_CARD (2 µg), pFlag-MDA5_CARD (2 µg), or empty vectors (2 µg) for 24 h, then infected with MNV-1 for 20 h. The viral titer was analyzed by TCID50 assay (n = 6). Data (A, C, D, E, and F) were normalized to the EV control (set as 1). *P < 0.05; **P < 0.01. β-actin was used as a loading control. For immunoblot results (B, C, D and E), band intensity of NS1/2 protein in each lane was quantified by Odyssey software, and the quantification results were normalized to β-actin expression (EV control, set as 1).

RIG-I and MDA5 restrict MNV replication, which is augmented by NS7 overexpression

We evaluated the anti-MNV activity of RIG-I and MDA5 in HEK293T cells. We found that RIG-I overexpression inhibited MNV infection in CD300lf transduced HEK293T cells, as shown at both viral RNA (Fig. 5A) and NS1/2 protein level (Fig. 5B). Consistently, the CARDS of RIG-I exerted similar inhibitory effects (Fig. 5C). Moreover, the viral titers were also decreased by RIG-I CARDS overexpression (Fig. 5F). Similar results were observed for the N-terminus and full-length of MDA5 (Fig. 5D-5F).

JAK/STAT cascade is a key component of the IFN signaling. Thus, we examined whether blocking JAK/STAT pathway would affect RIG-I and MDA5 mediated antiviral activity. HEK293T cells were co-transfected with pFlag-CD300lf and pFlag-RIG-I_CARD, or pFlag-MDA5_CARD for 20 h, treated with JAK inhibitor 1 for 6 h, and then infected with MNV-1 for 20 h. We found the inhibitory effects on viral RNA by CARDS of RIG-I or and MDA5 were partially reversed by JAK inhibitor, respectively (Fig. 6A). Consistently, the induction of IFN-β, IFIT1 and IFIT3 transcription was also attenuated (Fig. 6B and 6C). These results showed that the anti-MNV activity of RIG-I and MDA5 requires activation of the JAK/STAT pathway.

In HEK293T cells, overexpression of NS7 did not affect viral NS1/2 protein expression (supplementary Fig. 2E). Thus, we examined the effects of MNV NS7 on RIG-I mediated anti-MNV ability, by co-transfecting HEK293T cells with Flag-tagged CD300lf, RIG-I or its CARDS and NS7 for 24 h, and then infected with MNV-1 for 20 h. The results showed that NS7 enhanced RIG-I or CARDS of RIG-I mediated inhibition of viral RNA (Fig. 7A and 7B). Similar effects were observed for MDA5 (Fig. 7C and 7D). Interestingly, the N- or C-terminus of NS7 overexpression also did not affect viral NS1/2 protein expression (supplementary Fig. 2E), and the CARDS of RIG-I and MDA5 mediated inhibition of viral RNA (supplementary Fig. 2F and 2G). These results revealed that the intact version of MNV NS7 enhances the anti-MNV activity of RIG-I and MDA5.

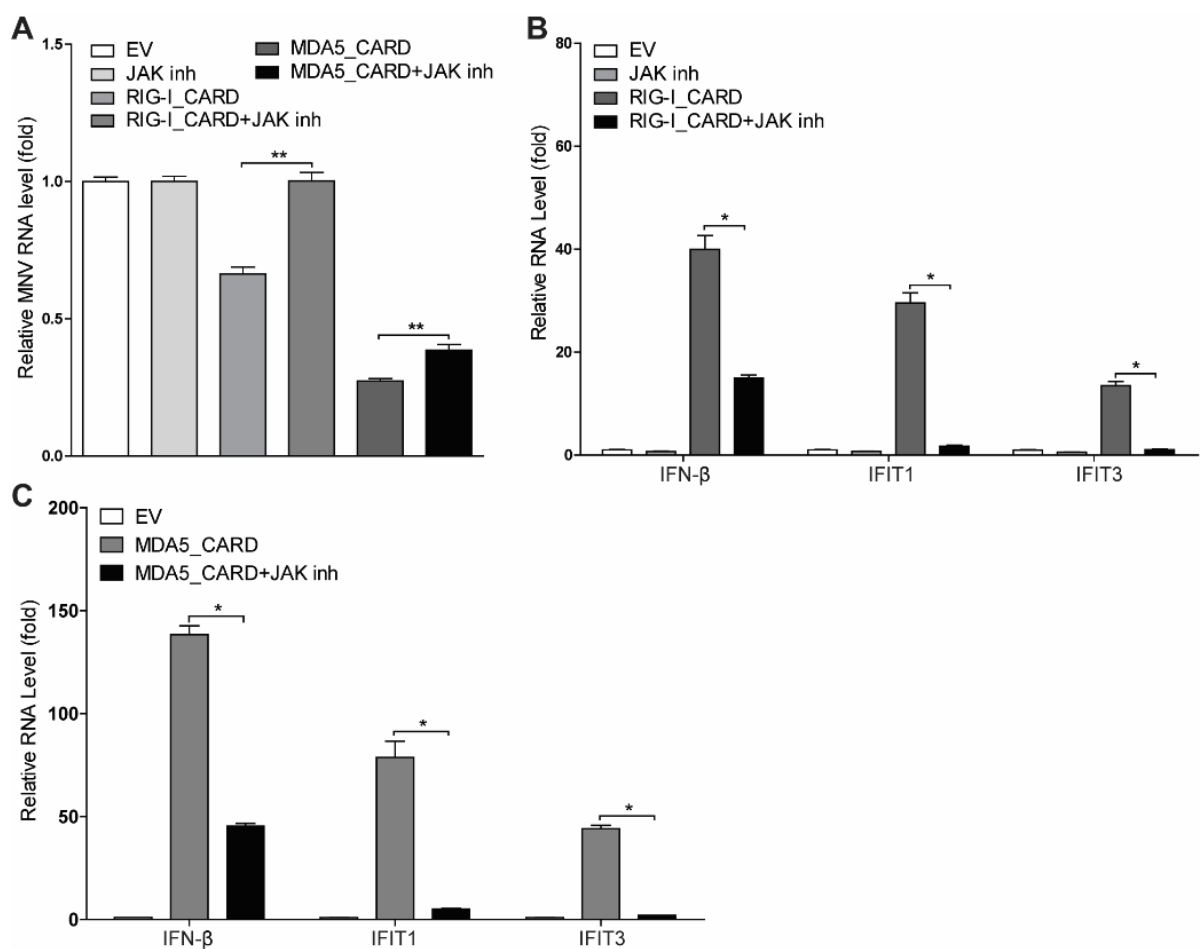


Figure 6. Anti-MNV activity of RIG-I and MDA5 requires activation of the JAK/STAT pathway. HEK293T cells were transfected with pFlag-CD300lf (0.5 μ g) and pFlag-RIG-I_CARD (1 μ g), or pFlag-MDA5_CARD (1 μ g) for 20 h, then treated with JAK inhibitor 1 (5 mM) for 6 h, then infected with MNV-1 for 20 h. The viral RNA levels (A) were analyzed by qRT-PCR (n = 6). HEK293T cells were transfected with (B) pFlag-RIG-I_CARD (1 μ g), or (C) pFlag-MDA5_CARD (1 μ g) for 20 h, then treated with JAK inhibitor 1 (5 mM) for 6 h. The mRNA level of IFN- β , IFIT1 and IFIT3 were analyzed by qRT-PCR (n = 4). Data (A) were normalized to the EV and JAK inh control (both set as 1). Data (B and C) were normalized to the EV control (set as 1). *P < 0.05; **P < 0.01.

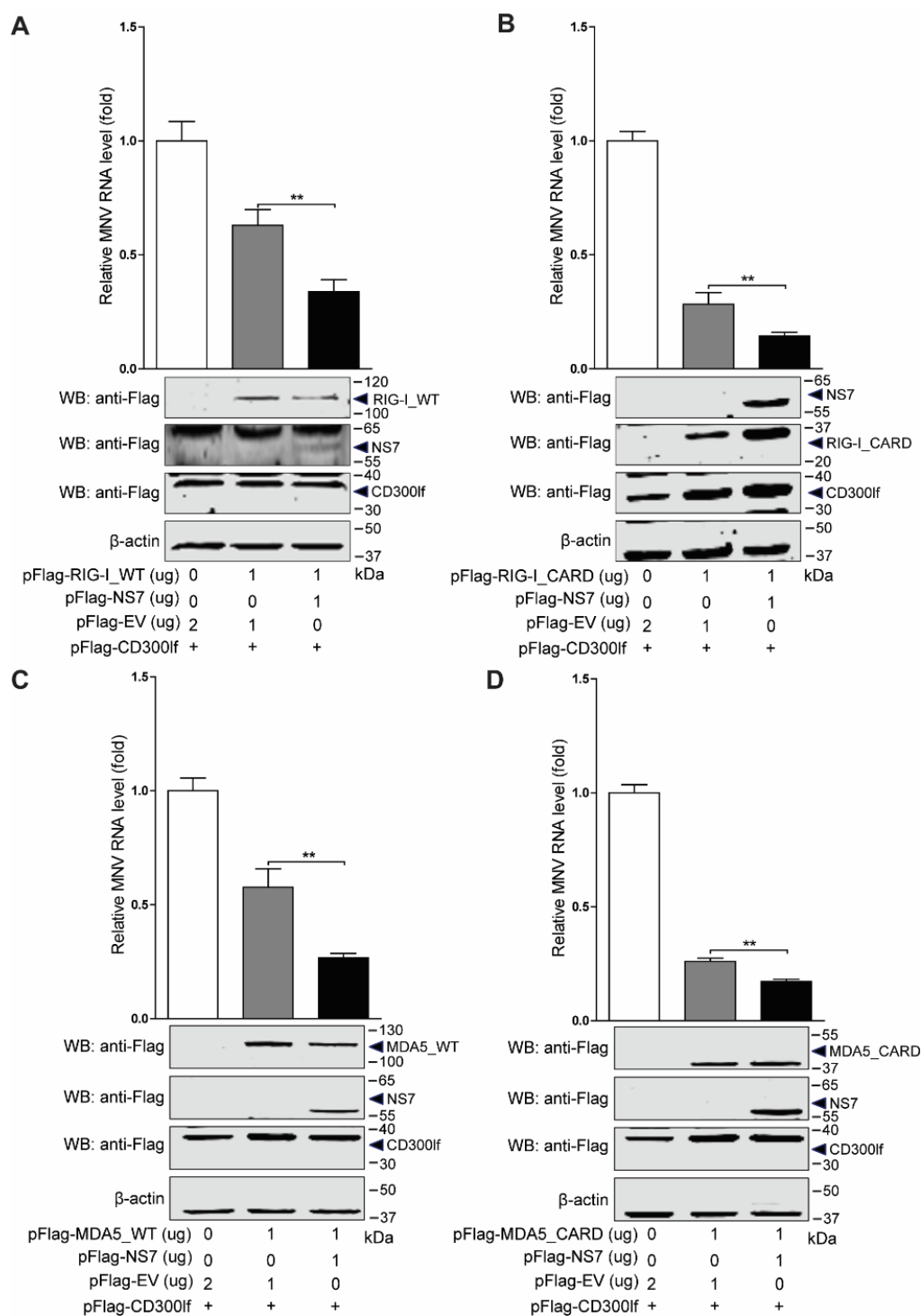


Figure 7. NS7 enhances RLRs-mediated inhibition of MNV RNA replication. (A) HEK293T cells were transfected with pFlag-CD300lf (0.5 μ g) and pFlag-RIG-I_WT, pFlag-NS7, or empty vectors with indicated concentrations for 24 h, then infected with MNV-1 for 20 h. The viral RNA level and the expression of transfected vectors were analyzed by qRT-PCR (n = 6-9) and western blotting, respectively. (B) HEK293T cells were transfected with pFlag-CD300lf (0.5 μ g) and pFlag-RIG-I_CARD, pFlag-NS7, or empty vectors with indicated concentrations for 24 h, then infected with MNV-1 for 20 h. The viral RNA level and expression of transfected vectors were analyzed by qRT-PCR (n = 7-9) and western blotting, respectively. (C) The expression vector pFlag-CD300lf (0.5 μ g) and pFlag-MDA5_WT,

pFlag-NS7, or empty vectors were transfected into HEK293T cells with indicated concentrations for 24 h, then infected with MNV-1 for 20 h. The viral RNA level and expression of transfected vectors were analyzed by qRT-PCR (n = 4-6) and western blotting, respectively. (D) The expression vector pFlag-CD300lf (0.5 µg) and pFlag-MDA5_CARD, pFlag-NS7, or empty vectors were transfected into HEK293T cells with indicated concentrations for 24 h, then infected with MNV-1 for 20 h. The viral RNA level and expression of transfected vectors were analyzed by qRT-PCR (n = 7-9) and western blotting, respectively. Data were normalized to the EV control (set as 1). **P < 0.01. β-actin was used as a loading control.

Discussion

Numerous studies have reported that viruses explore different strategies to counteract host antiviral defense. By striking contract, our results demonstrated that MNV RdRp promotes host antiviral response. Although NS7 alone does not affect IFN signaling, it potently enhances RIG-I and MDA5 triggered antiviral IFN response.

RIG-I and MDA5 can recognize dsRNA or 5'-pppRNA in the cytoplasm to induce downstream IFN signaling. MNV has been reported to be recognized by MDA5 and activate IFN signaling in mouse macrophages (17,33). Although the main function of viral replicases is to drive viral replication and transcription, different regulatory functions of viral replicases on RLRs-mediated IFN signaling have been reported (23-27,34). Previous studies have revealed that MNV RdRp upregulates RIG-I mediated IFN-β promoter activation (26). Our results have demonstrated that MNV NS7 can augment both RIG-I and MDA5 mediated IFN antiviral response. The mechanism of assisting RLRs-mediated IFN response by viral replicases has been linked to the conversion or modification of host RNA into dsRNA (23,35). In contrast, inhibition of MDA5 triggered IFN activation by enteroviral replicases has been reported through direct protein-protein interactions (27). In this study, we demonstrated that MNV NS7 interacts with the CARDS of RIG-I and MDA5. These interactions may explain the augmentation of RLRs-mediated IFN activation by MNV NS7, although further studies are needed to provide definitive proof.

Toll-like receptors (TLRs) including TLR3, TLR7 and TLR8 are essential for activation of antiviral response upon viral infection, and can sense ssRNA or dsRNA in the cytosol (36). Studies have shown a slight increase of MNV viral titers in TLR3 deficient mice (17). Although HuNV RdRp does not enhance TLR3-mediated IFN-β promoter activation (26), we found that MNV NS7 increased the transcription of several ISGs triggered by poly (I:C). Besides RIG-I and MDA5 associated with poly (I:C) triggered IFN response, poly (I:C) is also the activator of TLR3

signaling. Thus, it is interesting to further investigate whether there is a regulatory role of MNV NS7 on TLRs-mediated IFN response.

Studies have shown that MNV-1 replicates to higher levels in MDA5 deficient mice (17), but HuNV replication is not affected by silencing RIG-I signaling (18). We have previously demonstrated that ectopic expression of RIG-I and MDA5 potentially inhibit HuNV replication in the HG23 replicon model (37). In this study, we demonstrated that RIG-I and MDA5 exert antiviral activity against MNV replication in human cells ectopically expressing MNV receptor. ISGs are considered as the ultimate antiviral effectors, and the essential role of STAT1 in controlling MNV replication has been demonstrated (38). By blocking the JAK/STAT pathway, the CARDS of RIG-I and MDA5 mediated ISG transcription and anti-MNV activity are partially attenuated, suggesting the requirement of JAK/STAT pathway for RLRs-mediated antiviral actions. We also revealed that NS7 overexpression enhances RIG-I and MDA5 mediated inhibition of viral RNA, consistent with the augmentation of IFN response.

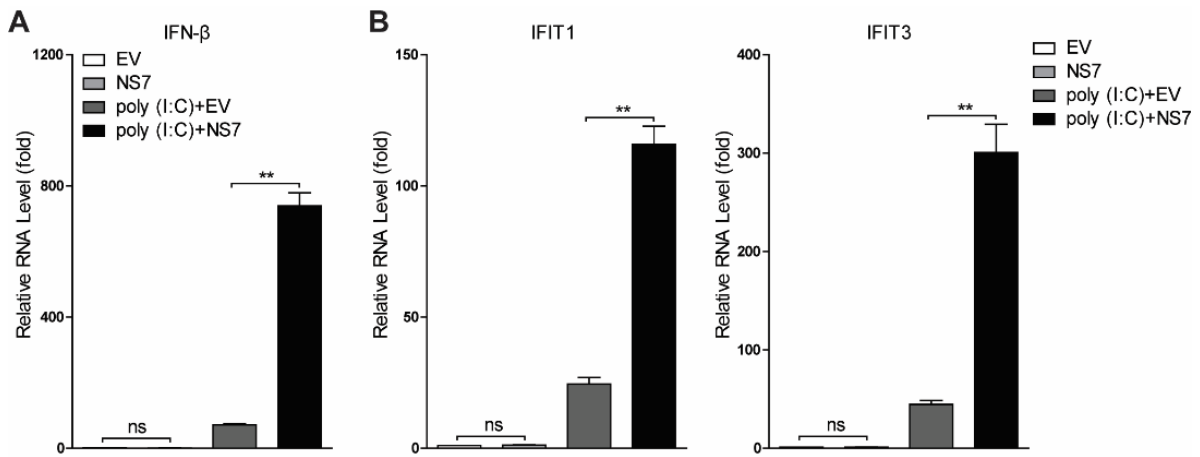
In summary, we demonstrated that MNV NS7 interacts with the N-terminus of RIG-I and MDA5 and enhances RIG-I and MDA5 triggered IFN response. Furthermore, RIG-I and MDA5 potentially inhibit MNV replication requiring the activation of JAK/STAT pathway, and this antiviral effect is augmented by NS7. We postulate that MNV has developed sophisticated strategies to efficiently replicate but also survive in the host cells. At the early stage of infection, viral proteins such as VF1 and VP2 can regulate cellular immune response to facilitate viral replication (8,9). In contrast, NS7 as a RdRp can sensitively recognize the level of viral replication. As a feedback reaction, NS7 can interact and augment RIG-I and MDA5 mediated antiviral IFN response to inhibit over-replication, and thus protect host cells from lysis in order to survive in the host. However, future experimental studies are required to further validate this theory. Furthermore, augmentation of antiviral response by MNV NS7 may have an impact on superinfection of other pathogens, as different pathogens cohabit in the intestine. Thus, this aspect is interesting to be further investigated.

References

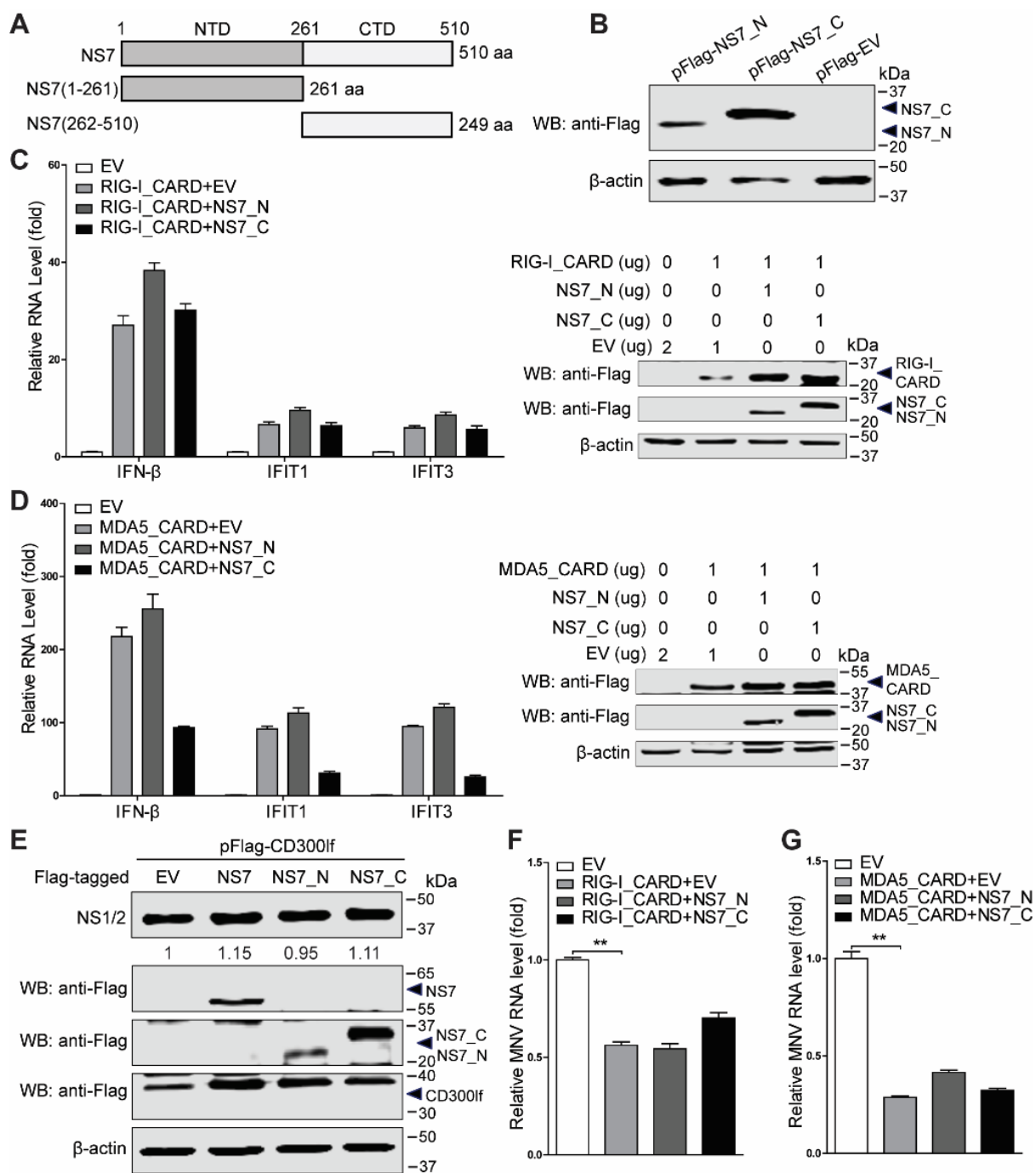
1. Karst, S. M., Wobus, C. E., Goodfellow, I. G., et al. (2014) Advances in norovirus biology. *Cell Host Microbe* 15, 668-680
2. Glass, R. I., Parashar, U. D., and Estes, M. K. (2009) Norovirus gastroenteritis. *New Engl J Med* 361, 1776-1785
3. Bok, K., and Green, K. Y. (2012) Norovirus gastroenteritis in immunocompromised patients. *New Engl J Med* 367, 2126-2132
4. Wobus, C. E., Karst, S. M., Thackray, L. B., et al. (2004) Replication of Norovirus in cell culture reveals a tropism for dendritic cells and macrophages. *PLoS Biol* 2, e432
5. Wobus, C. E., Thackray, L. B., and Virgin, H. W. (2006) Murine norovirus: a model system to study norovirus biology and pathogenesis. *J Virol* 80, 5104-5112
6. Orchard, R. C., Wilen, C. B., Doench, J. G., et al. (2016) Discovery of a proteinaceous cellular receptor for a norovirus. *Science* 353, 933-936
7. Orchard, R. C., Sullender, M. E., Dunlap, B. F., et al. (2019) Identification of antinorovirus genes in human cells using genome-wide CRISPR activation screening. *J Virol* 93, e01324-01318
8. McFadden, N., Bailey, D., Carrara, G., et al. (2011) Norovirus regulation of the innate immune response and apoptosis occurs via the product of the alternative open reading frame 4. *PLoS Pathog* 7, e1002413
9. Zhu, S., Regev, D., Watanabe, M., et al. (2013) Identification of immune and viral correlates of norovirus protective immunity through comparative study of intra-cluster norovirus strains. *PLoS Pathog* 9, e1003592
10. Hyde, J. L., Sosnovtsev, S. V., Green, K. Y., et al. (2009) Mouse norovirus replication is associated with virus-induced vesicle clusters originating from membranes derived from the secretory pathway. *J Virol* 83, 9709-9719
11. Hyde, J. L., Gillespie, L. K., and Mackenzie, J. M. (2012) Mouse norovirus 1 utilizes the cytoskeleton network to establish localization of the replication complex proximal to the microtubule organizing center. *J Virol* 86, 4110-4122
12. Zamyatkin, D. F., Parra, F., Alonso, J. M. M., et al. (2008) Structural insights into mechanisms of catalysis and inhibition in Norwalk virus polymerase. *J Biol Chem* 283, 7705-7712
13. Högbom, M., Jäger, K., Robel, I., et al. (2009) The active form of the norovirus RNA-dependent RNA polymerase is a homodimer with cooperative activity. *J Gen Virol* 90, 281-291
14. Wu, J., and Chen, Z. J. (2014) Innate immune sensing and signaling of cytosolic nucleic acids. *Ann Rev Immunol* 32, 461-488
15. Kato, H., Takeuchi, O., Sato, S., et al. (2006) Differential roles of MDA5 and RIG-I helicases in the recognition of RNA viruses. *Nature* 441, 101-105
16. Yoneyama, M., Kikuchi, M., Natsukawa, T., et al. (2004) The RNA helicase RIG-I has an essential function in double-stranded RNA-induced innate antiviral responses. *Nat Immunol* 5, 730-738
17. McCartney, S. A., Thackray, L. B., Gitlin, L., et al. (2008) MDA-5 recognition of a murine norovirus. *PLoS Pathog* 4, e1000108
18. Guix, S., Asanaka, M., Katayama, K., et al. (2007) Norwalk virus RNA is infectious in mammalian cells. *J Virol* 81, 12238-12248
19. Kawai, T., Takahashi, K., Sato, S., et al. (2005) IPS-1, an adaptor triggering RIG-I- and Mda5-mediated type I interferon induction. *Nat Immunol* 6, 981-988
20. Seth, R. B., Sun, L., Ea, C. K., et al. (2005) Identification and characterization of MAVS, a mitochondrial antiviral signaling protein that activates NF-kappaB and IRF 3. *Cell* 122, 669-682
21. Honda, K., Takaoka, A., and Taniguchi, T. (2006) Type I interferon [corrected] gene induction by the interferon regulatory factor family of transcription factors. *Immunity* 25, 349-360
22. Schoggins, J. W., Wilson, S. J., Panis, M., et al. (2011) A diverse range of gene products are effectors of the type I interferon antiviral response. *Nature* 472, 481

23. Nikonov, A., Molder, T., Sikut, R., et al. (2013) RIG-I and MDA-5 detection of viral RNA-dependent RNA polymerase activity restricts positive-strand RNA virus replication. *PLoS Pathog* 9, e1003610
24. Painter, M. M., Morrison, J. H., Zoecklein, L. J., et al. (2015) Antiviral Protection via RdRP-Mediated Stable Activation of Innate Immunity. *PLoS Pathog* 11, e1005311
25. Miller, C. M., Barrett, B. S., Chen, J., et al. (2020) Systemic Expression of a Viral RdRP Protects Against Retrovirus Infection and Disease. *J Virol*
26. Subba-Reddy, C. V., Goodfellow, I., and Kao, C. C. (2011) VPg-primed RNA synthesis of norovirus RNA-dependent RNA polymerases by using a novel cell-based assay. *J Virol* 85, 13027-13037
27. Kuo, R. L., Chen, C. J., Wang, R. Y. L., et al. (2019) Role of Enteroviral RNA-Dependent RNA Polymerase in Regulation of MDA5-Mediated Beta Interferon Activation. *J Virol* 93
28. Davies, C., Brown, C. M., Westphal, D., et al. (2015) Murine norovirus replication induces G0/G1 cell cycle arrest in asynchronously growing cells. *J Virol* 89, 6057-6066
29. Emmott, E., de Rougemont, A., Hosmillo, M., et al. (2019) Polyprotein processing and intermolecular interactions within the viral replication complex spatially and temporally control norovirus protease activity. *J Biol Chem* 294, 4259-4271
30. Hou, J., Zhou, Y., Zheng, Y., et al. (2014) Hepatic RIG-I predicts survival and interferon-alpha therapeutic response in hepatocellular carcinoma. *Cancer Cell* 25, 49-63
31. Yoneyama, M., Kikuchi, M., Matsumoto, K., et al. (2005) Shared and unique functions of the DExD/H-box helicases RIG-I, MDA5, and LGP2 in antiviral innate immunity. *J Immunol* 175, 2851-2858
32. Kato, H., Takeuchi, O., Sato, S., et al. (2006) Differential roles of MDA5 and RIG-I helicases in the recognition of RNA viruses. *Nature* 441, 101-105
33. Emmott, E., Sorgeloos, F., Caddy, S. L., et al. (2017) Norovirus-Mediated Modification of the Translational Landscape via Virus and Host-Induced Cleavage of Translation Initiation Factors. *Mol Cell Proteomics* 16, S215-S229
34. Moriyama, M., Kato, N., Otsuka, M., et al. (2007) Interferon-beta is activated by hepatitis C virus NS5B and inhibited by NS4A, NS4B, and NS5A. *Hepato Int* 1, 302-310
35. Yu, G. Y., He, G., Li, C. Y., et al. (2012) Hepatic expression of HCV RNA-dependent RNA polymerase triggers innate immune signaling and cytokine production. *Mol Cell* 48, 313-321
36. Jensen, S., and Thomsen, A. R. (2012) Sensing of RNA viruses: a review of innate immune receptors involved in recognizing RNA virus invasion. *J Virol* 86, 2900-2910
37. Dang, W., Xu, L., Yin, Y., et al. (2018) IRF-1, RIG-I and MDA5 display potent antiviral activities against norovirus coordinately induced by different types of interferons. *Antiviral Res* 155, 48-59
38. Karst, S. M., Wobus, C. E., Lay, M., et al. (2003) STAT1-dependent innate immunity to a Norwalk-like virus. *Science* 299, 1575-1578

Supplementary information



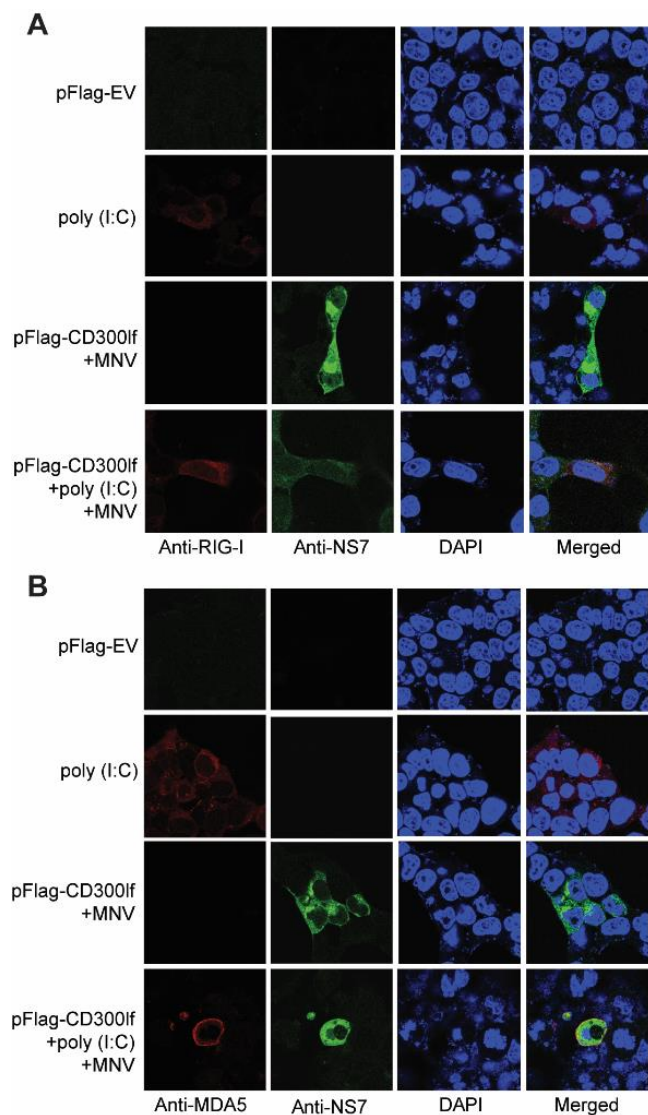
Supplementary Fig. 1 MNV NS7 enhances poly (I:C)-induced ISG transcription. HEK293T cells were transfected with poly (I:C) (1 μ g), pFlag-NS7 (1 μ g), or empty vectors (1 μ g) for 24 h. The mRNA levels of IFN- β (A), and IFIT1 and IFIT3 (B) were analyzed by qRT-PCR assay (n = 6). Data were normalized to the EV control (set as 1). **P < 0.01; ns, not significant.



Supplementary Fig. 2 Regulation of N- or C-terminus of MNV NS7 on RLRs-mediated IFN response and anti-MNV activity.

(A) Schematic representation of truncated NS7 domains. (B) The expression of truncated NS7 domains was determined by western blotting in HEK293T cells that were transfected with pFlag-NS7_N (1 μ g), pFlag-NS7_C (1 μ g) or empty vectors (1 μ g) for 24 h. (C) HEK293T cells were transfected with pFlag-RIG-I_CARD, pFlag-NS7_N, pFlag-NS7_C or empty vectors with indicated concentrations for 24 h. The expression of transfected vectors and the mRNA level of IFN- β , IFIT1 and IFIT3 were analyzed by western blotting and qRT-PCR assay (n = 9), respectively. (D) HEK293T cells were transfected with pFlag-MDA5_CARD, pFlag-NS7_N, pFlag-NS7_C or empty vectors with indicated concentrations for 24 h. The expression of transfected vectors and the mRNA level of IFN- β , IFIT1 and IFIT3 were analyzed by western blotting and qRT-PCR assay (n = 6), respectively. (E) HEK293T cells were

transfected with pFlag-CD300lf (0.5 µg) and pFlag-NS7, pFlag-NS7_N, pFlag-NS7_C, or empty vectors (1 µg/each) for 24 h, then infected with MNV-1 for 20 h. The expression of viral NS1/2 protein and transfected vectors was analyzed by western blotting. (F) HEK293T cells were transfected with pFlag-CD300lf (0.5 µg), pFlag-RIG-I_CARD (1 µg), or pFlag-NS7_N (1 µg) and pFlag-NS7_C (1 µg) for 24 h, then infected with MNV-1 for 20 h. The viral RNA level was analyzed by qRT-PCR (n = 6). (G) HEK293T cells were transfected with pFlag-CD300lf (0.5 µg), pFlag-MDA5_CARD (1 µg), or pFlag-NS7_N (1 µg) and pFlag-NS7_C (1 µg) for 24 h, then infected with MNV-1 for 20 h. The viral RNA level was analyzed by qRT-PCR (n = 6). Data (C, D, F and G) were normalized to the EV control (set as 1). **P < 0.01. β-actin was used as a loading control. For immunoblot results (E), band intensity of NS1/2 protein in each lane was quantified by Odyssey software, and the quantification results were normalized to β-actin expression (EV control, set as 1).



Supplementary Fig. 3
Co-localization of full-length RIG-I and MDA5 with viral NS7 in HEK293T cells.

HEK293T cells were transfected with pFlag-CD300lf (0.5ug), poly (I:C) (1 ug), or the empty vector (1 µg) for 24 h, then infected with MNV-1 for 20 h. The cells were subjected to a confocal assay by using the rabbit anti-MNV NS7, (A) mouse anti-RIG-I, and (B) mouse anti-MDA5 antibodies. (C) HEK293T cells were transfected with pFlag-CD300lf (0.5ug), poly (I:C) (1 ug), or the empty vector (1 µg)

for 24 h, then infected with MNV-1 for 20 h expression The expression of viral NS1/2 protein and transfected vectors was analyzed by western blotting. β-actin was used as a loading control.

Supplementary Table 1. The primers used for plasmid construction.

Primer	Sequence (5'to 3')
pFlag-NS7_F	TGCTCTAGAGGACCCCCATGCTTCCCCGCCCTCA
pFlag-NS7_R	CGGAATTCTTACTCATCCTCATTACAAAGAC
pMyc-NS7_F	CTAGCTAGCATGGGACCCCCATGCTTCCCCGCCCTCA
pMyc-NS7_R	CGGGATCCCTCATCCTCATTACAAAGACTGC
pFlag-NS7-N_F	TGCTCTAGAGGACCCCCATGCTTCCCCGCCCTCA
pFlag-NS7-N_R	CGGAATTCTTAAGCGCGCTTTAGGATGGCTCTC
pFlag-NS7-C_F	TGCTCTAGAGGCGACATCATGGTGCCTCTCC
pFlag-NS7-C_R	CGGGATCCCTCATCCTCATTACAAAGACTGC
pFlag-hMDA5-WT_F	CCGCTCGAGTCGAATGGGTATTCCACAGACG
pFlag-hMDA5-WT_R	CGGGGTACCTAATCCTCATCACTAAATAAAC
pFlag-hMDA5-CARD_F	CCGCTCGAGTCGAATGGGTATTCCACAGACG
pFlag-hMDA5-CARD_R	CGGGGTACCTACTCTTCATCTGAATCACTTC
pFlag-hRIG-I-WT_F	CCGCTCGAGACCACCGAGCAGCGACGCAGCC
pFlag-hRIG-I-WT_R	CGGGGTACCTCATTTGGACATTTCTGCTGGATC
pFlag-hRIG-I-CARD_F	CCGCTCGAGACCACCGAGCAGCGACGCAGCC
pFlag-hRIG-I-CARD_R	CGGGGTACCTCAATCAGACACTTCTGAAGGTGG
pMyc-hRIG-I-CARD-F	CCGCTCGAGATGACCACCGAGCAGCGACG
pMyc-hRIG-I-CARD-R	CGGGGTACCATCAGACACTTCTGAAGGTGG
pFlag-hRIG-I-ΔCARD_F	CCGCTCGAGACAACTGTACAGCCCATTTA
pFlag-hRIG-I-ΔCARD_R	CGGGGTACCTCATTTGGACATTTCTGCTGGATC

Supplementary Table 2. The primers used for qRT-PCR.

Gene	F-Sequences (5'to 3')	R-Sequences (5' to 3')
GAPDH	TGTCCCCACCCCAATGTATC	CTCCGATGCCTGCTTCACTACCTT
STAT1	ATGGCAGTCTGGCGGCTGAATT	CCAAACCAGGCTGGCACAATTG
ISG15	CTCTGAGCATCCTGGTGAGGAA	AAGGTCAGCCAGAACAGGTCGT
IFIT1	GCCTTGCTGAAGTGTGGAGGAA	ATCCAGGCGATAGGCAGAGATC
IFIT3	CCTGGAATGCTTACGGCAAGCT	GAGCATCTGAGAGTCTGCCCAA
MNV-1	CACGCCACCGATCTGTTCTG	GCGCTGCGCCATCACTC

Chapter 7

cGAS-STING effectively restricts murine norovirus infection but antagonizes the antiviral action of N-terminus of RIG-I in mouse macrophages

Peifa Yu, Zhijiang Miao, Yang Li, Ruchi Bansal, Maikel P. Peppelenbosch, Qiuwei Pan

Gut Microbes, 2021 (in press)

Abstract

Although cyclic GMP-AMP synthase (cGAS)-stimulator of interferon genes (STING) signaling has been well-recognized in defending DNA viruses, the role of cGAS-STING signaling in regulating infection of RNA viruses remains largely elusive. Noroviruses, as single-stranded RNA viruses, are the main causative agents of acute viral gastroenteritis worldwide. This study comprehensively investigated the role of cGAS-STING in response to murine norovirus (MNV) infection. We found that STING agonists potently inhibited MNV replication in mouse macrophages partially requiring the JAK/STAT pathway that induced transcription of interferon (IFN)-stimulated genes (ISGs). Loss- and gain-function assays revealed that both cGAS and STING were necessary for host defense against MNV propagation. Knocking out cGAS or STING in mouse macrophages led to defects in induction of antiviral ISGs upon MNV infection. Overexpression of cGAS and STING moderately increased ISG transcription but potently inhibited MNV replication in human HEK293T cells ectopically expressing the viral receptor CD300lf. This inhibitory effect was not affected by JAK inhibitor treatment or expression of different MNV viral proteins. Interestingly, STING but not cGAS interacted with mouse RIG-I, and attenuated its N-terminus-mediated anti-MNV effects. Our results implicate an essential role for mouse cGAS and STING in regulating innate immune response and defending MNV infection. This further strengthens the evidence of cGAS-STING signaling in response to RNA virus infection.

Keywords: murine norovirus, cGAS, STING, RIG-I, ISGs

Introduction

Noroviruses are positive sense single-stranded RNA viruses belonging to the Caliciviridae family [1]. The lack of robust cell culture systems for human norovirus (HuNV) impedes development of effective antiviral therapeutics. The closely related murine norovirus (MNV) shares similar structural and genetic features with HuNV and efficiently propagates *in vitro* and *in vivo*, representing as a useful model for studying norovirus biology [2]. The MNV genome is approximately 7.5 kilo bases in length, consisting of four open reading frames (ORFs). ORF1 encodes a polyprotein that is post-translationally cleaved into six non-structural proteins (NS1/2 to NS7), while ORF2 and ORF3 encode the major and minor structural viral proteins as VP1 and VP2, respectively. ORF4 overlaps with ORF2, and encodes the virulence factor (VF1), which has been reported to antagonize innate immune response [3].

Innate immune response plays a key role in the early recognition and restriction of viral infection. In the cytoplasm, viral RNA is mainly sensed by retinoic acid inducible gene-I (RIG-I)-like receptors (RLRs) including RIG-I and melanoma differentiation associated gene 5 (MDA5), and Toll-like receptors (TLRs) [4, 5]. Upon recognition, the RNA-stimulated signaling proceeds through adaptor mitochondrial antiviral signaling (MAVS; also called IPS-1, VISA, and Cardif) protein that activates transcription factors such as nuclear factor- κ B (NF- κ B) and interferon (IFN)-regulatory factors 3 (IRF3), which then translocate into the nucleus to drive secretion of various cytokines including IFNs, the potent inhibitors of viral replication [6-9]. Cytosolic DNA derived from pathogens is recognized by a DNA binding protein, cyclic GMP-AMP (cGAMP) synthase (cGAS) [8, 10]. Upon viral DNA recognition, cGAS produces 2'3'-cGAMP, which engages an endoplasmic reticulum (ER)-localized protein stimulator of interferon genes (STING; also called MITA, TMEM173, MPYS, and ERIS) [8, 11]. Binding of 2'3'-cGAMP to STING induces a conformational change and activates the following transcription factor IRF3, leading to expression of IFNs [8, 12]. The released IFNs can bind to their receptors and activate Janus kinase (JAK)/signal transducer and activator of transcription (STAT) signaling pathway, initiating transcription of hundreds of IFN-stimulated genes (ISGs). A subset of ISGs are considered as the ultimate antiviral effectors limiting viral replication, including norovirus [9, 13-15].

Besides the well-established role in innate immune responses to DNA viruses, emerging evidence indicates that cGAS-STING signaling is also involved in restricting RNA virus replication [16]. For instance, cells or mice that are deficient in cGAS or STING facilitate replication of several RNA viruses, such as vesicular stomatitis virus (VSV), Sendai virus (SeV), dengue virus (DENV), hepatitis C virus (HCV), and West Nile virus (WNV) [11, 17-20]. Moreover, cGAS and STING have been reported to be associated with RNA virus-induced immune responses. Cells lacking cGAS or STING show defects in IFN activation in response to the

infection of some RNA viruses, including SeV, VSV, IAV and Zika virus [21, 22]. Unlike DNA virus, RNA virus infection may not lead to quick ubiquitination and phosphorylation of STING, while SeV infection can induce STING expression [23]. Although the association between STING with RLRs in RNA virus-mediated immune responses has been indicated, the underlying mechanism remains unclear and awaits for further study. For norovirus, MDA5 has been recognized as a sensor mediating host immune response upon MNV infection [24], and both MDA5 and RIG-I overexpression can restrict HuNV and MNV replication in vitro [25-27].

To date, whether the cGAS-STING signaling plays a role in response to norovirus infection is still unknown. Thus, we investigated the potential involvement of cGAS-STING signaling mediated antiviral cellular response against MNV infection in this study.

Results

Regulation of STING agonists and inhibitor on MNV replication in mouse macrophages

Emerging studies have reported the potential involvement of cGAS-STING signaling in restricting RNA virus replication. DMXAA, as an agonist, has been identified to target the STING pathway in a mouse-specific manner [28], thus we first tested the effects of DMXAA on MNV replication in mouse macrophages. We found that DMXAA treatment inhibited viral RNA and NS1/2 protein expression (Figure 1a, b), showing a $89.93\% \pm 5.6$ (mean \pm SD, $n = 5$, $p < 0.01$) reduction of viral RNA with 10 $\mu\text{g/ml}$ of DMXAA. The antiviral effect was further confirmed by fluorescent staining showing low viral NS1/2 and NS7 protein expression (Figure 1c), and decreased viral titers by TCID50 assay (Figure 1j) in DMXAA-stimulated cells. Similar inhibitory effects were found in another two MNV strains, the acutely cleared strain MNV^{CW3} and persistent strain MNV^{CR6} both at viral RNA and NS1/2 protein levels (Figure 1d, e). In addition, another Sting agonist 2'3'-cGAMP also exerted anti-MNV effects in RAW264.7 cells (Figure 1j, and Figure S1a, b).

Based on the antiviral effects of STING agonists, we next tested the role of a STING inhibitor, H151, which can covalently bind to STING and inhibit STING-mediated signaling [29]. We found that both MNV RNA and NS1/2 protein levels were increased in H151 (5 $\mu\text{g/ml}$)-treated cells (Figure 1f, g). To further determine the involvement of cGAS-STING signaling during MNV replication, another macrophage cell line J774A.1 was used. Similarly, the inhibitory effects on MNV replication were observed in DMXAA- or 2'3'-cGAMP-stimulated cells (Figure 1h, i, and Figure S1c, d), whereas H151 treatment also facilitated viral replication in this cell line

(Figure 1h, i). No major cytotoxicity of DMXAA or 2'3'-cGAMP on both RAW264.7 and J774A.1 cells was observed (Figure S1h, and Figure S2e, f). These results suggested potential antiviral effects of cGAS-STING signaling against MNV infection.

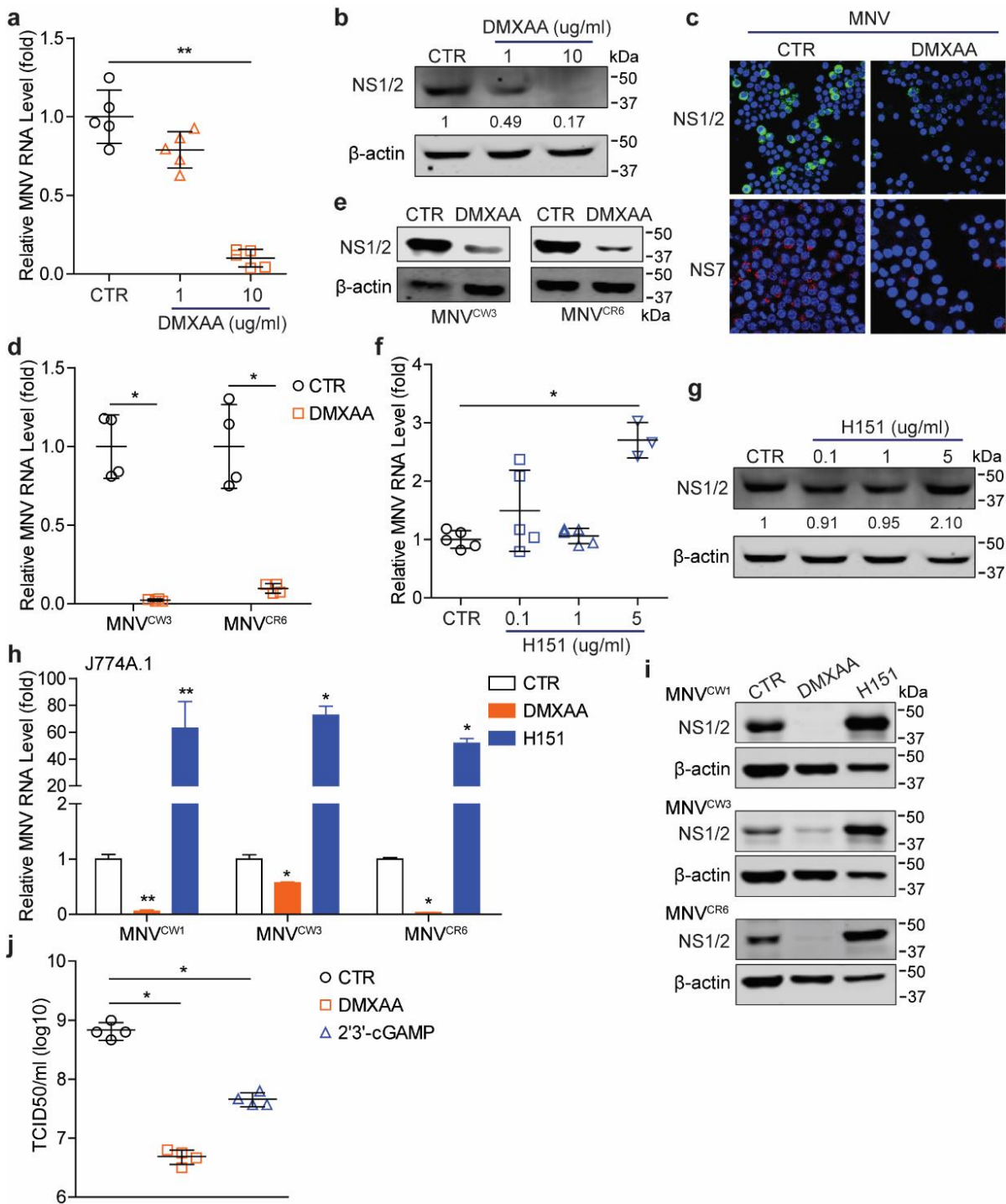


Figure 1. The effects of DMXAA and H151 on MNV replication in mouse macrophages. RAW264.7 cells were infected with MNV-1 for 1 h, then untreated or treated with DMXAA with indicated concentrations for 20 h. The viral RNA (a) and NS1/2 protein (b) expression were analyzed by qRT-PCR (n = 5) and western blotting, respectively. (c) RAW264.7 cells were infected with MNV-1 for 1 h, then

untreated or treated with DMXAA (10 µg/ml) for 20 h. The viral NS1/2 and NS7 protein expression were analyzed by confocal fluorescence microscopy. RAW264.7 cells were infected with MNV^{CW3} or MNV^{CR6} for 1 h, then untreated or treated with DMXAA (10 µg/ml) for 20 h. The viral RNA (d) and NS1/2 protein (e) expression were analyzed by qRT-PCR (n = 4) and western blotting, respectively. RAW264.7 cells were infected with MNV-1 for 1 h, then untreated or treated with H151 with indicated concentrations for 20 h. The viral RNA (f) and NS1/2 protein (g) expression were analyzed by qRT-PCR (n = 3-5) and western blotting, respectively. J774A.1 cells were infected with indicated MNV strains for 1 h, then untreated or treated with DMXAA (10 µg/ml) or H151 (5 µg/ml) for 20 h. The viral RNA (h) and NS1/2 protein (i) expression were analyzed by qRT-PCR (n = 4-5) and western blotting, respectively. (j) RAW264.7 cells were infected with MNV-1 for 1 h, then untreated or treated with DMXAA (10 µg/ml) or 2'3'-cGAMP (2 µg/ml) for 20 h. The viral titer was analyzed by TCID50 assay (n = 4). Data (a, d, f and h) were normalized to untreated control (set as 1). *P < 0.05; **P < 0.01. β-actin was used as a loading control. For immunoblot results (b and g), band intensity of NS1/2 protein in each lane was quantified by Odyssey software, and the quantification results were normalized to β-actin expression (untreated control, set as 1).

STING agonists mediate MNV inhibition through JAK/STAT pathway

Since DMXAA treatment of macrophages are associated with the downstream IFN response [28], we investigated whether STING agonists-mediated antiviral effects involves ISG response. DMXAA treatment of mouse macrophages increased the expression and phosphorylation of STAT1, and the transcription and protein expression of several antiviral ISGs, including the innate immune sensor MDA5 (Figure S2). Because JAK/STAT cascade is a key component of ISG response, we thus examined whether blocking JAK/STAT pathway could affect DMXAA-mediated ISG response and antiviral activity. We found that treatment with JAK inhibitor attenuated DMXAA-induced STAT1 expression and phosphorylation and downstream ISG transcription in macrophages (Figure 2a-d). Moreover, treatment with JAK inhibitor partially attenuated DMXAA-mediated anti-MNV ability in RAW264.7 cells, showing at increased viral RNA and NS1/2 protein levels (Figure 2e, f). The attenuated antiviral activity of DMXAA was also seen in JAK inhibitor-treated J774A.1 cells (Figure 2g, h). We also observed that inhibition of viral NS1/2 and NS7 protein expression by DMXAA was reversed upon treatment with JAK inhibitor (Figure 2i). Similar effects on 2'3'-cGAMP-mediated ISG induction and antiviral activity by JAK inhibitor were also observed (Figure S1).

In addition, we found that conditioned medium from DMXAA-treated cells stimulated IFN response, including increased IFN-β transcription, STAT1 expression and phosphorylation as well as transcription of some antiviral ISGs, whereas these effects were largely attenuated upon treatment with JAK inhibitor in RAW264.7 and J774A.1 cells (Figure S3a-g). The conditioned medium reduced viral RNA and NS1/2 protein levels, whereas the inhibitory effects were also reversed by JAK inhibitor (Figure S3h, i). These results collectively

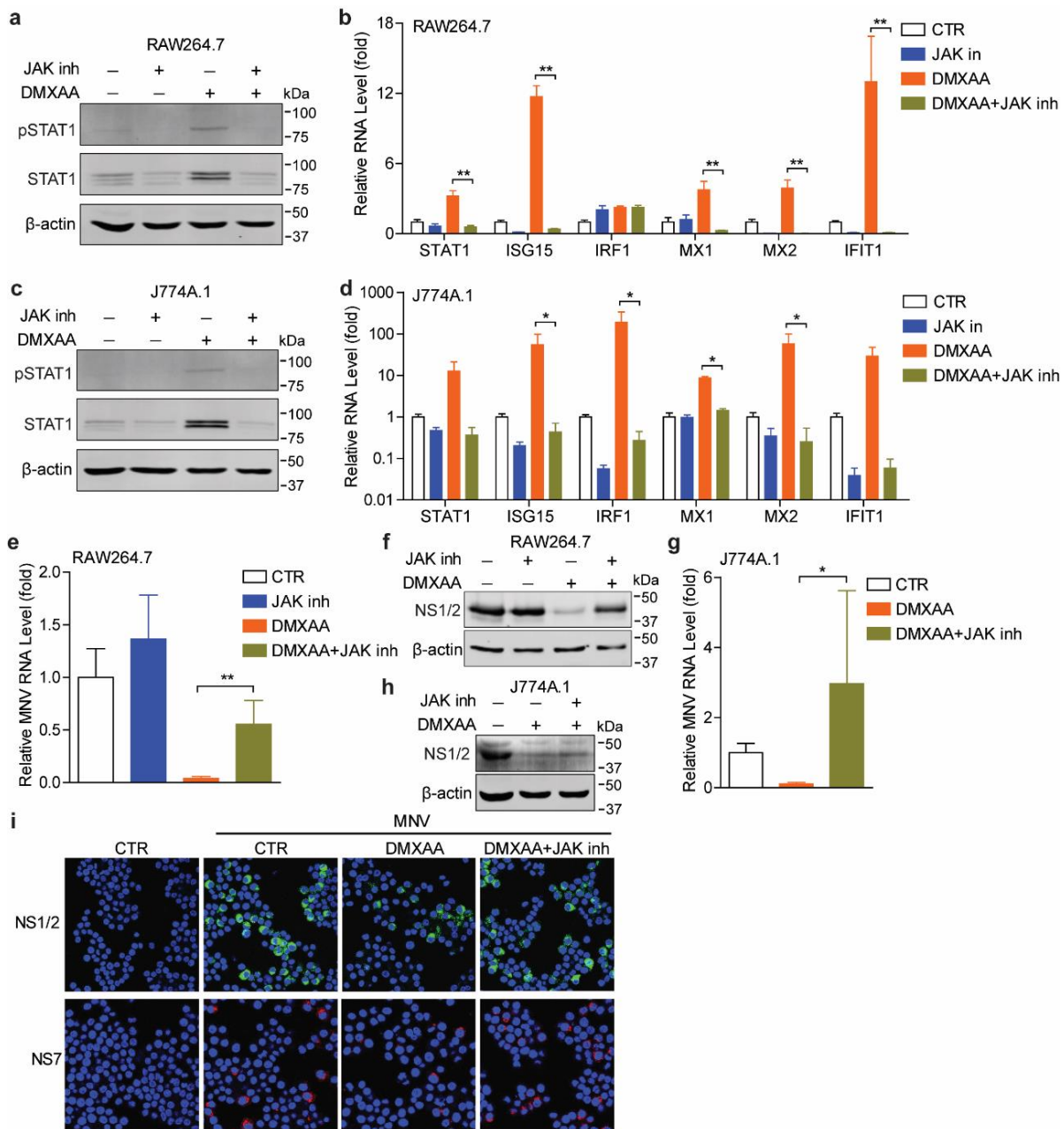


Figure 2. DMXAA mediates anti-MNV response through JAK/STAT pathway. (a) Western blotting analysis of STAT1 expression and phosphorylation, and (b) qRT-PCR analysis (n = 5) of mRNA levels of several ISGs in RAW264.7 cells untreated or treated with DMXAA (10 μ g/ml) or JAK inhibitor 1 (5 μ g/ml) for 20 h. (c) Western blotting analysis of STAT1 expression and phosphorylation, and (d) qRT-PCR analysis (n = 4) of mRNA levels of several ISGs in J774A.1 cells untreated or treated with DMXAA (10 μ g/ml) or JAK inhibitor 1 (5 μ g/ml) for 20 h. RAW264.7 cells were infected with MNV-1 for 1 h, then untreated or treated with DMXAA (10 μ g/ml) or JAK inhibitor 1 (5 μ g/ml) for 20 h. The viral RNA (e) and NS1/2 protein (f) expression were analyzed by qRT-PCR (n = 5) and western blotting, respectively. J774A.1 cells were infected with MNV-1 for 1 h, then untreated or treated with DMXAA (10 μ g/ml) or JAK inhibitor 1 (5 μ g/ml) for 20 h. The viral RNA (g) and NS1/2 protein (h) expression were analyzed by qRT-PCR (n = 4) and western blotting, respectively. (i) RAW264.7 cells were infected with MNV-1 for 1 h, then untreated or treated with DMXAA (10 μ g/ml) or JAK inhibitor 1 (5 μ g/ml) for 20 h. The viral

NS1/2 and NS7 protein expression were analyzed by confocal fluorescence microscopy. Data (b, d, e and g) were normalized to untreated control (set as 1). *P < 0.05; **P < 0.01. β -actin was used as a loading control.

demonstrated that STING agonists mediate anti-MNV effects through JAK/STAT pathway in mouse macrophages.

Absence of cGAS or STING facilitates MNV replication in mouse macrophages

Given the potential antiviral effects of STING agonists on MNV replication, we examined whether MNV infection could induce cGAS or STING expression. We found that expression of cGAS and STING appeared not to be changed in response to MNV infection in RAW264.7 cells (Figure 3a). To more specifically dissect the role of cGAS-STING signaling on MNV replication, we utilized the cGas or Sting-deficient RAW264.7 cells (Figure 3b). We found DMXAA-induced transcription of ISG15 and interferon-induced protein with tetratricopeptide repeats 1 (IFIT1) was largely abrogated in *Sting*^{-/-} but not *cGas*^{-/-} cells (Figure 3c), further confirming the specificity of DMXAA as a STING ligand. Compared with WT cells, *cGas*^{-/-} and *Sting*^{-/-} cells are more permissive in supporting MNV replication evidenced by increased viral RNA and NS1/2 protein expression levels (Figure 3d). Similar results were observed when inoculated with the MNV^{CW3} and MNV^{CR6} strains (Figure 3e, f). Even with stimulation of DMXAA or 2'3-cGAMP, the MNV replication levels still increased in *cGas*^{-/-} and *Sting*^{-/-} cells compared with WT cells (Figure 3g). In addition, we found that the viral titers of the same inoculum on *cGas*^{-/-} and *Sting*^{-/-} cells were moderately higher than that on the WT cells (Figure 3h), indicating more infectious viruses produced by the deficient cells. These results revealed that cGAS and STING are both necessary for inhibition of MNV replication in mouse macrophages.

cGAS and STING are necessary for antiviral ISG induction upon MNV infection

IFN-induced ISGs are ultimate antiviral effectors against many viral infections. MNV infection has been shown to induce ISG expression in mouse macrophages and dendritic cells [24, 30]. Thus, we investigated whether cGAS or STING could regulate MNV-induced ISG expression. The results showed that transcription of several ISGs including STAT1, ISG15 and IFIT1 induced by MNV infection were significantly inhibited by H151 treatment in RAW264.7 cells (Figure 4a). Consistently, induction of IFN- β and several antiviral ISGs (including ISG15, IFIT1, MX1 and MX2) by MNV infection were dramatically decreased in both *cGas*^{-/-} and *Sting*^{-/-} cells, compared to WT cells (Figure 4b, c). Notably, basal mRNA levels of tested antiviral ISGs were reduced in uninfected *cGas*^{-/-} and *Sting*^{-/-} RAW264.7 cells (Figure 4c), which might explain the increased viral replication in these deficient cells. Similar results were found when inoculated

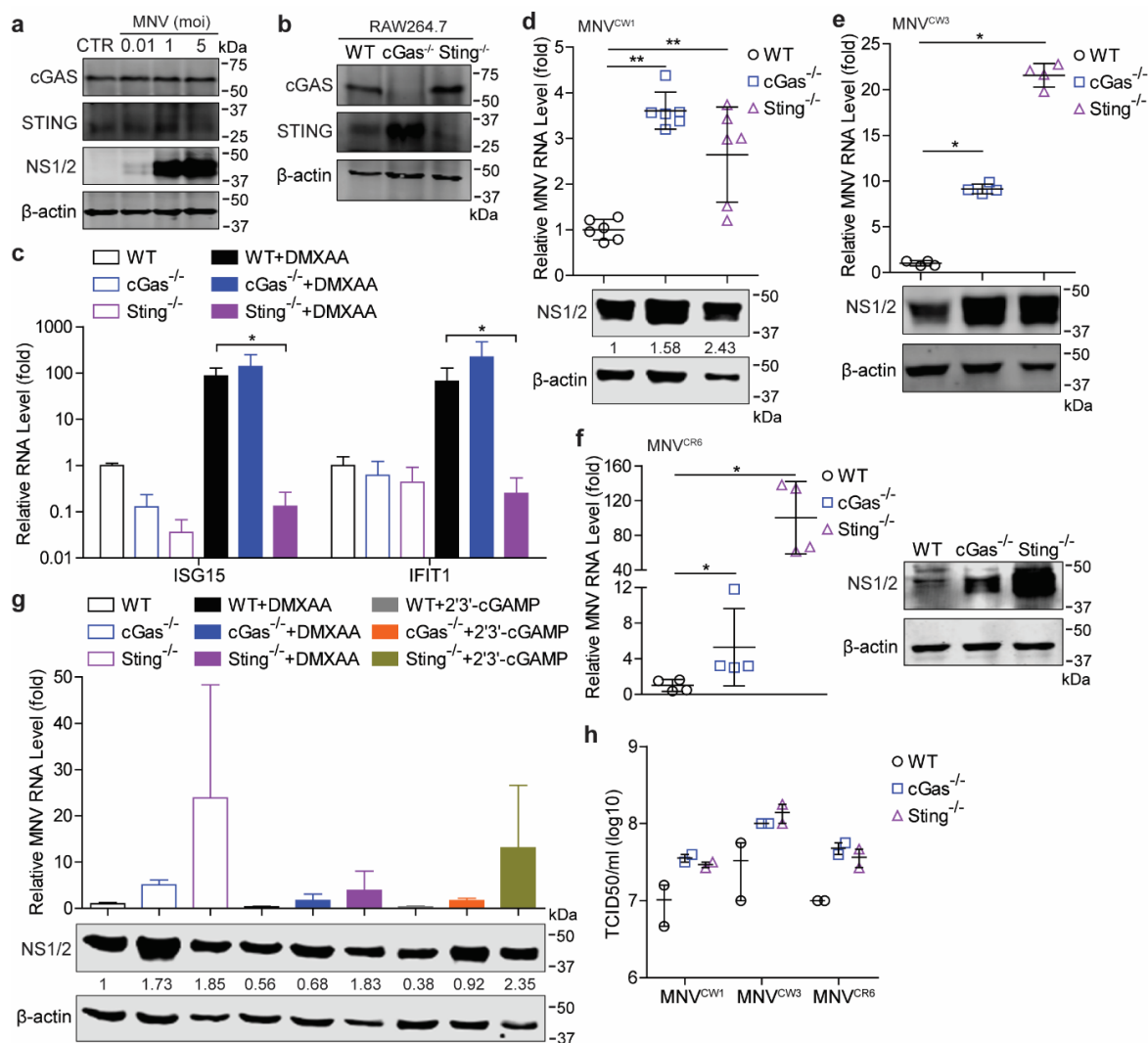


Figure 3. Absence of cGAS or STING facilitates MNV replication in mouse macrophages. (a) Western blotting analysis of cGAS and STING expression in RAW264.7 cells uninfected or infected with MNV in indicated MOIs. (b) Western blotting analysis of cGAS and STING expression in *cGas*^{-/-} and *Sting*^{-/-} RAW264.7 cells. (c) qRT-PCR (n = 4) analysis of mRNA levels of ISG15 and IFIT1 in the wild-type (WT), *cGas*^{-/-} and *Sting*^{-/-} RAW264.7 cells untreated or treated with DMXAA (10 μg/ml) for 20 h. RAW264.7 WT, *cGas*^{-/-} and *Sting*^{-/-} cells were infected with MNV-1 for 20 h. (d) The viral RNA and NS1/2 protein expression were analyzed by qRT-PCR (n = 6) and western blotting, respectively. qRT-PCR analysis of viral RNA and western blotting analysis of viral NS1/2 protein expression in WT, *cGas*^{-/-} and *Sting*^{-/-} RAW264.7 cells that infected with MNV^{CW3} (e) and MNV^{CR6} (f) for 20h, respectively. (g) RAW264.7 WT, *cGas*^{-/-} and *Sting*^{-/-} cells were infected with MNV-1 for 1 h, then untreated or treated with DMXAA (10 μg/ml) or 2'3'-cGAMP (2 μg/ml) for 20 h. The viral RNA and NS1/2 protein expression were analyzed by qRT-PCR (n = 4) and western blotting, respectively. (h) Viral titers of indicated MNV strains in RAW264.7 WT, *cGas*^{-/-} and *Sting*^{-/-} cells were examined by TCID50 assay (n = 2), data are presented as the mean ± SEM. Data were normalized to the WT control (set as 1). *P < 0.05; **P < 0.01. β-actin was used as a loading control. For immunoblot results (d and g), band intensity of NS1/2 protein in each lane was quantified by Odyssey software, and the quantification results were normalized to β-actin expression (WT control, set as 1).

with the MNV^{CW3} and MNV^{CR6} strains (Figure 4d, e). These data indicated that cGAS and STING are essentially required for MNV-induced antiviral IFN response in mouse macrophages.

Reconstitution of cGAS or STING expression in the deficient cells restores the antiviral state

Furthermore, we investigated whether reconstitution of cGAS or STING in cGas^{-/-} and Sting^{-/-} cells could restore the anti-MNV effects. We constructed and verified the expression of Myc-tagged plasmids expressing cGAS or STING in HEK293T cells, respectively (Figure 5a). Transient expression of cGAS in cGas-deficient cells restored the antiviral state of the cells, evidenced by decreased viral RNA with a 68.34% ± 10.4 (mean ± SD, n = 6, p < 0.01) reduction and NS1/2 protein expression compared with cGas^{-/-} cells transfected with the empty vectors (Figure 5b,

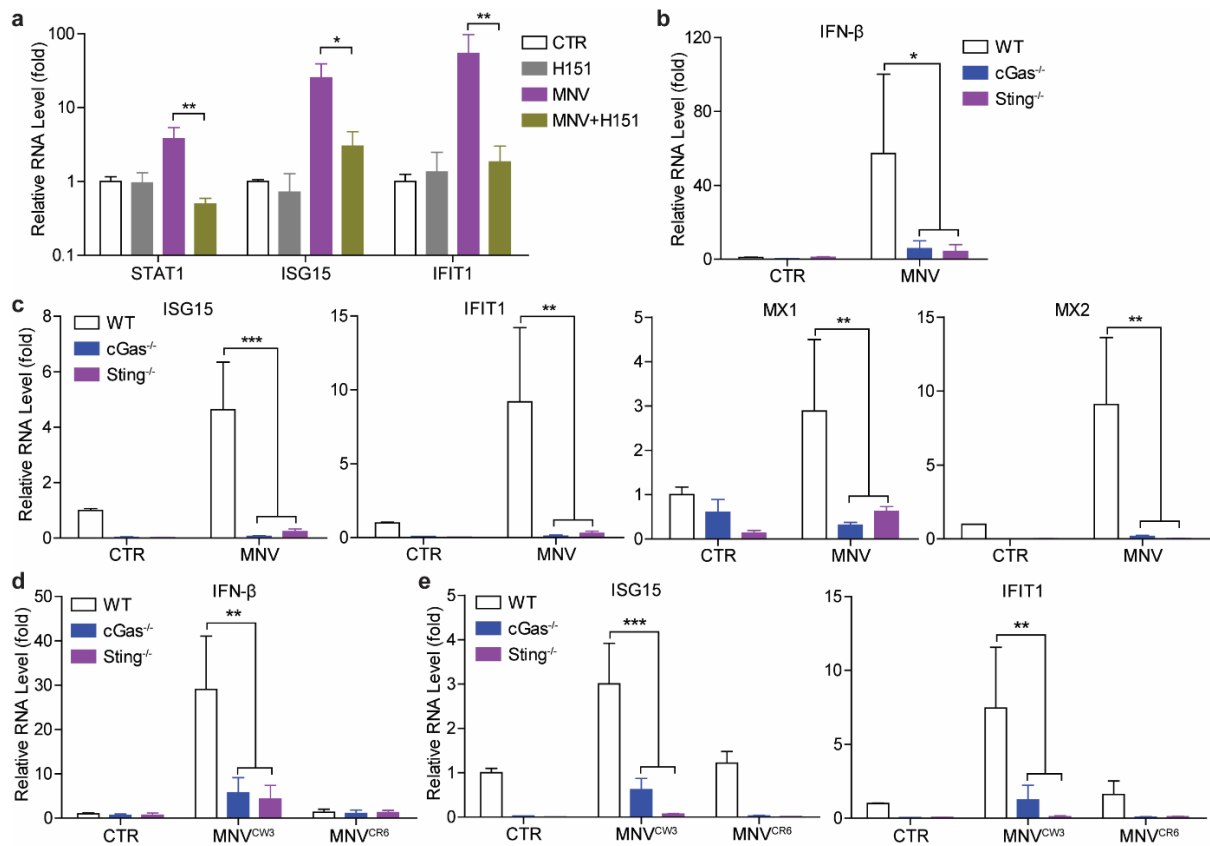


Figure 4. cGAS and STING are necessary for MNV infection-induced IFN response. (a) RAW264.7 cells were uninfected or infected with MNV-1 for 1 h, then untreated or treated with H151 (2 µg/ml) for 20 h. The mRNA levels of STAT1, ISG15 and IFIT1 were analyzed by qRT-PCR (n = 5). RAW264.7 WT, cGas^{-/-} and Sting^{-/-} cells were uninfected or infected with MNV-1 for 20 h. The mRNA levels of (b) IFN-β, and (c) ISG15, IFIT1, MX1 and MX2 were analyzed by qRT-PCR (n = 4), respectively. RAW264.7 WT, cGas^{-/-} and Sting^{-/-} cells were uninfected or infected with MNV^{CW3} or MNV^{CR6} for 20 h. The mRNA levels of (d) IFN-β, and (e) ISG15 and IFIT1 were analyzed by qRT-PCR (n = 4), respectively. Data were normalized to the uninfected WT control (set as 1). *P < 0.05; **P < 0.01 ; ***P < 0.001.

c). Similarly, reconstitution of STING expression in Sting-deficient cells also restored the antiviral state of these cells, shown by decreased viral RNA with a $66.01\% \pm 12.9$ (mean \pm SD, $n = 8$, $p < 0.001$) reduction and NS1/2 protein expression (Figure 5d, e). These data further confirmed the importance of cGAS and STING in restricting MNV replication in mouse macrophages.

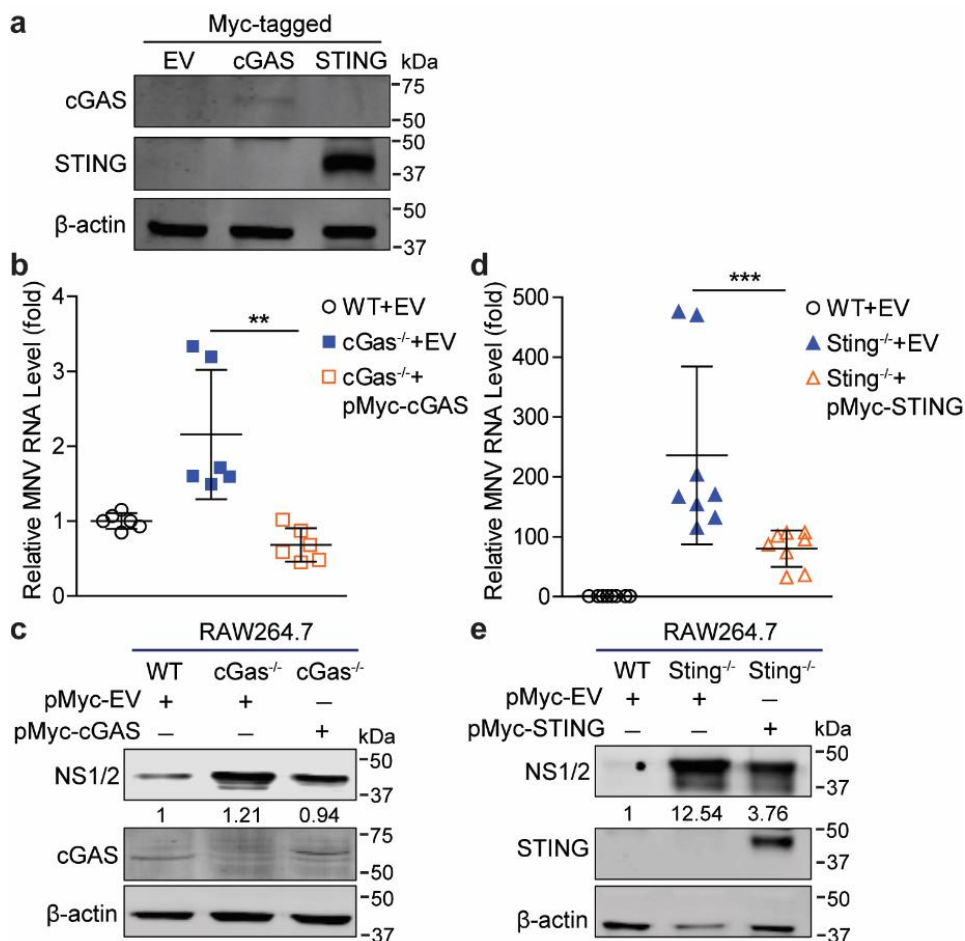


Figure 5. Reconstitution of cGAS and STING in the deficient cells restores the antiviral state. (a) HEK293T cells were transfected with pMyc-cGAS (1 μ g), pMyc-STING (1 μ g) or empty vectors (1 μ g) for 24 h. The expression of transfected vectors was detected by western blotting. RAW264.7 WT or cGas^{-/-} cells were transfected with pMyc-cGAS (1 μ g) or empty vectors (1 μ g) for 24 h, then infected with MNV for 20 h. The viral RNA (b) and NS1/2 protein (c) expression were analyzed by qRT-PCR ($n = 6$) and western blotting, respectively. RAW264.7 WT or Sting^{-/-} cells were transfected with pMyc-STING (1 μ g) or empty vectors (1 μ g) for 24 h, then infected with MNV for 20 h. The viral RNA (d) and NS1/2 protein (e) expression were analyzed by qRT-PCR ($n = 8$) and western blotting, respectively. Data were normalized to the WT control (set as 1). ** $P < 0.01$; *** $P < 0.001$. β -actin was used as a loading control. For immunoblot results (c and e), band intensity of NS1/2 protein in each lane was quantified by Odyssey software, and the quantification results were normalized to β -actin expression in WT cells (set as 1).

Overexpression of cGAS and STING restricts MNV replication

Since human cGAS and STING overexpression can activate antiviral immune response, thus we next evaluated whether overexpression of mouse cGAS and STING could also induce antiviral immune response. By using a transcriptional reporter system that mimics IFN response with a reporter luciferase gene driving by multiple ISREs, we found that expression of cGAS or STING alone, or their combination could increase ISRE-related luciferase activity (Figure 6a), and induce a moderate increase in the expression of IFN- β and several antiviral ISGs in HEK293T cells (Figure 6b). Because ectopic expression of the MNV receptor (mouse CD300lf) confers human cells to MNV infection [26, 31], we further characterized whether cGAS and STING overexpression could exert antiviral activity in HEK293T cells. As shown in Figure 6c and d, overexpression of cGAS or STING significantly inhibited MNV replication, showing at the decreased viral RNA and NS1/2 protein expression as well as virus production in the supernatant. This inhibitory effect is much stronger in the cells that overexpressing both cGAS and STING. In addition, cGAS and STING overexpression also reduced viral RNA levels in mouse macrophages (Figure 6e, f).

Overexpression of cGAS and STING had minimal effects on the induction of tested ISGs in RAW264.7 cells (Figure S4), and treatment of JAK inhibitor did not affect cGAS-STING mediated antiviral effects in HEK293T cells (Figure 6g), suggesting that cGAS-STING mediated anti-MNV activity is dispensable of ISG induction. Because viral proteins can be the targets of cGAS or STING [12, 17], we thus further investigated whether the MNV proteins (NS1/2, NS6 and NS7) could affect cGAS-STING mediated antiviral effects. The results showed that cGAS-STING mediated inhibition of MNV replication was not affected by expression of these viral proteins (Figure 6h).

STING but not cGAS interacts with RIG-I, and antagonizes N-terminus of RIG-I mediated antiviral effects

Human STING has been reported to interact with RIG-I, a key component of RNA sensing pathway [11, 32], and this prompted us to investigate whether this occurs in mouse cells. We constructed Flag-tagged vectors expressing WT (wild-type; 2-926 amino acids) and N-terminus (2-235 amino acids) of mouse RIG-I (RIG-I_N), and verified their expression in HEK293T cells (Figure 7a). Confocal microscopy revealed that STING could co-localize with either RIG-I or its N-terminus in the cytoplasm (Figure 7b), and co-immunoprecipitation assay showed that STING could interact with RIG-I and RIG-I_N (Figure 7c). In addition, we also examined the co-localization of cGAS with RIG-I. Although cGAS appeared to co-localize with RIG-I, it was not precipitated by RIG-I or its N-terminus (Figure 7d, e). Since MDA5 is a sensor for MNV infection, we further evaluated whether mouse cGas or Sting associates with MDA5. We constructed

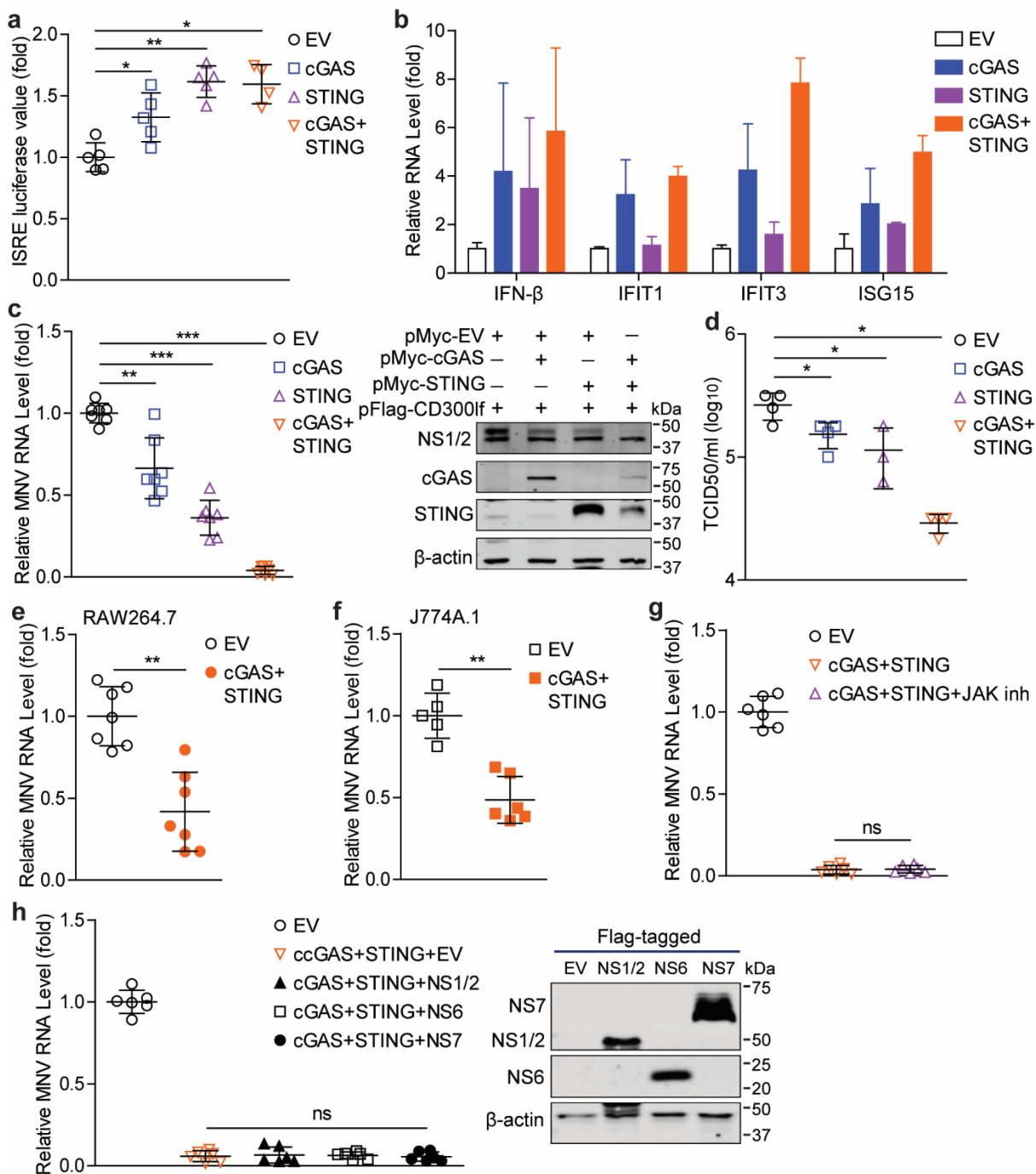


Figure 6. Overexpression of cGAS and STING restricts MNV replication. (a) Analysis of ISRE related firefly luciferase activity in Huh7-ISRE-Luc cells transfected with pMyc-cGAS (1 μ g), pMyc-STING (1 μ g) or empty vectors (1 μ g) for 48 h (n = 4-5). (b) HEK293T cells were transfected with pMyc-cGAS (1 μ g), pMyc-STING (1 μ g) or empty vectors (1 μ g) for 48 h. The mRNA levels of IFN- β , IFIT1, IFIT3 and ISG15 were analyzed by qRT-PCR (n = 2-5). HEK293T cells were transfected with pFlag-CD300lf (0.5 μ g) and pMyc-cGAS (1 μ g), pMyc-STING (1 μ g) or empty vectors (1 μ g) for 24 h, then infected with MNV-1 for 20 h. (c) Viral RNA, NS1/2 protein and expression of transfected vectors, and (d) viral titers were analyzed by qRT-PCR (n = 7), western blotting and TCID50 assay (n = 3-4), respectively. (e) RAW264.7 (n = 7) and (f) J774A.1 (n = 5-6) cells were transfected with pMyc-cGAS (1 μ g), pMyc-STING (1 μ g) or empty vectors (1 μ g) for 24 h, then infected with MNV-1 for 20 h. The viral RNA levels were analyzed

by qRT-PCR. (g) HEK293T cells were transfected with pFlag-CD300lf (0.5 μ g), pMyc-cGAS (1 μ g), and pMyc-STING (1 μ g) or empty vectors (1 μ g) for 24 h, then infected with MNV-1 for 1 h, and refreshed medium containing JAK inhibitor 1 (5 μ g/ml) for 20 h. The viral RNA levels were analyzed by qRT-PCR (n = 6). (h) Expression of Flag-tagged viral NS1/2, NS6 and NS7 vectors were analyzed by western blotting in HEK293T cells transfected with indicated constructs (1 μ g/each). HEK293T cells were transfected with pFlag-CD300lf (0.5 μ g), and pMyc-cGAS (1 μ g), pMyc-STING (1 μ g), pFlag-NS1/2 (1 μ g), pFlag-NS6 (1 μ g), pFlag-NS7 (1 μ g) or empty vectors (were used to maintain a constant amount of plasmid DNA per transfection) for 24 h, then infected with MNV-1 for 20 h. The viral RNA levels were analyzed by qRT-PCR (n = 6). Data were normalized to the EV control (set as 1). *P < 0.05; **P < 0.01; ***P < 0.001. β -actin was used as a loading control.

Flag-tagged vector expressing N-terminus (2-294 amino acids) of mouse MDA5 (MDA5_N), and verified its expression and co-localization with cGAS or STING in HEK293T cells (Figure S5a). Association between MDA5_N with cGAS or STING was not observed by co-immunoprecipitation assay (Figure S5b).

Our previous work has revealed that overexpression of human RIG-I restricts norovirus replication partially via ISG induction [25, 26]. Here, we characterized the effects of mouse RIG-I on MNV replication. By using the ISRE luciferase model, we found both the full-length RIG-I and its N-terminus increased ISRE-related luciferase activity (Figure 8a). In HEK293T cells, mRNA levels of IFN- β , ISG15 and IFIT1 were increased by RIG-I transfection (Figure 8b). It has been reported that the CARD domain in the N-terminus of RIG-I are responsible for signal transduction and activation of IRF-3 and NF- κ B, as well as subsequent IFN response [5]. We found that compared with the full-length RIG-I, its N-terminus induced much stronger levels of ISRE-related luciferase activity and ISG transcription (Figure 8a, b). Thus we further tested the antiviral effects of RIG-I_N, and found that RIG-I_N effectively inhibited viral RNA with a 88.2% \pm 6.8 (mean \pm SD, n = 5, p < 0.01) reduction and NS1/2 protein expression (Figure 8c), as well as production of infectious viruses in the supernatant (Figure 8d). RIG-I signaling stimulates downstream ISG expression mainly through JAK/STAT pathway [33]. We found that JAK inhibitor treatment substantially reduced RIG-I_N induced STAT1 expression and phosphorylation, as well as transcription of IFN- β , ISG15 and IFIT1 (Figure 8e). Moreover, RIG-I_N mediated inhibition of MNV replication was partially reversed by JAK inhibitor treatment in HEK293T cells (Figure 8f). The inhibitory effects of RIG-I_N against MNV replication were also observed in J774A.1 and RAW264.7 cells, respectively (Figure 8g).

As aforementioned, RIG-I_N can interact with STING (Figure 7c). We further examined whether STING could regulate RIG-I_N mediated antiviral response. Compared with the WT cells (showing an average 46.6% reduction of viral RNA; Figure 8g right panel), the antiviral activity of RIG-I_N was much stronger in cGas^{-/-} or Sting^{-/-} RAW264.7 cells, showing average 72.8% and 99.8% reduction of viral RNA, respectively (Figure 8h). Conversely, we found that

STING reconstitution in *Sting*^{-/-} cells significantly attenuated the anti-MNV activity of RIG-I_N, whereas this effect was not seen by cGAS reconstitution in *cGas*^{-/-} cells (Figure 8i). These results revealed that RIG-I_N exerts anti-MNV effect partially through JAK/STAT pathway, but this inhibitory effect is antagonized by STING expression in mouse macrophages.

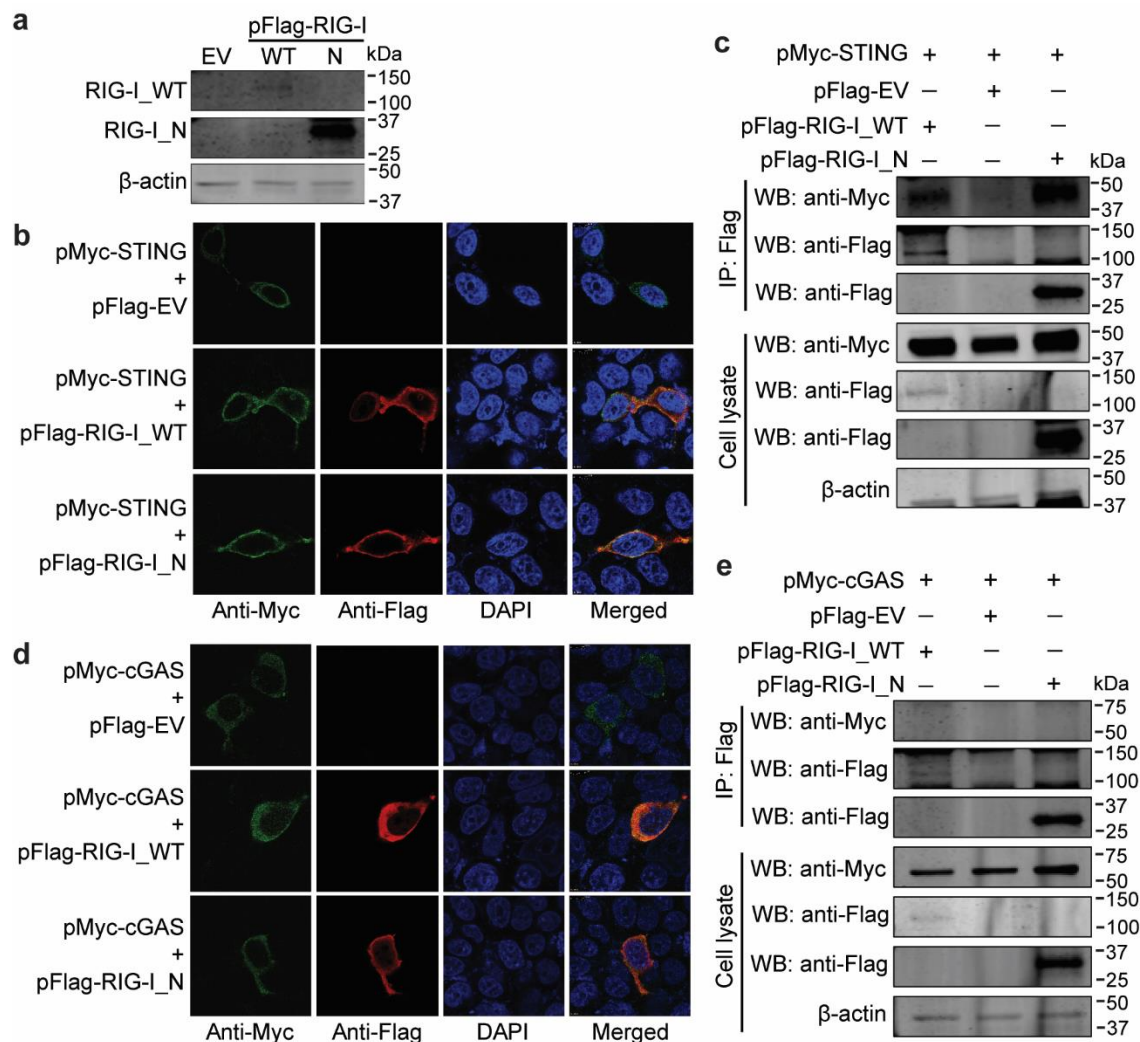


Figure 7. STING interacts with RIG-I. (a) HEK293T cells were transfected with pFlag-RIG-I_WT, pFlag-RIG-I_N, or the empty vectors (1 µg/each) for 24 h. Expression of transfected vectors were examined by western blotting. HEK293T cells were transfected with pMyc-STING, and pFlag-RIG-I_WT, pFlag-RIG-I_N or empty vectors (1 µg/each for confocal assay for 24 h; 1.5 µg/each for co-IP assay for 48 h). (b) Expression and co-localization of STING with RIG-I_WT and RIG-I_N were analyzed by confocal assay. (c) Co-IP assay was performed using anti-Flag MAb (1:1000). The precipitated proteins were analyzed by western blotting using anti-Flag and anti-Myc antibodies. HEK293T cells were transfected with pMyc-cGAS, and pFlag-RIG-I_WT, pFlag-RIG-I_N or empty vectors (1 µg/each for confocal assay for 24 h; 1.5 µg/each for co-IP assay for 48 h). (d) Expression and co-localization of cGAS with RIG-I_WT and RIG-I_N was analyzed by confocal assay. (e) Co-IP assay was performed using anti-Flag MAb (1:1000). The precipitated proteins were analyzed by western blotting using anti-Flag and anti-Myc antibodies. β-actin was used as a loading control.

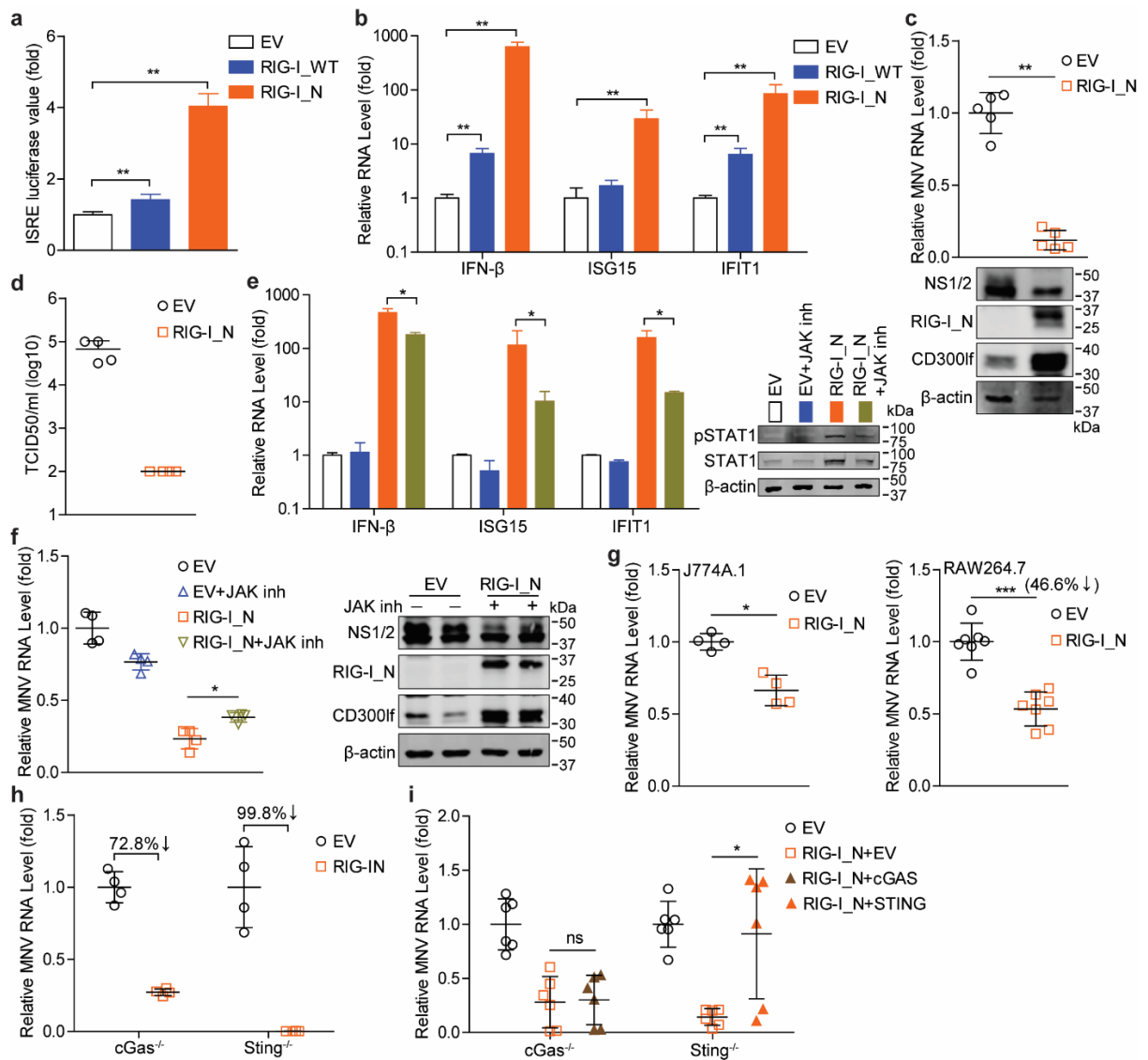


Figure 8. The N-terminus of RIG-I exerts antiviral effect, but is antagonized by STING expression. (a) Analysis of ISRE related firefly luciferase activity in Huh7-ISRE-Luc cells transfected with pFlag-RIG-I_WT (1 μ g), pFlag-RIG-I_N (1 μ g) or empty vectors (1 μ g) for 48 h (n = 6). (b) HEK293T cells were transfected with pFlag-RIG-I_WT (1 μ g), pFlag-RIG-I_N (1 μ g) or empty vectors (1 μ g) for 48 h. The mRNA levels of IFN- β , ISG15 and IFIT1 were analyzed by qRT-PCR (n = 5). (c) HEK293T cells were transfected with pFlag-CD300lf (0.5 μ g), pFlag-RIG-I_N (1 μ g) or empty vectors (1 μ g) for 24 h, then infected with MNV for 20 h. The viral RNA, NS1/2 protein and expression of transfected vectors were analyzed by qRT-PCR (n = 5) and western blotting, respectively. (d) HEK293T cells were transfected with pFlag-CD300lf (0.5 μ g), pFlag-RIG-I_N (1 μ g) or empty vectors (1 μ g) for 24 h, then infected with MNV for 20 h. The titers of produced viruses in the supernatant were analyzed by TCID50 assay (n = 4). (e) HEK293T cells were transfected with pFlag-RIG-I_N (1 μ g) or empty vectors (1 μ g) for 24 h, then untreated or treated with JAK inhibitor 1 (5 μ g/ml) for 20 h. The mRNA levels of IFN- β , ISG15 and IFIT1, and STAT1 expression and phosphorylation were analyzed by qRT-PCR (n = 4) and western blotting, respectively. (f) HEK293T cells were transfected with pFlag-CD300lf (0.5 μ g), pFlag-RIG-I_N (1 μ g) or empty vectors (1 μ g) for 24 h, then infected with MNV for 1 h, refreshed medium with or without JAK

inhibitor 1 (5 µg/ml) for 20 h. The viral RNA, NS1/2 protein and expression of transfected vectors were analyzed by qRT-PCR (n = 4) and western blotting, respectively. (g) J774A.1 and RAW264.7 cells were transfected with pFlag-RIG-I_N (1 µg) or empty vectors (1 µg) for 24 h, then infected with MNV for 20 h. The viral RNA levels were analyzed in J774A.1 (n = 4) and RAW264.7 (n = 7) cells by qRT-PCR. (h) RAW264.7 cGas^{-/-} or Sting^{-/-} cells were transfected with pFlag-RIG-I_N (1 µg) or empty vectors (1 µg) for 24 h, then infected with MNV for 20 h. The viral RNA levels were analyzed by qRT-PCR (n = 4). (i) RAW264.7 cGas^{-/-} or Sting^{-/-} cells were transfected with pFlag-RIG-I_N (1 µg), pMyc-cGAS (1 µg), pMyc-STING (1 µg), or empty vectors (1 µg) for 24 h, then infected with MNV for 20 h. The viral RNA levels in cGas^{-/-} (n = 6) or Sting^{-/-} (n = 6) RAW264.7 cells were analyzed by qRT-PCR. Data were normalized to the EV control (set as 1). *P < 0.05; **P < 0.01; ***P < 0.001; ns, not significant. β-actin was used as a loading control.

Discussion

IFN-mediated innate immune response provides the first line of host defense against viral infections. Within host cells, cyclic dinucleotides (CDNs) can be sensed by STING and stimulate IFN immune response. This antiviral mechanism has been widely described for defending DNA viruses, but emerging evidence indicates this may also function on some RNA viruses [18, 34, 35]. Here we demonstrated that two STING agonists, DMXAA and 2'3'-cGAMP, robustly inhibited MNV replication, whereas the STING inhibitor H151 promoted viral replication in mouse macrophages. Experimentally delivery of CDNs into host cells has been shown to activate IFN response and inhibit viral replication [18], and DMXAA treatment in macrophages has been reported to activate IFN activation and ISG expression [28, 36]. In this study, both DMXAA and 2'3'-cGAMP can stimulate IFN response and expression of antiviral ISGs in mouse macrophages. Blocking JAK/STAT pathway by JAK inhibitor significantly attenuates DMXAA and 2'3'-cGAMP induced antiviral actions, revealing the importance of antiviral ISG induction for their anti-MNV effects.

Studies have reported that infection of some RNA viruses (such as VSV, SeV, IAV and SINV) do not change STING electrophoretic mobility and stability, indicating that RNA virus infection does not induce hallmarks of STING activation that are associated with IFN response [19]. Here we also did not observe significant changes in cGAS or STING expression in response to MNV infection. Although a recent study has revealed an inverse effect that STING facilitates human rhinoviruses replication [37], most studies have demonstrated that compared with WT cells, the cells lacking cGAS or STING facilitate replication of some RNA viruses such as VSV and WNV [19, 20]. Consistently, our results showed that ablation of cGAS or STING enhances MNV replication, whereas reconstitution of cGAS or STING expression in the deficient cells partially restores the antiviral state. In addition, cGAS is also present in nucleus and nuclear-localized

cGAS can enhance antiviral immune response in a non-canonical manner [22]. Whether mouse cGAS can sense MNV infection in the cytoplasm needs to be further studied. We also revealed that more infectious viruses are produced in cGas- and Sting-deficient cells under same inoculum of MNV strains, which is consistent with previous reports demonstrating that the permissiveness of cells lacking STING was increased in response to VSV infection [19]. Loss of cGAS or STING has been reported to decrease the basal expression of some antiviral ISGs in uninfected cells [19, 20], and similar results were also observed in this study. Some studies showed that loss of cGAS or STING impairs RNA virus-induced IFN response, whereas others reported normal level of IFN activation in response to some RNA viruses in the absence of cGAS or STING [11, 19-22]. In this study, compared with the WT cells, MNV infection-induced transcription of some ISGs were reduced in cGas- and Sting-deficient RAW264.7 cells, showing a regulatory role of cGAS and STING on MNV triggered innate immune response. STING has been reported to possess dual functions in host defense by regulating protein synthesis or IFN response to prevent viral infection [19], and thus whether this regulation is directly attributed to the loss of cGAS and STING or indirectly through the altered host immune defense status remains to be investigated. We speculate this could also be virus and/or host cell type specific.

MNV can replicate in murine macrophages and dendritic cells, but not in epithelial cells or human cells because of a restriction at viral entry [31, 38, 39]. Discovery of the cell-surface expressed MNV receptor (CD300lf) enables MNV infection in human cells (like HeLa and HEK293T cells) and facilitates identification of antiviral cellular factors [9, 31, 40]. Overexpression of mouse cGAS and STING moderately upregulates ISG expression, but potently restricts MNV replication in HEK293T cells ectopically expressing viral receptor. However, this antiviral effect is not influenced by JAK inhibitor treatment, suggesting that ISG induction is dispensable for cGAS and STING mediated antiviral effects in human cells, and presenting a distinct antiviral effects compared with STING agonists in presence of JAK inhibitor. This might be attributed to the difference in cell types: immune vs epithelial cells. Emerging evidence indicates that some RNA viruses have evolved strategies to antagonize the antiviral activity of cGAS and STING. For instance, the nonstructural protein NS4B of yellow fever virus (YFV) interacts STING and inhibits STING-mediated IFN- β promoter-driven luciferase activity [12]. The DENV NS2B3 protease complex specifically cleaves human STING protein but not mouse STING, and attenuates STING-mediated IFN response [41], while the NS2B of DENV degrades cGAS in an autophagy-lysosome-dependent pathway and inhibits IFN production in the infected cells [17]. Several MNV nonstructural proteins are associated with immune response, including NS1/2 that mediates resistance to IFN- λ modulated clearance of persistent viral infection [42], and NS7 as the viral polymerase modulating innate immune response [26, 43]. Here we revealed that these two viral proteins along with NS6 did not exert clear effects on cGAS and STING mediated inhibitory activity, suggesting that these viral

proteins are likely not the target of cGAS and STING. Because MNV VF1 has been reported to attenuate RLRs-mediated immune response [3, 44], and thus whether other viral components including VF1 could influence or are the targets of cGAS and STING mediated antiviral activity needs to be further investigated.

Human STING interacts with RIG-I, and is necessary for RIG-I triggered IFN- β production in murine embryonic fibroblasts [32]. Besides IFN activation, STING restricts production of both viral and host proteins in a RIG-I/MDA5-dependent manner by initiating global translation inhibition [19]. Overexpression of human RIG-I or its N-terminus activates IFN response and exerts antiviral activity against HuNV and MNV infection [25, 26]. Similar actions mediated by

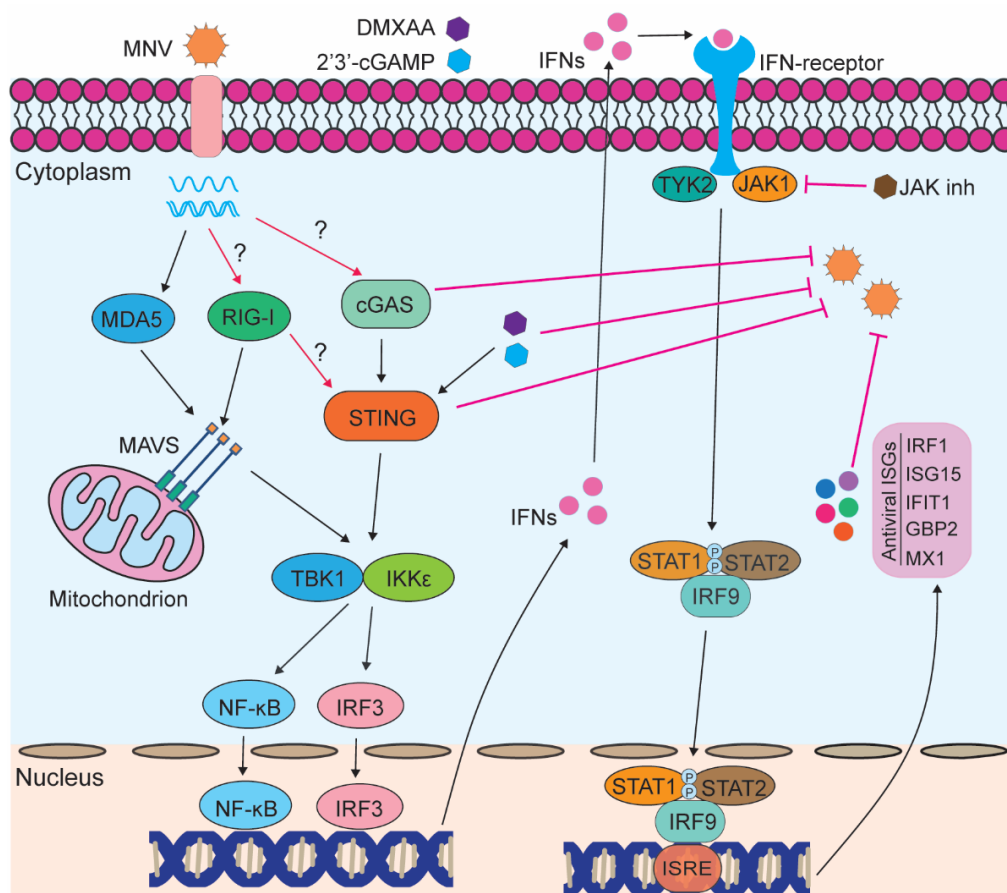


Figure 9. A proposed model for host immune response upon MNV infection. Upon infection, MNV is recognized by the pattern recognition receptor MDA5. This activates the downstream cascades, including NF- κ B and IRF3, inducing production of IFNs. Then, IFNs bind to the receptors and further activate JAK/STAT signaling pathway, leading to transcription of hundreds of ISGs. RIG-I, cGAS and STING can restrict MNV replication in mouse macrophages, but whether they are involved in MNV recognition needs further studies. Also, whether the interaction between RIG-I and STING involving the participation of other host factors needs to be further explored. STING agonists DMXAA and 2'3'-cGAMP inhibit MNV replication through induction of antiviral ISGs, and this effects is partially reversed by JAK inhibitor treatment. The red line with a blunt end indicates the inhibitory effect.

N-terminus of mouse RIG-I is also observed in this study, and this antiviral effect partially requires JAK/STAT signaling that triggers ISG induction in HEK293T cells. Unexpectedly, compared with the WT cells, RIG-I_N mediated antiviral effects are augmented in cGas- and Sting-deficient cells, whereas reconstitution of STING but not cGAS in the deficient cells impedes the antiviral effects of RIG-I_N. These results suggest that the interaction between mouse STING and RIG-I_N might affect their antiviral actions. However, we cannot rule out the possible participation of MAVS in our model, because human MAVS is known to associate with human STING, although it is not clear whether MAVS directly interacts with STING, or exists as a complex with RIG-I/STING [32]. Inactivating human RIG-I and MAVS has been reported to not affect HuNV replication [45, 46], and thus the potential role of basal mouse RIG-I and MAVS expression in response to MNV replication is interesting to be further studied. Theoretically, the RIG-I/MDA5-MAVS axis and cGAS-STING axis are distinct sensing pathways for cytosolic RNA and DNA, respectively. Crosstalk between these two pathways has been documented [19, 32], but there remain many knowledge gaps. In the context of MNV infection, we encourage future studies to decipher the potential crosstalk between the RIG-I/MDA5-MAVS and cGAS-STING axis.

In summary, this study reveals that the cGAS-STING signaling essentially contributes to the host defense in response to MNV infection, but these antiviral effects may only be partially through induced antiviral ISGs (Figure 9). Interestingly, mouse STING but not cGAS interacts with RIG-I, and attenuates RIG-I_N mediated inhibition of viral replication in mouse macrophages. Our results implicate a role for mouse cGAS and STING in controlling MNV replication and in regulating innate immune responses, and strengthen the evidence of cGAS-STING signaling in response to RNA virus infection. Nevertheless, future in vivo studies are required to validate our intriguing findings.

Materials and methods

Chemicals and antibodies

DMXAA, H151 and 2'3'-cGAMP were purchased from InvivoGen. JAK inhibitor 1 (SC-204021) was purchased from Santa Cruz Biotechnology (Santa Cruz, CA, USA). N-Acetyl-L-cysteine was purchased from Sigma-Aldrich. Rabbit polyclonal antisera to MNV NS1/2 was kindly provided by Prof. Vernon K. Ward (School of Biomedical Sciences, University of Otago, New Zealand) [45]. Rabbit polyclonal antisera to MNV NS7 was kindly provided by Prof. Ian Goodfellow (Department of Pathology, University of Cambridge, UK) [46]. Antibodies against STAT1 (#9172), pSTAT1 (Ser727, #9177), RIG-I (D14G6, #3743), MDA5 (D74E4, #5321), cGAS (D3O8O,

#31659), STING (D2P2F, #13647), Myc-tag (71D10, #2278) and Myc-Tag (9B11, #2276) were purchased from Cell Signaling Technology. Rabbit anti-GBP2 (11854-1-AP) and anti-GBP5 (13220-1-AP) antibodies were purchased from Proteintech. Mouse anti-Flag (F1804, Sigma-Aldrich) and anti- β -actin (#sc-47778, Santa Cruz Biotechnology) antibodies were used. Anti-rabbit and anti-mouse IRDye-conjugated secondary antibodies (Li-Cor Bioscience, Lincoln, USA) were used.

Cell lines

RAW264.7, J774A.1 and human embryonic kidney (HEK293T) cells were cultured in Dulbecco's modified Eagle's medium (DMEM; Lonza Verviers, Belgium) supplemented with 10% (vol/vol) heat-inactivated fetal calf serum (FCS; Hyclone, Logan, UT, USA), 100 μ g/mL of streptomycin and 100 IU/mL of penicillin. The cGas- and Sting-deficient RAW264.7 cells were kindly provided by Prof. Denise M. Monack (Department of Microbiology and Immunology, Stanford University Stanford School of Medicine) (45). ISRE (IFN-stimulated response element) activation reporter model (Huh7-ISRE-Luc) was based on Huh7 cells that expressing the firefly luciferase reporter gene driven by a promoter containing multiple ISRE elements (SBI Systems Biosciences, Mountain View, CA). Luciferase activity represents ISRE promoter activation level (46), and this cell line was also maintained in DMEM with 10% (vol/vol) heat-inactivated FCS, 100 μ g/mL of streptomycin and 100 IU/mL of penicillin.

Virus strains

Murine norovirus strains MNV-1 (MNV^{CW1}), the acutely cleared strain MNV^{CW3} and the persistent strain MNV^{CR6}, were produced by consecutively inoculating the virus (kindly provided by Prof. Herbert Virgin, Department of Pathology and Immunology, Washington University School of Medicine) into RAW264.7 cells (47). The MNV cultures were purified, aliquoted, and stored at -80 °C for subsequent experiments. The virus stock was quantified by the 50% tissue culture infective dose (TCID50). Without specific statement, the MNV strain used in most part of this study was MNV^{CW1}.

TCID50

TCID50 assay was used to determine the viral titers. Briefly, 10-fold dilutions of MNV were inoculated into RAW264.7 cells grown in 96-well tissue culture plate at 1,000 cells/well. Then the plate was incubated at 37 °C for another 5 days, followed by observing the cytopathic effect (CPE) of each well under a light scope. The TCID50 was calculated by using the Reed-Muench method.

Plasmid construction and cell transfection

The mouse cGAS and STING genes were amplified from a cDNA sample that isolated from RAW264.7 cells, and cloned into pcDNA3.1/Myc-His vector (kindly provided by Dr. Shuaiyang Zhao, Chinese Academy of Agricultural Sciences, China), respectively. The full-length mouse RIG-I gene and its N-terminus, and the N-terminus of mouse MDA5 were amplified from a cDNA sample that isolated from RAW264.7 cells and cloned into pcDNA3.1/Flag-HA vector (Addgene), respectively. The viral genes NS1/2 and NS6 were amplified from a cDNA sample that isolated from MNV-1 infected RAW264.7 cells, and cloned into pcDNA3.1/Flag-HA vector, respectively. Flag-tagged plasmid expressing MNV NS7 was previously described [9]. Flag-tagged plasmid expressing the MNV receptor CD300lf was kindly provided by Prof. Herbert Virgin (Department of Pathology and Immunology, Washington University School of Medicine, USA) [31]. The primer sequences used for plasmid construction are shown in Table S1.

The cells were transfected with various plasmids at indicated concentrations using FuGENE HD Transfection Reagent (E2311; Promega) according to the manufacturer's instructions. Where necessary, appropriate empty vectors were used to maintain a constant amount of plasmid DNA per transfection.

RNA isolation and qRT-PCR

The Macherey NucleoSpin RNA II Kit (Bioke, Leiden, The Netherlands) was used for total RNA isolation. The cDNA synthesis kit (TaKaRa Bio, Inc., Shiga, Japan) was used to synthesize cDNA from RNA samples, then targeted genes were quantified by SYBR-Green-based (Applied Biosystems) real-time PCR on the StepOnePlus™ System (Thermo Fisher Scientific LifeSciences) according to the manufacturer's instructions. Human and mouse glyceraldehyde-3-phosphate dehydrogenase (GAPDH) genes were used as reference genes to normalize gene expression. The relative expression of targeted genes were calculated using the $2^{-\Delta\Delta CT}$ method, and primer sequences used for quantification of targeted genes are shown in Table S2.

Western blotting

The cells were lysed in Laemmli sample buffer containing 0.1 M DTT and heated 5 min at 95 °C, then loaded onto a 10% or 12% sodium dodecyl sulfate polyacrylamide gel electrophoresis (SDS-PAGE) gel. Then proteins were further electrophoretically transferred onto a polyvinylidene difluoride (PVDF) membrane (pore size, 0.45 μM; Invitrogen) for 1.5 or 2 h with an electric current of 250 mA. Then the membrane was blocked with a mixture of 2.5 mL blocking buffer (Odyssey) and 2.5 mL PBS containing 0.05% Tween 20 for 1 h, followed by overnight incubation with appropriate primary antibodies at 4 °C. After washing 3-4 times, the

membrane was incubated with appropriate IRDye-conjugated secondary antibodies for 1 h. Then after washing 3 times, and protein bands on the membrane were detected with the Odyssey 3.0 Infrared Imaging System (Li-Cor Biosciences).

Confocal fluorescence microscopy

RAW264.7 cells (3×10^4 cells/well) were seeding into μ -slide 8-well chamber (Cat. no. 80826; ibidi GmbH) and were rested at 37 °C overnight. The cells were either left uninfected or infected with MNV for 1 h at 37 °C, and the virus inoculum was removed and cells were washed two times with phosphate-buffered saline (PBS). Then fresh medium containing DMXAA or JAK inhibitor 1 were added back onto cells for 20 h. For co-localization of mouse RIG-I or MDA5_N with cGas or Sting, HEK293T cells (3×10^4 cells/well) were co-transfected with pMyc-cGAS, pMyc-STING or pFlag-RIG-I_WT, pFlag-RIG-I_N, pFlag-MDA5_N (1 μ g/each) into μ -slide 8-well chamber for 24 h. The cells were washed and fixed with 4% paraformaldehyde in PBS, permeablized with 0.2% Triton X-100, blocked with blocking buffer (Odyssey) for 1 h, reacted with the rabbit polyclonal antisera to MNV NS1/2 and NS7, or anti-Flag and anti-Myc antibodies, and stained with 4',6-diamidino-2-phenylindole (DAPI). Anti-rabbit IgG (H+L), F(ab')₂ Fragment (Alexa Fluor[®] 488 and 594 conjugate) and Anti-mouse IgG (H+L), F(ab')₂ Fragment (Alexa Fluor[®] 594 conjugate) antibodies were used as secondary antibodies. Imaging was performed on a Leica SP5 confocal microscopy using a 63x oil objective.

Co-immunoprecipitation

HEK293T cells (1×10^5 cells/well) were co-transfected with pMyc-cGAS, pMyc-STING or pFlag-RIG-I_WT, pFlag-RIG-I_N, pFlag-MDA5_N (1.5 μ g/each) in 12-well tissue culture plate for 48 h. Then the cells were washed twice with cold PBS and lysed with cold NP-40 lysis buffer at 4 °C for 30 minutes. Halt™ Protease Inhibitor Cocktail (Thermo Fisher Scientific) was used during lysis according to the manufacturer's instructions. The cells collected by scraping and lysates were cleared by centrifugation at 12,000 rpm for 10 minutes at 4 °C. 10% of the supernatants were taken as input control, and the remaining supernatants were incubated with mouse anti-Flag antibody at 4 °C for 2 h, and then incubated with protein A/G plus-agarose (sc-2003; Santa Cruz) overnight at 4 °C. The agaroses were centrifuged and washed three times, and the bound proteins were analyzed by western blotting.

Antiviral assay with MNV

RAW264.7 wild-type (WT), cGas- or Sting-deficient cells, and J774A.1 (3×10^4 cells/well) were uninfected or infected with MNV for 1 h at 37 °C, and washed two times with PBS, and then fresh medium or medium containing indicated compounds were added back onto cells for 20 h in 48-well tissue culture plate. The total RNA, supernatant or protein samples were collected

for further analysis. To determine the potential antiviral effects of mouse cGAS, STING or RIG-I_N, cells were transfected with pMyc-cGAS, pMyc-STING or pFlag-RIG-I_N with indicated concentrations for 24 h, then infected with MNV for 20 h. For transfection of HEK293T cells, the cells were co-transfected with pFlag-CD300lf, whereas no pFlag-CD300lf was transfected into mouse macrophages. To investigate the role of viral NS1/2, NS6 and NS7 on cGas and Sting mediated antiviral effects, HEK293T cells were co-transfected with pFlag-CD300lf, pMyc-cGAS, pMyc-STING or Flag-tagged vectors expressing indicated viral proteins for 24 h, then the cells were washed and infected with MNV for 20 h. The total RNA, supernatant or protein samples were collected for further analysis.

Measurement of luciferase activity

Luciferin potassium salt (Sigma-Aldrich, Zwijndrecht, the Netherlands) was added to cells at a final concentration of 0.1 mM for 30 min at 37 °C. The luciferase activity was measured with a LumiStar Optima luminescence counter (BMG Lab Tech, Offenburg, Germany).

MTT assay

RAW264.7 or J774A.1 cells were seeded into 96-well tissue culture plates and treated with compounds for indicated time periods. The cell viability was assessed by adding 10 mM 3-(4,5-dimethyl-2-thiazolyl)-2,5-diphenyl-2H-tetrazolium bromide (MTT) (Sigma, Zwijndrecht, the Netherlands). After 3 h, the medium was replaced with DMSO (100 µL), and was incubated at 37 °C for 30 mins. The absorbance at 490 nm was recorded on the microplate absorbance reader (Bio-Rad, CA, USA).

Statistical analysis

Data are presented as the mean \pm SD without specific statement. Statistical analysis was performed using GraphPad Prism 5.0 (GraphPad Software Inc., La Jolla, CA, USA). Comparisons between two groups were performed with Mann-Whitney test. Comparisons among multiple groups were performed with one-way ANOVA with Newman-Keuls test. Differences were considered significant at a P value less than 0.05.

References

1. Karst, S. M., Wobus, C. E., Goodfellow, I. G., et al. (2014) Advances in norovirus biology. *Cell Host Microbe* 15, 668-680
2. Wobus, C. E., Thackray, L. B., and Virgin, H. W. (2006) Murine norovirus: a model system to study norovirus biology and pathogenesis. *J Virol* 80, 5104-5112
3. McFadden, N., Bailey, D., Carrara, G., et al. (2011) Norovirus regulation of the innate immune response and apoptosis occurs via the product of the alternative open reading frame 4. *PLoS Pathog* 7, e1002413

4. Kato, H., Takeuchi, O., Sato, S., et al. (2006) Differential roles of MDA5 and RIG-I helicases in the recognition of RNA viruses. *Nature* 441, 101-105
5. Yoneyama, M., Kikuchi, M., Natsukawa, T., et al. (2004) The RNA helicase RIG-I has an essential function in double-stranded RNA-induced innate antiviral responses. *Nat Immunol* 5, 730-737
6. Seth, R. B., Sun, L., Ea, C. K., et al. (2005) Identification and characterization of MAVS, a mitochondrial antiviral signaling protein that activates NF-kappaB and IRF 3. *Cell* 122, 669-682
7. Brubaker, S. W., Bonham, K. S., Zanoni, I., et al. (2015) Innate immune pattern recognition: a cell biological perspective. *Ann Rev Immunol* 33, 257-290
8. Wu, J., and Chen, Z. J. (2014) Innate immune sensing and signaling of cytosolic nucleic acids. *Ann Rev Immunol* 32, 461-488
9. Yu, P., Li, Y., Li, Y., et al. (2020) Guanylate-binding protein 2 orchestrates innate immune responses against murine norovirus and is antagonized by the viral protein NS7. *J Biol Chem* 295, 8036-8047
10. Wu, J., Sun, L., Chen, X., et al. (2013) Cyclic GMP-AMP is an endogenous second messenger in innate immune signaling by cytosolic DNA. *Science* 339, 826-830
11. Zhong, B., Yang, Y., Li, S., et al. (2008) The adaptor protein MITA links virus-sensing receptors to IRF3 transcription factor activation. *Immunity* 29, 538-550
12. Ishikawa, H., Ma, Z., and Barber, G. N. (2009) STING regulates intracellular DNA-mediated, type I interferon-dependent innate immunity. *Nature* 461, 788-792
13. Schoggins, J. W., Wilson, S. J., Panis, M., et al. (2011) A diverse range of gene products are effectors of the type I interferon antiviral response. *Nature* 472, 481-485
14. Maloney, N. S., Thackray, L. B., Goel, G., et al. (2012) Essential cell-autonomous role for interferon (IFN) regulatory factor 1 in IFN- γ -mediated inhibition of norovirus replication in macrophages. *J Virol* 86, 12655-12664
15. Rodriguez, M. R., Monte, K., Thackray, L. B., et al. (2014) ISG15 functions as an interferon-mediated antiviral effector early in the murine norovirus life cycle. *J Virol* 88, 9277-9286
16. Ni, G., Ma, Z., and Damania, B. (2018) cGAS and STING: At the intersection of DNA and RNA virus-sensing networks. *PLoS Pathog* 14, e1007148
17. Aguirre, S., Luthra, P., Sanchez-Aparicio, M. T., et al. (2017) Dengue virus NS2B protein targets cGAS for degradation and prevents mitochondrial DNA sensing during infection. *Nat Microbiol* 2, 17037
18. Yi, G., Wen, Y., Shu, C., et al. (2016) Hepatitis C Virus NS4B Can Suppress STING Accumulation To Evade Innate Immune Responses. *J Virol* 90, 254-265
19. Franz, K. M., Neidermyer, W. J., Tan, Y. J., et al. (2018) STING-dependent translation inhibition restricts RNA virus replication. *Proc Nat Acad Sci U S A* 115, E2058-e2067
20. Schoggins, J. W., MacDuff, D. A., Imanaka, N., et al. (2014) Pan-viral specificity of IFN-induced genes reveals new roles for cGAS in innate immunity. *Nature* 505, 691-695
21. Holm, C. K., Rahbek, S. H., Gad, H. H., et al. (2016) Influenza A virus targets a cGAS-independent STING pathway that controls enveloped RNA viruses. *Nat Commun* 7, 10680
22. Cui, S., Yu, Q., Chu, L., et al. (2020) Nuclear cGAS Functions Non-canonically to Enhance Antiviral Immunity via Recruiting Methyltransferase Prmt5. *Cell Rep* 33, 108490
23. Liu, Y., Goulet, M. L., Sze, A., et al. (2016) RIG-I-Mediated STING Upregulation Restricts Herpes Simplex Virus 1 Infection. *J Virol* 90, 9406-9419
24. McCartney, S. A., Thackray, L. B., Gitlin, L., et al. (2008) MDA-5 recognition of a murine norovirus. *PLoS Pathog* 4, e1000108
25. Dang, W., Xu, L., Yin, Y., et al. (2018) IRF-1, RIG-I and MDA5 display potent antiviral activities against norovirus coordinately induced by different types of interferons. *Antiviral Res* 155, 48-59
26. Yu, P., Li, Y., Li, Y., et al. (2020) Murine norovirus replicase augments RIG-I-like receptors-mediated antiviral interferon response. *Antiviral Res* 182, 104877
27. Li, Y., Yu, P., Qu, C., et al. (2020) MDA5 against enteric viruses through induction of interferon-like response partially via the JAK-STAT cascade. *Antiviral Res* 176, 104743

28. Conlon, J., Burdette, D. L., Sharma, S., et al. (2013) Mouse, but not human STING, binds and signals in response to the vascular disrupting agent 5,6-dimethylxanthenone-4-acetic acid. *J Immunol* 190, 5216-5225
29. Haag, S. M., Gulen, M. F., Reymond, L., et al. (2018) Targeting STING with covalent small-molecule inhibitors. *Nature* 559, 269-273
30. Yu, P., Li, Y., Wang, Y., et al. (2020) Lipopolysaccharide restricts murine norovirus infection in macrophages mainly through NF- κ B and JAK-STAT signaling pathway. *Virology* 546, 109-121
31. Orchard, R. C., Wilen, C. B., Doench, J. G., et al. (2016) Discovery of a proteinaceous cellular receptor for a norovirus. *Science* 353, 933-936
32. Ishikawa, H., and Barber, G. N. (2008) STING is an endoplasmic reticulum adaptor that facilitates innate immune signalling. *Nature* 455, 674-678
33. Xu, L., Wang, W., Li, Y., et al. (2017) RIG-I is a key antiviral interferon-stimulated gene against hepatitis E virus regardless of interferon production. *Hepatology* 65, 1823-1839
34. Cai, H., Holleufer, A., Simonsen, B., et al. (2020) 2' 3'-cGAMP triggers a STING-and NF- κ B-dependent broad antiviral response in *Drosophila*. *Sci Signal* 13
35. Ablasser, A., Goldeck, M., Cavlar, T., et al. (2013) cGAS produces a 2'-5'-linked cyclic dinucleotide second messenger that activates STING. *Nature* 498, 380-384
36. Prantner, D., Perkins, D. J., Lai, W., et al. (2012) 5,6-Dimethylxanthenone-4-acetic acid (DMXAA) activates stimulator of interferon gene (STING)-dependent innate immune pathways and is regulated by mitochondrial membrane potential. *J Biol Chem* 287, 39776-39788
37. McKnight, K. L., Swanson, K. V., Austgen, K., et al. (2020) Stimulator of interferon genes (STING) is an essential proviral host factor for human rhinovirus species A and C. *Proc Nat Acad Sci U S A* 117, 27598-27607
38. Wobus, C. E., Karst, S. M., Thackray, L. B., et al. (2004) Replication of Norovirus in cell culture reveals a tropism for dendritic cells and macrophages. *PLoS Biol* 2, e432
39. Ward, V. K., McCormick, C. J., Clarke, I. N., et al. (2007) Recovery of infectious murine norovirus using pol II-driven expression of full-length cDNA. *Proc Nat Acad Sci U S A* 104, 11050-11055
40. Orchard, R. C., Sullender, M. E., Dunlap, B. F., et al. (2019) Identification of antinorovirus genes in human cells using genome-wide CRISPR activation screening. *J Virol* 93
41. Aguirre, S., Maestre, A. M., Pagni, S., et al. (2012) DENV inhibits type I IFN production in infected cells by cleaving human STING. *PLoS Pathog* 8, e1002934
42. Lee, S., Liu, H., Wilen, C. B., et al. (2019) A Secreted Viral Nonstructural Protein Determines Intestinal Norovirus Pathogenesis. *Cell Host Microbe* 25, 845-857.e845
43. Subba-Reddy, C. V., Goodfellow, I., and Kao, C. C. (2011) VPg-primed RNA synthesis of norovirus RNA-dependent RNA polymerases by using a novel cell-based assay. *J Virol* 85, 13027-13037
44. Zhu, S., Regev, D., Watanabe, M., et al. (2013) Identification of immune and viral correlates of norovirus protective immunity through comparative study of intra-cluster norovirus strains. *PLoS Pathog* 9, e1003592
45. Guix, S., Asanaka, M., Katayama, K., et al. (2007) Norwalk virus RNA is infectious in mammalian cells. *J Virol* 81, 12238-12248.
46. Qu, L., Murakami, K., Broughman, J., et al. (2016) Replication of Human Norovirus RNA in Mammalian Cells Reveals Lack of Interferon Response. *J Virol* 90, 8906-8923.
47. Baker, E. S., Luckner, S. R., Krause, K. L., et al. (2012) Inherent structural disorder and dimerisation of murine norovirus NS1-2 protein. *PLoS One* 7, e30534
48. Emmott, E., and de Rougemont, A. (2019) Polyprotein processing and intermolecular interactions within the viral replication complex spatially and temporally control norovirus protease activity. *J Biol Chem* 294, 4259-4271
49. Storek, K. M., Gertszov, N. A., Ohlson, M. B., et al. (2015) cGAS and Ifi204 cooperate to produce type I IFNs in response to *Francisella* infection. *J Immunol* 194, 3236-3245
50. Pan, Q., de Ruiter, P. E., Metselaar, H. J., et al. (2012) Mycophenolic acid augments interferon-stimulated gene expression and inhibits hepatitis C Virus infection in vitro and in vivo. *Hepatology* 55, 1673-1683

Supplementary information

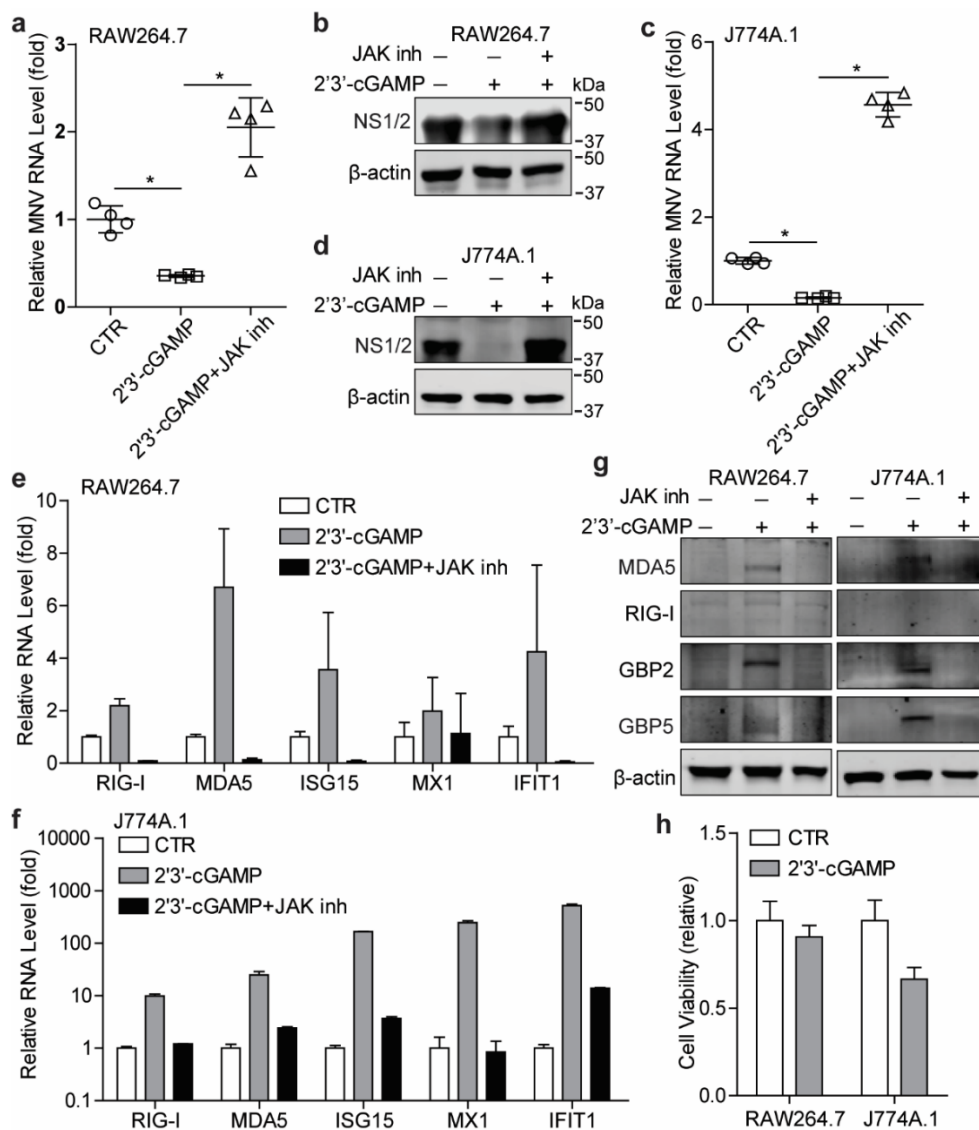


Fig. S1 2'3'-cGAMP restricts MNV replication. RAW264.7 cells were infected with MNV-1 for 1 h, then untreated or treated with 2'3'-cGAMP (2 μ g/ml) or JAK inhibitor 1 (5 μ g/ml) for 20 h. The viral RNA (a) and NS1/2 protein (b) expression levels were analyzed by qRT-PCR (n = 4) and western blotting, respectively. J774A.1 cells were infected with MNV-1 for 1 h, then untreated or treated with 2'3'-cGAMP (2 μ g/ml) or JAK inhibitor 1 (5 μ g/ml) for 20 h. The viral RNA (c) and NS1/2 protein (d) expression levels were analyzed by qRT-PCR (n = 4) and western blotting, respectively. qRT-PCR analysis of mRNA levels of RIG-I, MDA5, ISG15, MX1 and IFIT1 in RAW264.7 (e, n = 3-4) and J774A.1 (f, n = 2) cells untreated or treated with 2'3'-cGAMP (2 μ g/ml) or JAK inhibitor 1 (5 μ g/ml) for 20 h. (g) RAW264.7 or J774A.1 cells were untreated or treated with 2'3'-cGAMP (2 μ g/ml) or JAK inhibitor 1 (5 μ g/ml) for 20 h. Expression of MDA5, RIG-I, GBP2 and GBP5 proteins were analyzed by western blotting. (h) RAW264.7 or J774A.1 cells were untreated or treated with 2'3'-cGAMP (2 μ g/ml) for 20 h. The cytotoxicity was determined by MTT assay (n = 16). Data were normalized to untreated control (set as 1). *P < 0.05. β -actin was used as a loading control.

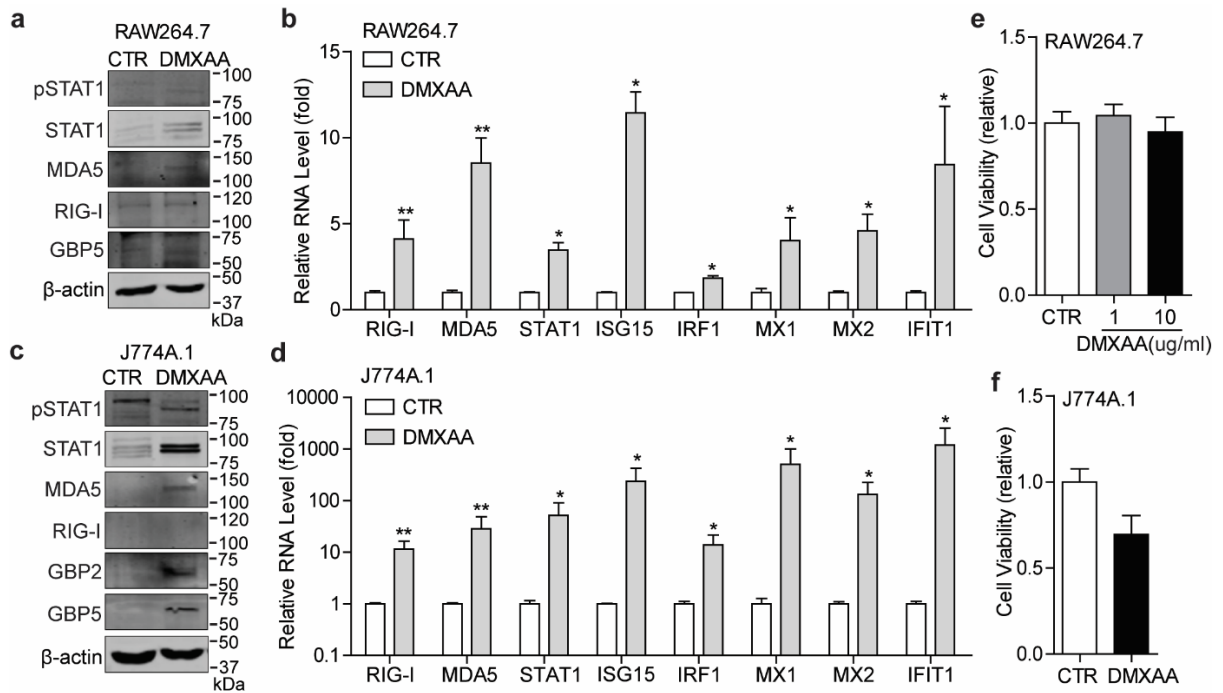


Fig. S2 DMXAA treatment induces ISG transcription. RAW264.7 cells were untreated or treated with DMXAA (10 μ g/ml) for 20 h. (a) STAT1 expression and phosphorylation, MDA5, RIG-I and GBP5 expression, and (b) mRNA levels of indicated ISGs were analyzed by western blotting and qRT-PCR (n = 4-5), respectively. J774A.1 cells were untreated or treated with DMXAA (10 μ g/ml) for 20 h. (c) STAT1 expression and phosphorylation, MDA5, RIG-I, GBP2 and GBP5 expression, and (d) mRNA levels of indicated ISGs were analyzed by western blotting and qRT-PCR (n = 4-5), respectively. (e) RAW264.7 cells were untreated or treated with DMXAA (1 or 10 μ g/ml) for 20 h. The cytotoxicity was determined by MTT assay (n = 16). (f) J774A.1 cells were untreated or treated with DMXAA (10 μ g/ml) for 20 h. The cytotoxicity was determined by MTT assay (n = 16). Data were normalized to the untreated control (set as 1). *P < 0.05; **P < 0.01. β -actin was used as a loading control.

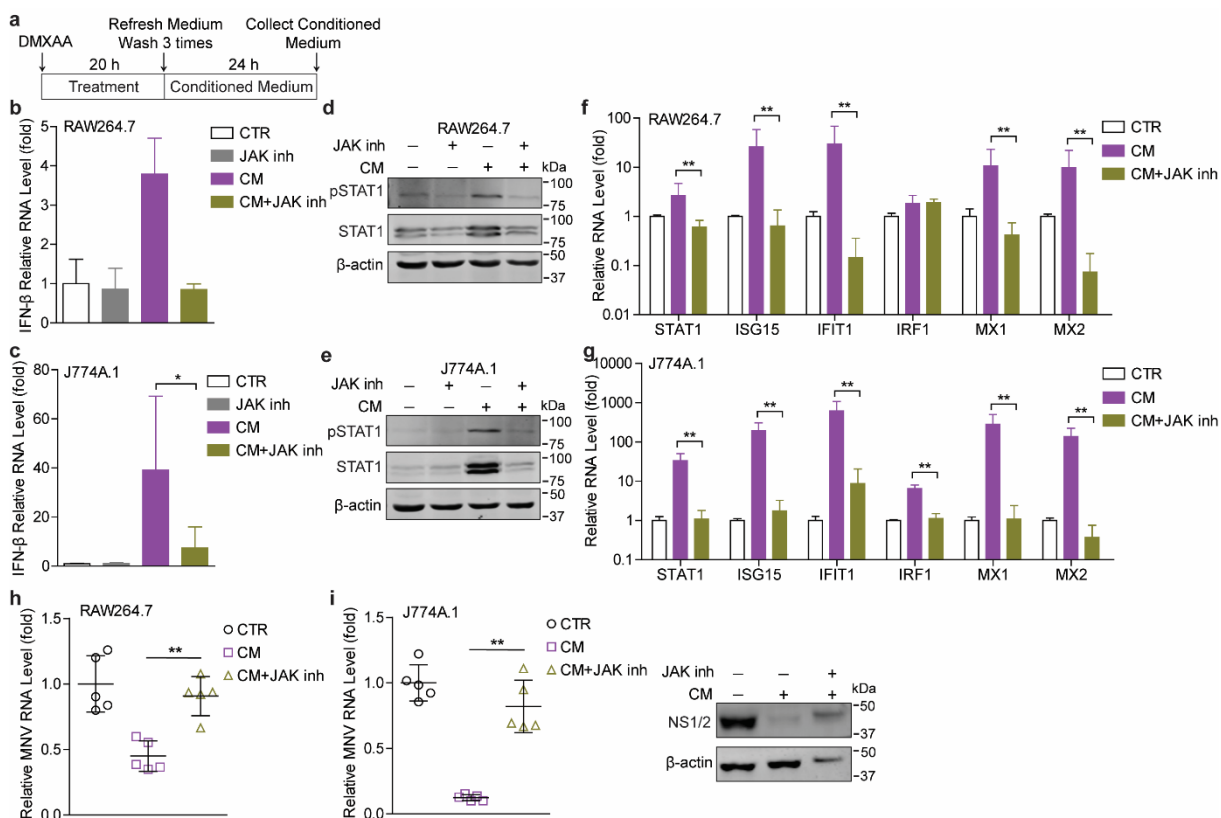


Fig. S3 The conditioned medium (CM) from DMXAA-treated cells exerts anti-MNV activity. (a) Production of conditioned medium (supernatant). RAW264.7 or J774A.1 cells were treated with DMXAA (10 $\mu\text{g}/\text{ml}$) for 20 h, then were washed 3 times and medium was refreshed. Cells were further cultured for 24 h and supernatant was collected as conditioned medium. RAW264.7 and J774A.1 cells were untreated or treated with JAK inhibitor 1 (5 $\mu\text{g}/\text{ml}$) or conditioned medium (CM) from DMXAA-treated RAW264.7 or J774A.1 cells for 20 h, respectively. The IFN- β mRNA level in (b) RAW264.7 ($n = 2$) and (c) J774A.1 ($n = 5$) cells, and mRNA levels of several ISGs in (f) RAW264.7 ($n = 5$) and (g) J774A.1 ($n = 5$) cells were analyzed by qRT-PCR, respectively. Western blotting analysis of STAT1 expression and phosphorylation in (d) RAW264.7 and (e) J774A.1 cells untreated or treated with JAK inhibitor 1 (5 $\mu\text{g}/\text{ml}$) or CM from DMXAA-treated RAW264.7 or J774A.1 cells for 20 h. (h) RAW264.7 cells were infected with MNV-1 for 1 h, then untreated or treated with CM from DMXAA-treated RAW264.7 cells or combinations with JAK inhibitor 1 (5 $\mu\text{g}/\text{ml}$) for 20 h. The viral RNA level was analyzed by qRT-PCR ($n = 5$). (i) J774A.1 cells were infected with MNV-1 for 1 h, then untreated or treated with CM from DMXAA-treated J774A.1 cells or combinations with JAK inhibitor 1 (5 $\mu\text{g}/\text{ml}$) for 20 h. The viral RNA and NS1/2 protein expression levels were analyzed by qRT-PCR ($n = 5$) and western blotting, respectively. Data were normalized to the untreated control (set as 1). * $P < 0.05$; ** $P < 0.01$. β -actin was used as a loading control.

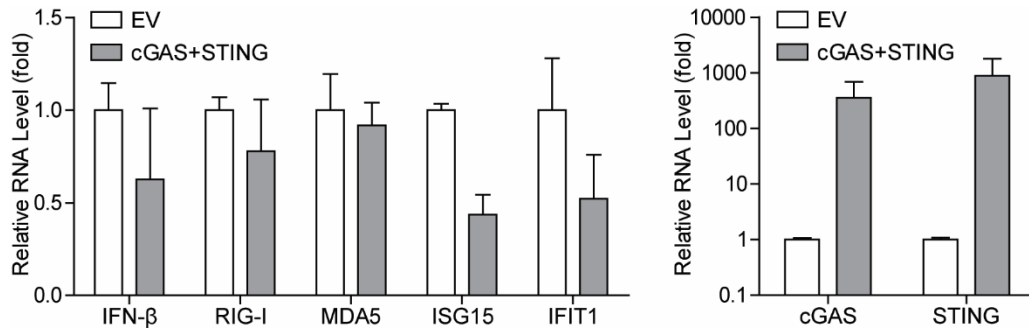


Fig. S4 RAW264.7 cells were transfected with pMyc-cGAS and pMyc-STING (1 μ g/well) or empty vectors for 48 h. The mRNA levels of indicated genes were analyzed by qRT-PCR (n = 4). Data were normalized to the EV control (set as 1).

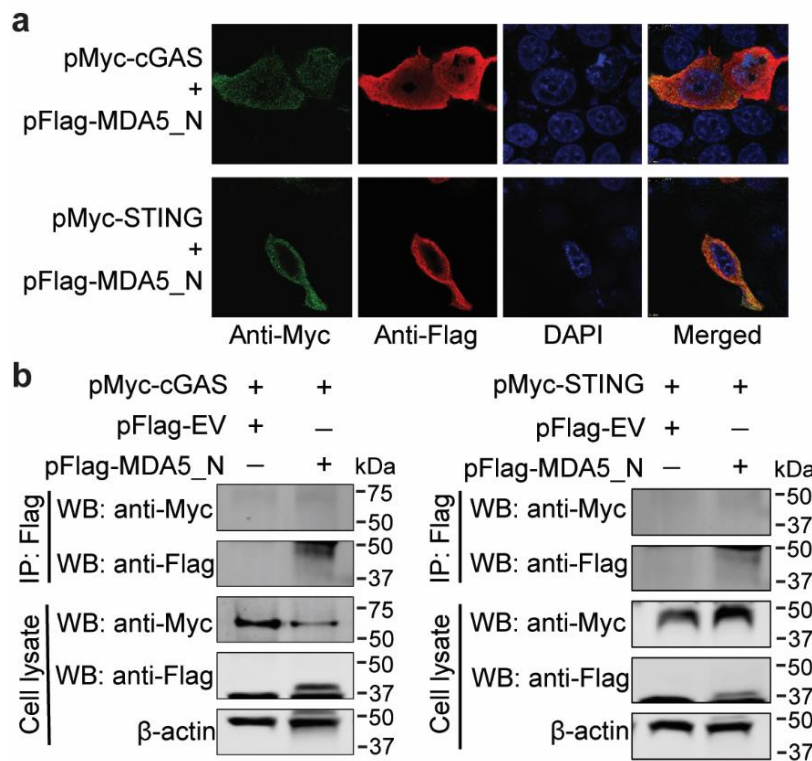


Fig. S5 (a) HEK293T cells were transfected with pFlag-MDA5_N and pMyc-cGAS or pMyc-STING (1 μ g/each) for 24 h. Expression and co-localization of MDA5_N with cGAS or STING were analyzed by confocal assay. (b) HEK293T cells were transfected with pMyc-cGAS or pMyc-STING and pFlag-MDA5_N or empty vectors (1.5 μ g/each) for 48 h. Co-IP assay was performed using anti-Flag MAb (1:1000). The precipitated proteins were analyzed by western blotting using anti-Flag and anti-Myc antibodies. β -actin was used as a loading control.

Table S1. The primers used for plasmid construction.

Primer	Sequence (5' to 3')	Usage for amplification
pMyc-cGAS-F	CCGCTCGAGATGGAAGATCCGCGTAGA	mouse cGAS
pMyc-cGAS-R	GGGGTACCAAGCTTGTCAAAAATTGG	
pMyc-STING-F	CTAGCTAGCATGCCATACTCCAACCTGC	mouse STING
pMyc-STING-R	CCAAGCTTGATGAGGTCAAGTGC GGAGTG	
pFlag-NS1/2-F	CCGCTCGAGAGGATGGCAACGCCATCTTCTG	MNV NS1/2
pFlag-NS1/2-R	CGGGGTACCTTATTCGGCCTGCCATCCCCGA	
pFlag-NS6-F	CCGCTCGAGGCCCCAGTCTCCATCTGGTCCC	MNV NS6
pFlag-NS6-R	CGGGGTACCTTACTGGA ACTCCAGAGCCTCAAG	
pFlag-RIG-I_WT-F	TGCTCTAGAACAGCGGAGCAGCGGCAGAATCTG	full-length mouse RIG-I
pFlag-RIG-I_WT-R	CGGGGTACCTCATA CGGACATTTCTGCAGGATC	
pFlag-RIG-I_N-F	TGCTCTAGAACAGCGGAGCAGCGGCAGAATCTG	mouse RIG-I_N
pFlag-RIG-I_N-R	CGGGGTACCTCAAGAAGACGCTTCTGAAGG	
pFlag-MDA5_N-F	CCGCTCGAGTCGATTGTCTGTTCTGCAG	mouse MDA5_N
pFlag-MDA5_N-R	CGGGGTACCCTAACTTTCATCTGAATCAC	

Table S2. The primers used for qRT-PCR.

Primer	F-Sequence (5' to 3')	R-Sequence (5' to 3')
mGAPDH	TTCCAGTATGACTCCACTCACGG	TGAAGACACCAGTAGACTCCACGAC
mSTAT1	GCCTCTCATTGTCACCGAAGAAC	TGGCTGACGTTGGAGATCACCA
mIRF1	CAGAGGAAAGAGAGAAAGTCC	CACACGGTGACAGTGCTGG
mISG15	TGACGCAGACTGTAGACACG	TGGGGCTTTAGGCCATACTC
mMX1	GGGGAGGAAATAGAGAAAATGAT	GTTTACAAAGGGCTTGCTTGCT
mMX2	CCAGTTCCTCTCAGTCCCAAGATT	TACTGGATGATCAAGGGAACGTGG
mIFIT1	CCATAGCGGAGGTGAATATC	GGCAGGACAATGTGCAAGAA
mIFN- β	AAGAGTTACTACTGCCTTTGCCATC	CACTGTCTGCTGGTGGAGTTCATC
mcGAS	GGCAGCTACTATGAACATGTG	CTCAGCGGATTTCTCGTGAA
mSTING	TATACCTCAGTTGGATGTTTGGC	CTGGAGTCAAGCTCTGAAGGC
hGAPDH	TGTCCCCACCCCAATGTATC	CTCCGATGCCTGCTTCACTACCTT
hIFN- β	CTTGGATTCTACAAAGAAGCAGC	TCCTCCTTCTGGA ACTGCTGCA
hISG15	CTCTGAGCATCCTGGTGAGGAA	AAGGTCAGCCAGAACAGGTCGT
hIFIT1	GCCTTGCTGAAGTGTGGAGGAA	ATCCAGGCGATAGGCAGAGATC
hIFIT3	CCTGGAATGCTTACGGCAAGCT	GAGCATCTGAGAGTCTGCCCAA
MNV-1	CACGCCACCGATCTGTTCTG	GCGCTGCGCCATCACTC

Chapter 8

Summary and Discussion

Norovirus is the most common global etiology of diarrheal illness, causing both sporadic and epidemic infection and imposing a substantial health and economic burden (1). Genetically, this virus is genetically highly diverse, posing a challenge for vaccine development efforts (2). Moreover, the lack of a robust system for cultivating human norovirus (HuNV) largely impedes our understanding of norovirus biology and pathogenesis, as well as the associated immune response. As a surrogate model, murine norovirus (MNV) is capable of replicating in vitro and in vivo, and shares similar characteristics with HuNV in structural and genetic features, and has thus been widely used for norovirus research, as well as in this thesis. Currently, no licensed norovirus vaccines are available, thus novel antiviral treatment is urgently needed to combat norovirus infection.

Potential inhibitors of noroviruses have been identified and some of these have been demonstrated efficacy in experimental models, including ribavirin, mycophenolic acid (MPA) and favipiravir (3-5). A nucleoside analogue named 2'-Fluoro-2'-deoxycytidine (2'-FdC) has been recently reported to exert broad antiviral activities against Lassa virus, Crimean-Congo hemorrhagic fever virus and bunyaviruses (6,7). Thus in **Chapter 2**, I profiled its antiviral effects on norovirus, and showed that 2'-FdC potently inhibits replication of different strains of MNV in macrophages, and exerts moderate inhibition on HuNV replication. Since 2'-FdC is an analogue of cytidine and fluorine is isosteric with a hydroxyl group, the antiviral effects can be partially reversed by CTP but not GTP. Moreover, 2'-FdC acts synergistically with the well-known antivirals including MPA, ribavirin or favipiravir. Although 2'-FdC can serve as a potential backbone for anti-norovirus drug design, the potential side effects as well as combination with other compounds, should be carefully evaluated in future studies.

The inflammasome machinery has recently been recognized as an emerging pillar of innate immunity, and plays an important role in controlling viral infections, examples being infections by rotavirus or influenza virus (8,9). Studies have reported that MNV infection can induce secretion of mature IL-1 β by activating NLRP3 inflammasome in primary bone marrow-derived macrophages (BMDMs) with TLR2 priming, and in STAT1 deficient BMDMs (10). In **Chapter 3**, I revealed that MNV infection induces IL-1 β transcription but not release of mature IL-1 β in mouse macrophages. Then I profiled the antiviral action of LPS, a potent activator of inflammasome action in pathophysiology. My results demonstrated that inflammasome inhibitors slightly counteract LPS-mediated antiviral effects and especially those that at least partially requires the induction of interferon-stimulated genes (ISGs) and that LPS effects in this are mainly mediated through the NF- κ B and JAK-STAT signaling pathways. I feel these results hold promise for understanding the potential crosstalk between IFN response and inflammasome activation in response to norovirus, although the exact mechanisms involved need to be further studied in order to make definitive statements in this respect.

IFN-mediated innate immune responses provide the first line of host defense against viral infections, and a subset of ISGs are considered to be the ultimate antiviral effectors limiting viral replication and spread (11). Currently, only a few ISGs have been identified that inhibit MNV infection, but those identified include interferon regulatory factor 1 (IRF1), interferon-stimulated gene 15 (ISG15) and guanylate-binding proteins (GBPs) (12-14). In **Chapter 4**, I profiled the anti-MNV effects of GBP2 and I observe it requires the presence of IFN- γ in murine macrophages but can act without IFN- γ in HEK293T cells that ectopically expressing MNV receptor (CD300lf). Possible explanations here are the differences in species, cell type and the expression pattern of GBP2. I modeled the different domains of mouse GBP2 including the G, M and E domains, and my experiments revealed that the N-terminal G domain of GBP2 is necessary for this antiviral action. Viruses have developed sophisticated strategies to evade host defense, and accordingly I also established that viral replicase (NS7) antagonizes GBP2-mediated antiviral effects. Potential interaction of NS7 with GBP2, and a possible inhibitory role of NS7 on GTPase activity of GBP2 are interesting to be studied further, for instance by my potential successor with respect to this research. Similarly, as innate immune sensors and antiviral ISGs, both RIG-I and MDA5 have been reported to restrict infection of some RNA viruses. In **Chapter 5 and 6**, I profiled the antiviral actions of RIG-I and MDA5 against norovirus (HuNV and MNV). Overexpression of RIG-I and MDA5 induces some antiviral ISG induction through an interferon-like response, whereas blocking the JAK-STAT cascade partially attenuates ISG induction and their associated antiviral functions. Regulation of viral replicases on RLRs-mediated IFN response have been documented (15,16). I further investigated the regulation of MNV NS7 on RIG-I and MDA5-mediated antiviral immune response in **Chapter 6**. I showed that viral NS7 enhances RIG-I and MDA5-triggered antiviral IFN response, which conceivably involves interactions with the CARDs of RIG-I and MDA5. Moreover, the antiviral effects mediated by RIG-I and MDA5 are further enhanced by NS7 overexpression in HEK293T cells that ectopically expressing CD300lf. These findings shed new light on norovirus-host interactions and shall be helpful for developing new antiviral strategies.

Besides the well-established role in innate responses to DNA viruses, emerging evidence indicates that cGAS-STING signaling is also involved in restricting RNA virus replication. For instance, cells or mice that are deficient in cGAS or STING facilitate replication of several RNA viruses, such as vesicular stomatitis virus (VSV) and West Nile virus (WNV) (17,18). In **Chapter 7**, I explored the role of cGAS-STING in response to MNV infection. MNV replication is restricted in the presence of STING agonists, but increased in the presence of STING inhibitor in mouse macrophages, which partially involves the ISG response. Meanwhile, I established that silencing mouse cGAS or STING leads to defects in antiviral ISGs induction upon MNV infection, and enhances viral replication in mouse macrophages. Overexpression of cGAS and STING moderately increases ISG transcription but potently inhibits MNV replication in

HEK293T cells that ectopically expressing CD300lf, whereas JAK inhibitor treatment or expression of different MNV viral proteins doses not affect this antiviral effect. I further learned that the N-terminus of RIG-I exerts anti-MNV activity, but that this effect is attenuated by STING, I attributed this effect to the interaction between RIG-I and STING. However, the possibility of participation of MAVS in the signaling or interaction should also be considered. Indeed, human MAVS associates with human STING, although it is not clear whether MAVS directly interacts with STING, or exists as a complex with RIG-I/STING (19). Whether human cGAS and STING are also necessary in restricting human norovirus replication is still unknown, and future studies are needed to investigate their potential association. Thus, in conjunction I hope my studies improve our understanding of norovirus-host interactions, and provide insight to develop new antiviral strategies for combating norovirus infection.

References

1. Atmar, R. L., and Ramani, S. (2021) Birth Cohort Studies: Toward Understanding Protective Immunity to Human Noroviruses. Oxford University Press US
2. Chhabra, P., de Graaf, M., Parra, G. I., et al. (2019) Updated classification of norovirus genogroups and genotypes. *J Gen Virol* 100, 1393
3. Dang, W., Xu, L., Ma, B., et al. (2018) Nitazoxanide inhibits human norovirus replication and synergizes with ribavirin by activation of cellular antiviral response. *Antimicrob Agents Chemother* 62
4. Dang, W., Yin, Y., Wang, Y., et al. (2017) Inhibition of calcineurin or IMP dehydrogenase exerts moderate to potent antiviral activity against norovirus replication. *Antimicrob Agents Chemother* 61
5. Ruis, C., Brown, L.-A. K., Roy, S., et al. (2018) Mutagenesis in norovirus in response to favipiravir treatment. *New Engl J Med* 379, 2173-2176
6. Smee, D. F., Jung, K.H., Westover, J., et al. (2018) 2'-Fluoro-2'-deoxycytidine is a broad-spectrum inhibitor of bunyaviruses in vitro and in phleboviral disease mouse models. *Antiviral Res* 160, 48-54
7. Welch, S. R., Scholte, F. E., Flint, M., et al. (2017) Identification of 2'-deoxy-2'-fluorocytidine as a potent inhibitor of Crimean-Congo hemorrhagic fever virus replication using a recombinant fluorescent reporter virus. *Antiviral Res* 147, 91-99
8. Zhu, S., Ding, S., Wang, P., et al. (2017) Nlrp9b inflammasome restricts rotavirus infection in intestinal epithelial cells. *Nature* 546, 667-670
9. Ichinohe, T., Lee, H. K., Ogura, Y., et al. (2009) Inflammasome recognition of influenza virus is essential for adaptive immune responses. *J Exp Med* 206, 79-87
10. Dubois, H., Sorgeloos, F., Sarvestani, S. T., et al. (2019) Nlrp3 inflammasome activation and Gasdermin D-driven pyroptosis are immunopathogenic upon gastrointestinal norovirus infection. *PLoS Pathog* 15, e1007709
11. Schoggins, J. W., Wilson, S. J., Panis, M., et al. (2011) A diverse range of gene products are effectors of the type I interferon antiviral response. *Nature* 472, 481-485
12. Maloney, N. S., Thackray, L. B., Goel, G., et al. (2012) Essential cell-autonomous role for interferon (IFN) regulatory factor 1 in IFN- γ -mediated inhibition of norovirus replication in macrophages. *J Virol* 86, 12655-12664
13. Rodriguez, M. R., Monte, K., Thackray, L. B., et al. (2014) ISG15 functions as an interferon-mediated antiviral effector early in the murine norovirus life cycle. *J Virol* 88, 9277-9286
14. Biering, S. B., Choi, J., Halstrom, R. A., et al. (2017) Viral replication complexes are targeted by LC3-guided interferon-inducible GTPases. *Cell Host Microbe* 22, 74-85. e77
15. Miller, C. M., Barrett, B. S., Chen, J., et al. (2020) Systemic expression of a viral RdRP protects against retrovirus infection and disease. *J Virol* 94
16. Kuo, R.L., Chen, C.J., Wang, R. Y., et al. (2019) Role of enteroviral RNA-dependent RNA polymerase in regulation of MDA5-mediated beta interferon activation. *J Virol* 93
17. Schoggins, J. W., MacDuff, D. A., Imanaka, N., et al. (2014) Pan-viral specificity of IFN-induced genes reveals new roles for cGAS in innate immunity. *Nature* 505, 691-695
18. Franz, K. M., Neidermyer, W. J., Tan, Y.J., et al. (2018) STING-dependent translation inhibition restricts RNA virus replication. *Proc Nat Acad Sci U S A* 115, E2058-E2067
19. Ishikawa, H., and Barber, G. N. (2008) STING is an endoplasmic reticulum adaptor that facilitates innate immune signalling. *Nature* 455, 674-678

Chapter 9

Nederlandse Samenvatting

Dutch Summary

Eén van de belangrijkste oorzaken van diarree is het norovirus. Dit virus kan binden aan receptoren die aanwezig zijn op darmcellen en zal dan vervolgens door de darmcel worden opgenomen. Nadat het virus aangekomen in celvloeistof van de darmcel pakt het virus haar genetisch materiaal uit. Dit bestaat enkelstrengs RNA wat onmiddellijk kan worden afgeschreven door de cellulaire machinerie van de darmcel tot virale eiwitten, die op hun beurt het genetisch materiaal van het virus kunnen vermenigvuldigen en het inpakken in virale eiwitten om daar weer nieuwe virussen van te maken. De gastheercel, die het virus dus gebruikt om nieuwe virale eiwitten en viraal genetisch materiaal te maken, overleeft dit parasitisme vaak niet. De stervende cellen leiden tot het ontstaan van gaten in darmbekleding en samen met het immuunantwoord van het lichaam tegen het norovirus, leidt dit dan weer tot ziekte. Ongeveer de helft van alle acute episoden van gastro-enteritis (buikgriep) wereldwijd wordt door norovirusinfectie veroorzaakt, vooral omdat het virus zeer besmettelijk is. Het virus verspreidt zich via voedsel en water dat besmet is met ontlasting, maar ook via aerosolen die verschillende oppervlakten besmettelijk kunnen maken. Vooral de deurkruk of het lichtknopje van het toilet zijn berucht in dit opzicht. Anders dan bijvoorbeeld rotavirus, wat vooral kinderen treft, zijn mensen van alle leeftijden gevoelig voor norovirus. Ook door gebrek aan inzicht in hoe onze cellen zich tegen norovirus infectie verzetten en wapenen, is er nog geen goede norovirus medicatie ontwikkeld. Met dit proefschrift probeer ik het nodige inzicht te verschaffen. **Hoofdstuk 1** geeft een uitgebreide adstructie bij de visie die ik hierbij gevolgd heb.

Een eerste stap hierbij was het ontwikkelen van een kapstok waarlangs verdere antivirale therapie tegen het norovirus mee ontwikkeld kan worden. Een aanzet hiertoe geef ik in **Hoofdstuk 2**. In dit hoofdstuk laat ik zien dat de gemodificeerde nucleoside 2'-Fluoro-2'-deoxycytidine, een verbinding die een veelheid van virussen in haar replicatie kan remmen, effectief in ieder geval het muizenorovirus kan remmen. Deze bevinding heb ik verspreid in de wetenschappelijke wereld middels een publicatie in het vaktijdschrift "Archives of Virology" (2020, 165(11): 2605-2613). Op basis van deze vinding kan dan verdere medicatie en behandeling ontworpen voor de menselijke varianten van dit virus. Ik realiseerde me echter wel dat dit meer inzicht zou vergen in hoe de menselijke cel zich in het algemeen verdedigt tegen het norovirus en in de rest van dit proefschrift zou ik dit verder ontrafelen.

In eerste instantie heb ik daarbij onderzocht in welke mate de verdediging van de gastheercel zich conformeerde aan de gedachten die er in veld van biomedische wetenschappers heersten over deze weerstand, maar nooit formeel waren bevestigd. In **Hoofdstuk 3**, waarvan ik de tekst ook publiek heb gemaakt middels een artikel in het vaktijdschrift "Virology" (2020, 546: 109-121), onderzoek de rol van interferonen (belangrijke antivirale hormoonachtige stoffen gemaakt door het lichaam om virusinfectie te bestrijden) en hun relatie met de activatie van het zogenaamde inflammasoom (een intracellulaire structuur die verdediging en vernietiging

van virussen coördineert in de gastheercel). Anders dan de gedachten in het veld leken interferonen nauwelijks betrokken het activeren van het inflammasoom na norovirusinfectie, maar leken mechanismen die we normaal meer associëren met de verdediging tegen bacteriële infectie belangrijk bij inflammasoomactivatie. Op haar beurt leidt inflammasoomactivatie wel weer tot interferonproductie. Dit gaf al een belangrijke aanwijzing dat de verdediging van de gastheercel tegen norovirus unieke aspecten vertoonde en dus meer studie zou vergen.

Hierdoor aangemoedigd ging ik verder op zoek naar eiwitten die belangrijk zijn bij het bestrijden van het norovirus door de gastheer. Een eerste succes hierbij was de identificatie van GBP2 als een belangrijke effector hierbij. Dit eiwit wordt actief nadat de cel wordt geïnfecteerd door norovirus en nog veel meer na de door het norovirus opgeroepen interferon productie. Het kunstmatig laten maken van GBP2 door de darmepitheel blijkt voldoende om de darmepitheel te beschermen tegen infectie met het norovirus. Het belang van GBP2 bij de verdediging tegen norovirus wordt verder geïllustreerd door mijn observatie dat het norovirus zelf op haar beurt het GBP2 eiwit probeert te remmen, een waar gevecht dus. Ik beschrijf deze bevindingen in **Hoofdstuk 4** en ik heb ze gedeeld met de wetenschappelijke wereld middels publicatie in het vaktijdschrift “Journal of Biological Chemistry” (2020, 295: 8036-8047).

In **Hoofdstuk 5**, wat ik ook gepubliceerd heb in het vaktijdschrift “Antiviral Research” (2020, 176: 104743) verkreeg ik verder inzicht in hoe het interferon-onafhankelijke initiële tegen norovirus opgestart zou kunnen worden. Hierin laat ik namelijk zien dat het zogenaamde MDA5 (een intracellulaire receptor die vaak effectief virussen kan herkennen en dus de cellulaire verdediging kan activeren) ook bij het norovirus een dergelijke functie kan hebben, maar dat de receptor dit kan doen zonder dat met een interferon-opgeroepen processen daar een allesbepalende rol in hebben. Ook voor andere verwante moleculen, zoals ik beschrijf in **Hoofdstuk 6** en heb gepubliceerd in een tweede publicatie in het vaktijdschrift “Antiviral Research” (2020, 182: 104877), blijkt een analoge situatie te spelen. Hiermee kon ik dus de gastheerverdediging tegen infectie met het norovirus weer een stukje beter in kaart brengen en begrijpen.

In **Hoofdstuk 7** weet ik het overzicht met betrekking tot de interactie norovirus, intracellulaire intravirale receptoren en de activatie van het inflammasoom grotendeels te complementeren. Hier vestig ik mijn aandacht op de antivirale eiwitten cGAS/STING. Van deze eiwitten was al bekend dat ze betrokken zijn bij de verdediging van onze cellen tegen DNA virussen, maar of ze ook betrokken zijn bij de afweer tegen RNA virussen, zoals norovirussen, was nog niet onderzocht. Wij zagen dat het kunstmatig activeren of inbrengen van deze eiwitcassette

cellen resistent maakte tegen norovirusinfectie. Opnieuw leek het belang van de interferensignalering weer beperkt.

In **Hoofdstuk 8** vat ik al mijn bevindingen samen en probeer de samenhang tussen deze bevindingen, ook in het licht van het corpus van beschikbare biomedische literatuur, te duiden. Ik concludeer dat ik een onverwacht moleculair netwerk, wat waar maar gedeeltelijk afhankelijk is van de vroeger zo cruciaal geachte interferon signaal transductie, heb blootgelegd dat onze natuurlijke weerstand tegen het norovirus in stand houdt. Farmacologische activatie van dit netwerk, eventueel samen met breedspectrum antivirale middelen zou heel wel een betere therapeutische optie kunnen zijn dan de huidige praktijk van alleen ondersteunende therapie, vooral bij ernstig zieke patiënten. Ik schets mogelijkheden hoe dit verder zou kunnen worden uitgewerkt. Ik spreek aan het eind van dit proefschrift dan ook de hoop uit dat dit werk zal bijdragen aan reduceren van de last die het norovirus de menselijke soort bezorgt.

Appendix

Acknowledgements

Publications

PhD Portfolio

Curriculum Vitae

Acknowledgements

Four years ago, I started my PhD studies in the delightful city-Rotterdam. My heart overflows with gratitude and thanksgiving as I reflect on this incredible experience. I hereby would like to express my heartfelt gratitude to all of you, my families, my promotor, co-promoter, colleagues, friends, and the China Scholarship Council (CSC). This work would not be feasible without all your support and help.

First and foremost, I want to express my gratitude to Dr. Qiuwei (Abdullah) Pan, my co-promotor and daily supervisor. Thank you so much for your enormous encouragement and support throughout my PhD studies. You are a brilliant and hard-working scientist with a good sense of smell on the research field. I admire the way how you train us to conduct research and to think scientifically. You have allowed me enough of time and space to proceed my studies, and you have always been helpful for guiding me through the challenges I have faced. I have learned a lot from you during the last four years of my studies. Thank you very much for supervising me.

To my promotor Prof. dr. Maikel P. Peppelenbosch, thank you so much for offering me the opportunity to join the MDL large group. Thank you for your advice and guidance on my research. I really enjoy the group discussions that you attended, since you always come up with new and creative ideas, and contribute to the resolution of our experimental difficulties. I am so impressed by your innovative and creative ideas for our different research projects. Thank you for your insightful remarks on my manuscript as well as this thesis. Thank you once again for your support throughout my PhD studies.

To Dr. Ron Smits, thank you for providing me some cells for my research and experimental tips while working in the lab. You are full of knowledge and kindness, and always willing to give a hand when we meet experimental difficulties. To Dr. Gwenny Fuhler, thanks for the outstanding questions and thoughts you raised in our seminars, and these have aided me a lot in improving my understanding towards different topics.

To Dr. Ruchi Bansal, thank you very much for your assistance in revising our manuscript and providing critical feedback. You are full of kindness, and tell me the detailed routes to reach your lab to obtain the experimental materials.

To Prof. dr. Herbert W. Virgin, Prof. dr. Vernon K. Ward, Prof. dr. Ian Goodfellow, Prof. dr. Denise M. Monack, Prof. dr. Andrea Kröger, Dr. Sanna M. Mäkelä, Dr. Kyeong-Ok Chang, Dr. Shuaiyang Zhao and Dr. Rui-Lin Kuo, thank you all very much for providing us important experimental materials that are very helpful for my research projects. I also would like to

thank the Erasmus Biomics Center for providing me with useful shRNA clones for my research. Thank you all very much.

To Dr. Wen Dang, Dr. Changbo Qu, Dr. Buyun Ma, Dr. Sunrui Chen, Dr. Jiaye Liu, Dr. Wenshi Wang, Dr. Wanlu Cao, Dr. Guoying Zhou, Dr. Meng Li, Dr. Shan Li, Dr. Pengyu Liu, Dr. Xumin Ou and Dr. Qin Yang, my respectful elder fellows, thank you for sharing your various experimental skills with me. I am delighted to have met you in Rotterdam, and I wish you all and your family healthy and happy.

To Yang, Zhijiang, Yunlong and Ling, we arrived in Rotterdam and started our PhD study in the same year. Yang, I am so glad to meet you in Lanzhou. We worked together for the past four years, and you gave me much help and support for my projects and I have learned a lot from you. You are intelligent and hard-working, I hope you can achieve great success in the future. Zhijiang, we meet each other in Beijing before traveling to the Netherlands. You are really kind and hard-working person, thank you for your assistance with my experiments and for treating me so well, I am really enjoy the time we had together. Hoping you a bright future. Yunlong, I am happy to meet you in the Netherlands and we shared a spacious office desk. You are very nice and helpful for my research. Hope you achieve big success in your research career. Ling, we came to the Netherlands together and started our research in the same department. You are very helpful and friendly. Thanks for your help for my projects, I wish you get great achievements in your future.

To Yining, Pengfei and Ruyi, I am happy to meet you in Rotterdam. Thanks for your help and support for my research work in the lab. You are very hard-working and intelligent, I wish you a great success in your future and enjoy the life in the Netherlands. To Shaojun, Bingting, Shihao, Zhouhong, Junhong, Shanshan and Xiaopei, you are all very friendly and helpful, thank you all for your help to my projects, hope all of you can achieve success in your research field.

To roommates in Ee830, Jorker, Floris, Rachid, Ruby, Pauline, Suk yee Lam, Michiel, Gulce, Ketaryna and other colleagues in this office. I am very happy for sharing the office with all of you, that is a very precious memory for my life. Hoping a bright future to all of you.

To Leonie, Jan and Auke, thank you very much for your help in primer/reagents ordering and lab management. Because of your assistance, I am able to concentrate on my research projects. To all MDL colleagues: Henk, Sonja, Marla, Andre, Hugo, Luc, Jaap, Lucia, Natasha, Kelly, Patrick, Anthonie, Marcel, Monique, Shanta, Petra, Lianne, and everyone in our lab. We are a large group, I want to thank all of you for your help and support during my study in the lab, and wish all of you happiness and good health.

To my master supervisor Prof. dr. Hong Yin, and co-supervisors Dr. Zhijie Liu, Dr. Qingli Niu and Jifei Yang, thank you all for guiding me through my master study, giving me a lot of experimental skills, allowing me to attend some helpful conferences that broadened my horizons. Also, thanks for your help and support for my PhD study abroad. I wish you and your family happy and healthy.

To my friends in China, thank you all very much for your help and support for my life and study, you bring me a lot of joy and good fortune, and I believe you all are the wealth of my life. I wish you all succeed and have a happy life.

To my cousin Peixue and friend Xingli, thank you very much for guaranteeing us to go abroad and continue our study in the Netherlands. I really enjoy the time and food we had together. I hope you both can achieve great success in your educational careers, and wish you and your family have a happy life.

I want to express my gratitude to the China Scholarship Council (CSC) for financially supporting me to study in the Netherlands for four years. Also, I would like to sincerely thank the Education Section, Embassy of the People's Republic of China in the Netherlands, who provided more assistance and support throughout my study in the Netherlands. 诚挚地感谢中国留学基金委（CSC）和中国驻荷兰大使馆教育处对我学习的资助与支持。

致我的家人和亲人们：感谢您们对我（和春燕）国外求学的支持。四年的时间一晃而过，我依然记得出国前您们对我们的嘱托，以及求学期间的牵挂与帮助。我们将完成博士阶段的学习，并将开始新的征程，希望您们会一如既往的支持。感谢亲人们对我们家庭的关心与帮助，祝我的家人亲人们工作顺利，幸福安康！

To my beloved wife, Chunyan, thank you very much for your unwavering love and support. Company is the most affectionate confession, you are the one who always encourage and support me when I meet hardship. The time we spend living and studying in the Netherlands is destined to be precious and unforgettable. Thank you for everything you have done for our family and me. Best wishes for a prosperous future to us.

Publications

1. **Yu, P.**, Miao, Z., Li, Y., Bansal, R., Peppelenbosch, M.P. and Pan, Q., 2021. cGAS-STING effectively restricts murine norovirus infection but antagonizes the antiviral action of N-terminus of RIG-I in mouse macrophages. **Gut Microbes**. (In press)
2. **Yu, P.**, Li, Y., Li, Y., Miao, Z., Peppelenbosch, M.P. and Pan, Q., 2020. Guanylate-binding protein 2 orchestrates innate immune responses against murine norovirus and is antagonized by the viral protein NS7. **J Biol Chem**, 295(23): 8036-8047.
3. **Yu, P.**, Li, Y., Li, Y., Miao, Z., Wang, Y., Peppelenbosch, M.P. and Pan, Q., 2020. Murine norovirus replicase augments RIG-I-like receptors-mediated antiviral interferon response. **Antiviral Res**, 182: 104877.
4. **Yu, P.**, Li, Y., Wang, Y., Peppelenbosch, M. and Pan, Q., 2020. Lipopolysaccharide restricts murine norovirus infection in macrophages mainly through NF- κ B and JAK-STAT signaling pathway. **Virology**, 546: 109-121.
5. **Yu, P.**, Wang, Y., Li, Y., Li, Y., Miao, Z., Peppelenbosch, M.P. and Pan, Q., 2020. 2'-Fluoro-2'-deoxycytidine inhibits murine norovirus replication and synergizes MPA, ribavirin and T705. **Arch Virol**, 165(11): 2605-2613.
6. Miao, Z., Li, Y., **Yu, P.**, Yu, B., Peppelenbosch, M. P. and Pan, Q., 2021. The dynamics of hepatitis delta virus prevalence and its potential association with hepatitis B virus vaccination. **Clin Res Hepatol Gastroenterol**, 101677.
7. Li, Y., **Yu, P.**, Qu, C., Li, P., Li, Y., Ma, Z., Wang, W., Robert, A., Peppelenbosch, M.P. and Pan, Q., 2020. MDA5 against enteric viruses through induction of interferon-like response partially via the JAK-STAT cascade. **Antiviral Res**, 176: 104743.
8. Li, Y., Li, P., Li, Y., Zhang, R., **Yu, P.**, Ma, Z., Kainov, D.E., Robert, A., Peppelenbosch, M.P. and Pan, Q., 2020. Drug screening identified gemcitabine inhibiting hepatitis E virus by inducing interferon-like response via activation of STAT1 phosphorylation. **Antiviral Res**, 184: 104967.
9. Li, Y., Qu, C., **Yu, P.**, Ou, X., Pan, Q. and Wang, W., 2019. The interplay between host innate immunity and hepatitis E virus. **Viruses**, 11(6): 541.
10. Qu, C., Li, Y., Li, Y., **Yu, P.**, Li, P., Donkers, J.M., van de Graaf, S.F., Robert, A., Peppelenbosch, M.P. and Pan, Q., 2019. FDA-drug screening identifies depropine inhibiting hepatitis E virus involving the NF- κ B-RIPK1-caspase axis. **Antiviral Res**, 170: 104588.
11. **Yu, P.**, Liu, Z., Niu, Q., Yang, J., Abdallah, M.O., Chen, Z., Liu, G., Luo, J. and Yin, H., 2017. Molecular evidence of tick-borne pathogens in *Hyalomma anatolicum* ticks infesting cattle in Xinjiang Uygur Autonomous Region, Northwestern China. **Exp Appl Acarol**, 73(2): 269-281.
12. **Yu, P.**, Niu, Q., Liu, Z., Yang, J., Chen, Z., Guan, G., Liu, G., Luo, J. and Yin, H., 2016. Molecular epidemiological surveillance to assess emergence and re-emergence of tick-borne infections in tick samples from China evaluated by nested PCRs. **Acta Trop**, 158: 181-188.
13. Niu, Q., Liu, Z., Yang, J., **Yu, P.**, Pan, Y., Zhai, B., Luo, J. and Yin, H., 2016. Genetic diversity and molecular characterization of *Babesia motasi*-like in small ruminants and ixodid ticks from China. **Infect Genet Evol**, 41: 8-15.

14. Wang, C., **Yu, P.**, He, X., Fang, Y., Cheng, W. and Jing, Z., 2016. $\alpha\beta$ T-cell receptor bias in disease and therapy. **Int J Oncol**, 48(6): 2247-2256.
15. Niu, Q., Liu, Z., Yang, J., **Yu, P.**, Pan, Y., Zhai, B., Luo, J., Guan, G. and Yin, H., 2016. Expression of sheep pathogen *Babesia* sp. Xinjiang rhoptry-associated protein 1 and evaluation of its diagnostic potential by enzyme-linked immunosorbent assay. **Parasitology**, 143(14): 1990-1999.
16. Niu, Q., Liu, Z., Yang, J., **Yu, P.**, Pan, Y., Zhai, B., Luo, J., Moreau, E., Guan, G. and Yin, H., 2016. Expression analysis and biological characterization of *Babesia* sp. BQ1 (Lintan)(*Babesia motasi*-like) rhoptry-associated protein 1 and its potential use in serodiagnosis via ELISA. **Parasite Vector**, 9(1): 1-14.
17. Abdallah, M.O., Niu, Q., Yang, J., Hassan, M.A., **Yu, P.**, Guan, G., Chen, Z., Liu, G., Luo, J. and Yin, H., 2017. Identification of 12 piroplasms infecting ten tick species in China using reverse line blot hybridization. **J Parasitol**, 103(3): 221-227.
18. Abdallah, M.O., Niu, Q., **Yu, P.**, Guan, G., Yang, J., Chen, Z., Liu, G., Wei, Y., Luo, J. and Yin, H., 2016. Identification of piroplasm infection in questing ticks by RLB: a broad range extension of tick-borne piroplasm in China?. **Parasitol Res**, 115(5): 2035-2044.
19. Niu, Q., Liu, Z., **Yu, P.**, Yang, J., Abdallah, M.O., Guan, G., Liu, G., Luo, J. and Yin, H., 2015. Genetic characterization and molecular survey of *Babesia bovis*, *Babesia bigemina* and *Babesia ovata* in cattle, dairy cattle and yaks in China. **Parasite Vector**, 1(8): 1-13.

PhD Portfolio

Name of PhD student	Peifa Yu
Department	Gastroenterology and Hepatology, Erasmus MC - University Medical Center, Rotterdam
PhD Period	October 2017 – September 2021
Promotor	Prof. dr. Maikel P. Peppelenbosch
Copromotor	Dr. Qiuwei Pan

PhD training

Seminars

- 2017-2021, Weekly MDL seminar program in experimental gastroenterology and hepatology (attending); (42 weeks/year; @1.5 h) (ECTS, 9.0)
- 2017-2021, Weekly MDL seminar program in experimental gastroenterology and hepatology (presenting); (preparation time 16 h; 2 times/year) (ECTS, 4.6)
- 2017-2021, Biweekly research group education (attending); (20 times/year; @1.5 h) (ECTS, 4.3)
- 2017-2021, Biweekly research group education (presenting); (preparation time 8 h; 8 times/year) (ECTS, 8.6)
- 2019-2020, Weekly organoid meeting (attending); (4 times) (ECTs, 0.2)

Teaching Activity

- 2019, Supervising two students (Junior Medicine); (4 weeks; 20 h/week) (ECTs, 2.9)

General Courses and Workshops

- 2018, The Course in Virology 2018 (ECTS, 1.4)
- 2018, The Introduction in GraphPad Prism Version 6 (ECTS, 0.3)
- 2018, The Workshop on Microsoft Excel 2010: Basic (ECTS, 0.3)
- 2018, The Workshop on Microsoft Excel 2010: Advanced (ECTS, 0.4)

- 2018, The English Social Skills Course
- 2019, The Introduction in Confocal Course
- 2021, The Research Integrity Course (ECTS, 0.3)
- 2021, PowerPoint: Tips & Tricks you didn't know (ECTS, 0.3)

National and International Conferences

- 2018, Annual Day of the Molecular Medicine, Postgraduate School Molecular Medicine, Rotterdam, the Netherlands
- 2019, Annual Day of the Molecular Medicine, Postgraduate School Molecular Medicine, Rotterdam, the Netherlands (Poster)
- 2020, Innovative Training Network Antiviral Immunometabolism (INITIATE) Kick-Off Meeting, Rotterdam, the Netherlands
- 2021, Dutch Annual Virology Symposium (DAVS), the Netherlands
- 2021, The 5th Dutch Arbovirus Research Network (DARN) meeting

Academic Awards

- 2017, China Scholarship Council (CSC) Scholarship

Curriculum Vitae

Peifa Yu was born on November 27th, 1989 in Jinan, Shandong province, China. He grew up in his hometown and attended primary, secondary, and high school there.

In 2009, he started his undergraduate study in veterinary medicine at Shandong Agricultural University. In 2013, he initiated his master study at Graduate School of Chinese Academy of Agricultural Science (CAAS), Beijing, China. One year later, he formally started his master research training at the Department of Vector and Vector-Borne Disease, Lanzhou Veterinary Research Institute, CAAS. Under the supervision of Prof. dr. Hong Yin and Dr. Zhijie Liu, he completed his master with a thesis book, entitled “Study on Characterization and Antigenicity of P66 Gene of *Borrelia garinii*”.

In 2017, with the support of China Scholarship Council (CSC), he got an opportunity to start his PhD research at the Department of Gastroenterology and Hepatology, Erasmus University Medical Center, Rotterdam, the Netherlands. Under the supervision of Prof. dr. Maikel P. Peppelenbosch and Dr. Qiuwei Pan, he focused on the norovirus-host interactions and development of novel antiviral strategies against norovirus infection.